The structure of borosilicate glasses

THE STRUCTURE OF BOROSILICATE GLASSES

W. L. KONIJNENDIJK

THE STRUCTURE OF BOROSILICATE GLASSES

PROEFSCHRIFT

TER VERKRIJGING VAN DE GRAAD VAN DOCTOR IN DE TECHNISCHE WETENSCHAPPEN AAN DE TECHNISCHE HOGESCHOOL EINDHOVEN, OP GEZAG VAN DE RECTOR MAGNIFICUS, PROF. DR. IR. G. VOSSERS, VOOR EEN COMMISSIE AANGEWEZEN DOOR HET COLLEGE VAN DEKANEN IN HET OPENBAAR TE VERDEDIGEN OP VRIJDAG 11 APRIL 1975 TE 16.00 UUR

DOOR

WILLEM LEENDERT KONIJNENDIJK

GEBOREN TE OSS

DIT PROEFSCHRIFT IS GOEDGEKEURD DOOR DE PROMOTOREN
PROF. DR. J. M. STEVELS EN PROF. DR. G. C. A. SCHUIT

Zonder glas zou de chemie blind zijn

Dankbetuiging

De direktie van het Natuurkundig Laboratorium van de N.V. Philips' Gloeilampenfabrieken ben ik erkentelijk voor de toestemming het verrichte onderzoek aan borosilikaatglazen in de vorm van een dissertatie te mogen publiceren.

Voor de uitvoering van de vele experimenten dank ik in het bijzonder Mevr. M. van Duuren-Baarda en J. H. J. M. Buster en daarnaast Mej. W. Rexwinkel, Mevr. R. L. Goor-Driesen, Mej. C. M. Haex, G. P. Melis, W. Loendersloot, R. E. Breemer en C. Langereis.

Aan Ir. T. W. Bril ben ik veel dank verschuldigd voor de vele en uitvoerige diskussies alsmede de nauwe samenwerking tijdens het Raman onderzoek.

Voor het kritisch doorlezen van het manuskript van deze dissertatie ben ik dank verschuldigd aan Dr. Ir. H. M. J. M. van Ass, Ing. H. van den Boom, Dr. A. Bril, Dr. Ir. R. G. Gossink en Dr. H. J. L. Trap.

CONTENTS

1. INTRODUCTION

1.1. The structure of glass

For an understanding of the structure of glass it is very important to know the coordination numbers and type of bonding of the atoms. These coordination numbers and type of bonding are primarily determined by the kind of atoms present. Differences in the structure of glasses also mean differences in their physical and chemical properties. Thus, for a better understanding and even in order to predict the properties of glass it is important to know the coordination number and type of bonding of the atoms present in the glass.

Up to now a good deal is known about the structure of many glasses; however, the current impossibility to describe the structure of glasses in detail as fine as for crystals, has led to different approaches to describe the structure. Two main approaches may be observed, viz. the random-network hypothesis and the crystallite hypothesis. In the random-network hypothesis it is thought for instance that the SiO_4 tetrahedra in vitreous silica are bonded irregularly to each other. In the crystallite hypothesis it is suggested that in vitreous silica submicroscopically small areas with an ordered structure are present, and are connected to each other by areas with a disordered structure. To-day the crystallite hypothesis finds but little support. On the other hand, the random-network hypothesis is also in discussion. Usually it is assumed that there is a certain short-range order in glass, somewhat similar to the order as observed in crystals but there is a definite absence of long-range order.

For the study of the structure of crystalline solids the use of X-ray diffraction has been of vital importance. Due to the absence of long-range order in glass, X-ray diffraction cannot reveal the complete structure. From a historical point of view one should say that precisely the method of X-ray diffraction revealed the absence of long-range order in glass. By the recently developed method of fluorescence excitation, the background scattering has been largely eliminated and it has become possible to calculate some interatomic distances and the number of neighbouring atoms from so called "pair-distribution" functions. Mozzi and Warren [1-1]) in this way showed the smallest silicon–oxygen distance in vitreous silica to be 1·62 Å and the smallest oxygen–oxygen distance to be 2·65 Å, confirming earlier studies, which however had theoretical and experimental limitations. These distances are close to those found in many crystalline silicates. It was also shown that each silicon atom is tetrahedrally coordinated by oxygen. Furthermore it was shown that the distribution of bond angles is rather narrow compared to a completely random distribution of bond angles. Thus the structure of vitreous silica shows something like regularity at a short range, although there is no order beyond several units of SiO_4 tetrahedra.

In multicomponent silicate glasses, X-ray-diffraction studies have shown that the alkali ions are not uniformly distributed throughout the glass, the average first-neighbour distance of alkali ions being considerably less than for a uniform distribution. This clustering of alkali ions is reminiscent of the structure of for instance crystalline alkali disilicates. The first-neighbour distance of alkali ions in the disilicate crystals is also considerably less than if the ions had been distributed evenly throughout the crystal. It is therefore suggested that in certain cases small areas in the glass have a structure somewhat similar to that of crystals. This structure will deviate to some extent from the ideal situation, so that the randomness at longer distance is retained.

Other experimental techniques used to study the molecular structure of glass, for instance are infrared and Raman spectroscopy, nuclear magnetic resonance, and measurement of viscosity, thermal expansion, electrical conduction, dielectric and mechanical losses, density and refractive index. Study of the nature of colour centres in glass by electron spin resonance and optical-absorption measurements has also been very helpful in understanding the structure. Usually these measurements are done on glasses in certain composition series. By the systematic variation of the composition of the glasses one obtains insight into the characteristics of certain elements.

A drawback usually encountered in the study of the structure of glass is that one experimental technique reveals only a part of the structural characteristics or that more than one structural model explains the experimental results. This has made the study of the structure of glass very time-consuming. The study of the structure of glass often results in an intelligent speculation on this structure with the experimental evidence available.

Another factor that sometimes interferes in the study of the structure of glass is metastable subliquidus phase separation. What is usually meant by this type of phase separation is that composition fluctuations are present in the glass, extending from about 5 nm to higher values. In this case both phases (or even more than two) are glasses. It will be clear that an interpretation in terms of molecular groups present, for instance, of viscosity measurements, may be hampered greatly by the phenomenon of phase separation. The electron microscope has been of great help in studying this phase separation in glass.

Apart from its scientific interest, the study of the structure is also of great technological importance. To study the process of formation of glass one must be able to characterize the intermediate product at different moments of this process. The characterization in terms of molecular structure has been of great help for crystalline materials. The characterization of glass in terms of the molecular units has also been useful up to now, although it is not so far reaching as in the crystalline materials. Knowledge on the relationship between the structure, the composition and viscosity of glass is of vital importance for the industrial production of all kinds of glass products.

1.2. Borosilicate glasses

Borosilicate glasses are of technological interest because they have many applications. They generally have a lower thermal expansion than soda-lime silica glasses, have good chemical resistance, high dielectric strength and a higher softening temperature than soda-lime silica glasses. For these reasons they are used for laboratory glassware, household cooking ware, industrial piping, bulbs for hot lamps and electronic tubes of high wattage such as X-ray tubes. Besides these applications one must mention the use of barium crown glasses for optical purposes. Furthermore, borosilicate glass plays an important role in the production of what is known as Vycor glass. This glass contains about 96% SiO_2 and is an important substitute for fused silica. Vycor glass can be produced at lower working temperatures than fused silica, which is of economic interest. It is used, for instance, in projection lamps.

In spite of this technological importance, the exact glass-forming regions and phase relations in borosilicate glasses have not been determined as yet. Also, the information on the molecular groups in these glasses is scattered and very incomplete.

The system Li_2O–B_2O_3–SiO_2 was studied by Sastry and Hummel [1-2,3]) and later by Galakhov and Alekseeva [1-4]). In this ternary system, compositions with less than about 20 mol % Li_2O showed liquid–liquid phase separation, compositions with more than about 33 mol % Li_2O showed a strong tendency to crystallization. Close to the boundary Li_2O–B_2O_3 the glass-forming tendency improves.

The phase relations in the system Na_2O–B_2O_3–SiO_2 were studied by many workers. The oldest work, worth citing, was done by Morey [1-5]). At atmospheric pressure no ternary-compound formation was indicated in this ternary diagram. In that work the fields of the binary compounds are outlined and isotherms determined. Later Skatulla, Vogel and Wessel [1-6]) studied metastable-phase-separation phenomena in this system. Vogel [1-7]) studied the structure of glass of the Vycor type, this study being extended by Kühne and Skatulla [1-8]). More-recent studies on the metastable immiscibility surface in the system were carried out by Haller, Blackburn, Wagstaff and Charles [1-9]) and Scholes and Wilkinson [1-10]). The area of glass formation of the system Na_2O–B_2O_3–SiO_2 is shown in fig. 1.1.

No ternary phase diagram of the system K_2O–B_2O_3–SiO_2 is available. Scattered experimental evidence suggests that the phase relations and glass-forming region are similar to the system Na_2O–B_2O_3–SiO_2.

The phase diagram of the system CaO–B_2O_3–SiO_2 was given by Levin, McMurdie and Hall [1-11]). This system shows a large area of a stable liquid–liquid phase separation. Phase relations and the glass-forming regions in the system BaO–B_2O_3–SiO_2 were studied by Levin and Ugrinic [1-12]) and Hamilton, Cleek and Graner [1-13]). This system shows a large area of a stable liquid–liquid

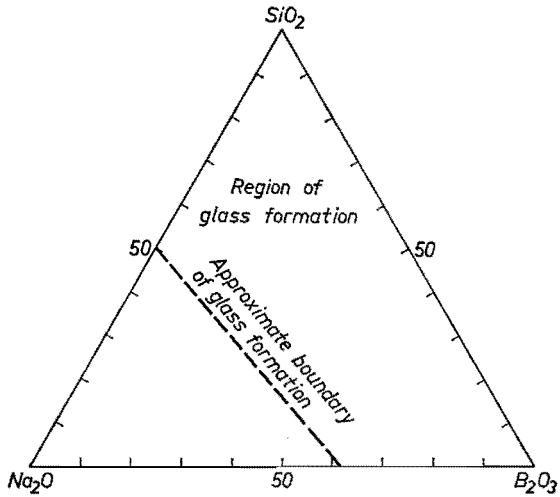

Fig. 1.1. The region of glass formation in the system Na_2O–B_2O_3–SiO_2.

phase separation. Glasses in this system are formed much more easily than in the corresponding calcium-borosilicate system. For an indication of the approximate glass-forming region in the system BaO–B_2O_3–SiO_2, see fig. 1.2.

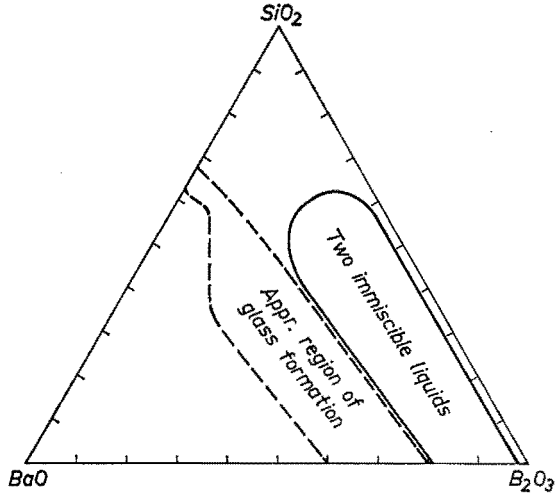

Fig. 1.2. The region of glass formation and region of liquid–liquid-phase separation in the system BaO–B_2O_3–SiO_2.

1.3. Metastable subliquidus phase separation in silicate, borate and borosilicate glasses

Immiscibility in oxide systems may occur above or below the liquidus. The latter is often called metastable subliquidus phase separation. Silicate melts that

exhibit phase separation above the liquidus can be found in a certain area of the system $CaO–SiO_2$. Metastable subliquidus immiscibility is often found in silicate, borate and borosilicate systems that have an s-shaped liquidus. The phenomenon of metastable subliquidus immiscibility leads to a phase separation on a very fine scale, often only detectable by the electron microscope or by small-angle X-ray scattering.

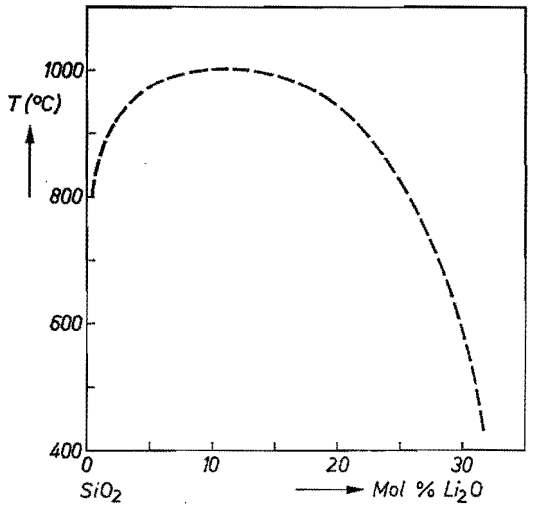

Fig. 1.3. Boundary of the region of metastable subliquidus phase separation in the system $Li_2O–SiO_2$ (from Tomozawa [1–14]).

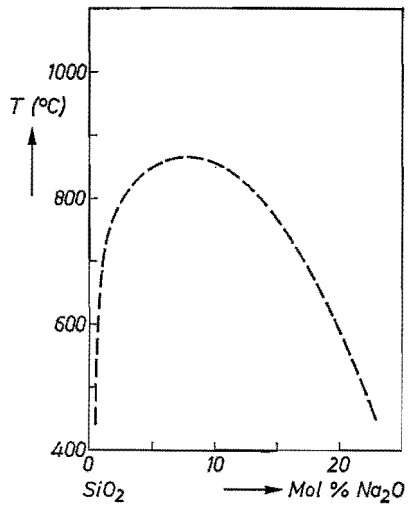

Fig. 1.4. Boundary of the region of metastable subliquidus phase separation in the system $Na_2O–SiO_2$ (from Tomozawa et al.[1–15]).

In the last decade it has become obvious that the understanding and interpretation of many physical and chemical properties of glass has been influenced considerably by the discovery of this metastable subliquidus phase separation in many glasses previously thought to be homogeneous. This means too that care must be taken in the interpretation of physical and chemical properties in terms of structural units.

The metastable subliquidus immiscibility boundary of Li_2O–SiO_2 glass was determined with small-angle X-ray scattering by Tomozawa [1–14]) and others mentioned in the references in his work. This boundary is reproduced in fig. 1.3.

The same boundary in the system Na_2O–SiO_2 was also determined with small-angle X-ray scattering by Tomozawa, MacCrone and Herman [1–15]) and Neilson [1–16]). This boundary is shown in fig. 1.4.

A recent discussion on miscibility gaps in alkali-silicate glasses was given by Haller, Blackburn and Simmons [1–17]).

The boundaries of the metastable subliquidus miscibility gaps in a number of alkali-borate systems were determined by Shaw and Uhlmann [1–18]) using electron microscopy. The boundaries of the lithium-, sodium- and potassium-borate systems are shown in figs 1.5 to 1.7. A recent review on the boundaries of miscibility gaps in alkali-borate systems is given by Macedo and Simmons [1–19]). A study of the metastable immiscibility in the system B_2O_3–SiO_2 was made by Charles and Wagstaff [1–20]). They proposed a boundary that was rather flat and extended across the complete binary system, cf. fig. 1.8.

Studies on metastable-subliquidus-phase-separation phenomena in the system Na_2O–B_2O_3–SiO_2 are numerous. The boundary of the immiscibility dome, reproduced from the work of Haller, Blackburn, Wagstaff and Charles [1–9]), is shown in fig. 1.9. It was determined by "opalescence" and "clearing" techniques. The results indicate the existence of a three-liquid region which underlies the immiscibility surface (cf. fig. 1.10). The reader is also referred to the work of Scholes and Wilkinson [1–10]) on this subject. A study on the metastable region of phase separation in the system Li_2O–B_2O_3–SiO_2 was made by Galakhov and Alekseeva [1–4]). The results on first approximation are similar to those of the corresponding Na_2O–B_2O_3–SiO_2 system. The boundary of this region will not be shown here because it mainly falls outside the glass-forming region.

An interesting study on phase-separation phenomena of BaO–B_2O_3–SiO_2 glasses was carried out by Vogel, Schmidt and Horn [1–21]) where it was shown that phase separation in oxide melts is a very complicated process. The phase-separation processes may be incomplete after cooling of the melt. In this way the phase boundaries of the micro-glass phases are not well developed and the concentration differences do not reach the final situation.

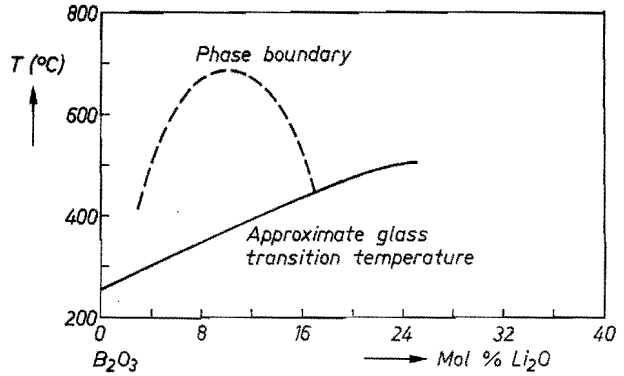

Fig. 1.5. Boundary of the region of metastable subliquidus phase separation in the system Li_2O–B_2O_3 (from Shaw and Uhlmann [1–18]).

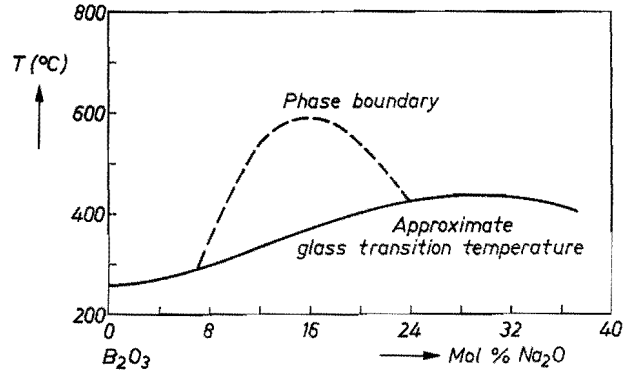

Fig. 1.6. Boundary of the region of metastable subliquidus phase separation in the system Na_2O–B_2O_3 (from Shaw and Uhlmann [1–18]).

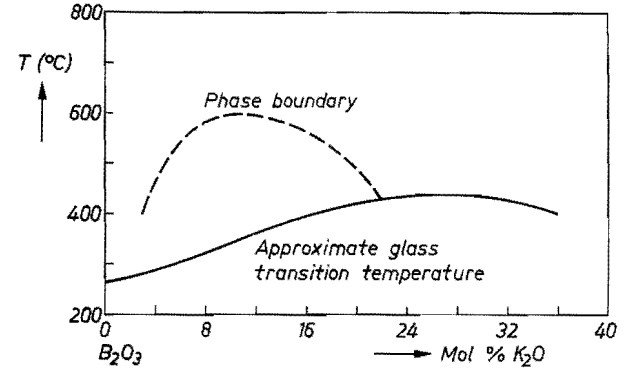

Fig. 1.7. Boundary of the region of metastable subliquidus phase separation in the system K_2O–B_2O_3 (from Shaw and Uhlmann [1–18]).

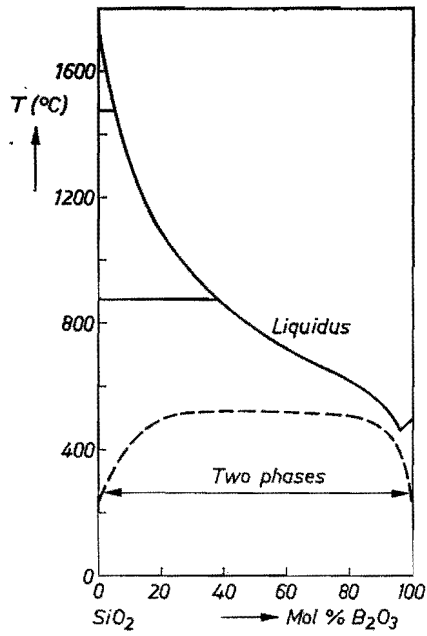

Fig. 1.8. Predicted boundary of the region of metastable subliquidus phase separation in the system B_2O_3–SiO_2 (from Charles and Wagstaff [1-20]).

1.4. The structure of binary silicate and borate glasses

Glass formation in the binary system Li_2O–SiO_2 is continuous from SiO_2 to a limiting composition with about 35 mol % Li_2O. In the corresponding Na_2O–SiO_2 and K_2O–SiO_2 system the limiting composition lies at about 50 mol % alkali oxide. The exact limiting composition depends on the experimental conditions such as the size of the melt and the cooling rate.

Glass formation in the binary system CaO–SiO_2 goes up to about 55 mol % CaO; however, in a large part of this area liquid–liquid phase separation prevents single-phase glasses from being made. In the corresponding BaO–SiO_2 system the limiting composition is about 40 mol % BaO and also in this system liquid–liquid phase separation spoils single-phase-glass formation over a part of this area.

In all crystalline silicates the silicon ions are coordinated by four oxygen ions. The simplest silicate glass is vitreous silica. As pointed out in somewhat more detail in sec. 1.1, in vitreous silica all silicon ions are also coordinated by four oxygen ions. There is a certain distribution in the bond angles, evidenced by X-ray analysis, which makes the structure of vitreous silica quite uniform at a short range, but there is no order beyond several units of SiO_4 tetrahedra. Various other properties of vitreous silica are also in agreement with the random-

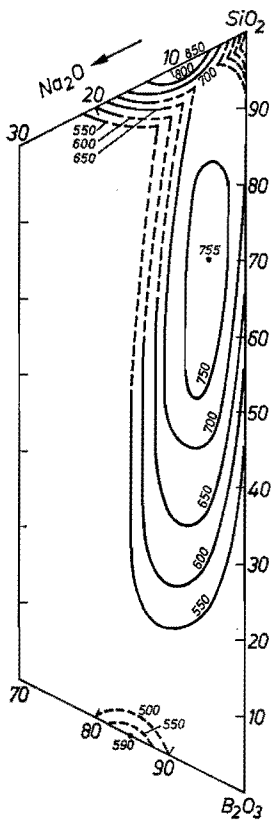

Fig. 1.9. Boundaries of the metastable subliquidus immiscibility dome in the system Na_2O–B_2O_3–SiO_2 (from Haller et al.[1–9]).

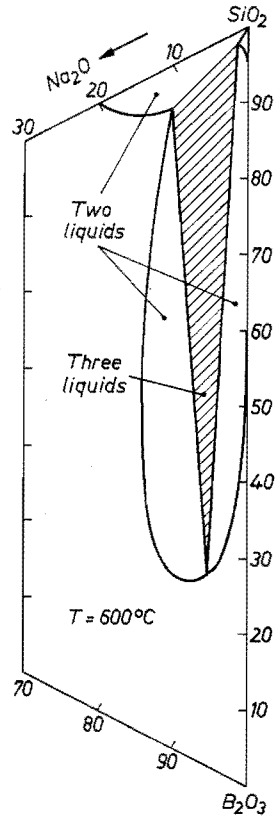

Fig. 1.10. Estimated three-phase incompatibility triangle of the system Na_2O–B_2O_3–SiO_2 at 600 °C (from Haller et al.[1–9]).

network model, for instance infrared absorption, Raman scattering, inelastic neutron scattering and thermal behaviour.

The introduction of alkali or alkaline-earth oxide in silica leads to a breaking up of the silicon–oxygen network. This is evidenced by the much lower viscosity and higher thermal-expansion coefficient of these glasses compared to vitreous silica. However, silicons remain coordinated by four oxygen ions, although part of these oxygens will be of the non-bridging type. Thus the random network is preserved.

X-ray-diffraction studies have shown that the alkali ions are not distributed evenly throughout the glass. The average first-neighbour separation is much lower than would be the case for a uniform distribution. As already discussed in sec. 1.1 this clustering of alkali ions suggests areas with a structure that resembles the structure of $Li_2O \cdot 2\,SiO_2$ and α-$Na_2O \cdot 2\,SiO_2$ on a small scale. In these crystals too, the alkali distribution is not uniform. The alkali-silicate glasses show an area of metastable subliquidus phase separation, as

evidenced primarily by electron microscopy and small-angle X-ray scattering. Also outside this region of metastable phase separation such clustering of alkali ions seems to persist (Milberg and Peters [1-22]).

Glass formation becomes progressively more difficult close to a composition having about 50 mol % Na_2O or K_2O. Near this composition a metasilicate chain-like structure is assumed to exist in these glasses.

Small differences in physical and chemical properties may be observed between lithium-silicate, sodium-silicate and potassium-silicate glasses at equal alkali-oxide content. This is explained by differences in the bond strength of the alkali-ion and the oxygen coordination. The coordination number of alkali ions in glass is not very clear, in crystalline $Li_2O \cdot 2\,SiO_2$ this coordination is four (Liebau [1-23]), in α-$Na_2O \cdot 2\,SiO_2$ it is five, with varying Na–O distances (Pant and Cruickshank [1-24]) and in $Na_2O \cdot SiO_2$ sodium is coordinated by five oxygen ions in a distorted trigonal bipyramid (McDonald and Cruickshank [1-25]). Of course, at least one of the ions of the oxygen coordination of alkali ions in glass will be of the non-bridging type. Table 1-I summarizes the X-ray crystallography work on alkali-silicate compounds.

The presence of alkaline-earth ions also leads to the formation of non-bridging oxygen ions; however, in contrast to the alkali ions, in this case the introduction of one alkaline-earth ion leads to the formation of two non-bridging ions, which will necessarily belong to the oxygen coordination of the alkaline-earth ions. The bonding, for instance, of calcium to the network is much stronger than in case of sodium. This is reflected in properties such as the viscosity and thermal-expansion behaviour of the glass.

The introduction of Al_2O_3 in alkali-silicate glass leads to a decrease in the number of non-bridging oxygen ions and the formation of AlO_4 tetrahedra, the negative charge of these AlO_4 tetrahedra being compensated by an alkali ion. In crystalline aluminosilicates Al^{3+} replaces an Si^{4+} ion in a tetrahedral position, so that aluminosilicates show structures that resemble silicate structures. It is not clear how far these structures on a small scale are retained in aluminosilicate glasses, although it is highly probable that this is the case.

The structure and physical properties of binary borate glasses are quite different from the binary silicate glasses. Vitreous boron oxide is primarily built up of boroxol rings (cf. fig. 1.12) as evidenced by Mozzi and Warren [1-28]) using the fluorescence-excitation method. Krogh-Moe [1-29]) in a review of the structure of vitreous boron oxide, concluded from the experimental evidence available (primarily n.m.r., infrared and Raman data) that the boroxol group is the most important group. In this six-membered boroxol ring all boron ions are triangularly coordinated. The best fit to the experimental results of Mozzi and Warren [1-28]) was to assume that, besides the linking of the boroxol groups, a small part of the BO_3 units was linked randomly to the boroxol groups and was not in boroxol rings.

TABLE 1-I
Structural units present in crystalline silicates

compound	structural units present	literature reference crystal structure	ASTM-index
$Li_2O \cdot 2\,SiO_2$	SiO_4^- units with one non-bridging oxygen ion, layered with 6 SiO_4 tetrahedra in a ring	Liebau [1-23])	17-447
α-$Na_2O \cdot 2SiO_2$	SiO_4^- units with one non-bridging oxygen ion, layered with 6 SiO_4 tetrahedra in a ring	Liebau [1-26]), Pant and Cruickshank [1-24]), Pant [1-27])	
$Na_2O \cdot SiO_2$	SiO_4^{2-} units with two non-bridging oxygen ions, chains of tetrahedra	McDonald and Cruickshank [1-25])	16-818

The binary sodium- and potassium-borate systems show glass formation up to nearly 40 mol % alkali oxide. The change in properties of borate glass when alkali oxide is added is in many cases the reverse of that observed in silicate glasses. For instance, the addition of alkali oxide leads to an increase in viscosity and a decrease in thermal expansion compared to vitreous boron oxide. The increase in viscosity and decrease in thermal expansion proceed up to 20 to 30 mol % alkali oxide after which the tendency is reversed and addition of more alkali oxide leads to a decrease in viscosity and increase in thermal expansion. This behaviour is generally referred to as the boron-oxide anomaly. This anomaly is related to the change in the coordination number of boron from three to four when alkali oxide is added. This coordination change is clearly indicated by nuclear-magnetic-resonance spectroscopy. Bray and O'Keefe [1–30]) determined the fraction of tetrahedrally coordinated boron ions in alkali-borate glasses by this method. This fraction, usually called N_4, is shown in fig. 1.11. From this figure it becomes clear that up to about 30 mol % alkali oxide

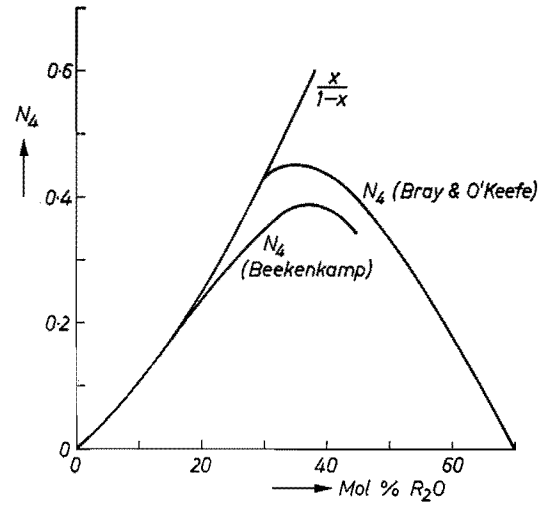

Fig. 1.11. The fraction of boron ions in four-coordination N_4, after Bray and O'Keefe [1–30]) and Beekenkamp [1–31]). The curve $x/(1-x)$ represents the maximum possible value of N_4.

the maximum number of BO_3 triangles is converted into BO_4 tetrahedra. At higher alkali-oxide concentrations the relative number of BO_4 tetrahedra begins gradually to decrease and for lithium-borate glasses has been shown to decrease to zero at about 70 mol % Li_2O. It is suggested that if the addition of a molecule of alkali oxide does not lead to the formation of BO_4 tetrahedra, then in that case non-bridging oxygen ions are formed, so it is suggested from the n.m.r. data that from about 30 mol % alkali oxide onwards a significant number of non-bridging oxygen ions is formed.

A quantitative hypothesis of the structure of alkali-borate glasses has been

given by Beekenkamp [1-31]). In this hypothesis it is suggested that various types of structural units are formed which may consist of the following ions: triangularly coordinated boron ions, tetrahedrally coordinated boron ions, bridging and non-bridging oxygen ions, and alkali ions. Two further structural rules are suggested, viz.:

— BO_4 tetrahedra cannot be bound to each other;
— non-bridging oxygen ions occur in BO_3 triangles only and are absent in BO_4 tetrahedra.

From these rules it can be concluded that this hypothesis does not suggest the formation of a random network in the strict sense of the word. It can also be concluded that the rules are not based on ideas of a similarity between groups in the glass and groups in crystalline borates.

Beekenkamp's hypothesis goes even further and suggests the following quantitative relation between the fraction of tetrahedrally coordinated boron ions N_4 and the mole fraction of alkali oxide x:

$$N_4 = \frac{x/(1-x)}{1 + \exp(11{\cdot}5\,x - 4{\cdot}8)}.$$

See fig. 1.11 for a graphical representation of this equation.

An equation of this form satisfies certain experimental data that non-bridging oxygen ions begin to occur at $x \approx 0{\cdot}15$ in detectable numbers. This assumption is primarily based on the position of the absorption edge in the u.v. spectrum of sodium-borate glasses as a function of the sodium-oxide concentration (McSwain et al.[1-32]). For $x < 0{\cdot}60$ this relation is consistent with the shape of the experimental N_4 versus x curve as given by Bray and O'Keefe [1-30]). This model of the structure of alkali-borate glasses provides a qualitative explanation of the viscosity and thermal expansion versus composition behaviour, it offers an explanation for the position of the u.v. absorption edge and also the position from where a mechanical-loss peak in the alkali borates may be observed.

However, there is some experimental evidence which is inconsistent with this hypothesis of the structure. From X-ray analysis it became evident that vitreous boron oxide is primarily built up of boroxol rings. The model by Beekenkamp [1-32]) does not suggest this, it suggests a network of BO_3 triangles without further specification.

Further, a considerable amount of combined evidence from X-ray crystallography, infrared spectra and melting-point-depression measurements seems to indicate the presence of large borate groups in vitreous alkali and alkaline-earth borates.

Just to give an example, Willis and Hennessy [1-33]) observed that silver ions in silver-borate melts (below 20 mol % silver oxide) appear to occur in pairs. This, together with the similarity of the infrared spectra of vitreous and crys-

talline $Ag_2O \cdot 4\ B_2O_3$ suggests the formation of tetraborate groups in vitreous $Ag_2O \cdot 4\ B_2O_3$ (cf. fig. 1.14). This pair formation may also be observed in caesium-borate glasses up to 20 mol % Cs_2O (Krogh-Moe [1-34]).

To mention another example, X-ray studies of barium-borate glasses (Krogh-Moe [1-35]) and of strontium-borate glasses (Block and Piermarini [1-36]) indicate that the cations are not randomly distributed throughout these glasses, but are instead restricted to characteristic positions. These positions show a certain similarity with the positions of these cations in crystalline borates.

Nuclear-magnetic-resonance studies of the structure of caesium-borate glasses also suggest the presence of large borate groups (Rhee and Bray [1-59]). These are of the same type as can be found in the crystalline caesium borates. Nuclear-magnetic-resonance studies of vitreous and crystalline sodium borates (Rhee [1-60]) suggest that in the region below approximately 20 mol % Na_2O the boroxol group and the tetraborate group as occurring in crystalline $Na_2O \cdot 4\ B_2O_3$ are the major groups. In the region 20–33⅓ mol % Na_2O groups are present that also occur in the compounds $Na_2O \cdot 4\ B_2O_3$, $Na_2O \cdot 3\ B_2O_3$ and $Na_2O \cdot 2\ B_2O_3$. In the region 33⅓–40 mol % Na_2O the diborate group and the metaborate group are proposed to be present in major amounts.

Riebling [1-61]) studied volume relations in sodium-borate melts at 1300 °C. He concluded that at 40 mol % Na_2O 50% of the boron ions is in tetrahedral coordination, which is in agreement with the n.m.r. measurements of Bray and O'Keefe [1-30]) on sodium-borate glasses. Thus, contrary to other suggestions, BO_4 tetrahedra appear to be quite stable at high temperatures, which tends to strengthen the conclusion that significant structural similarities can exist between a borate glass and the corresponding high-temperature liquid.

From X-ray analysis of many crystalline borates it is known that crystalline borates are built up of large borate groups (cf. table 1-II and figs 1.12 to 1.23). It is one of the aims of this thesis to show that in vitreous borates these large groups are retained to some extent. Melting-point-depression studies in sodium-borate melts confirm this picture (Krogh-Moe [1-58]).

In figs 1.12 to 1.23 the types of structure elements in anhydrous crystalline borates are shown. In table 1-II the results of all X-ray analyses of anhydrous borates are summarized.

With the experimental evidence available the existence of a random distribution of BO_4 tetrahedra and BO_3 triangles in vitreous borates can be ruled out. The hypothesis of Beekenkamp [1-31]) of the structure of borate glasses is not strictly a random-network hypothesis of BO_3 and BO_4 units, but at the time of his publication he could not dispose of the evidence of the occurrence of large borate groups. His quantitative relation between N_4 and the composition may be fairly accurate, but with present-day knowledge it must be concluded that his picture of the structure of borate glasses is incomplete.

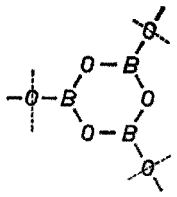

Fig. 1.12. The boroxol ring (a_3), observed in vitreous B_2O_3.

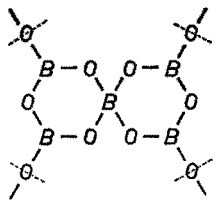

Fig. 1.13. The pentaborate group (a_4c), observed in the compounds α-K_2O . 5 B_2O_3 and β-K_2O . 5 B_2O_3.

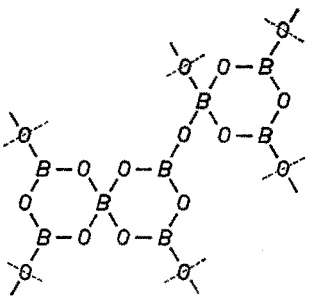

Fig. 1.14. The tetraborate group (a_6c_2), observed in the compound Na_2O . 4 B_2O_3.

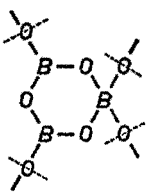

Fig. 1.15. The triborate group (a_2c), observed in the compound Cs_2O . 3 B_2O_3.

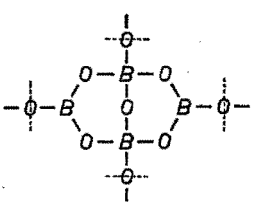

Fig. 1.16. The diborate group (a_2c_2), observed in the compound Li_2O . 2 B_2O_3.

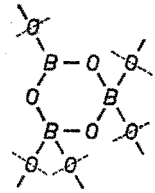

Fig. 1.17. The di-triborate group (ac_2), observed in the compound $K_2O \cdot 2\,B_2O_3$.

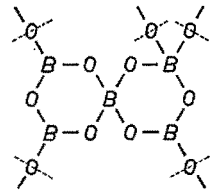

Fig. 1.18. The di-pentaborate group (a_3c_2), observed in the compound $Na_2O \cdot 2\,B_2O_3$.

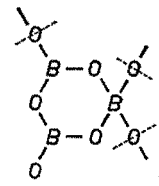

Fig. 1.19. The triborate group with one non-bridging oxygen ion (abc), observed in the compound $Na_2O \cdot 2\,B_2O_3$.

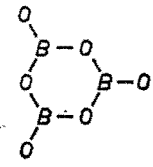

Fig. 1.20. The ring-type metaborate group (b_3), observed in the compounds $Na_2O \cdot B_2O_3$ and $K_2O \cdot B_2O_3$.

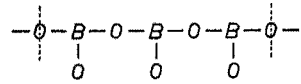

Fig. 1.21. The chain-type metaborate group (b_∞), observed in the compounds $Li_2O \cdot B_2O_3$ and $CaO \cdot B_2O_3$.

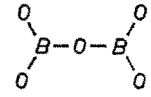

Fig. 1.22. The pyroborate group (b_2''), observed in the compounds $2\,MgO \cdot B_2O_3$ and $2\,CaO \cdot B_2O_3$.

Fig. 1.23. The orthoborate group (b'''), observed in the compounds $3\,MgO \cdot B_2O_3$ and $3\,CaO \cdot B_2O_3$.

TABLE 1-II

Structural units and groups present in crystalline borates

compound	structural units and groups	literature reference crystal structure	ASTM-index
$3\,Na_2O\,.\,B_2O_3$		Milman and Bouaziz [1-37])	
$3\,MgO\,.\,B_2O_3$	isolated planar BO_3^{3-} units (b''')	Berger [1-38])	5-648
$3\,CaO\,.\,B_2O_3$	isolated planar BO_3^{3-} units (b''')	Weir and Schroeder [1-39])	22-142
$2\,Na_2O\,.\,B_2O_3$		Milman and Bouaziz [1-37])	
$2\,MgO\,.\,B_2O_3$	isolated $B_2O_5^{4-}$ groups (b_2'')	Takeuchi [1-40])	15-537
$2\,CaO\,.\,B_2O_3$	isolated $B_2O_5^{4-}$ groups (b_2'')	Weir and Schroeder [1-39])	18-279
$3\,Li_2O\,.\,2\,B_2O_3$			18-721
$Li_2O\,.\,B_2O_3$	BO_3^- triangles in chain (b_∞)	Zachariasen [1-41])	11-407
$Na_2O\,.\,B_2O_3$	$B_3O_6^{3-}$ ring-type groups (b_3)	Marezio, Plettinger and Zachariasen [1-42])	12-492
$K_2O\,.\,B_2O_3$	$B_3O_6^{3-}$ ring-type groups (b_3)	Schneider and Carpenter [1-43])	19-979
$CaO\,.\,B_2O_3$	BO_3^- triangles in chain (b_∞)	Marezio, Plettinger and Zachariasen [1-44])	22-522
$Li_2O\,.\,2\,B_2O_3$	diborate groups, connected (a_2c_2)	Krogh-Moe [1-45])	22-140
$Na_2O\,.\,2\,B_2O_3$	dipentaborate (a_3c_2), triborate groups with one non-bridging oxygen (abc)	Krogh-Moe [1-48])	9- 14
$Na_2O\,.\,2\,B_2O_3\,.\,10\,H_2O$	diborate groups, not connected		
$K_2O\,.\,2\,B_2O_3$	diborate (a_2c_2), di-triborate (ac_2) groups, BO_3 units (a)	Krogh-Moe [1-47])	19-948

TABLE 1-II (continued)
Structural units and groups present in crystalline borates

$SrO \cdot 2\,B_2O_3$	BO_4 units (c)	Krogh-Moe [1-48])	15-801
$ZnO \cdot 2\,B_2O_3$	diborate groups (a_2c_2)	Martinez-Ripoll, Martinez-Carrera and Garcia-Blanco [1-49])	16-283
$BaO \cdot 2\,B_2O_3$	di-triborate (ac_2) and di-pentaborate groups (a_3c_2)	Block and Perloff [1-50])	16-283
α-$Na_2O \cdot 3\,B_2O_3$	pentaborate, (a_4c), diborate groups (a_2c_2)	Krogh-Moe [1-51])	
β-$Na_2O \cdot 3\,B_2O_3$	pentaborate, (a_4c), triborate groups (a_2c), BO_4 units (c)	Krogh-Moe [1-52])	
$K_2O \cdot 3\,B_2O_3$		Krogh-Moe [1-53])	
$Cs_2O \cdot 3\,B_2O_3$	triborate groups (a_2c)	Krogh-Moe [1-54,71])	
$Na_2O \cdot 4\,B_2O_3$	pentaborate (a_4c), triborate groups (a_2c) paired to tetraborate groups (a_6c_2)	Hyman, Perloff, Mauer and Block [1-55])	21-622
$K_2O \cdot 3{\cdot}8\,B_2O_3$	pentaborate (a_4c) and triborate groups (a_2c), BO_4 (c) and BO_3 units (a)	Krogh-Moe [1-70])	
α-$K_2O \cdot 5\,B_2O_3$	pentaborate groups (a_4c)	Krogh-Moe [1-56])	
β-$K_2O \cdot 5\,B_2O_3$	pentaborate groups (a_4c)	Krogh-Moe [1-57])	

It is believed that the group model primarily suggested by Krogh-Moe gives a better description of the structure of borate glasses. According to Krogh-Moe, in the region below 20 mol % sodium oxide the boroxol group and the tetraborate groups are predominant. Between 20 and 30 mol% the tetraborate and diborate groups predominate. Krogh-Moe suggested that this structural model, in which the sodium-borate glasses are described as a random network of large borate groups similar to those present in crystalline sodium borates, may also apply to other alkali-borate systems. In this thesis the evidence is given that Krogh-Moe's suggestion applies to borosilicate glasses as well.

1.5. Review of experimental studies of borosilicate glasses

Experimental studies on the glass formation and subliquidus phase separation were discussed in secs 1.2 and 1.3. In this section a review will be given of experimental studies such as nuclear magnetic resonance, viscosity, electrical conduction, thermal expansion, density and electron spin resonance of these glasses.

The relative proportions of three- and four-coordinated boron ions in Na_2O–B_2O_3–SiO_2 glasses were determined by Milberg, O'Keefe, Verhelst and Hooper [1-62]) and Scheerer, Müller-Warmuth and Dutz [1-63]) using ^{11}B nuclear magnetic resonance. Scheerer et al.[1-63]) concluded that there was a preferred association of the alkali oxide with the boron units up to a certain saturation concentration by the formation of BO_4 tetrahedra. The maximum fraction of four-coordinated borons is greater than in alkali-borate glasses and increases with increasing silica content. According to Scheerer et al.[1-63]), the decrease in the line width of the BO_4 resonance with increasing silica content is due to a statistical distribution of the boron and silicon polyhedra. Milberg et al.[1-62]) concluded from their study that in sodium-borosilicate glasses with sodium-to-boron ratios of 0·5 or less behave with regard to boron coordination as if they were sodium-borate glasses diluted by silica. In glasses with sodium-to-boron ratios greater than 0·5, the fraction of boron atoms in fourfold coordination lies between this ratio and the values reported for lithium-borate glasses [1-30]) and tends to increase with increasing silica content. Furthermore, Milberg et al.[1-62]) concluded that glasses with sodium-to-boron ratios of less than 0·5 contain essentially no non-bridging oxygen ions, while in those glasses with greater sodium-oxide content, the fraction of non-bridging oxygen ions increases with increasing sodium-oxide content at fixed silica content and with increasing silica content at fixed sodium-oxide content.

A study of the coordination of boron in potassium-borosilicate glasses by the ^{11}B n.m.r. method was made by Zvyagin, Kalinin, Kaplun and Shevelevich [1-64]). The conclusions reached by these authors are similar to those on the sodium-borosilicate glasses mentioned above.

Viscosity measurements of borosilicate glasses were made by Abe [1-65]). He

found that at various compositions of the system Na_2O–B_2O_3–SiO_2 the viscosity measured by the fibre-elongation method was time-dependent. It was shown that certain glasses show a characteristic decrease in the elongation rate with time, at constant temperature and weight in a certain temperature range between the softening and the transition temperatures. Later it became clear that the above-mentioned effect takes place in the composition area where subliquidus phase separation is observed. Abe [1–65]) further explained various anomalous properties of borosilicate glasses by the assumption that atomic groups are formed in these glasses consisting of one BO_4 tetrahedron and four BO_3 triangles bonded to this tetrahedron.

Linear-expansion measurements in the system Na_2O–B_2O_3–SiO_2 were carried out by Gooding and Turner [1–66]). These measurements showed a behaviour of the linear thermal-expansion coefficient with sodium-oxide content (at constant SiO_2 content) similar to that of the sodium-borate glasses, so a continuation of the "boron-oxide anomaly" can be observed for the ternary system.

From his study on volume relations Riebling [1–61]) concluded that BO_4 tetrahedra were present in sodium-borosilicate melts at 1300 °C. Hence by analogy with the sodium-borate glasses, the BO_4 tetrahedra seem to be quite stable at high temperatures.

Karapetyan and Yudin [1–67]), from their electron-spin-resonance study of the effect of ionizing radiation on sodium-borosilicate glasses concluded that at least four structural units were present. They are SiO_4 tetrahedra without and with one non-bridging oxygen ion and BO_3 and BO_4 units.

Otto [1–68]) investigated the electrical conductivity of glasses in the system Li_2O–B_2O_3–SiO_2 and Na_2O–B_2O_3–SiO_2. In these systems three concentration ranges can be distinguished for the description of the activation energies. A rather steep but linear decrease is found from 0 to 25 mol % alkali oxide if the mole fraction of SiO_2 is kept constant. An abrupt change is observed at 25 mol % Li_2O or Na_2O. The activation energy still decreases linearly but the proportionality constant is only about one fourth of the value at lower concentrations. Raising the alkali-oxide concentration above 50 mol % does not lower the activation energy further.

Densities, refractive indices, liquidus temperatures and primary phases of glass compositions in the glass-forming region of the system BaO–B_2O_3–SiO_2 were determined by Hamilton, Cleek and Grauer [1–69]). Anomalous changes in properties were observed for a continuous change in composition. It is suggested that there are relations between the actual units in the glass and the compounds indicated by the phase diagram.

1.6. Nomenclature

A possibility for naming the borate groups makes use of the nomenclature recommended by IUPAC (1957) for complexes. However, this nomenclature

is never used in inorganic borate chemistry. Therefore the names of the different borate groups described in this thesis are those used by Krogh-Moe. However, the reader unfamiliar with inorganic borate chemistry may easily confuse these names. In order to facilitate reading this thesis, symbols will be labelled to each borate group, as explained below.

Firstly, the term "*unit*" will be used for structural elements having only one boron atom, for example the BO_4 tetrahedron. Secondly, the term "*group*" will only be used for structural elements containing more than one boron atom, for example the triborate group.

Up to now, five structural units are known in crystalline anhydrous borates. These are the BO_3 triangle and the BO_4 tetrahedron having only bridging oxygen ions, and BO_3 triangles having one, two or three non-bridging oxygen ions.

Throughout this thesis the BO_3 unit with three bridging oxygen ions will be called *a*, the BO_4 unit *c* and the BO_3 units with one, two or three non-bridging oxygen ions *b*, *b''* and *b'''* respectively *). Now it is possible to ascribe a combined symbol to every borate group. Thus the triborate group (cf. fig. 1.15) has the symbol a_2c because it contains two *a*-units (BO_3) and one *c*-unit (BO_4). The symbol for every known borate group is given in the legends to figs 1.12 to 1.23.

1.7. Hypothesis for the structure of borosilicate glasses

The experimental results of measurements of some properties of borosilicate glasses, discussed in sec. 1.5, suggest a continuation of the boron-oxide anomaly into the ternary alkali-borosilicate glasses. This means that there is a tendency of the alkali ions to bonding to borate groups and the formation of BO_4 tetrahedra in the borosilicate glasses is also indicated. At low SiO_2 concentration this SiO_2 seems only to dilute the borate network. With increasing SiO_2 content and increasing alkali-oxide content an increasing amount of non-bridging ions will be formed. Due to this the boron-oxide anomaly becomes less well pronounced when the amount of SiO_2 in borosilicate glasses is increased.

Most probably the structural groups present in binary alkali-silicate and -borate glasses are retained to some extent in the borosilicate glasses, there is no statistical distribution of B and Si in the network, but there is to some extent a tendency to a phase separation on a very small scale. It is thus suggested that in borosilicate glasses the same different types of borate and silicate groups can be found as in the binary alkali-silicate and alkali-borate compounds.

The purpose of this work is to investigate how far this hypothesis is supported by experimental evidence given in the following chapters.

*) *b* is used instead of *b'*; *a*, *b* and *c* are retained because they are used already by Beekenkamp.

REFERENCES

1–1) R. L. Mozzi and B. E. Warren, J. appl. Cryst. **2**, 164, 1969.
1–2) B. S. R. Sastry and F. A. Hummel, J. Am. ceram. Soc. **42**, 81, 1959.
1–3) B. S. R. Sastry and F. A. Hummel, J. Am. ceram. Soc. **43**, 23, 1960.
1–4) F. Ya. Galakhov and O. S. Alekseeva, Izvestiya Akademi Nauk SSSR neorganicheskie Materialy **4**, 2161, 1968.
1–5) G. W. Morey, J. Soc. Glass Technol. **35**, 270, 1951.
1–6) W. Skatulla, W. Vogel and H. Wessel, Silikattechn. **9**, 51, 1958.
1–7) W. Vogel, Silikattechn. **9**, 323, 1958.
1–8) K. Kühne and W. Skatulla, Silikattechn. **10**, 105, 1959.
1–9) W. Haller, D. H. Blackburn, F. E. Wagstaff and R. J. Charles, J. Am. ceram. Soc. **53**, 34, 1970.
1–10) S. Scholes and F. C. F. Wilkinson, Disc. Far. Soc. **50**, 175, 1970.
1–11) E. M. Levin, H. F. McMurdie and F. P. Hall, Phase diagrams for ceramists, The American ceramic Society, 1956.
1–12) E. M. Levin and G. M. Ugrinic, J. Res. natl Bur. Standards **51**, 37, 1953.
1–13) E. H. Hamilton, G. W. Cleek and O. H. Graner, J. Am. ceram. Soc. **41**, 209, 1958.
1–14) M. Tomozawa, Phys. Chem. Glasses **13**, 161, 1972.
1–15) M. Tomozawa, R. K. MacCrone and H. Herman, Phys. Chem. Glasses **11**, 136, 1970.
1–16) G. F. Neilson, Phys. Chem. Glasses **10**, 54, 1969.
1–17) W. Haller, D. H. Blackburn and J. H. Simmons, J. Am. ceram. Soc. **57**, 120, 1974.
1–18) R. R. Shaw and D. R. Uhlmann, J. Am. ceram. Soc. **51**, 377, 1968.
1–19) P. B. Macedo and J. H. Simmons, J. Res. natl Bur. Standards **78A**, 53, 1974.
1–20) R. J. Charles and F. E. Wagstaff, J. Am. ceram. Soc. **51**, 16, 1968.
1–21) W. Vogel, W. Schmidt and L. Horn, Z. Chem. **9**, 401, 1969.
1–22) M. E. Milburg and C. R. Peters, Phys. Chem. Glasses **4**, 99, 1969.
1–23) F. Liebau, Acta cryst. **14**, 389, 1961.
1–24) A. K. Pant and D. W. J. Cruickshank, Acta cryst. **B24**, 13, 1968.
1–25) W. S. McDonald and D. W. J. Cruickshank, Acta cryst. **22**, 37, 1967.
1–26) F. Liebau, Acta cryst. **14**, 395, 1961.
1–27) A. K. Pant, Acta cryst. **B24**, 1077, 1968.
1–28) R. L. Mozzi and B. E. Warren, J. appl. Cryst. **3**, 251, 1970.
1–29) J. Krogh-Moe, J. non-cryst. Solids **1**, 269, 1969.
1–30) P. J. Bray and J. G. O'Keefe, Phys. Chem. Glasses **4**, 37, 1963.
1–31) P. Beekenkamp, Philips Res. Repts Suppl. 1966, No. 4.
1–32) B. D. McSwain, N. F. Borelli and Gouq-Jen Su, Phys. Chem. Glasses **4**, 1, 1963.
1–33) G. M. Willis and F. L. Hennessy, J. Metals **5**, 1367, 1953.
1–34) J. Krogh-Moe, Ark. Kemi **14**, 451, 1959.
1–35) J. Krogh-Moe, Phys. Chem. Glasses **3**, 208, 1962.
1–36) S. Block and G. J. Piermarini, Phys. Chem. Glasses **5**, 138, 1964.
1–37) T. Milman and R. Bouaziz, Ann. Chim. **3**, 311, 1968.
1–38) S. V. Berger, Acta chem. Scand. **3**, 660, 1949.
1–39) C. E. Weir and R. A. Schroeder, J. Res. natl Bur. Standards **68A**, 465, 1964.
1–40) Y. Takeuchi, Acta cryst. **5**, 574, 1952.
1–41) W. H. Zachariasen, Acta cryst. **17**, 749, 1964.
1–42) M. Marezio, H. A. Plettinger and W. H. Zachariasen, Acta cryst. **16**, 594, 1963.
1–43) W. Schneider and G. B. Carpenter, Acta cryst. **B26**, 1189, 1970.
1–44) M. Marezio, H. A. Plettinger and W. H. Zachariasen, Acta cryst. **16**, 390, 1963.
1–45) J. Krogh-Moe, Acta cryst. **15**, 190, 1962; **B24**, 179, 1968.
1–46) J. Krogh-Moe, Acta cryst. **B30**, 578, 1974.
1–47) J. Krogh-Moe, Acta cryst. **B28**, 3089, 1972.
1–48) J. Krogh-Moe, Acta chem. Scand. **18**, 2055, 1964.
1–49) M. Martinez-Ripoll, S. Martinez-Carrera and S. Garcia-Blanco, Acta cryst. **B27**, 672, 1970.
1–50) S. Block and A. Perloff, Acta cryst. **19**, 297, 1965.
1–51) J. Krogh-Moe, Acta cryst. **B30**, 747, 1974.
1–52) J. Krogh-Moe, Acta cryst. **B28**, 1571, 1972.
1–53) J. Krogh-Moe, Acta cryst. **14**, 68, 1961.
1–54) J. Krogh-Moe, Acta cryst. **13**, 889, 1960.
1–55) A. Hyman, A. Perloff, F. Mauer and S. Block, Acta cryst. **22**, 815, 1967.
1–56) J. Krogh-Moe, Acta cryst. **B28**, 168, 1972.

[1-57]) J. Krogh-Moe, Acta cryst. **18**, 1088, 1965.
[1-58]) J. Krogh-Moe, Phys. Chem. Glasses **3**, 101, 1962.
[1-59]) C. Rhee and P. J. Bray, Phys. Chem. Glasses **12**, 165, 1971.
[1-60]) C. Rhee, J. Korean phys. Soc. **4**, 51, 1971.
[1-61]) E. F. Riebling, J. Am. ceram. Soc. **50**, 46, 1967.
[1-62]) M. E. Milberg, J. G. O'Keefe, R. A. Verhelst and H. O. Hopper, Phys. Chem. Glasses **13**, 79, 1972.
[1-63]) J. Scheerer, W. Müller-Warmuth and H. Dutz, Glastechn. Ber. **46**, 109, 1973
[1-64]) A. I. Zvyagin, P. S. Kalinin, V. A. Kaplun and R. S. Shevelevich, Izvestiya Akademi Nauk SSSR **7**, 350, 1971.
[1-65]) T. Abe, J. Am. ceram. Soc. **35**, 284, 1952.
[1-66]) E. J. Gooding and W. E. S. Turner, J. Soc. Glass Techn. **18**, 32, 1934.
[1-67]) G. O. Karapetyan and D. M. Yudin, Sov. Phys. solid State **4**, 1943, 1963.
[1-68]) K. Otto, Phys. Chem. Glasses **7**, 29, 1966.
[1-69]) E. H. Hamilton, G. W. Cleek and O. H. Grauer, J. Am. ceram. Soc. **41**, 209, 1958.
[1-70]) J. Krogh-Moe, Acta cryst. **B30**, 1827, 1974.
[1-71]) J. Krogh-Moe, Acta cryst. **B30**, 1178, 1974.

2. EXPERIMENTAL METHODS

2.1. Preparation of the samples

Two factors, related to the preparation of the samples, may interfere with the interpretation of the results of several measurements in terms of structural units. These factors are the homogeneity and the hydroxyl-ion concentration of the glasses.

Preparation of borosilicate glasses without visible sandstones and striae by the usual laboratory methods poses no problems. But as was shown earlier by Konijnendijk, Van Duuren and Groenendijk [2-1]) borosilicate glasses prepared by the classical method of mixing dry powders and melting gives rise to a considerable submicroscopic inhomogeneity of the glasses as revealed by electron microscopy. It was shown, too, that by using wet-chemical preparation methods the submicroscopic homogeneity is improved considerably. In spite of the use of wet-chemical preparation techniques small submicroscopic inhomogeneities in the final unannealed glasses can still be observed by electron microscopy. The inhomogeneities seemed to be of the order of 20–30 nm, this value being somewhat higher in the composition areas inclined to phase separation. These values were obtained by electron microscopy of shadowed carbon replicas of freshly broken and etched glass surfaces, and thus are only slightly above the resolution of about 20 nm of this technique and therefore give only qualitative information. Of course no indication can be obtained on this scale of the intensity of the observed concentration fluctuations.

It became evident during this investigation that no reproducible and useful results could be obtained from viscosity and electrical-conduction measurements of borosilicate glasses prepared by the classical method. However, the results could be considerably improved by using wet-chemical preparation methods. Therefore, all glasses used for viscosity, electrical-conduction and thermal-expansion measurements were prepared by these methods. Nearly all glasses used for infrared-absorption and Raman-scattering measurements were also prepared in this way, although no difference was observed in the spectra of glasses of equal composition prepared either by the classical or the wet-chemical method.

The advantages of the wet-chemical preparation methods were extensively described earlier (Konijnendijk, Van Duuren and Groenendijk [2-1]) and Konijnendijk and Groenendijk [2-2])). In all these methods the compounds constituting the final glass composition are brought into a regular or colloidal solution. The solvent is evaporated at a low temperature in such a way that a fine, homogeneous powder results. This powder can be melted easily to yield homogeneous glass. For the glasses prepared by the wet-chemical method reagent-grade chemicals were used except for SiO_2. Lithium, sodium, potassium, calcium, barium ions were introduced as nitrates, boron as boric acid and

silicon as a colloidal solution of SiO_2. This colloidal silica solution was usually Ludox AS, a commercially available product from Dupont, or in some cases Ludox LS. The chemical composition and physical properties of Ludox AS and LS are summarized in table 2-I.

For the preparation of the borosilicate glasses the sol–gel method was chosen as the first stage. In this method H_3BO_3 is dissolved in the colloidal SiO_2 sol, if necessary the sol was heated or diluted. To this solution a second solution of all the other glass constituents, as nitrates, was added. After evaporation of a part of the water or adding ammonia the sol sets to a gel. This gel is dried at 200 °C for 16 hours, which usually results in a friable product that was ball-milled for about 1 hour. In this way one obtains a fine powder in which all elements are intimately mixed.

TABLE 2-I

The chemical composition and physical properties of colloidal silica solutions Ludox AS and Ludox LS

	Ludox AS	Ludox LS
silica as SiO_2 (%)	30·5	30·3
Na_2O (titrable alkali) (%)		0·10
ammonia (%)	0·25	
chloride as NaCl (%)	0·001	0·002
sulphate as Na_2SO_4 (%)	0·005	0·010
viscosity at 25 °C, cps	12	9
pH at 25 °C	9·6	8·3
appr. particle diam. (nm)	13–14	15–16
surface area (m^2/g) (B.E.T.)	220–235	195–215
specific gravity	1·206	1·209

This powder is melted in a Pt–Rh crucible in an electric furnace to a bubble-free glass in two hours at temperatures varying from 800 to 1400 °C depending on the composition of the glasses. In this way glasses were obtained that showed a reasonable reproducibility in properties such as viscosity and electrical conduction. However, the glasses produced in this way contain an amount of hydroxyl ions that influenced the properties such as the viscosity and electrical conduction considerably. Therefore, interpretation of these measurements in terms of structural units for these glasses is impossible. For this reason all glasses were remelted in a vacuum furnace for approximately 2 hours at about the same melting temperature as used earlier, at pressures between 10^{-5} to 10^{-4} mm Hg and again in a Pt–Rh crucible.

After this vacuum melting the hydroxyl-ion content had diminished by a factor of 10 to 100 resulting in a maximum hydroxyl-ion content of about 300 ppm. This hydroxyl-ion concentration was measured by infrared spectroscopy using the OH absorption band at 2·8 μm. The extinction coefficient of this band was taken between 140 and 60 l mol^{-1} H_2O cm^{-1}, depending upon the alkali-oxide content and type of glass. These latter extinction coefficients were taken from the work of Franz [2–3]).

The preparation of the glasses starting by wet-chemical methods and combined with vacuum melting resulted in reproducible values for the viscosity and the electrical conduction. For this reason nearly all samples were prepared in this way. All measurements were made on the same samples. Vacuum melting has in some cases influence on the infrared spectra in the spectral area 400–1600 cm^{-1}. The Raman spectra, however, remain completely unaltered in the spectral region 200–1600 cm^{-1} after vacuum melting.

Chemical analyses of samples of twelve different compositions after the vacuum-melting operation showed that B_2O_3 evaporation was practically negligible. The difference between analysed and intended compositions was less than 3% B_2O_3. This difference was 1% for the other oxides. For this reason the batch composition of the samples described in this thesis is taken as representative for the composition.

2.2. Raman and infrared measurements

The Raman-scattering experiments were made with two types of apparatus. The spectra produced with these apparatus are shown in chapter 3 of this thesis. In the one apparatus the scattered radiation is measured as a linear function of the wavenumber, in the other the scattered radiation is measured as a linear function of the wavelength.

The apparatus that records the Raman spectra as a linear function of the wavenumber is a relatively simple instrument *). In this equipment the 632·8-nm line of a 6-mW He–Ne laser is used for excitation. The monochromator is of the double Ebert type with additive dispersion. The detector consists of an EMI 9659 B photomultiplier, thermoelectrically cooled to —20 °C. The scattered radiation is measured at a 90° angle from the incident laser beam. The equipment gives the possibility to measure the direction of incident and scattered polarized light for the following combinations $x(zz + zx)y$, $x(zz)y$ and $x(zx)y$. The symbol $x(zz + zx)y$ means that the direction of the incident radiation was along the x-axis and was polarized in the z-direction, the scattered radiation was collected along the y-axis, and was the sum of the light polarized in the z- and x-directions. The differences in the spectra recorded for the combinations $x(zz + zx)y$ and $x(zz)y$ were negligible. The glass-sample

*) This instrument was developed by the Philips Industrial Products Division.

dimensions are about $15 \times 10 \times 3$ mm^3, with the appropriate surfaces polished. The scattered radiation is collected from up to 5 to 10 mm of the path of the primary laser beam through the glass.

All spectra were recorded at room temperature. The band width was usually 10 cm^{-1} for the glasses, for the crystalline samples the band width was lowered to 8 cm^{-1}.

The second Raman apparatus *) has more facilities than the one described above, but a number of the special features are of little value for measuring Raman scattering from glass samples. Spectra of this instrument can be recognized by the linear wavelength scale on the horizontal abscissa. The 514·5-nm line of an Ar laser (Coherent Radiation model 52) is used for excitation in the experiments described in chapter 3 of this thesis. The monochromator in this equipment was of the Jarrell-Ash 25-100 series dual monochromator type. The detector consists of an I.T.T. type FW 130S photomultiplier, thermoelectrically cooled to —15 °C. The cathode dark current then amounts to about 2 electrons/s. The sample dimensions are $15 \times 10 \times 1$ mm^3, the appropriate surfaces are polished. The scattered radiation is collected from at most 10 mm of the path of the primary laser beam through the sample. All spectra were recorded at room temperature of the samples, the band width usually being 10 cm^{-1}.

The Raman spectra obtained for one sample with either of the two instruments do not show significant differences. In a few cases it was advantageous to use one of the spectrometers above the other because of luminescence of the samples (different excitation lines).

The infrared-absorption measurements were made with a model EPI-G2 Hitachi double-beam grating infrared spectrometer. All spectra were recorded with a band width of approximately 1 cm^{-1}. The recording speed in the range 400–1600 cm^{-1} was 40 cm^{-1}/min, from 1600 to 4000 cm^{-1} it was 400 cm^{-1}/min. Of every borosilicate-glass sample the infrared absorption of a thin film (of a few microns thickness) was measured in the 400–4000 cm^{-1} range. The films were mounted in an evacuated Dewar vessel suitable for infrared-absorption measurements at about liquid-N_2 temperatures. This vessel is analogous to the one described by Beekenkamp [2–4]) for his optical-absorption measurements, except that windows made of KBr now are mounted instead of vitreous silica. The infrared spectra of silicate and aluminosilicate glasses were measured at room temperature. The infrared absorption of all polycrystalline borates and silicates was measured by the usual KBr technique at room temperature. The ordinate of all figures represents the transmission which increases in the upward direction. The spectra are vertically displaced for display purposes.

*) This apparatus was built by J. H. Haanstra and A. W. de Jager.

2.3. Viscosity measurements

The viscosity versus composition was measured for selected composition series by the fibre-elongation method. By this method the viscosity η (poises) can be determined as a function of the temperature in the range $\log_{10} \eta = 7$ to $\log_{10} \eta = 12$. Uniform fibres 1 mm thick and 15 mm in length are drawn in a flame. The fibres are vertically suspended in a furnace and a certain load is attached to the lower end of the fibre. After attachment of the load the elongation rate of the fibre is measured with a suitable simple optical system. In this way several elongation rates at different temperatures can be obtained. The following equation gives the relation with the viscosity:

$$\eta = \frac{g\,l\,F}{3\pi\,r^2\,v}$$

in which g is the gravity constant, l the length of the fibre, F the load on one end of the fibre, r the radius of the fibre and v the elongation rate.

The values of η obtained at different temperatures can be plotted on a semi-log scale versus the reciprocal of the absolute temperature. Usually a linear relationship is observed between $\log \eta$ and $1/T$.

2.4. Thermal-expansion measurements

The linear thermal-expansion coefficient of the samples was measured with an instrument developed by the Central Laboratory of the Elcoma division and adapted at the Philips Research Laboratories. The expansion of the samples was measured continuously up to a temperature just below the transformation temperature T_g or at maximum just above 300 °C. From the expansion curve the expansion coefficient was calculated at 200, 250 and 300 °C.

This instrument is a displacement-measuring dilatometer: the thermal displacement of the sample, with an initial length of 10 mm, is transmitted by a fused-silica assembly to a linearly variable differential transformer, having a sensitivity of about 4 mV/μm at an excitation voltage of 24 V dc and the output characteristic linear for displacements varying from −1·5 up to +1·5 mm. A fused-silica bar is pressed against the sample at a constant load of 15 mg. The core of the transducer is mounted at the other end of the bar, suspended so as to be nearly frictionless. The transducer is placed in a thermostatic bath, held at a constant temperature a little above room temperature to eliminate the influence of fluctuations of the room temperature.

The samples in their holder are placed in an electric furnace with a temperature-control unit consisting of a millivolt current converter, a PID controller, a program control for the heating rate and a thyristor unit. The supply voltage of the furnace is raised quadratically to shorten the time necessary for one measurement. The normal heating rate is 2 °C/min. A coaxial Chromel–Alumel thermocouple is placed just underneath the sample. The furnace consists of a

fused-silica tube, approximately 27 cm long with 18 mm inner diameter. The tube is provided with an external heating coil, approximately 15 cm long.

Pure Pt and Al_2O_3 are used as standards together with two standard glasses. The expansion coefficient was measured of two samples of each composition. In each case the thermal-expansion coefficient was determined during a heating and a cooling period.

2.5. Electrical-conduction measurements

The direct-current conductivity of the samples was measured as a function of temperature in the range $\varrho = 10^5$ to 10^8 ohm cm, where ϱ is the specific resistance. The samples of glass obtained in the way described earlier were sawn into rods $25 \times 5 \times 5$ mm^3 in dimension. The plane-parallel faces were ground perpendicularly to the longest axis and coated with a layer of silver paste which was allowed to dry at room temperature.

The sample was inserted into an electrode assembly consisting of two flat circular silver discs mounted on fused-silica supports and connected by metal springs to ensure a good contact between the electrodes and the silver-coated faces of the sample.

Several electrode assemblies are attached to a circular cover which fits exactly into a horizontal cylindrical electric furnace. During the measurement the furnace was heated at an average rate of about 2 °C/minute and measurements were carried out over a temperature range of about 100 °C.

The principle underlying the determination of the resistivity consists simply in the application of Ohm's law. The method used involved the measurement of the direct current flowing through the sample when a stabilised voltage of 100 V was applied.

At a given temperature two readings were taken. This could be carried out rapidly enough, and to eliminate electrode polarization the direction of the current was reversed after each reading. The average conduction was calculated for each temperature. Values of $\log \varrho$ based on these averages were plotted against the reciprocal of the absolute temperature, usually giving straight lines and in some cases straight lines with a knick. This means that the conduction behaviour can be described by the Rasch-and-Hinrichsen law

$$\log \varrho = A + \frac{B}{T}.$$

As a rule two samples were taken from each glass composition and the values in the tables are average values for these two samples.

REFERENCES

2–1) W. L. Konijnendijk, M. van Duuren and H. Groenendijk, Verres Réfract. **27**, 11, 1973.
2–2) W. L. Konijnendijk and H. Groenendijk, Klei en Keramiek **22**, 7, 1972.
2–3) H. Franz, J. Am. ceram. Soc. **49**, 473, 1966.
2–4) P. Beekenkamp, Philips Res. Repts Suppl. 1966, No. 4.

3. RAMAN SPECTRA OF BORATE, SILICATE AND BOROSILICATE GLASSES

3.1. Introduction

The development of laser Raman spectrometers during the last five years has made Raman spectroscopy of glasses a very interesting technique. The use of lasers in the equipment has been of vital importance because the Raman effect is generally very weak.

Raman and infrared spectroscopy may be considered as supplementary methods, both supplying information on the vibrational behaviour of the atoms. It was shown by Schuker and Gamon [3–1]) that Raman scattering in amorphous materials is due to first-order Raman processes, and that the spectra are related to the vibrational density of states. Raman scattering in disordered systems differs from the scattering in crystals in that it is related to a spectrum of the vibrations in the material rather than to specific modes of vibration. Raman lines arise from the induced polarization of the vibrating molecular groups.

The interpretation of vibrational spectra of crystals has improved considerably in the last decade. However, for the vibrational spectroscopy of glasses, in which no long-range order exists, there is no generally agreed theory of vibrations available. For the interpretation of the vibrational spectra of glasses one generally starts with the free molecule. The absorption bands in the infrared spectra and the bands in the Raman spectra are assigned to vibrations in the free molecule influenced by its surroundings. In this way it has been possible to obtain a rough but consistent picture of the vibrations in different types of glasses, mainly based on the infrared spectra *).

The Raman bands in the spectra of glasses are generally broader than in comparable crystals. This is caused by the deformation of the vibrating groups in the vitreous state, consequently leading to a broader density of states. This does not facilitate the interpretation of the vibrational spectra of glasses.

For the above-mentioned reasons it is difficult to give a sound theoretical interpretation of the Raman spectra of the borate, silicate and borosilicate glasses. However, by comparison of the Raman spectra of glasses with those of appropriate compounds whose crystal structure is known it is possible to obtain qualitative and sometimes semiquantitative information on the presence of certain structural units in the glasses. This is based on the assumption that structural units or groups are present in oxide melts and oxide glasses that resemble the units or groups in comparable compounds. For instance, the Raman spectra of molten and crystalline carbonates show a high degree of similarity, thus suggesting that the same types of units are present in the melt

*) For a general background on vibrational spectroscopy of glasses the reader is referred to the review articles by Neuroth [3–2]), Wong and Angell [3–3]) and Simon [3–4]) and the references given in these articles.

and in the crystal (Maroni and Cairns [3–5]).

From the comparison of spectra of glasses in which the composition is varied systematically one obtains information on the change of structure with the composition. This change of structure is also reflected in some physical properties such as viscosity behaviour, thermal expansion, electrical conductivity and in the infrared spectra. By comparison of the Raman data with the other experimental results it will be possible to obtain a consistent picture of the structure of borosilicate glasses.

For reasons mentioned above, the Raman spectra of polycrystalline borates and silicates will be presented and discussed first. The discussion of these spectra must be rather superficial and restricted to those items of interest for the spectra of the glasses. In this thesis the spectra of the crystalline compounds are only used as a fingerprint to demonstrate the presence of certain structural units in the glass. Comparison of the Raman spectra of crystalline compounds with those of glasses suggests that the same type of units are present in the glasses as in the comparable crystalline compounds. This similarity in structural units or groups is of course no necessity but in a number of cases X-ray work on glasses strongly suggests this similarity. A difference in the type of structural units or groups in glass and a crystal of the same composition may possibly be due to the lower density of the glass.

The comparison of the spectra of crystalline compounds and glasses may further be hampered by intensity differences and shift of Raman lines due to bond-strength differences and differences in symmetry between the structural units in glass and the crystal. It is most likely that the borate units in glasses will be distorted somewhat compared to the units in the corresponding crystals. This distortion will not be the same for every unit. This deviation from the ideal will lead to line-width increases in the vibrational spectra which will make the comparison of the spectra of the glasses and the compounds more difficult and interpretation of the spectra of the glasses less certain.

It must be noted, too, that numerous borate compounds with different crystal structures and different types of molecular groups are known. The generally low crystallization tendency of borate glasses suggests no high similarity between the glass and the corresponding crystal. It also suggests that a mixture of many types of borate groups is present in the glass and that these groups are irregularly bonded to each other.

3.2. Raman spectra of polycrystalline borates and silicates

3.2.1. *Experimental results*

The Raman spectra of a number of polycrystalline borates are shown in figs 3.1 to 3.9, and the spectra of some polycrystalline silicates are shown in fig. 3.10. Nearly all borate and silicate compounds indicated in tables 1-I and

1-II were prepared. These tables also indicate which structural units are present in the compounds, and references are given to the literature in which the crystal structure is described or in which the X-ray powder spectra can be found. By X-ray analysis of every sample a check was made to ensure that the correct compound had been prepared and, in the appropriate cases, that the sample had the same crystal structure as described in the literature.

The powdered sample was introduced into a glass capillary which was illuminated by the laser beam. All Raman spectra were recorded at room temperature, the excitation line had the wavelength 632·8 nm of the He–Ne laser and the band width was 8 cm^{-1} for every sample. Smaller band widths, down to 2 cm^{-1} generally did not give better-resolved spectra. The scattered light was collected at a 90° angle and the intensity was measured as a function of the wavenumber in cm^{-1}. For more details about the equipment used, see sec. 2.2.

Spectra of many crystalline borate compounds were also recorded by Bril [3–6]) at about the same time.

3.2.2. *Discussion of results*

As explained in sec. 3.1 only a superficial discussion of the Raman spectra of the crystalline compounds will be given in this thesis. The Raman spectra of the compounds are intended to be used only as a fingerprint to reveal the presence of certain structural units in the corresponding glasses.

Due to the complex structure of many borate compounds, the study of the vibrational spectra of borates has not attracted much interest in the past. Interpretation of these spectra is further complicated because the crystal structure of a number of borates is unknown. Together with the complex structure of many borate compounds it can also be observed from table 1-II that many types of borate groups exist. In a number of borate compounds more than one type of group is present and it may also be observed that different types of cations lead to different borate groups although the compositions may be comparable.

Vibrational spectra of simple boron-containing compounds were studied by Pinchas and Shamir [3–7]), Frey and Funck [3–8]) and Bates et al.[3–9]). They interpreted the spectra by assigning all peaks in the spectra to vibrations of simple borate units as for instance the BO_3 triangle.

From the work of Bril [3–6]) it is evident that some peaks in the Raman spectrum, for instance of crystalline $Na_2O \cdot B_2O_3$ have to be assigned to vibrations within the ring-type metaborate group (b_3), thus to a larger group than the basic BO_3 triangle. Bril also suggests that the strong Raman line observed at about 770 cm^{-1} in many crystalline borates is due to a vibration in which all oxygen ions of the six-membered ring take part (for instance of the triborate group (a_2c)). A six-membered ring is present in many alkali-borate compounds; it may contain one or two BO_4 tetrahedra and is coupled in many

different ways with its surroundings in the different compounds.

Parsons [3-10]) and Krogh-Moe [3-11]) suggested that the Raman peak at 806 cm^{-1} which they observed in vitreous B_2O_3 should be assigned to the ring-deformation motion of the boroxol ring (a_3), therefore to a group larger than a simple BO_3 triangle.

Thanks to the marked differences in the Raman spectra of the crystalline borates, they may indeed serve as a fingerprint for the presence of certain types of larger structural units, for instance the ring-type metaborate group, in the corresponding glasses.

Unfortunately the crystal structure of some crystalline borates has not been revealed up to now, so that the information as to which groups are present in these compounds is lacking. Furthermore, some compounds are composed of several groups, thus in some cases it is difficult to take certain Raman peaks as characteristic of a group. At the same time it can be observed that different types of alkali ions give rise to different types of borate groups although the composition of the borate compound is similar. This shows the influence of the cation on the borate network in the compounds. In glass this situation may be different because of the lower density, which leaves more space to accomodate the ions.

Thereabove Raman spectra of polycrystalline samples cannot be further refined by polarization measurements, so that symmetrical vibrations cannot be distinguished from antisymmetrical ones. This problem may be overcome by dispersing the sample in a liquid with a matched index of refraction. However, Bril [3-6]) found that, because of double refraction of the borate compounds, no additional interesting information could be obtained.

Orthoborate compounds

The simplest borate group known is the isolated orthoborate BO_3^{3-} unit (b''', cf. fig. 1.23) present in a number of borates shown in table 1-II. In isolation this anion has the planar symmetrical structure arising from the sp^2 hybridization of the boron orbitals. It thus has the symmetry D_{3h}, giving rise to four fundamental vibrations. When such an ion is placed in a crystal lattice the symmetry class may be lowered, degeneracies can be removed and more peaks in the Raman spectrum perhaps observed than in the case of the isolated ion.

The Raman spectra of three orthoborate compounds are shown in fig. 3.1. The strongest peak in the Raman spectra of the Mg- and Ca-orthoborate compounds is observed at 920 and 930 cm^{-1} respectively. Due to its absence in the infrared spectra of these compounds (cf. fig. 4.1) this peak can tentatively be assigned to the symmetric stretching vibration of the BO_3^{3-} unit. In this explanation only the molecular symmetry is taken into account.

For a sample described as $3\,Na_2O\,.\,B_2O_3$ a strong Raman peak at 905 cm^{-1} is also observed, but in the first place it could not be confirmed by

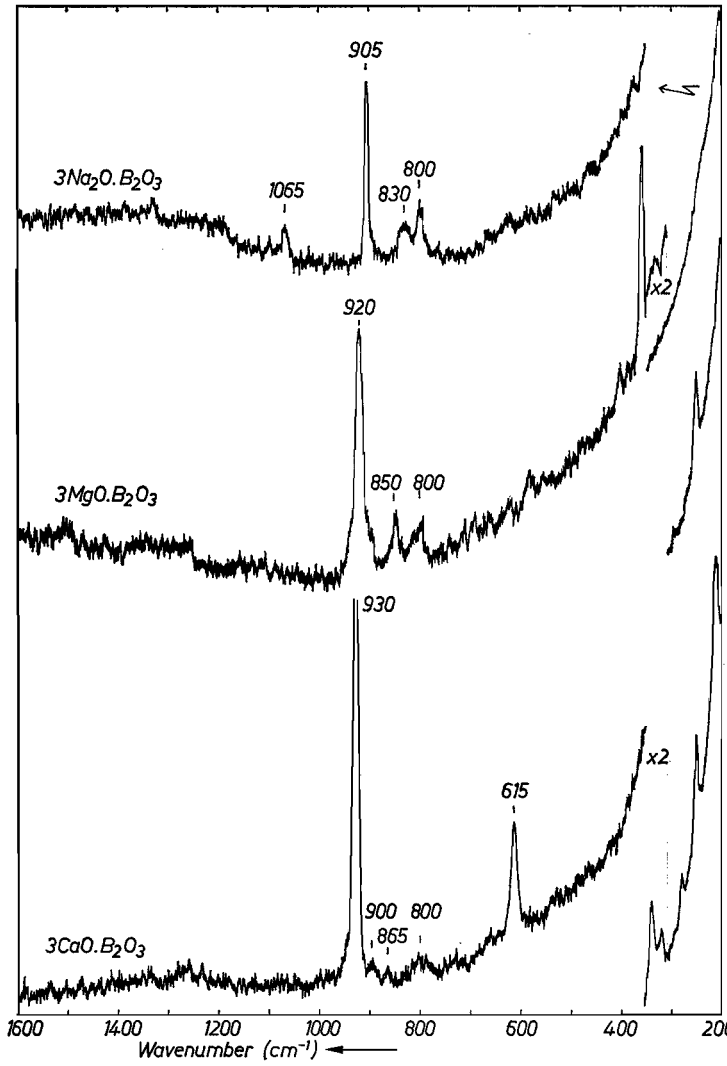

Fig. 3.1. Raman spectra of polycrystalline orthoborates (direction $x(zz + zx)y$).

X-ray analysis that this sample was indeed $3\,Na_2O\,.\,B_2O_3$, in the second place the sample contained a fair amount of water, as evidenced by its infrared spectrum. Possibly this peak is also due to the symmetric stretching vibration but this is less certain than in the case of the Mg and Ca compounds.

Pyroborate compounds

The Raman spectra of the pyroborate compounds $2\,Na_2O\,.\,B_2O_3$, $2\,MgO\,.\,B_2O_3$

and 2 $CaO \cdot B_2O_3$ are shown in fig. 3.2. The Raman spectra are not of a high quality but for the interpretation of the spectra of some glasses they are supposed to be sufficiently detailed.

Again as in the case of the orthoborate compounds, it could not be confirmed by X-ray analysis that the sample with the intended composition $2\,Na_2O \cdot B_2O_3$ is indeed this compound; moreover, from the infrared spectrum of the sample it becomes evident that it contains a fair amount of water.

The two mentioned alkaline-earth borates are built up of isolated $B_2O_5^{4-}$

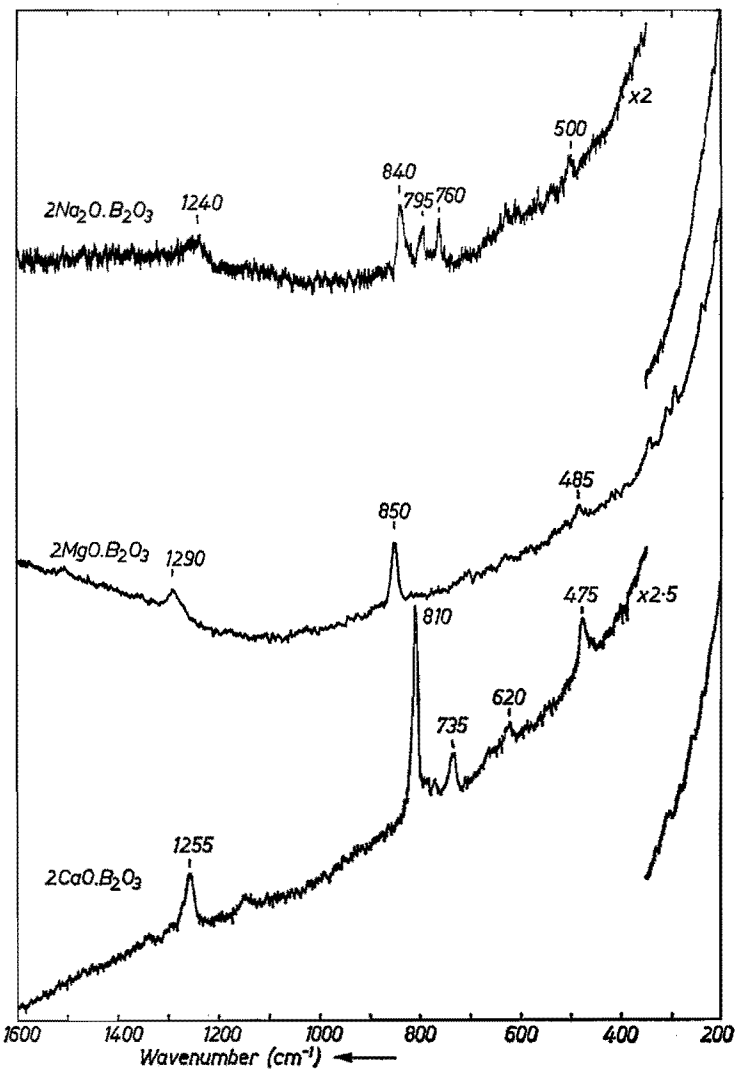

Fig. 3.2. Raman spectra of polycrystalline pyroborates (direction $x(zz + zx)y$).

groups (b_2'', cf. fig. 1.22). If the vibrational spectra of these pyroborates can be interpreted in terms of the corresponding vibrations of the parent BO_3^{3-} unit, then again the peak at 820 cm^{-1} for 2 CaO . B_2O_3 and 850 cm^{-1} for 2 MgO . B_2O_3 might be attributed to the symmetric stretching of the oxygen ions. Attention is drawn to the band at approximately 1250 cm^{-1}; at this position no Raman band with this intensity has been observed in any other crystalline borate, so that with some caution, it might be taken as characteristic of the pyroborate group.

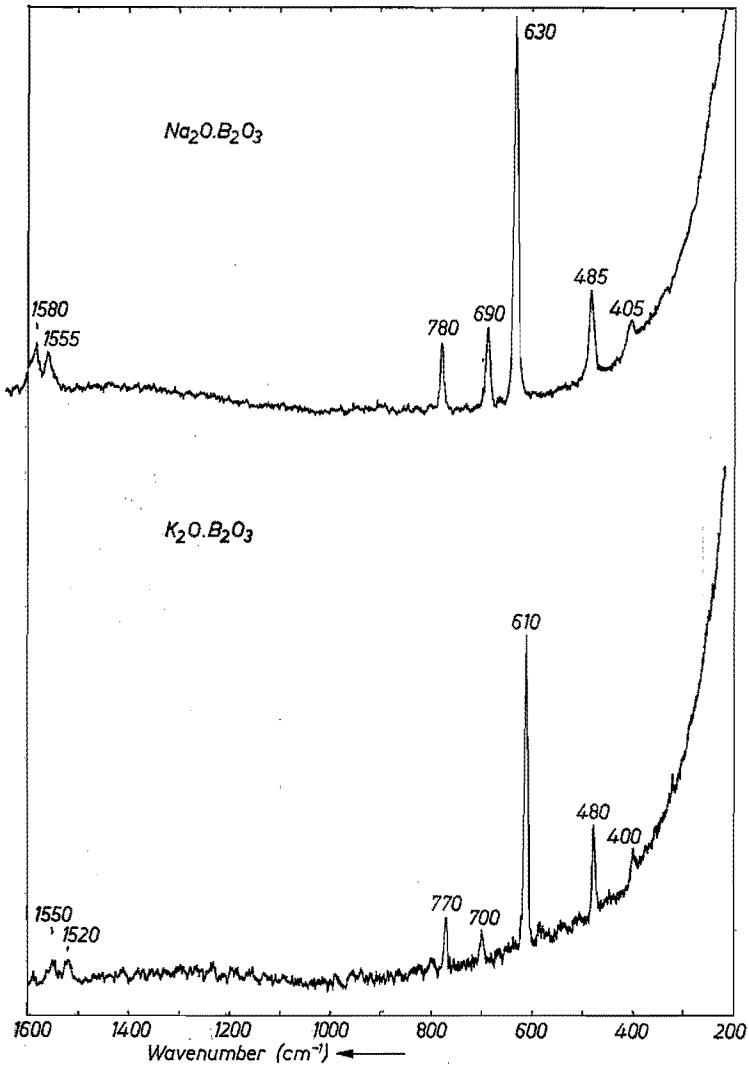

Fig. 3.3. Raman spectra of polycrystalline metaborates (direction $x(zz + zx)y$).

Metaborate compounds

The Raman spectra of four metaborate compounds, $Li_2O \cdot B_2O_3$, $Na_2O \cdot B_2O_3$, $K_2O \cdot B_2O_3$ and $CaO \cdot B_2O_3$ are shown in figs 3.3 and 3.4. From X-ray analysis $Li_2O \cdot B_2O_3$ (Zachariasen [3-12]) and $CaO \cdot B_2O_3$ (Marezio, Plettinger and Zachariasen [3-13]) are known to contain endless chains of BO_2^- ions (b_∞, cf. fig. 1.21). $Na_2O \cdot B_2O_3$ (Marezio, Plettinger and Zachariasen [3-14]) and $K_2O \cdot B_2O_3$ (Schneider and Carpenter [3-15]) contain the ring-type planar $B_3O_6^{3-}$ group (b_3, cf. fig. 1.20). The Raman spectra of those compounds clearly

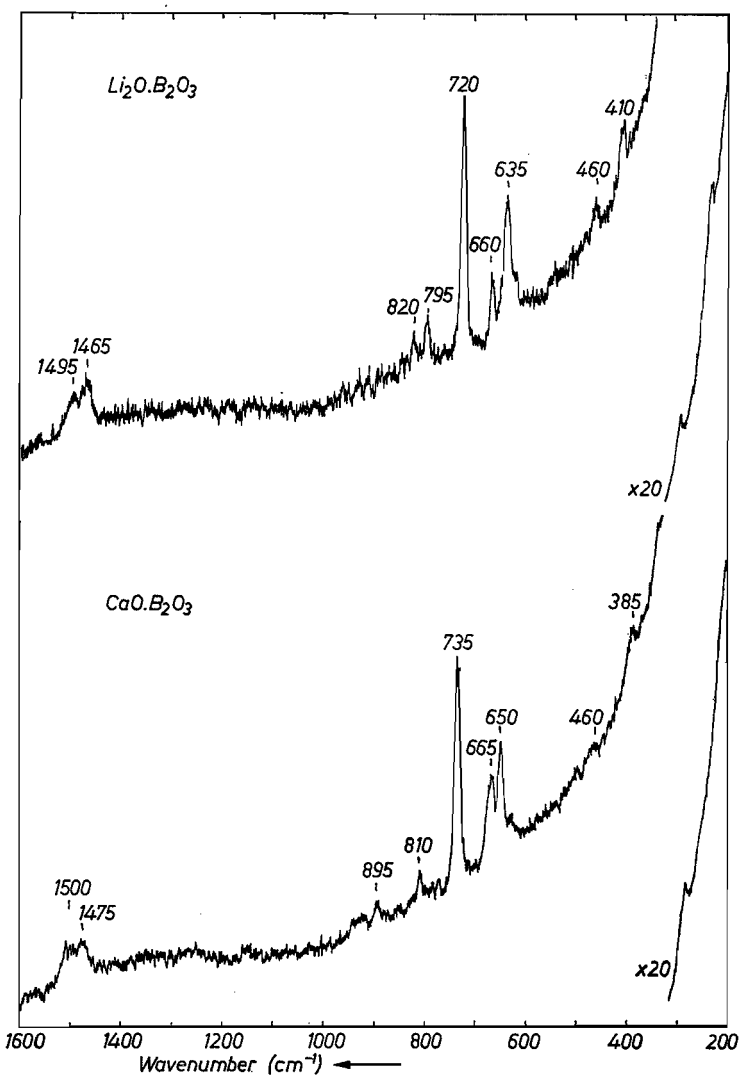

Fig. 3.4. Raman spectra of polycrystalline metaborates (direction $x(zz + zx)y$).

show the different types of groups in these borates, on the other hand the compounds with the same type of groups show highly similar Raman spectra.

For a complete interpretation of the spectra of the compounds $Na_2O \cdot B_2O_3$ and $K_2O \cdot B_2O_3$ the reader is referred to the work of Bril [3–6]). Bril assigns the peak observed at 610 cm^{-1} for the potassium compound and at 630 cm^{-1} for the sodium compound to a stretching-type vibration in which all six atoms of the metaborate ring take part. Thus this peak is characteristic of the ring-type metaborate group. The peaks in the range about 1500 cm^{-1} are assigned to a symmetric vibration of the three non-bridging oxygen ions. These peaks are thus characteristic of the presence of non-bridging oxygen ions in this particular group.

Diborate compounds

The Raman spectra of the crystalline diborates studied are shown in figs 3.5–3.9. From X-ray analysis it is known that all these diborate compounds have a different crystal structure. The compound $Li_2O \cdot 2\,B_2O_3$ is built up of diborate groups (a_2c_2) only (Krogh-Moe [3–16,17]), cf. fig. 1.16) in which all oxygen ions are bridging and two BO_4 tetrahedra are connected to each other. The crystal structure of $Na_2O \cdot 2\,B_2O_3$ was recently revealed by Krogh-Moe [3–18]), the borate network is built up of di-pentaborate (a_3c_2) groups and triborate groups with one non-bridging oxygen ion (*abc*, cf. figs 1.18 and 1.19). $Na_2O \cdot 2\,B_2O_3 \cdot 10\,H_2O$ also contains a diborate-like group but this group is isolated from the network because four oxygen ions now are non-bridging. The compound $K_2O \cdot 2\,B_2O_3$ consists of diborate (a_2c_2), di-triborate groups (ac_2) and loose BO_3 units (a) (Krogh-Moe [3–19])). The compound $ZnO \cdot 2\,B_2O_3$ is built up of diborate groups (a_2c_2) only (Martinez-Ripoll, Martinez-Carrera and Garcia-Blanco [3–20])), $BaO \cdot 2\,B_2O_3$ contains di-triborate (ac_2) and di-pentaborate groups (a_3c_2) (Block and Perloff [3–21])) and finally $SrO \cdot 2\,B_2O_3$ has a completely deviating structure (Krogh-Moe [3–22])).

As can be observed, the Raman spectra of these diborate compounds show important differences. Interpretation of these spectra is rather difficult, it can however be observed that in spectra of the compounds containing the diborate group (a_2c_2) a number of the stronger peaks is observed in the areas 700–800 cm^{-1} and around 500 cm^{-1}.

Bril [3–6]) suggests that the large peak observed at about 770 cm^{-1} is due to a vibration in which all oxygen ions take part of the six-membered ring of a borate group with one or two BO_4 units in this ring (a_pc_q groups). It is clear that many borate groups are built up of these rings as, for instance, the diborate (a_2c_2) and the pentaborate groups (a_4c). In some diborate compounds the di-triborate (ac_2) and di-pentaborate group (a_3c_2) are observed which contain rings with two BO_4 tetrahedra.

Although $ZnO \cdot 2\,B_2O_3$ contains only diborate groups (a_2c_2) and the bond

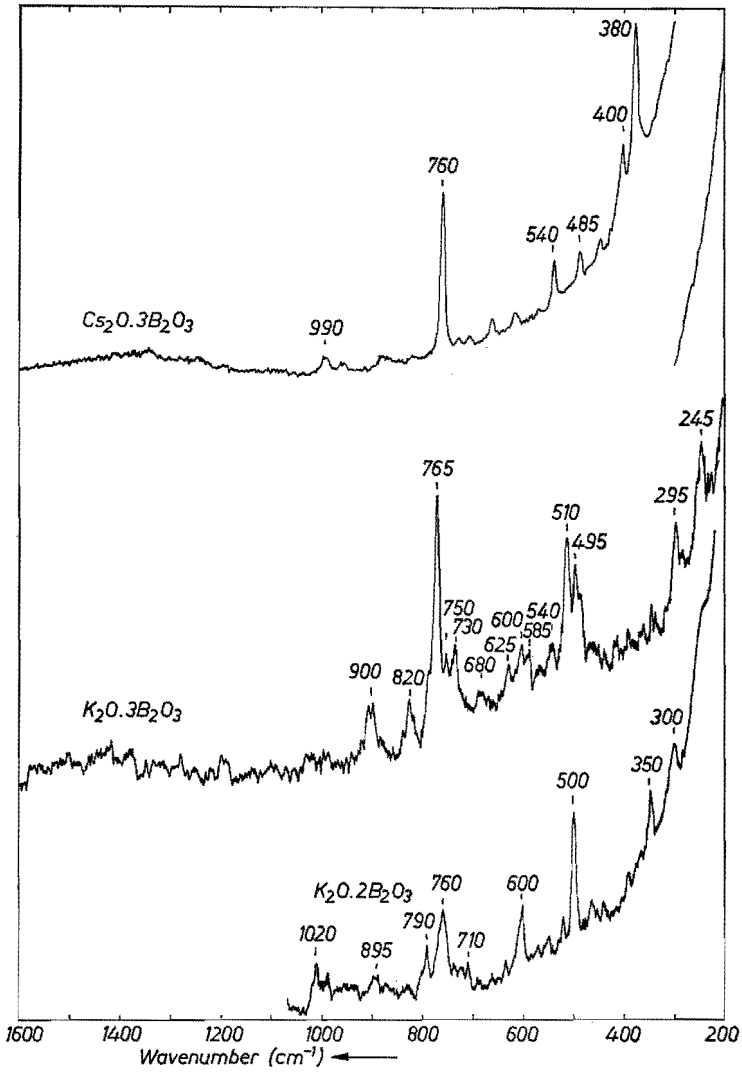

Fig. 3.5. Raman spectra of polycrystalline di- and triborates (direction $x(zz + zx)y$).

lengths and angles do not differ strongly from the diborate groups (a_2c_2) in $Li_2O \cdot 2\,B_2O_3$, the Raman spectra of the two compounds are very different. Assuming that the crystal structures described in the literature are indeed correct, this strong difference in the Raman spectra must be caused by the influence of the Zn^{2+} ion on the vibrations of the diborate group.

Unfortunately it could not be confirmed by X-ray analysis that the sample with intended composition $BaO \cdot 2\,B_2O_3$ had the crystal structure of this compound described by Block and Perloff [3–21]. The Raman spectrum in

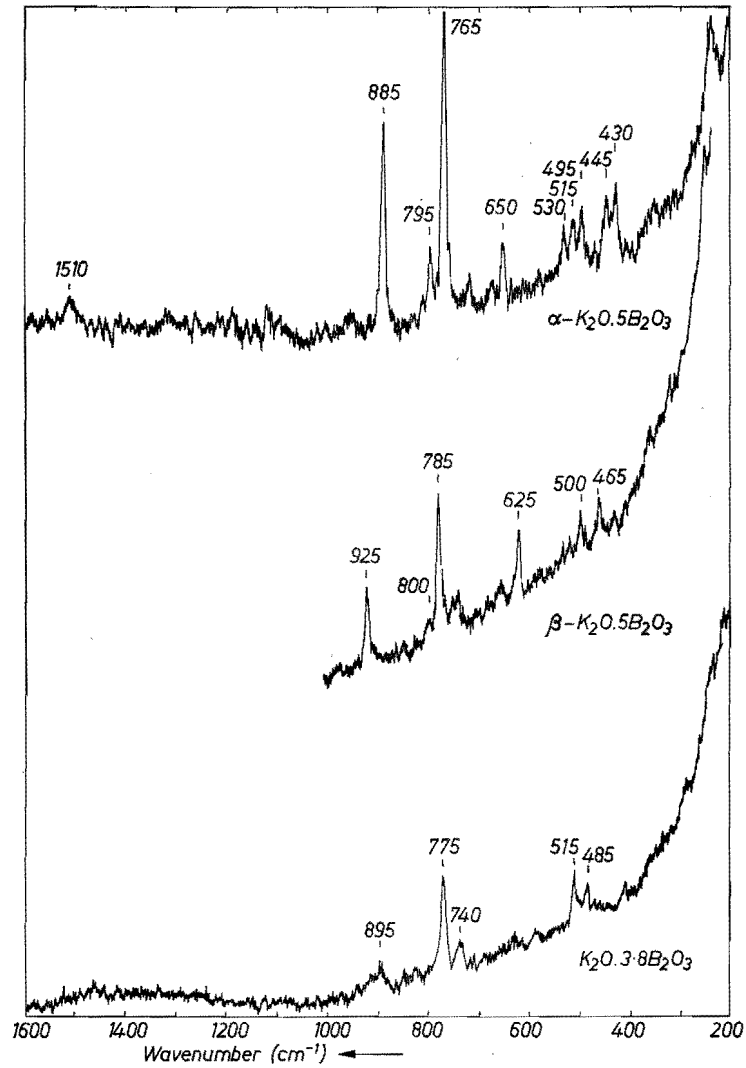

Fig. 3.6. Raman spectra of polycrystalline potassium borates (direction $x(zz + zx)y$).

fig. 3.8, however, shows some similarity with the spectrum of the compound $K_2O \cdot 2\,B_2O_3$. The Raman spectrum of the compound $SrO \cdot 2\,B_2O_3$ differs completely from other spectra of diborates, but this is not strange because the crystal structure of this compound is completely different from other diborates, containing all boron ions in an unusual tetrahedral coordination.

The Raman spectrum of the compound $Na_2O \cdot 2\,B_2O_3 \cdot 10\,H_2O$, shown in fig. 3.9 differs greatly from the spectrum of the compound $Li_2O \cdot 2\,B_2O_3$, although both compounds are built up of diborate groups. However, in the

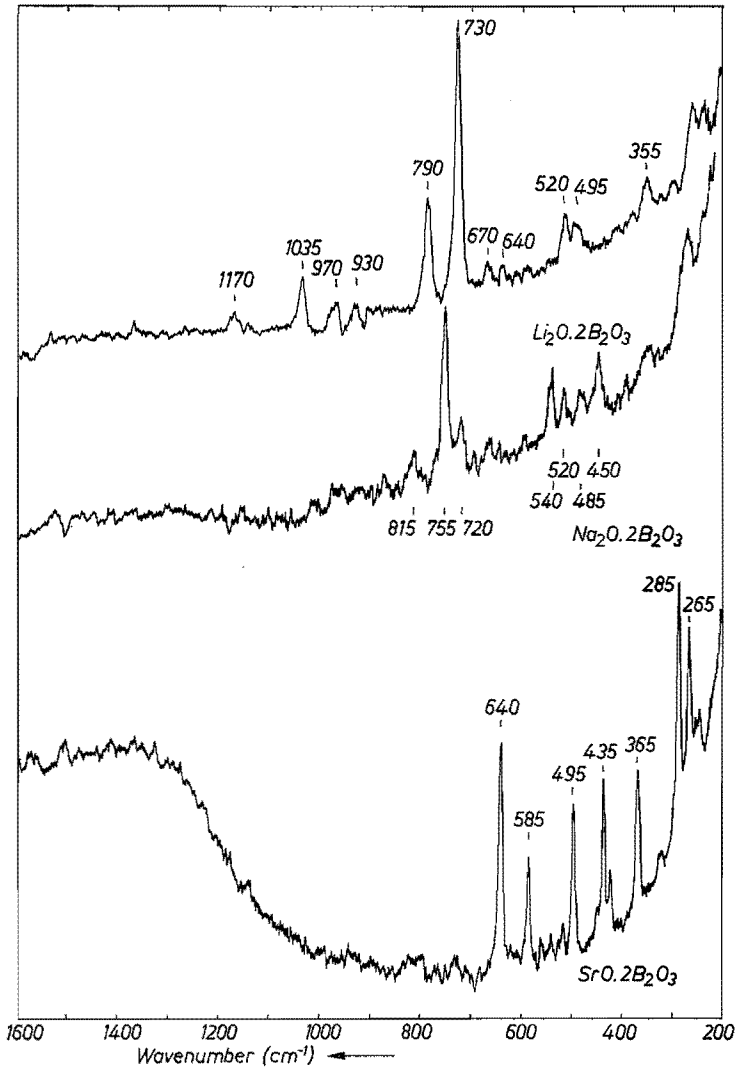

Fig. 3.7. Raman spectra of polycrystalline diborates (direction $x(zz + zx)y$).

compound $Na_2O \cdot 2\,B_2O_3 \cdot 10\,H_2O$ these diborate groups are not connected to the network with bridging oxygen ions, as is the case with the groups in $Li_2O \cdot 2\,B_2O_3$. The absence of a strong absorption band at 580 cm^{-1} in the infrared spectrum of $Na_2O \cdot 2\,B_2O_3 \cdot 10\,H_2O$ suggests that the Raman line at 580 cm^{-1} is probably due to a symmetric vibration.

The compound $3\,Li_2O \cdot 2\,B_2O_3$, of which the crystal structure is unknown, could have had the same type of diborate groups as the compound $Na_2O \cdot 2\,B_2O_3 \cdot 10\,H_2O$. The Li^+ ions could have replaced the H^+ ions bonded to

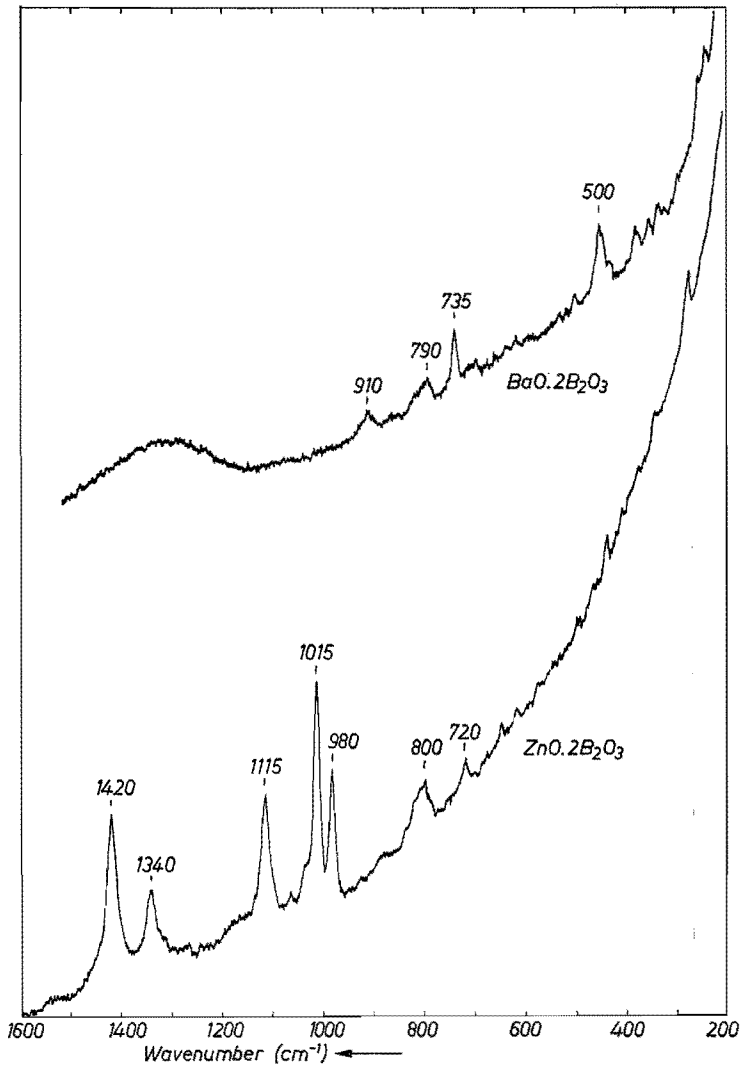

Fig. 3.8. Raman spectra of polycrystalline diborates (direction $x(zz + zx)y$).

the non-bridging oxygen ions. The Raman spectra of the two compounds are completely different, however (cf. fig. 3.9). This probably means that the compound 3 Li_2O . 2 B_2O_3 contains an other type of borate group than Na_2O . 2 B_2O_3 . 10 H_2O. The strong peak at 780 cm^{-1} again suggests the presence of six-membered borate rings (a_pc_q). However, the infrared spectrum of 3 LiO_2 . 2 B_2O_3 (cf. fig. 4.8) shows a strong absorption band in the same wavenumber area, hence, with this information the Raman line at 780 cm^{-1} cannot unequivocally be attributed to a symmetric vibration. The presence of

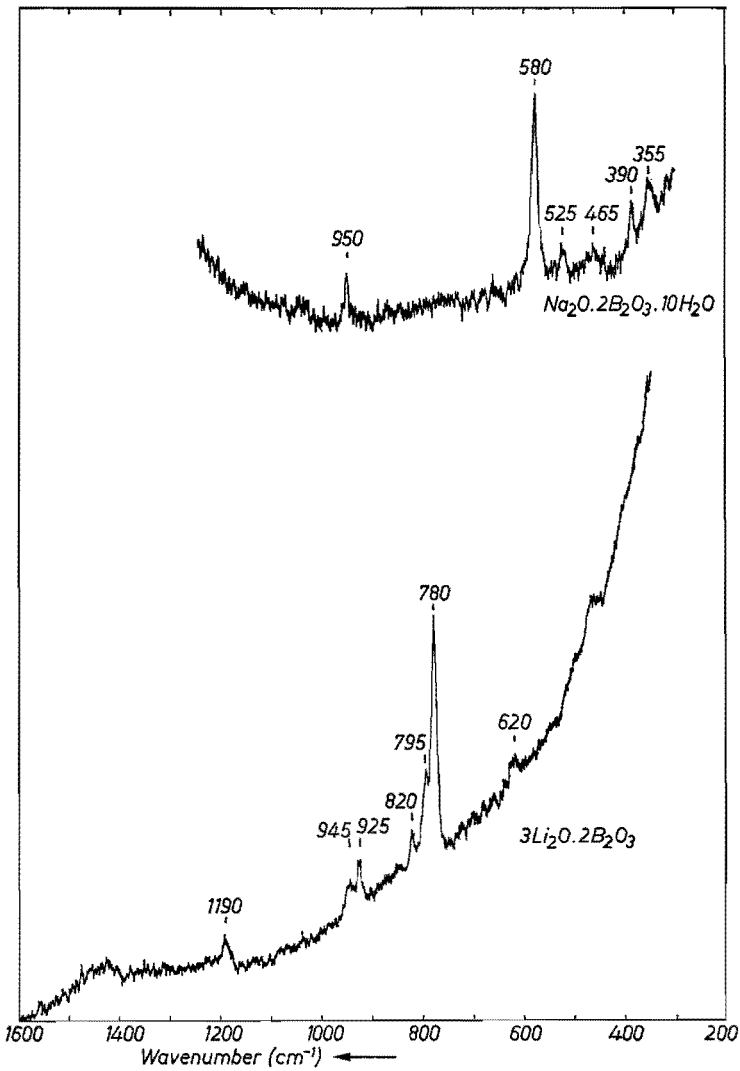

Fig. 3.9. Raman spectra of polycrystalline borates (direction $x(zz + zx)y$).

a small Raman band between 1400 and 1500 cm^{-1} is reminiscent of the spectrum of $Li_2O \cdot B_2O_3$. The infrared spectra of $3\ Li_2O \cdot 2\ B_2O_3$ and $Li_2O \cdot B_2O_3$ also show a high degree of similarity, which suggests that the structure is analogous to some extent.

Triborate compounds

The Raman spectra of two crystalline triborates are shown in fig. 3.5. The crystal structure of the compound $K_2O \cdot 3\ B_2O_3$ is unknown, so that the

borate groups which are present are also unknown. The crystal structure of Cs_2O . 3 B_2O_3 is known (Krogh-Moe [3-23,62]), the compound being built up of triborate groups (a_2c) only (cf. fig. 1.15). The Raman spectra of these two compounds are not identical, which probably means that the compounds have a different borate network structure, although this difference will not be extreme (cf. fig. 3.5). Also, the compound β-Na_2O . 3 B_2O_3, whose Raman spectrum was recorded by Bril [3-6]), shows little similarity to the other two spectra mentioned. The crystal structure of β-Na_2O . 3 B_2O_3 was elucidated by Krogh-Moe [3-24]) and contains pentaborate (a_4c), triborate groups (a_2c) and loose BO_4 units (c). The crystal structure of α-Na_2O . 3 B_2O_3 was recently revealed by Krogh-Moe [3-25]), the borate network being built up of pentaborate (a_4c) and diborate groups (a_2c_2).

One thing these spectra all have in common is that the strongest Raman peak is observed between 760 and 790 cm^{-1}. As in some diborates, this is probably due to the vibration of the six-membered ring (a_pc_q), as suggested by Bril [3-6]).

Tetraborate compounds

The crystal structure of the compound Na_2O . 4 B_2O_3 is known (Hyman, Perloff, Mauer and Block [3-26])). The borate network in this compound is built up of pairs of pentaborate (a_4c) and triborate groups (a_2c, cf. fig. 1.14). Potassium-borate glasses of the tetraborate composition, K_2O . 4 B_2O_3, may be crystallized to give a compound of the composition K_2O . 3·8 B_2O_3, as has been found by Krogh-Moe [3-63]). The structure consists of a three-dimensional framework, built up of interconnected pentaborate groups (a_4c), triborate groups (a_2c) and BO_4 tetrahedra (c) and BO_3 triangles (a).

The Raman spectrum of Na_2O . 4 B_2O_3 was recorded by Bril [3-6]) and shows close similarity to the Raman spectrum of K_2O . 3·8 B_2O_3 (fig. 3.6). The strongest peak in the spectrum of K_2O . 3·8 B_2O_3 is observed at 775 cm^{-1} and that of Na_2O . 4 B_2O_3 at 786 cm^{-1} (Bril [3-6])) which in both cases seem to be peaks related to the vibration of the six-membered rings (a_pc_q) as suggested by Bril [3-6]).

Pentaborate compounds

The compounds α-K_2O . 5 B_2O_3 and β-K_2O . 5 B_2O_3 of the pentaborates were prepared, α being the higher-temperature modification. The Raman spectra of both compounds are shown in fig. 3.6.

From X-ray analysis it is known that they both contain the double-ring pentaborate group (a_4c, cf. fig. 1.13, Krogh-Moe [3-27,28])). The Raman spectra of the two compounds show similarity. The crystals of both belong to the same symmetry class, the cell dimensions are somewhat different which results in a calculated density of 1·93 g/cm^3 for the α-compound and 2·29 g/cm^3 for the β-compound (Krogh-Moe [3-28])). This shows to some extent that the influence

of the network on the vibrational frequencies is not too drastic although the density difference is about 17%. This suggests that in first approximation most vibrations are located within the elementary pentaborate group and it may be concluded therefore that the Raman spectra are characteristic of the type of borate group present in the crystalline borates. The strongest peak observed at 765 cm^{-1} for the α-compound and at 785 cm^{-1} for the β-compound is probably connected with the vibration of the six-membered borate ring ($a_p c_q$) as suggested by Bril [3-6]).

Silica compounds

The Raman spectrum of α-quartz has been published and discussed by Scott and Porto [3-29]), the spectrum of β-quartz by Bates and Quist [3-30]). The Raman spectra of α- and β-crystobalite have been published and discussed by Bates [3-31]).

The Raman spectra of α- and β-quartz have their strongest peak at 464 cm^{-1}. This peak is attributed to a bending-type vibration of the O–Si–O group (Etchepare [3-64])).

The Raman spectrum of α-crystobalite has its strongest peaks at 426 cm^{-1} and 233 cm^{-1} (at 77 K). Both peaks are attributed to vibrations with A_1 symmetry [3-31]). The Raman spectrum of β-crystobalite has weak lines at 292, 777 and 1077 cm^{-1} [3-31]). It has been concluded by Bates [3-31]) that β-crystobalite is a poor model for vitreous SiO_2.

Disilicate compounds

The crystal structure of $Li_2O \cdot 2\,SiO_2$ was revealed by Liebau [3-32]). This disilicate was shown to have a layered structure, built up of SiO_4 units. These layers contain ring-type structures with six SiO_4 tetrahedra in the ring. The crystal structure of α-$Na_2O \cdot 2\,SiO_2$ was first determined by Liebau [3-33]), but later corrected by Pant and Cruickshank [3-34]). The structure of α-$Na_2O \cdot 2\,SiO_2$ was shown to be very similar to $Li_2O \cdot 2\,SiO_2$ although the space groups are different. α-$Na_2O \cdot 2\,SiO_2$ also contains two-dimensional corrugated layers of tetrahedra with one non-bridging oxygen ion. These layers contain rings of six SiO_4 tetrahedra.

The similarity in structure is reflected in the similarity of the Raman spectra of these compounds (cf. fig. 3.10) and also by the similarity of the infrared spectra (cf. fig. 4.9).

Etchepare [3-55]) attributed the peaks at 1080 cm^{-1} in the spectrum of α-$Na_2O \cdot 2\,SiO_2$ and at 1105 cm^{-1} of $Li_2O \cdot 2\,SiO_2$ to a bond-stretching vibration of the $Si–O^-$ unit. The peaks at 530 and 550 cm^{-1} are assigned to a vibration of the Si–O–Si group.

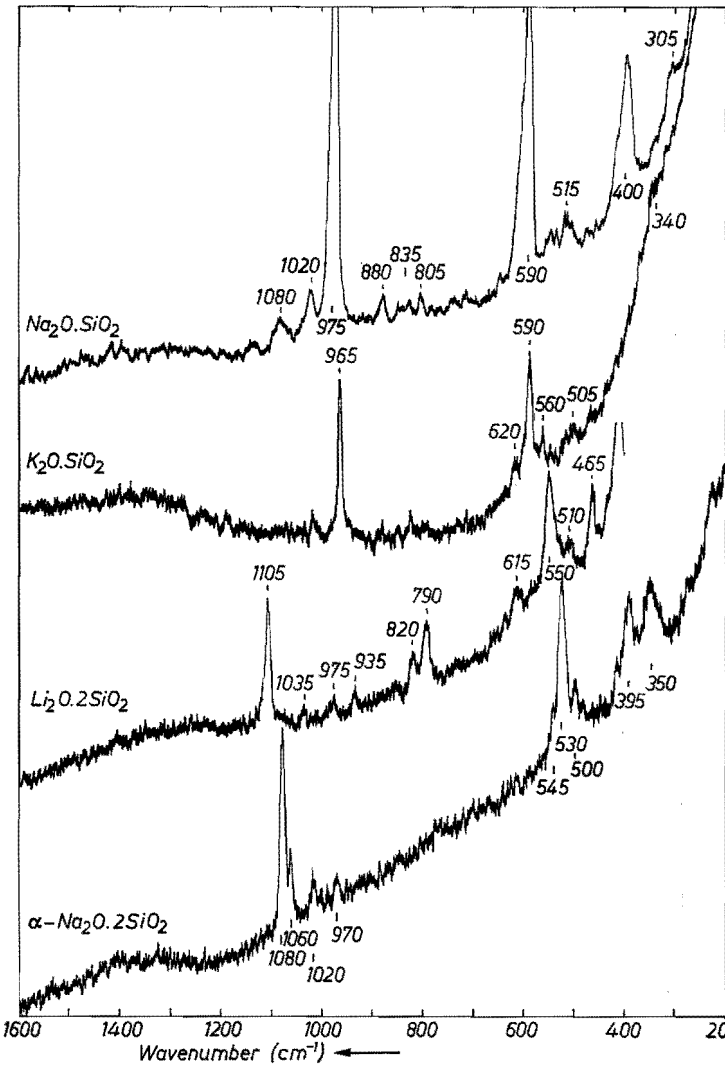

Fig. 3.10. Raman spectra of polycrystalline silicates (direction $x(zz + zx)y$).

Metasilicate compounds

The most recent investigation into the crystal structure of the metasilicate Na_2O . SiO_2 was done by McDonald and Cruickshank [3–36]). The structure was shown to consist of metasilicate chains, chains with two non-bridging oxygen ions per SiO_4 tetrahedron. The crystal structure of the compound K_2O . SiO_2 is unknown but due to the similarity of the Raman and infrared spectra of K_2O . SiO_2 and Na_2O . SiO_2 the structure of K_2O . SiO_2 will be similar to that of Na_2O . SiO_2 (cf. figs 3.10 and 4.9).

Etchepare [3-55]) attributed the peaks at 975 cm^{-1} in the spectrum of Na_2O . SiO_2 to a bond-stretching vibration of the Si–O^- unit. The peak at 590 cm^{-1} is assigned to a vibration of the Si–O–Si groups.

3.2.3. *Conclusions*

The Raman spectra of the borate compounds seem primarily to be characteristic of medium-large borate groups, for instance the pentaborate (a_4c) or the ring-type metaborate groups (b_3). The peak at about 770 cm^{-1} in the spectra seems to be characteristic of the six-membered borate ring with one or two BO_4 tetrahedra (a_pc_q groups). The peak at 610–630 cm^{-1} seems to be characteristic of the ring-type metaborate group (b_3). The influence of the network on the vibrational spectra cannot be excluded for a number of the smaller peaks.

The Raman spectra of the silicate compounds are primarily characteristic of small groups, such as the Si–O–Si bridging group. A clear difference can be observed in the spectra of the compounds built up of SiO_4 tetrahedra with none, one or two non-bridging oxygen ions. The peaks at 530 to 550 cm^{-1} and 1080 to 1105 cm^{-1} are characteristic of SiO_4 tetrahedra with one non-bridging oxygen ion. The peaks at 590 cm^{-1} and 965 to 975 cm^{-1} are characteristic of SiO_4 tetrahedra with two non-bridging oxygen ions.

The influence of alkali and alkaline-earth ions seems to be negligible in the 250–1600 cm^{-1} wavenumber range.

3.3. Raman spectra of borate glasses

3.3.1. *Experimental results*

The Raman spectra of the binary vitreous borate systems $x\,Na_2O\,.\,(1-x)\,B_2O_3$ and $x\,K_2O\,.\,(1-x)\,B_2O_3$ are shown in figs 3.12 to 3.16 for several values of x. In figs 3.17 and 3.18 some Raman spectra of mixed alkali-borate glasses are shown with a relatively high proportion of alkali oxide. In figs 3.19, 3.20 and 3.21 a number of spectra of glasses containing alkaline-earth ions are shown and in figs 3.22 and 3.23 the spectra are shown of borate glasses containing increasing amounts of Al_2O_3. In fig. 3.24 the Raman spectrum is shown of a crystallized mixed Li-, Na- and K-borate glass. In the same figure the spectrum is shown of a glass with composition $0{\cdot}25\,Cs_2O\,.\,0{\cdot}75\,B_2O_3$.

All Raman spectra were recorded at room temperature, however, with two different spectrometers. With the one spectrometer the spectra were recorded as a linear function of the wavelength, for excitation the 514·5-nm line of an Ar laser was used, the band width was 10 cm^{-1}. With the other spectrometer the spectra were recorded as a linear function of the wavenumber, for excitation the 632·8-nm line of a 6-mW He–Ne laser was used, the band width was 10 cm^{-1}. No significant differences could be observed between the spectra

recorded with the two different spectrometers, so that for the interpretation of the results these spectra from the different spectrometers are completely interchangeable. Lowering the band width to 2 cm^{-1} did not give increased resolution of the spectra compared to the 10 cm^{-1} generally used. For more details about the equipment the reader is referred to sec. 2.2.

Numbers in the Raman spectra close to the peaks show the position of the maxima of these peaks in cm^{-1}. In all spectra the direction of the incident and scattered light is shown, using symbols that are explained in sec. 2.2. Spectra of a number of borate glasses were separately recorded by Bril [3–6]) at about the same time.

3.3.2. *Qualitative discussion of results*

Boron-oxide glass

A recent X-ray study of the structure of vitreous boron oxide by Mozzi and Warren [3–37]) has revealed that the major part of the glass is made up of boroxol groups B_3O_6 (a_3), see fig. 1.12. This was already suggested by Goubeau and Keller [3–38]) and later by Krogh-Moe [3–11]). Their conclusion was based on the observation that the strongest peak in the Raman spectrum of B_2O_3 glass at 806 cm^{-1} (cf. also fig. 3.12) coincides with a strong Raman peak in several boroxol derivatives. Due to the relatively strong polarization of this peak it must be attributed to a totally symmetric vibration. Parsons [3–18]) and Krogh-Moe [3–11]) attribute this peak to a trigonal deformation of the boroxol ring, shown in fig. 3.11.

More evidence for this suggestion was given by Kristiansen and Krogh-Moe [3–39]) when they calculated the vibrational spectra of boroxol groups with different groups attached to the boroxol ring and compared this to the observed spectra.

In a review paper on the structure of boron-oxide glass Krogh-Moe [3–40]) compared the random-network model of BO_3 groups with the group model based on boroxol groups and, with the experimental evidence available, concluded that the group model was by far the most probable.

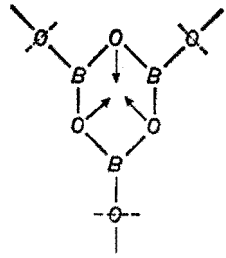

Fig. 3.11. The trigonal deformation of the boroxol ring after Parsons [3–10]) and Krogh-Moe [3–11]).

Borate glasses with up to 25 mol % alkali oxide

The Raman spectra of the binary sodium- and potassium-borate glasses show a close resemblance (cf. figs 3.12 to 3.16). The most striking feature, at low alkali-oxide concentration, is the rapid decrease of the peak at about 806 cm^{-1} and the rapid increase at the same time of a peak at about 770 cm^{-1} with increasing alkali-oxide content. At 20 mol % alkali oxide the 806-cm^{-1} peak is still just visible as a shoulder of the 770-cm^{-1} peak but in the case of vitreous sodium borate at 25 mol % Na_2O the 806-cm^{-1} peak has completely disappeared, just as in the spectrum of the glass of composition 0·25 Cs_2O . 0·75 B_2O_3 (cf. fig. 3.24).

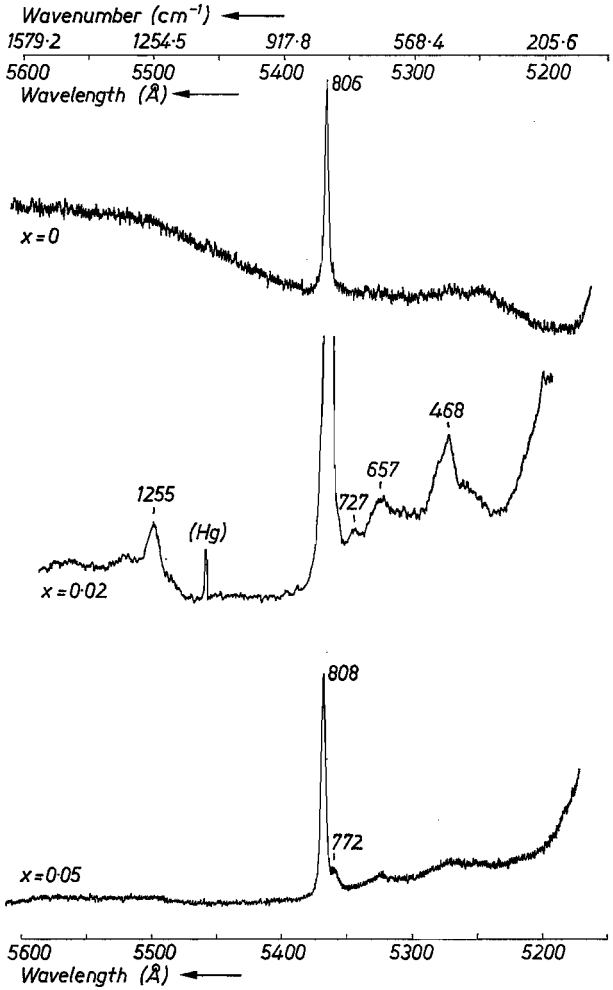

Fig. 3.12. Raman spectra of glasses in the system $x\ Na_2O\ .\ (1 - x)\ B_2O_3$ (direction $x(zz)y$).

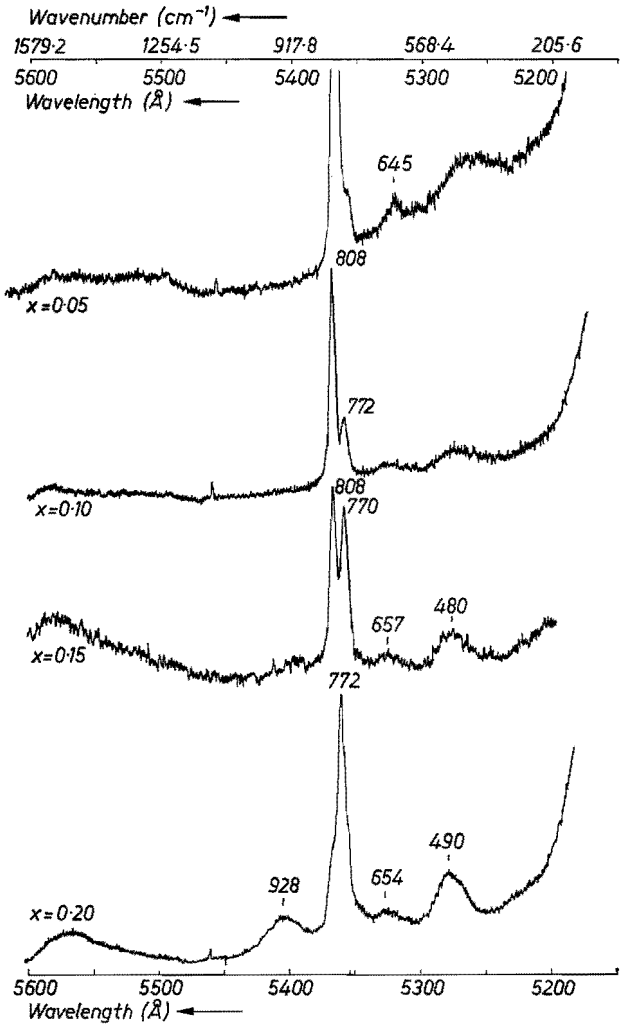

Fig. 3.13. Raman spectra of glasses in the system $x\ Na_2O\ .\ (1-x)\ B_2O_3$ (direction $x(zz)y$).

Because this 806-cm^{-1} peak is characteristic of the boroxol group it becomes quite clear that on addition of alkali oxide to boron oxide the boroxol groups are converted into other groups. The fact that this 806-cm^{-1} peak has disappeared at about 25 mol % alkali oxide makes it less certain that vitreous boron oxide consists of a random network of BO_3 units. If that were so, the only regular basic unit with a high abundance would have been this BO_3 triangle, hence the peaks observed in the vibrational spectra should be due to vibrations in this BO_3 triangle. At 25 mol % alkali oxide not all these BO_3 triangles with three bridging oxygen ions can be converted into other types of groups,

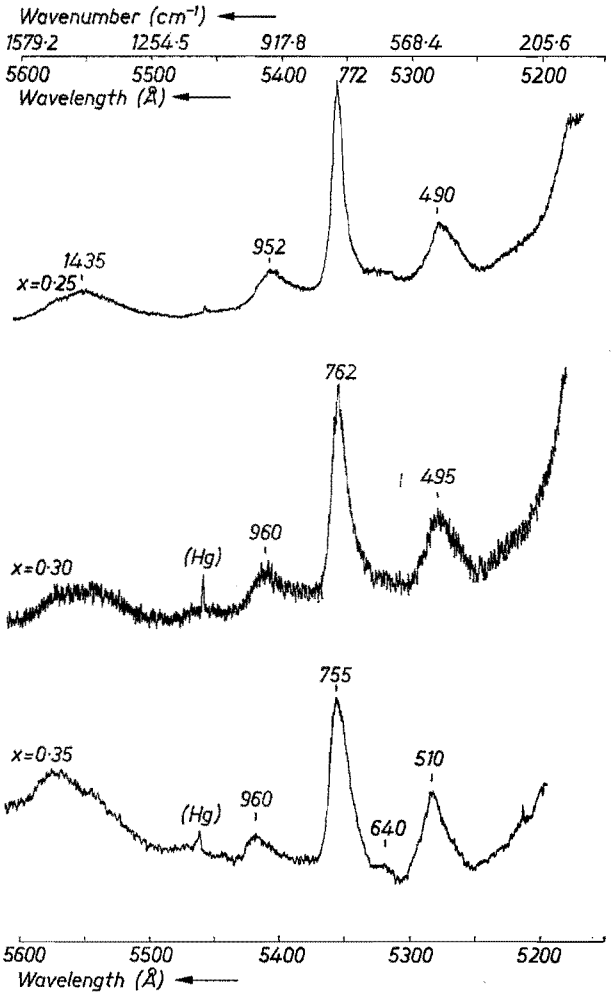

Fig. 3.14. Raman spectra of glasses in the system $x\ Na_2O\ .\ (1-x)\ B_2O_3$ (direction $x(zz)y$).

so that it is again doubtful that boron-oxide glass is built up of a random network of BO_3 triangles, as has already been proposed by Krogh-Moe [3–40]).

From the fact that at the composition $0{\cdot}20\ R_2O\ .\ 0{\cdot}80\ B_2O_3$ the 806-cm^{-1} peak is still observable it can be concluded too that in this composition borate groups with an average sodium-to-boron ratio of about $\frac{1}{4}$ to $\frac{1}{3}$ are present because otherwise the boroxol groups would already have been consumed at lower alkali-to-boron ratios or persisted longer at higher ratios.

From the appearance of new bands in the Raman spectra on addition of alkali oxide to boron oxide some conclusions can be drawn about the existence of certain types of borate groups in alkali-borate glasses. It can be observed from

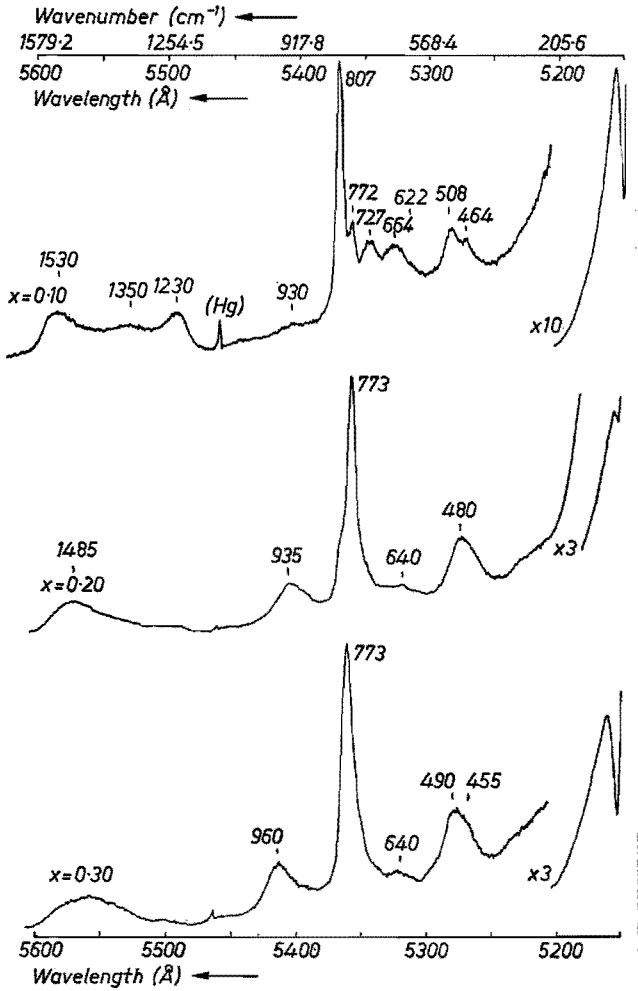

Fig. 3.15. Raman spectra of glasses in the system $x\,K_2O\,.\,(1-x)\,B_2O_3$ (direction $x(zz + zx)y$).

the spectra of the binary sodium- and potassium-borate glasses in figs 3.12 to 3.16, that a strong peak arises at about 770 cm^{-1}, a peak that is polarized, too. This peak is assigned to a symmetric vibration of the six-membered borate ring with one BO_4 unit (a_2c) (Bril [3–6]).

From the Raman spectra of the sodium- and potassium-borate glasses with 20 mol % alkali oxide or less it becomes probable that not only pentaborate groups (a_4c) of the type present in α- and β-$K_2O\,.\,5\,B_2O_3$ are present. This is based on the absence of the peaks at 885 and 915 cm^{-1} in the spectra of the glasses, which are present in the spectra of crystalline α- and β-$K_2O\,.\,5\,B_2O_3$. Formation of pentaborate groups (a_4c) only would also lead to a

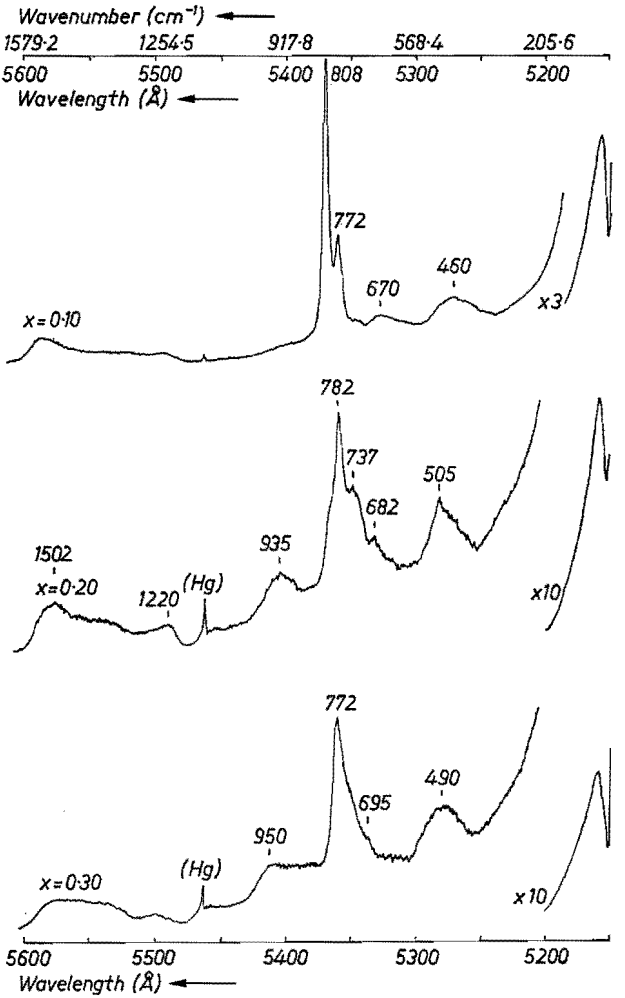

Fig. 3.16. Raman spectra of glasses in the system $x\ K_2O\ .\ (1-x)\ B_2O_3$ (direction $x(yz + yx)y$).

consumption of all the boroxol groups at a lower alkali-oxide content than is actually observed. Formation of only pentaborate groups (a_4c) at about 16 mol % K_2O in vitreous potassium-borate glass is also improbable because the density of potassium-borate glass at 16 mol % K_2O (Coenen [3–41])) is significantly higher than the density of the high-temperature form α-$K_2O\ .\ 5\ B_2O_3$ (Krogh-Moe [3–28])).

The spectra of the sodium- and potassium-borate glasses with 20 mol % alkali oxide (cf. figs 3.13 and 3.16) and the spectra of the compounds $Na_2O\ .\ 4\ B_2O_3$ (Bril [3–6])) and $K_2O\ .\ 3{\cdot}8\ B_2O_3$ show a reasonable similarity. The similarity with the Raman spectra of the compounds β-$Na_2O\ .\ 3\ B_2O_3$

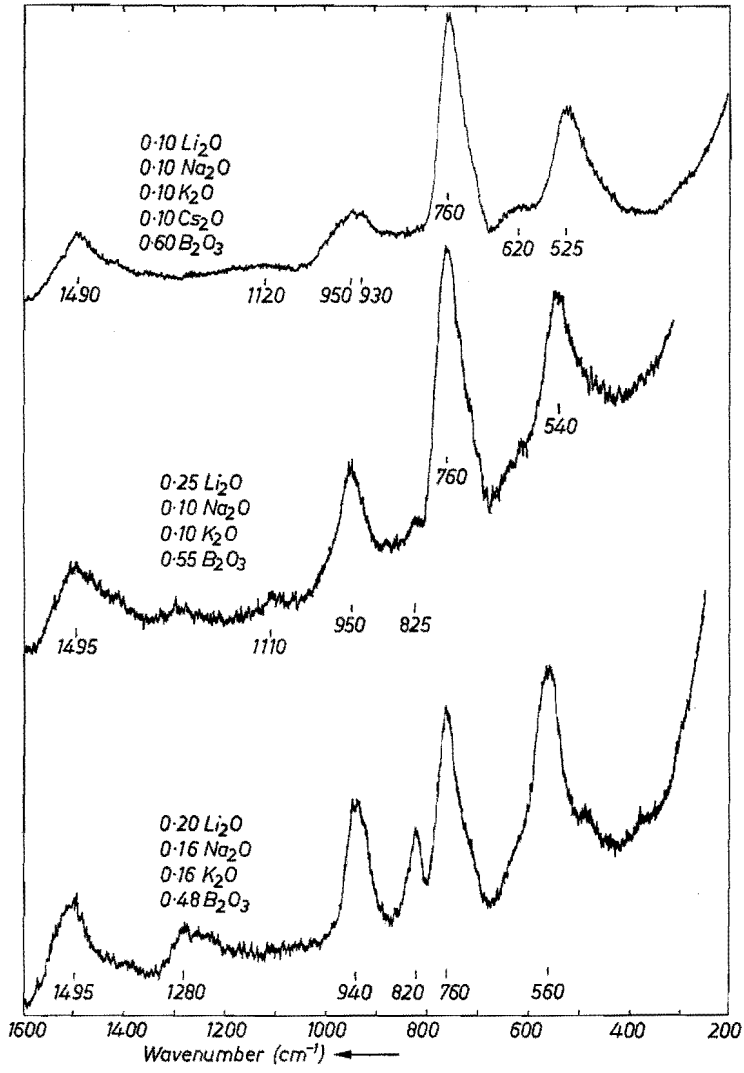

Fig. 3.17. Raman spectra of mixed alkali-borate glasses (direction $x(zz + zx)y$).

(Bril [3–6]), $K_2O \cdot 3\,B_2O_3$, $Cs_2O \cdot 3\,B_2O_3$, $Na_2O \cdot 2\,B_2O_3$ and $K_2O \cdot 2\,B_2O_3$ is definitely less (cf. figs 3.5 and 3.7). This means that probably tetraborate groups (a_6c_2), that is, a couple consisting of one pentaborate (a_4c) and one triborate group (a_2c) are formed in the concentration range 0–20 mol % alkali oxide.

Due to the similarity of the infrared spectra of crystalline $K_2O \cdot 3{\cdot}8\,B_2O_3$, $Na_2O \cdot 4\,B_2O_3$ and the corresponding glasses the latter conclusion is confirmed by infrared spectroscopy. The conclusion is also confirmed by X-ray

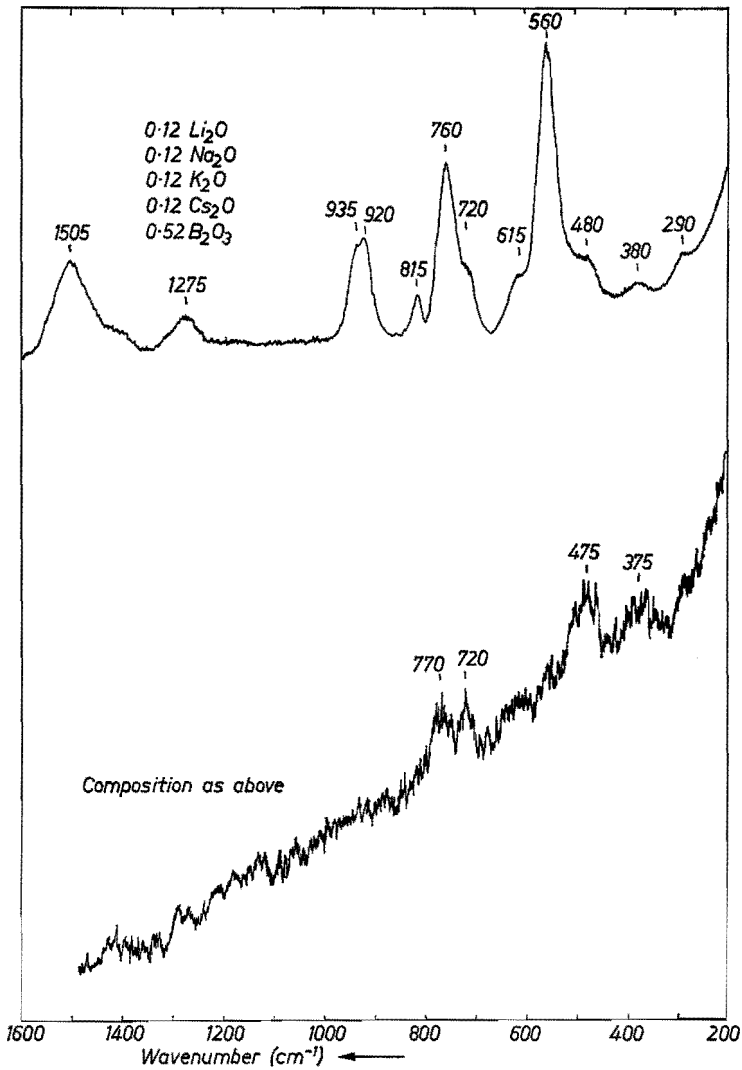

Fig. 3.18. Raman spectrum of mixed alkali-borate glass. Upper trace direction $x(zz)y$, lower trace direction $x(zx)y$.

analysis of glasses in this concentration range, n.m.r. measurements of sodium-borate glasses and melting-point-depression results (cf. sec. 1.4).

Another explanation that can be considered is to propose the presence of a random network of six-membered borate rings with usually one BO_4 tetrahedron in the ring (a_2c) as the major basic group in alkali-borate glasses with about 20 mol % alkali oxide. This is consistent with the interpretation of the 770-cm^{-1} peak in the Raman spectrum as given by Bril. Formation of these

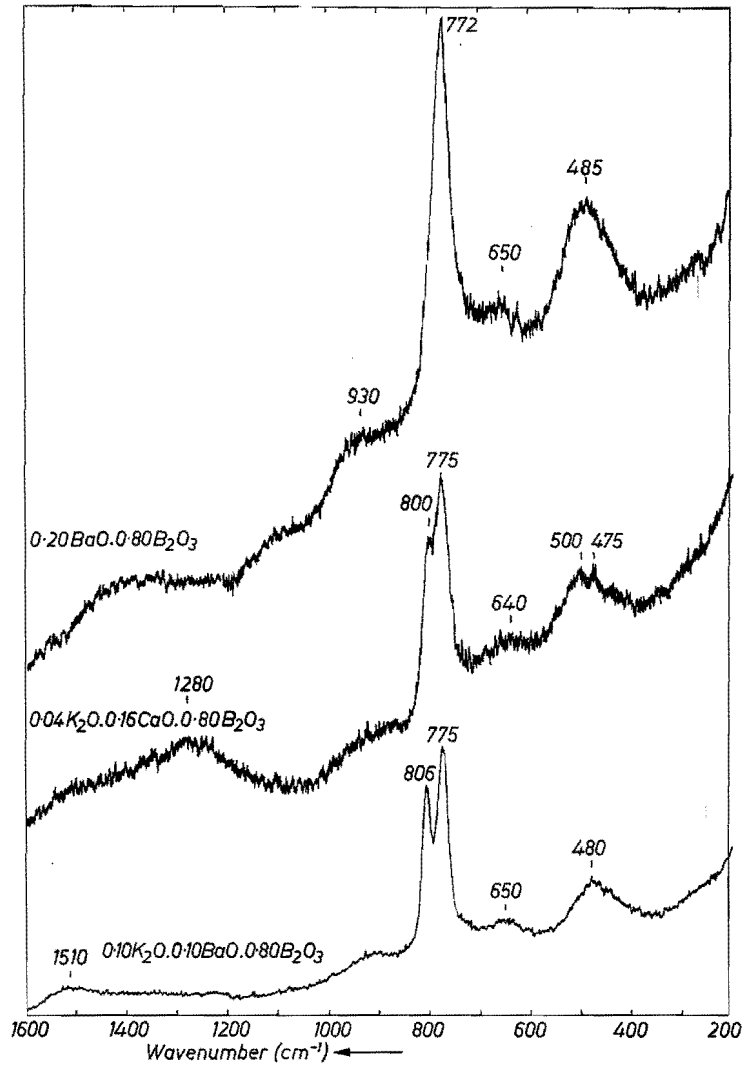

Fig. 3.19. Raman spectra of borate glasses containing alkaline-earth oxides (direction $x(zz + zx)y$).

a_2c groups also fits in exactly with the disappearance of the boroxol groups (a_3) at about 25 mol % alkali oxide.

The calculations in sec. 3.3.3 show that, based on the values of N_4 and the alkali-to-boron ratios at $x = 0{\cdot}17$ and $x = 0{\cdot}20$, the structure may indeed be built up of a major number of triborate groups, a reasonable number of boroxol groups and small numbers of diborate and metaborate groups. However, these same calculations show that the structure may also be built up of a major

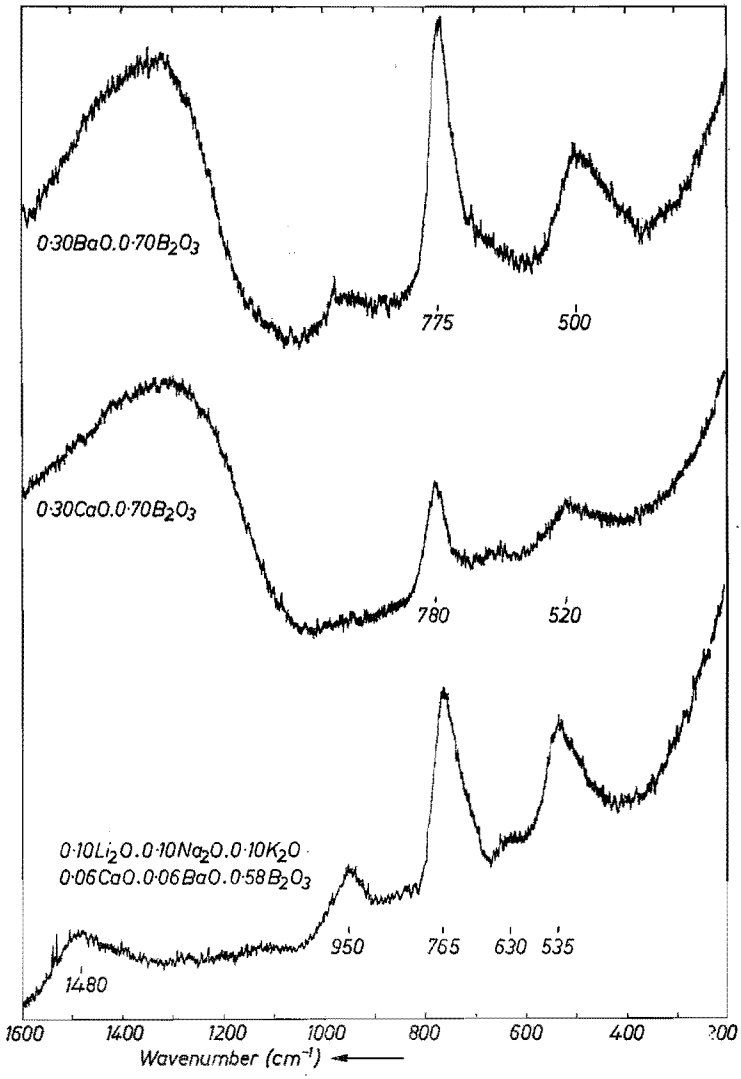

Fig. 3.20. Raman spectra of borate glasses containing alkaline-earth oxides (direction $x(zz + zx)y$).

number of tetraborate groups (a_6c_2), a minor number of boroxol groups (a_3), a minor number of "loose" BO_3 triangles (a) and a small number of "loose" BO_4 tetrahedra (c). This latter explanation is supported by the coincidence of the smaller peaks in the Raman spectra of glasses and crystals at $x = 0{\cdot}20$, the similarity of the infrared spectra of glasses and crystals and the X-ray, n.m.r., and melting-point-depression results, discussed in sec. 1.4.

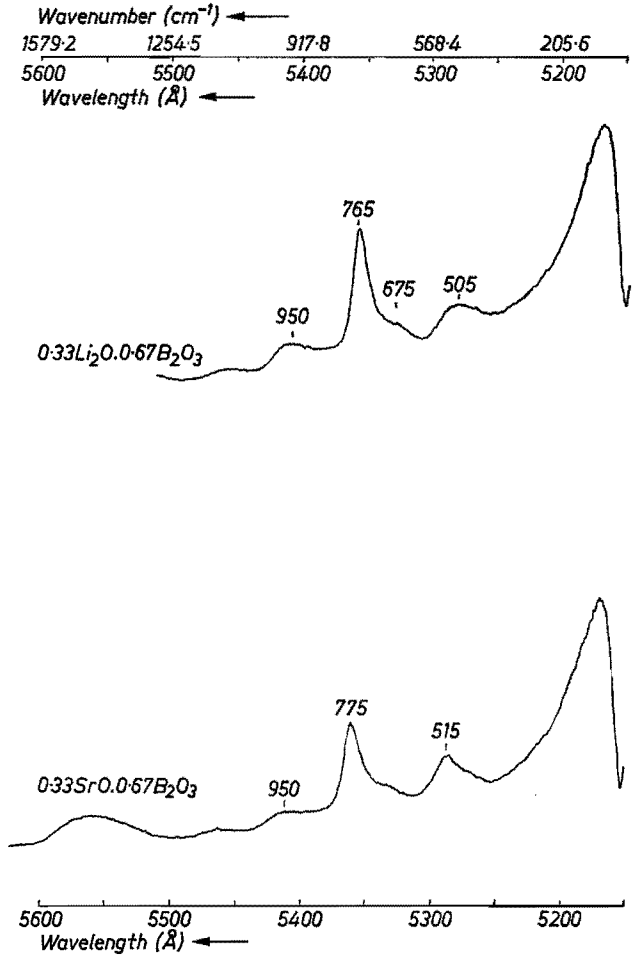

Fig. 3.21. Raman spectra of borate glasses (direction $x(zz + zx)y$).

It is concluded that up to about 20 *mol* % *alkali oxide mainly tetraborate groups* (a_6c_2) *are formed on addition of alkali oxide to boron-oxide glass. At* 20 *mol* % *alkali oxide the structure of the borate glass is mainly built up of tetraborate groups* (a_6c_2), *a minor number of boroxol groups* (a_3), *a minor number of "loose"* BO_3 *triangles* (*a*) *and a small number of "loose"* BO_4 *tetrahedra* (*c*).

Borate glasses with 20 *to* 35 *mol* % *alkali oxide*

The Raman spectra show that in the alkali-oxide concentration range 20 to 35 mol % a_pc_q groups are present in substantial amounts: again the strongest peak is observed at 770 to 755 cm^{-1}.

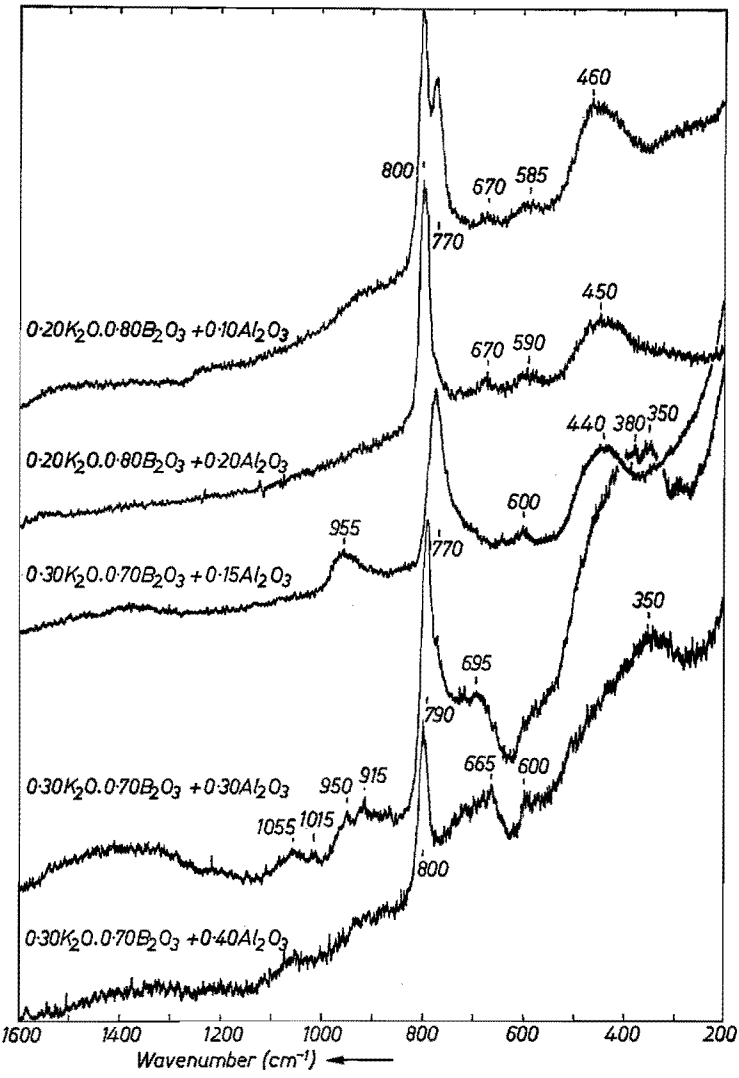

Fig. 3.22. Raman spectra of aluminoborate glasses (direction $x(zz + zx)y$).

For the sodium-borate glasses it seems most probable that the groups present in the crystalline compound Na_2O . 2 B_2O_3 are not formed in major amounts, viz. di-pentaborate groups (a_3c_2) and triborate groups with a non-bridging oxygen ion (*abc*). This is based on the observed higher density of vitreous Na_2O . 2 B_2O_3 compared to that of the compound.

From the absence of a strong peak at about 630 cm^{-1} in the spectrum of the glass of composition 0·35 Na_2O . 0·65 B_2O_3 it can be concluded that no significant number of ring-type metaborate groups (b_3) is present. This means

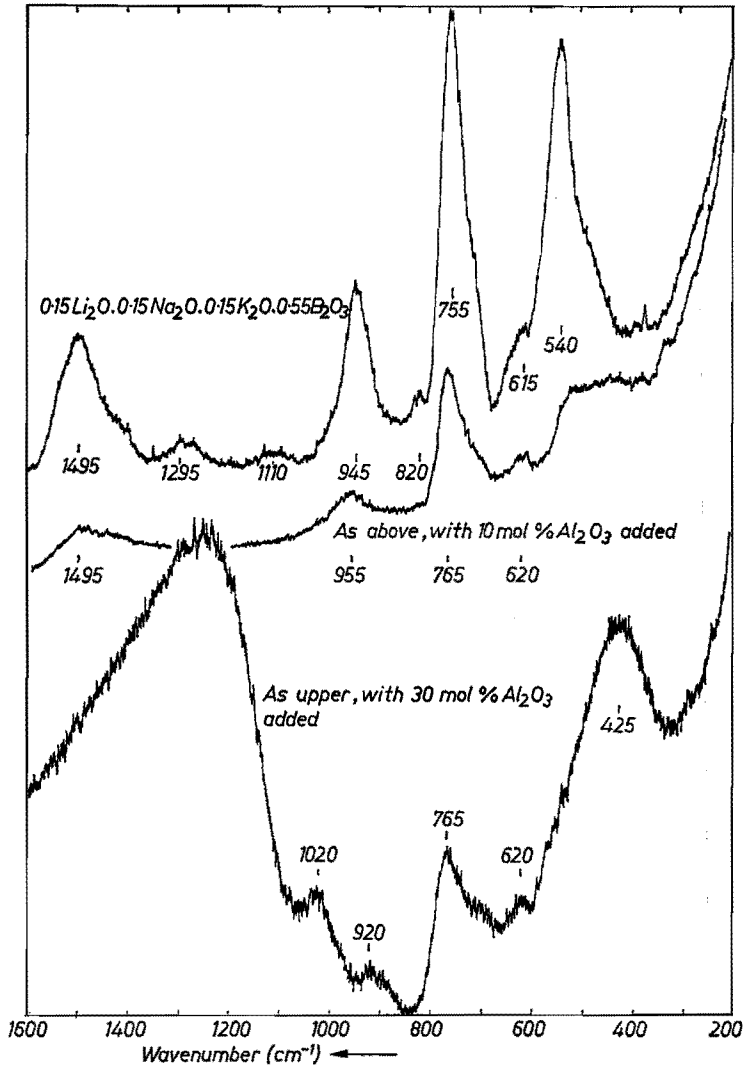

Fig. 3.23. Raman spectra of aluminoborate glasses (direction $x(zz + zx)y$)

that not many borate groups with a sodium-to-boron ratio of $\frac{1}{3}$ or lower are present in this glass.

Most probably di-triborate (ac_2) or diborate groups (a_2c_2) are formed. The formation of paired BO_4 groups is confirmed by the n.m.r. experiments on sodium-borate glass by Rhee [3–42]). Rhee measured an increase in the quadrupole coupling constant and dipolar line width of the ^{11}B resonance of BO_4 units for increasing amounts of Na_2O above 20 mol % Na_2O which indicates the coupling of BO_4 units. Krogh-Moe [3–43]) concluded from melting-point-

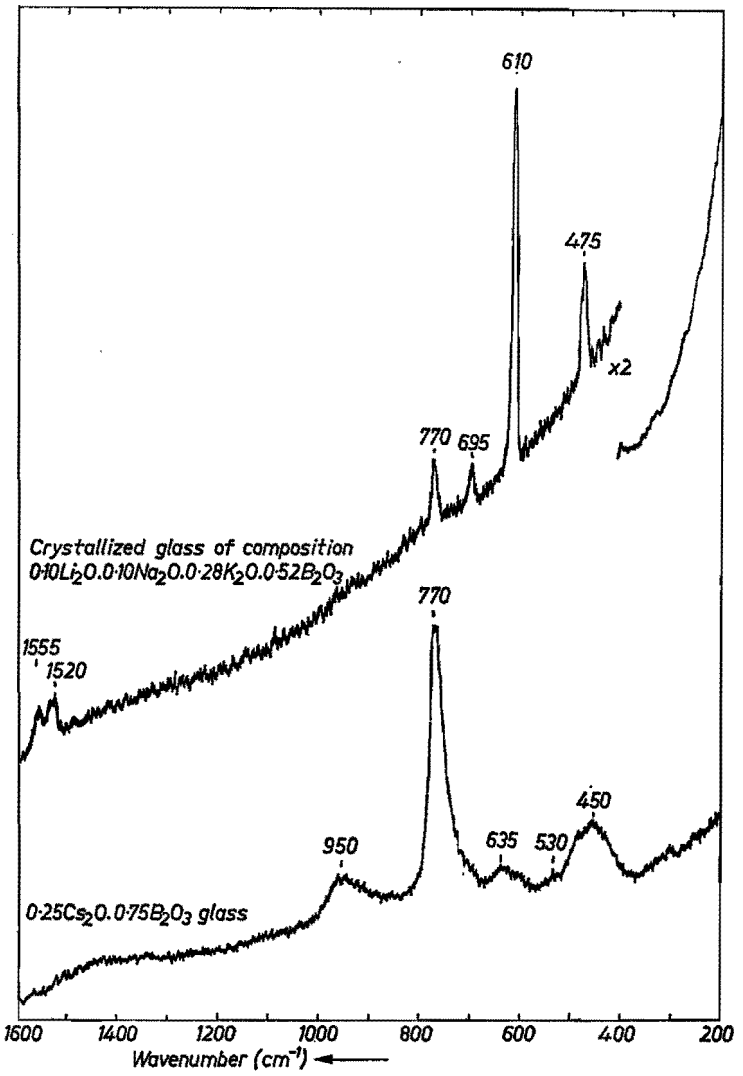

Fig. 3.24. Raman spectra of a crystallized borate glass (upper trace) and caesium-borate glass (lower trace) (direction $x(zz + zx)y$).

depression measurements that at about the glass composition with 33 mol % Na_2O the diborate group (a_2c_2) was the predominant group. Kumar [3-44]), using the free-volume theory for viscosity described by Cohen and Turnbull, calculated that the average size of the flow unit in the melt around 33 mol % Na_2O is approximately that of a B_4O_7 group, that is the diborate group (a_2c_2). Nagel and Bergeron [3-45]) estimated that the relative number of boron ions in four-coordination was about 50% for a melt of composition $Na_2O \cdot 2\,B_2O_3$ at temperatures near the transformation range.

All this evidence suggests that the diborate group (a_2c_2) is the predominant group in sodium-borate glasses at about 33 mol % Na_2O. A minor number of "loose" BO_3 triangles (a) and a small number of "loose" BO_4 tetrahedra (c) is probably present too.

The Raman spectra of the glasses 0·30 Na_2O . 0·70 B_2O_3 and 0·30 K_2O . 0·70 B_2O_3 show a close similarity. However, the strongest peak is observed at slightly different cm^{-1} values. This may indicate that in the glass 0·30 K_2O . 0·70 B_2O_3 the network is not built up of diborate groups (a_2c_2) only. The calculations in sec. 3.3.3 show that di-triborate groups (ac_2) may be present if also a reasonable number of "loose" BO_3 triangles is formed. Crystalline K_2O . 2 B_2O_3 is built up of diborate groups (a_2c_2), di-triborate groups (ac_2) and "loose" BO_3 triangles. However, the Raman spectra of vitreous 0·30 K_2O . 0·70 B_2O_3 and crystalline K_2O . 2 B_2O_3 do not show a close similarity. This suggests no close similarity in structure. Hence, most probably, the glass of composition 0·30 K_2O . 0·70 B_2O_3 is built up of a major number of diborate groups (a_2c_2), a minor number of "loose" BO_3 triangles and a small number of "loose" BO_4 tetrahedra. The presence of small numbers of di-triborate (ac_2) and ring-type metaborate groups (b_3) is not excluded.

The Raman spectrum of lithium-borate glass with 33 mol % Li_2O is shown in fig. 3.21. Due to the similarity of the spectrum to that of the sodium-borate glass at $x = 0{\cdot}30$ it is suggested that in this case also diborate groups (a_2c_2) are formed in major numbers.

The Raman spectra of vitreous and crystalline Cs_2O . 3 B_2O_3 are not identical (cf. figs 3.24 and 3.5). This indicates that the glass is not built up of a random network of triborate groups (a_2c). The spectrum of the glass shows a close similarity to that of the glass 0·25 Na_2O . 0·75 B_2O_3. This suggests that tetraborate (a_6c_2) and diborate groups (a_2c_2) and "loose" BO_3 triangles (a) and "loose" BO_4 tetrahedra (c) are present. It is evident that no boroxol groups (a_3) are present. This picture on the structure is confirmed by the n.m.r. measurements of Rhee and Bray [3-65]).

It can be concluded that in the composition range 20 *to* 35 *mol % alkali oxide the tetraborate groups (a_6c_2) are gradually replaced by diborate groups (a_2c_2) on increase of the alkali-oxide content. At the diborate composition ($x = 0{\cdot}33$) the network is mainly built up of diborate groups (a_2c_2). Minor numbers of "loose"* BO_3 *triangles (a) and small numbers of "loose"* BO_4 *tetrahedra (c) and ring-type metaborate groups (b_3) are probably present too.*

Borate glasses with 40 *to* 50 *mol % alkali oxide*

Figures 3.17 and 3.18 show some spectra of borate glasses containing a mixture of 40 mol % and more alkali oxides. In the spectra one may observe a shift and rise of the peak at about 540 cm^{-1} on decreasing the amount of B_2O_3. In the spectrum of the glass with 48 mol % B_2O_3 (cf. fig. 3.17) this peak

is very strong, lies at 560 cm^{-1} and is strongly polarized. This becomes clear from fig. 3.18 showing the spectra for the directions $x(zz)y$ and $x(zx)y$ for a glass with 52 mol % B_2O_3. Due to its polarization behaviour the peak must be assigned to a symmetric vibration, a conclusion which is not contradicted by the infrared spectra. The Raman spectra of the crystalline compounds do not indicate clearly what type of group may be involved. The Raman spectrum of the compound $Na_2O \cdot 2\,B_2O_3 \cdot 10\,H_2O$ shows a strong peak at 580 cm^{-1}, so it may be that the peak in the spectra is caused by an "isolated" diborate group as in the compound $Na_2O \cdot 2\,B_2O_3 \cdot 10\,H_2O$. This means that where H^+ ions are bonded to non-bridging oxygen ions of the "isolated" diborate group in $Na_2O \cdot 2\,B_2O_3 \cdot 10\,H_2O$, in the case of the glasses, alkali ions are now bonded to these non-bridging oxygen ions. The Raman spectrum of the compound $3\,Li_2O \cdot 2\,B_2O_3$ which could have had this type of groups shows no strong peak at 560 cm^{-1} (cf. fig. 3.9), hence analogous groups are probably not formed.

Another reason that makes it uncertain that this peak should be ascribed to the suggested type of "isolated" diborate group is the presence of peaks at 820 cm^{-1} and 940 cm^{-1} in the spectra. These peaks should be attributed to pyroborate groups ($B_2O_5^{4-}$) and orthoborate units (BO_3^{3-}) as becomes clear on comparison with spectra of compounds containing these groups (cf. figs 3.1 and 3.2). The presence of a significant number of such groups leaves no possibility of the existence of "isolated" diborate groups due to the alkali-to-boron ratio in these glasses.

The presence of the peak at 760 cm^{-1} reveals the presence of a significant amount of BO_4 units up to 48 mol % B_2O_3, most probably in diborate groups (a_2c_2). This view is supported by some calculations given in sec. 3.3.3. It is clear from figs 3.17 and 3.18 that no high proportion of ring-type or chain-type metaborate groups are formed in borate glasses with about 50 mol % B_2O_3. This is based on the absence of strong peaks at about 630 and 730 cm^{-1} in the spectra. The non-bridging oxygen ions are probably primarily formed in connection with pyroborate groups (b_2''), orthoborate units (b''') or "loose" BO_3 triangles with a non-bridging oxygen ion (b). Calculations, given in sec. 3.3.3, support this view. Crystallization of these mixed alkali glasses around 50 mol % B_2O_3 results primarily in the formation of ring-type metaborate groups (cf. fig. 3.24).

It can be concluded that at $x = 0{\cdot}50$ *the structure is built up of a major number of diborate groups* (a_2c_2), *reasonable numbers of orthoborate units* (b'''), *pyroborate groups* (b_2'') *and "loose"* BO_3 *triangles with or without a non-bridging oxygen ion* (b *and* a). *The presence of a small number of ring-type metaborate groups* (b_3) *is indicated.*

Borate glasses with alkaline-earth oxides

In figs 3.19, 3.20 and 3.21 some spectra are shown of glasses containing alkaline-earth ions. From the spectrum of the glass of composition 0·20 BaO . 0·80 B_2O_3, melted at 1200 °C, it becomes evident that no boroxol groups are present in this glass and that in principle all the BaO is used for the formation of BO_4 units, as evidenced by the characteristic peak at about 775 cm^{-1}.

One is inclined to think that these BO_4 tetrahedra are connected to each other, so that one Ba^{2+} ion can compensate the negative charge of two BO_4 units close to one another. An indication of this is found in the structure of the compound BaO . 2 B_2O_3. From the Raman spectra it is not suggested that pairs of BO_4 tetrahedra are formed in vitreous 0·20 BaO . 0·80 B_2O_3. Pairs of BO_4 tetrahedra in diborate (a_2c_2) or di-triborate groups (ac_2) present in this glass necessarily results in the presence of boroxol groups which is not indicated.

Krogh-Moe [3–47]) showed by X-ray analysis the Ba–Ba distance in the glass of composition 0·20 BaO . 0·80 B_2O_3 to be 6·9 Å. This is an indication that the Ba^{2+} ions are not distributed randomly throughout the borate network. Moreover, this distance of 6·9 Å of Ba^{2+} ions is also found in the compound BaO . 4 B_2O_3. In the same article Krogh-Moe [3–47]) suggested the presence of tetraborate groups (a_6c_2) in glass of composition 0·20 BaO . 0·80 B_2O_3, similar to the tetraborate groups in the compound Na_2O . 4 B_2O_3. Unfortunately the crystal structure of the compound BaO . 4 B_2O_3 has not been revealed up to now; however, the unit-cell data of this compound show a high degree of similarity to those of Na_2O . 4 B_2O_3 (Krogh-Moe [3–47])). The suggestion of Krogh-Moe means that the BO_4 tetrahedra are not paired in vitreous 0·20 BaO . 0·80 B_2O_3.

Except for the 806-cm^{-1} peak the Raman spectra of the glasses of composition 0·20 BaO . 0·80 B_2O_3 and 0·20 Na_2O . 0·80 B_2O_3 (cf. figs 3.19 and 3.13) show great similarity. The infrared spectra of both glasses also show this close similarity. Thus, the glass of composition 0·20 BaO . 0·80 B_2O_3 is probably mainly built up of tetraborate groups (a_6c_2). In these tetraborate groups, however, the BO_4 tetrahedra are not connected to each other. This means that when the same type of tetraborate groups are present in glass of composition 0·20 BaO . 0·80 B_2O_3, the Ba^{2+} ions have to compensate the charges of BO_4 tetrahedra belonging to different borate groups. This is not impossible because the cations in Na_2O . 4 B_2O_3 appear in two crystallographically different environments and apparently serve to hold two independent networks together. The same may apply to the compound BaO . 4 B_2O_3.

It must be concluded along with Krogh-Moe [3–47]) that without evidence to the contrary, it is reasonable to believe that the borate network in the glass of composition 0·20 BaO . 0·80 B_2O_3 consists primarily of tetraborate groups (a_6c_2). The complete determination of the crystal structure of the compound

$BaO \cdot 4\ B_2O_3$ may solve the problem of the charge compensation. As for the alkali-borate glasses, most probably a minor number of "loose" BO_3 triangles (a) and "loose" BO_4 tetrahedra is present too.

Borate glasses containing 20 mol % mixed potassium oxide and alkaline-earth oxide show Raman spectra in which the peak at about 806 cm^{-1} is relatively stronger than in the spectrum of the glass of composition $0{\cdot}20\ K_2O \cdot 0{\cdot}80\ B_2O_3$ (cf. figs 3.19 and 3.15). This suggests that more boroxol groups are present in the mixed glasses than in the unmixed systems. That means that in the mixed systems there is a tendency to the formation of borate groups with a higher cation-to-boron ratio than of the tetraborate groups (a_6c_2), when one alkaline-earth ion is counted as equal to two alkali ions. The Raman spectra of the mixed systems further reveal the presence of BO_4 units, as can be expected, but do not allow a decision as to the type of borate group in which these BO_4 tetrahedra are incorporated. It is not clear why the replacement of BaO by K_2O should lead to a glass structure at the composition $0{\cdot}10\ K_2O \cdot 0{\cdot}10\ BaO \cdot 0{\cdot}80\ B_2O_3$ with more boroxol groups than in the unmixed glasses. It may mean that this effect shows the instability of the tetraborate groups (a_6c_2) in barium-tetraborate glass.

The spectra of the glasses of composition $0{\cdot}33\ SrO \cdot 0{\cdot}67\ B_2O_3$, $0{\cdot}30\ BaO \cdot 0{\cdot}70\ B_2O_3$ and $0{\cdot}30\ CaO \cdot 0{\cdot}70\ B_2O_3$ are rather similar to the spectra of the glasses of composition $0{\cdot}30\ Na_2O \cdot 0{\cdot}70\ B_2O_3$ and $0{\cdot}30\ K_2O \cdot 0{\cdot}70\ B_2O_3$ (cf. figs 3.21, 3.20, 3.14 and 3.15). This suggests a structural similarity of the glasses, and that in the case of the alkaline-earth-borate glasses also six-membered borate rings (a_pc_q) are formed. Block and Piermarini [3–48]) have shown that in vitreous and crystalline barium borates around the diborate composition, the shortest Ba–Ba distance is about equal in both cases. This suggests that the same types of borate groups are present in the crystal and in the glass. The $BaO \cdot 2\ B_2O_3$ crystals contain di-triborate (ac_2) and di-pentaborate groups (a_3c_2), so perhaps the same types of groups are present in vitreous $0{\cdot}30\ BaO \cdot 0{\cdot}70\ B_2O_3$. However, the X-ray results may also be explained by supposing that diborate groups (a_2c_2) are formed. The Raman spectra support this view.

A Raman spectrum of a glass of composition $0{\cdot}33\ SrO \cdot 0{\cdot}67\ B_2O_3$ could be obtained. The compound $SrO \cdot 2\ B_2O_3$ has a crystal structure deviating somewhat from other borate compounds of this composition, which is reflected in its Raman spectrum. Due to the low similarity of the spectra of vitreous and crystalline $SrO \cdot 2\ B_2O_3$ it may be concluded that no structural units are present in the glass that resemble the units in the crystal. This is confirmed by infrared spectroscopy.

Influence of Al_2O_3

The influence of increasing amounts of Al_2O_3 on the Raman spectra is shown in figs 3.22 and 3.23. For the glass of composition $0{\cdot}20\ K_2O \cdot 0{\cdot}80\ B_2O_3$

one may observe that the addition of 10 mol % Al_2O_3 results in an increase of the peak at 806 cm^{-1} and a decrease of the peak at 770 cm^{-1} (cf. figs 3.15 and 3.22). Adding 20 mol % Al_2O_3 results in the disappearance of the peak at 770 cm^{-1} in the Raman spectrum (fig. 3.22). This means that the addition of Al_2O_3 leads to a decrease in the amount of BO_4 tetrahedra and a back formation of boroxol groups. Al_2O_3, probably incorporated in the structure as AlO_4 units, unfortunately does not produce new peaks in the Raman spectra in the wavenumber range studied, so that this hypothesis cannot be directly checked.

The effect of the addition of up to 40 mol % Al_2O_3 to a glass of composition 0·30 K_2O . 0·70 B_2O_3 is also shown in fig. 3.22. The spectrum of the base glass is shown in fig. 3.15. In this case also the BO_4 units are most probably replaced by AlO_4 units, and boron ions are present in boroxol groups.

Addition of increasing amounts of Al_2O_3 to a glass of composition 0·15 Li_2O . 0·15 Na_2O . 0·15 K_2O . 0·55 B_2O_3 leads to the disappearance of the unidentified peak at 540 cm^{-1} (cf. fig. 3.23). The spectrum of the glass with 30 mol % is difficult to interpret completely. It becomes clear that BO_4 units are still present and that back-formation of boroxol groups has probably not taken place. The peak at 620 cm^{-1} is probably due to ring-type metaborate groups (b_3).

3.3.3. *Semiquantitative discussion of results*

Introduction

Krogh-Moe [3–49]) and Bray and O'Keefe [3–46]) have concluded from the results of their n.m.r. measurements that the excess of oxygen ions in borate glass, introduced by alkali oxide up to a content of about 30 mol % alkali oxide, are exclusively used for the formation of BO_4 tetrahedra. Only beyond this composition will part of the excess oxygen ions be used for the formation of non-bridging oxygen ions.

In his work on the structural interpretation of melting-point depression in sodium-borate melts, Krogh-Moe [3–43]) has concluded to the presence of boroxol (a_3), tetraborate (a_6c_2) and diborate groups (a_2c_2) in the melt up to about 33 mol % Na_2O. The concentration of these groups depends on the composition of the melt.

Beekenkamp [3–50]) has proposed a hypothesis for the structure of alkali-borate glasses which enabled him to explain qualitatively the viscosity, electrical conduction, optical absorption and thermal expansion versus composition behaviour of borate glasses. In this model the following assumptions were made:

— BO_4 tetrahedra cannot be bonded to each other,
— non-bridging oxygen ions occur only in BO_3 triangles and are absent in BO_4 tetrahedra.

Except for these rules this model is essentially a random-network model. In this model it is further proposed that from about 15 mol % alkali oxide on a significant amount of non-bridging oxygen ions is gradually formed. The relative number of boron ions in four-coordination by oxygen N_4 is given by the semi-empirical formula

$$N_4 = \frac{x}{100 - x} \frac{1}{1 + \exp(0{\cdot}115\,x - 4{\cdot}8)}$$

in which x is the mol percentage alkali oxide. The values of N_4 that can be calculated in this way do not differ greatly from the proposals by Krogh-Moe [3-43,49]) and Bray and O'Keefe [3-46]).

The Raman spectra shown in this chapter clearly indicate that up to about 30 mol % alkali oxide no significant amount of ring-type metaborate groups are formed. This result is fairly consistent with the n.m.r. data of Krogh-Moe [3-49]) and Bray and O'Keefe [3-46]). It also fits in with the results of the melting-point depression, discussed by Krogh-Moe [3-43]). From the Raman spectra the presence of $a_p c_q$ groups cannot be excluded. The melting-point-depression results, as discussed by Krogh-Moe [3-43]), exclude the presence of loose triborate groups (a_2c) in sodium-borate melts. From the Raman spectra it becomes clear that pentaborate groups (a_4c) are not formed in any significant amount, which is in accordance with the conclusions of Krogh-Moe [3-43]) of the melting-point-depression data and the X-ray work on silver-borate and caesium-borate glasses (Willis and Hennessy [3-51]) and Krogh-Moe [3-52])) that revealed pair formation of the cations in these glasses, supporting the idea that tetraborate groups (a_6c_2) are formed in the appropriate composition area.

According to Beekenkamp's [3-50]) formula for N_4, at 30 mol % alkali oxide, 9 % of the boron ions should be bonded to a non-bridging oxygen ion. If this formula for N_4 is correct then these boron triangles with a non-bridging oxygen ion should be a part of a borate group, as for instance the diborate group, rather than be grouped together in ring-type metaborate as suggested by the Raman spectra. This remains a problem because it is not known how the presence of a non-bridging oxygen ion in a large borate group influences the vibrational frequencies of this borate group. If indeed 9 % of the boron atoms is bonded to a non-bridging oxygen ion, and if, according to Krogh-Moe [3-43]) the melt at 30 mol % Na_2O primarily contains diborate (a_2c_2) and tetraborate groups (a_6c_2), then on average one in every two to three diborate groups (a_2c_2) is disturbed, and practically all the tetraborate groups are disturbed.

The general qualitative conclusion may be that the Raman spectra are fairly consistent with the work of Krogh-Moe [3-43]) showing the presence of boroxol (a_3), tetraborate (a_6c_2) and diborate groups (a_2c_2) in borate melts up to about 30 mol % sodium oxide. The Raman spectra also fit in well with the n.m.r. data of Krogh-Moe [3-47]) and Bray and O'Keefe [3-46]).

Discussion

For the presence of certain groups in borate glasses three equations can be derived between a number of variables that will be defined below:

$$a + b + c + d + \ldots = 1,$$
$$p_a a + p_b b + p_c c + p_d d + \ldots = N_4,$$
$$q_a a + q_b b + q_c c + q_d d + \ldots = x/(1-x),$$

in which

$a, b, c, d \ldots$ are the fractions of boron ions in different types of borate groups,
$p_a, p_b, p_c, p_d, \ldots$ are the fractions of the boron ions of a certain type of borate group that are in four-coordination by oxygen ions,
$q_a, q_b, q_c, q_d, \ldots$ are the alkali-to-boron ratios of different types of borate groups,
N_4 is the total relative amount of boron ions in four-coordination of oxygen ions,
x is the mol fraction of alkali oxide,
$1 - x$ is the mol fraction of boron oxide.

For example, if a stands for the fraction of boron ions present in diborate groups, then $p_a = \frac{1}{2}$ because diborate groups are built up of two BO_4 tetrahedra and two BO_3 triangles, and $q_a = \frac{1}{2}$ because the diborate group contains 4 boron ions and 2 alkali ions.

For the values of $x = 0{\cdot}17$, $0{\cdot}20$, $0{\cdot}33$ and $0{\cdot}50$, calculations will be given for the relative presence of certain groups and the possible variation in this amount.

$x = 0{\cdot}17$

From the qualitative discussion in sec. 3.3.2 it has become clear that mainly six-membered rings with a BO_4 tetrahedron are formed. These rings can be present as triborate groups (a_2c) or tetraborate groups (a_6c_2). Hence at $x = 0{\cdot}17$ the most probable groups and units are boroxol (a_3), triborate (a_2c) and tetraborate groups (a_6c_2), "loose" BO_3 triangles (a) and "loose" BO_4 tetrahedra (c) not present in a six-membered ring.

If a is the fraction of boron ions in boroxol groups, b the fraction in triborate groups, c the fraction in tetraborate groups, d the fraction in "loose" BO_3 triangles and e the fraction in "loose" BO_4 tetrahedra, then the equations become

$$a + b + c + d + e = 1,$$
$$\tfrac{1}{3} b + \tfrac{1}{4} c + e = N_4 = x/(1-x) \approx 0{\cdot}20.$$

If $c = d = e = 0$, then $a = 0{\cdot}40$ and $b = 0{\cdot}60$. Hence, the ratio boroxol groups/triborate groups $= \frac{2}{3}$, which is very reasonable in comparison with the Raman spectra.

If $c = 0{\cdot}20$ and $d = e = 0$, then $b = 0{\cdot}45$ and $a = 0{\cdot}35$. Hence the proportion boroxol : triborate : tetraborate $= 0{\cdot}35/3 : 0{\cdot}45/3 : 0{\cdot}20/8 \approx 40 : 51 : 9$. This proportion is also not unreasonable in comparison with the spectra.

If $c = 0{\cdot}50$ and $d = e = 0$, then $b = 0{\cdot}225$ and $a = 0{\cdot}275$. Hence the proportion boroxol : triborate : tetraborate $= 0{\cdot}275/3 : 0{\cdot}225/3 : 0{\cdot}50/8 \approx 40 : 33 : 27$. This proportion does not fit in so well with the spectra because according to this result the boroxol peak in the spectrum should have about $\frac{1}{3}$ the height of the peak at 770 cm^{-1}, which is not the case.

The conclusion from the above calculations can be that borate glass at $x = 0{\cdot}17$ may be built up of a major number of boroxol and triborate groups and a minor number of tetraborate groups. However, these calculations are uncomplete because d and e were always taken zero.

The calculations will now be confined to a model of the structure with boroxol, tetraborate groups, "loose" BO_3 units and "loose" BO_4 tetrahedra. Hence the equations become

$$a + c + d + e = 1,$$

$$\tfrac{1}{4}c + d = N_4 \approx 0{\cdot}20.$$

If $d = 0$, then $c = 0{\cdot}80$ and $a + e = 0{\cdot}20$; if $e = 0$ then $a = 0{\cdot}20$ and the proportion boroxol : tetraborate $= 0{\cdot}20/3 : 0{\cdot}80/8 = 40 : 60$. This proportion does not fit in so well with the spectra because according to this result the boroxol peak in the spectrum should have about $\frac{1}{4}$ the height of the peak at 770 cm^{-1}, which is not the case. Thus the network is not built up of boroxol and tetraborate groups only. A small increase of e would sufficiently correct the above result.

If $d = 0{\cdot}1$, then $c = 0{\cdot}40$ and $a + e = 0{\cdot}50$, if $e = 0$ then $a = 0{\cdot}50$. This result does not fit in with the spectra because the calculated relative number of boroxol groups is too high. If $e = 0{\cdot}30$ then $a = 0{\cdot}20$. Then the proportion boroxol : tetraborate : BO_3 : $BO_4 = 0{\cdot}20/3 : 0{\cdot}40/8 : 0{\cdot}1 : 0{\cdot}30 \approx 13 : 10 : 20 : 67$. This result fits in with the spectra, although the total number of boroxol and tetraborate groups seems too low.

The conclusion from these calculations at $x = 0{\cdot}17$ is that the network is built up of

(1) a major number of boroxol groups and triborate groups and a minor number of tetraborate groups, or

(2) a major number of boroxol and tetraborate groups with at the same time a reasonable number of "loose" BO_3 triangles and a small number of "loose" BO_4 tetrahedra.

This discussion on the structure is continued for the composition with $x = 0{\cdot}20$.

$x = 0{\cdot}20$

At $x = 0{\cdot}20$ the most probable groups are boroxol (a_3), triborate (a_2c),

tetraborate (a_6c_2), diborate (a_2c_2) and possibly a few metaborate groups (b_3). BO_3 triangles (a) and BO_4 tetrahedra (c) may be present as "loose" units, not belonging to a typical borate ring.

Analogous to the calculations at $x = 0{\cdot}17$, first d and e will be taken zero. The equations then become

$$a + b + c + f + g = 1,$$
$$\tfrac{1}{3}b + \tfrac{1}{4}c + \tfrac{1}{2}f = N_4,$$
$$\tfrac{1}{3}b + \tfrac{1}{4}c + \tfrac{1}{2}f + g = x/(1-x) = 0{\cdot}25,$$

in which f is the fraction of boron ions in diborate groups and g the fraction of boron ions in metaborate groups.

According to Beekenkamp [3-50] $N_4 = 0{\cdot}23$, hence $g = 0{\cdot}02$ and the equations become

$$a + b + c + f = 0{\cdot}98,$$
$$\tfrac{1}{3}b + \tfrac{1}{4}c + \tfrac{1}{2}f = 0{\cdot}23.$$

If $c = f = 0$, then $b = 0{\cdot}69$ and $a = 0{\cdot}29$. In this case the ratio boroxol groups/triborate groups fits in with the spectra.

If $c = 0{\cdot}20$ and $f = 0$, then $b = 0{\cdot}56$ and $a = 0{\cdot}22$. The proportion then becomes boroxol : triborate : tetraborate : metaborate = $0{\cdot}22/3 : 0{\cdot}56/3 : 0{\cdot}20/8 : 0{\cdot}02/3 \approx 25 : 65 : 8 : 2$. This proportion is quite reasonable.

If $c = 0{\cdot}50$ and $f = 0$, then $b = 0{\cdot}315$ and $a = 0{\cdot}165$. The proportion then becomes boroxol : triborate : tetraborate : metaborate = $0{\cdot}165/3 : 0{\cdot}315/3 : 0{\cdot}50/8 : 0{\cdot}02/3 \approx 24 : 46 : 27 : 3$. This result does not fit in well. Compared to the spectra the calculated number of boroxol groups is too small.

If $b = f = 0$, then $c = 0{\cdot}92$ and $a = 0{\cdot}06$. The ratio boroxol groups/tetraborate groups then becomes about $\frac{1}{6}$, which is too low compared to the spectra.

If $b = 0$ and $f = 0{\cdot}1$, then $c = 0{\cdot}56$ and $a = 0{\cdot}32$. The proportion then becomes boroxol : tetraborate : diborate : metaborate = $0{\cdot}32/3 : 0{\cdot}56/3 : 0{\cdot}10/4 : 0{\cdot}02/3 \approx 33 : 57 : 8 : 2$. This proportion is reasonable compared to the spectra.

If $b = 0$ and $f = 0{\cdot}2$, then $c = 0{\cdot}39$ and $a = 0{\cdot}39$. The proportion then becomes boroxol : tetraborate : diborate : metaborate = $0{\cdot}39/3 : 0{\cdot}39/3 : 0{\cdot}20/4 : 0{\cdot}02/3 \approx 41 : 41 : 16 : 2$. Compared to the spectra the number of calculated boroxol groups is too high.

For the case that $d = e = 0$ the conclusions on the structure of borate glass are as follows:

(1) a major number of triborate groups is present, a reasonable number of boroxol groups and small numbers of diborate and metaborate groups, or
(2) a major number of tetraborate groups is present, a reasonable number of boroxol groups (somewhat higher than under (1)) and small numbers of diborate and metaborate groups.

Now the situation will be looked at in which d and/or e are unequal to zero. If $b = f = 0$ and $g = 0{\cdot}02$ then the equations become

$$a + c + d + e = 0{\cdot}98,$$

$$\tfrac{1}{4}c + d = 0{\cdot}20.$$

If $d = 0$, then $c = 0{\cdot}80$ and $a + e = 0{\cdot}18$. If $e = 0{\cdot}05$ then $a = 0{\cdot}63$. The proportion then becomes boroxol : tetraborate : BO_3 : BO_4 : metaborate = $0{\cdot}13/3 : 0{\cdot}80/8 : 0{\cdot}25 : 0 : 0{\cdot}02/3 \approx 21 : 50 : 25 : 0 : 4$. Compared to the spectra the calculated numbers are reasonable.

If $d = 0{\cdot}1$, then $c = 0{\cdot}40$ and $a + e = 0{\cdot}48$. If $e = 0{\cdot}40$ then $a = 0{\cdot}08$. The proportion then becomes boroxol : tetraborate : BO_3 : BO_4 : metaborate = $0{\cdot}08/3 : 0{\cdot}40/8 : 0{\cdot}1 : 0{\cdot}4 : 0{\cdot}02/3 \approx 6 : 8 : 17 : 68 : 1$. Compared to the spectra the calculated ratio boroxol groups/tetraborate groups is reasonable, but the total calculated number of these groups seems relatively low.

The conclusion from the calculations with $b = 0$ and d and e unequal to zero is that the structure indeed may be built up of a major number of tetraborate groups, a minor number of boroxol groups, a minor number of "loose" BO_3 triangles, and a small number of "loose" BO_4 tetrahedra and metaborate groups.

As is discussed in sec. 3.3.2 this last conclusion is the most probable when other results are also taken into account.

$x = 0{\cdot}33$

At $x = 0{\cdot}33$ the most probable groups are tetraborate (a_6c_2), triborate (a_2c), diborate (a_2c_2) and metaborate groups (b_3), and "loose" BO_3 triangles (a) and "loose" BO_4 tetrahedra (c).

If the concentration of triborate groups (a_2c) and "loose" BO_3 triangles and "loose" BO_4 tetrahedra is taken zero, then the equations become

$$c + f + g = 1,$$

$$\tfrac{1}{4}c + \tfrac{1}{2}f = N_4,$$

$$\tfrac{1}{4}c + \tfrac{1}{2}f + g = x/(1 - x) = 0{\cdot}50.$$

If $N_4 = 0{\cdot}32$, according to Beekenkamp, then $g = 0{\cdot}18$ and the equations become

$$c + f = 0{\cdot}82,$$

$$\tfrac{1}{4}c + \tfrac{1}{2}f = 0{\cdot}32,$$

giving $c = 0{\cdot}36$ and $f = 0{\cdot}46$. Then the proportion becomes tetraborate : diborate : metaborate $\approx 21 : 52 : 27$.

If we compare the results of these calculations with the actual Raman spectra, then the impression arises that if non-bridging oxygen ions are present in borate

glasses up to 33 mol % alkali oxide according to the formula given by Beekenkamp, these cannot be grouped together to a large extent in ring-type metaborate groups (b_3). Based on the Raman spectra, the presence of non-bridging oxygen ions connected to borate groups cannot be excluded but n.m.r. and melting-point-depression-data, discussed earlier, do not suggest this presence in a significant amount in sodium-borate glass of this composition. The conclusion is that the value of N_4 given by Beekenkamp is probably too low at $x = 0{\cdot}33$.

The Raman spectra of sodium- and potassium-borate glasses at $x = 0{\cdot}30$ indicate the presence of only a very small number of metaborate groups (b_3). Hence g will be taken zero in the calculations below. This means that no tetraborate (a_6c_2) and triborate groups (a_2c) can be present, if no groups are present with a sufficiently high alkali-to-boron ratio.

Thus, if no groups are present with a higher alkali-to-boron ratio than 0·5, then the network must mainly be built up of diborate groups (a_2c_2) and a minor number of "loose" BO_3 triangles and "loose" BO_4 tetrahedra (c). However, crystalline $Na_2O \cdot 2\ B_2O_3$ and $K_2O \cdot 2\ B_2O_3$ contain groups with six-membered borate rings with two BO_4 tetrahedra in the ring. Therefore, di-triborate groups (ac_2) may be present in the glasses of this composition. Some calculations are given below for the situation that the network is built up of diborate groups (a_2c_2), di-triborate groups (ac_2), "loose" BO_3 triangles and "loose" BO_4 tetrahedra. If h is the fraction of boron ions in di-triborate groups (ac_2), then the equations become (N_4 is taken 0·50, this is the maximum value)

$$d + e + f + h = 1,$$
$$e + \tfrac{1}{2}f + \tfrac{2}{3}h = N_4 = 0{\cdot}50.$$

If $e = 0{\cdot}1$, then the equations become

$$d + f + h = 0{\cdot}9,$$
$$\tfrac{1}{2}f + \tfrac{2}{3}h = 0{\cdot}40.$$

If $h = 0{\cdot}1$, then

$$d + f = 0{\cdot}8,$$
$$\tfrac{1}{2}f = 0{\cdot}33,$$

which yields $d = 0{\cdot}14$ and $f = 0{\cdot}66$.

If $h = 0{\cdot}3$ then

$$d + f = 0{\cdot}70,$$
$$\tfrac{1}{2}f = 0{\cdot}20,$$

which yields $d = 0{\cdot}30$ and $f = 0{\cdot}40$.

These calculations learn that di-triborate groups (ac_2) may indeed be present if a reasonable number of "loose" BO_3 triangles is present at the same time.

$x = 0{\cdot}50$

At $x = 0{\cdot}50$ the most probable groups are orthoborate (b'''), pyroborate (b_2''), metaborate (b_3), diborate (a_2c_2), di-triborate groups (ac_2), "loose" BO_3 triangles (a) and "loose" BO_4 tetrahedra (c).

Suppose that the fractions of boron ions in orthoborate and pyroborate groups are respectively i and j. According to Beekenkamp $N_4 = 0{\cdot}28$ at $x = 0{\cdot}50$.

If $d = e = h = 0$, then the equations become

$$f + g + i + j = 1,$$
$$\tfrac{1}{2}f = N_4 = 0{\cdot}28,$$
$$\tfrac{1}{2}f + g + 3i + 2j = x/(1 - x) = 1{\cdot}00.$$

This yields $f = 0{\cdot}56$ and the equations become

$$g + i + j = 0{\cdot}44,$$
$$g + 3i + 2j = 0{\cdot}72;$$

hence

$$2i + j = 0{\cdot}28.$$

Thus, if $i = 0{\cdot}10$, then $j = 0{\cdot}08$ and $g = 0{\cdot}26$.

Compared to the spectra this value of g (metaborate groups) is too high. Other reasonable values of i and j give also too high values of g. A higher value of N_4 would decrease the calculated fraction of metaborate groups. This would fit in better with the spectra. Lower values of g are also obtained if the presence of "loose" BO_3 triangles with one non-bridging oxygen ion (b) is allowed.

The presence of di-triborate groups (ac_2) would also give rise to too high values of g. This means on the other hand that the presence of di-triborate groups (ac_2) is not very probable. The presence of "loose" BO_3 triangles (a) would lower the value of g.

The conclusion from these calculations is that at 50 mol % alkali oxide the network contains a reasonable number of diborate groups (a_2c_2) and minor numbers of orthoborate units (b'''), pyroborate groups (b_2''), "loose" BO_3 triangles (a), "loose" BO_3 triangles with one non-bridging oxygen ion (b) and a small number of metaborate groups (b_3). A small number of "loose" BO_4 tetrahedra (c) cannot be excluded.

3.3.4. *Conclusions*

All the results of the Raman spectroscopy of borate glasses are summarized in table 3-I. This table gives a qualitative impression of the presence of borate groups in several composition areas.

TABLE 3-I

The presence of borate groups in alkali-borate glasses in several composition areas

0–20 mol % R_2O	20–35 mol % R_2O	35–50 mol % R_2O
boroxol (a_3)		
	tetraborate (a_6c_2)	diborate (a_2c_2)
tetraborate (a_6c_2)	diborate (a_2c_2)	
"loose" BO_3 triangles (a)	"loose" BO_3 triangles (a)	metaborate (b_3)
"loose" BO_4 tetrahedra (c)	"loose" BO_4 tetrahedra (c)	pyroborate (b_2'')
		orthoborate (b''')
		"loose" BO_3 triangles (a)
		"loose" BO_3 triangles (b)

Raman spectroscopy of sodium- and potassium-borate glasses has proved the gradual decrease of the number of boroxol groups (a_3) in the composition area 0–25 mol % alkali oxide. In this same composition area tetraborate groups (a_6c_2) are formed primarily on increase of the alkali-oxide content.

Somewhat before the 20 mol % alkali oxide, borate groups are formed with a higher cation-to-boron ratio than in tetraborate groups. Raman spectroscopy does not reveal the nature of these groups exactly, but probably these are diborate groups (a_2c_2).

At about 30 mol % alkali oxide the borate glasses contain only a very small number of ring-type metaborate groups (b_3). From 40 to 50 mol % alkali oxide the formation of orthoborate units (b''') and pyroborate (b_2'') groups is clear. At 50 mol % alkali oxide the ring- and chain-type metaborate groups are not the most abundant groups. The BO_4 tetrahedra are probably mainly present in diborate groups (a_2c_2).

Due to the increase in line width of the bands in the spectra of the glasses compared to the spectra of the crystalline borates it is clear that the borate groups in the glasses are distorted. This distortion may take place in the bond angles and the lengths of the B–O bond. These distortions will not be the same for every borate group. From the Raman spectra it does not become clear how many non-bridging oxygen ions connected to the borate groups are formed. It may be, as in the triborate groups (*abc*) in the compound $Na_2O \cdot 2\ B_2O_3$, that this type of non-bridging oxygen ions is present in increasing amounts in borate glasses with more than about 20 mol % alkali oxide. This would explain the viscosity and thermal expansion versus composition behaviour of these borate

glasses.

Raman spectra of alkaline-earth-borate glasses show much similarity to those of corresponding alkali-oxide glasses. At 20 mol % BaO or CaO and 80 mol % B_2O_3 no boroxol groups (a_3) are present, most probably tetraborate groups (a_6c_2) are predominant in the glasses of this composition. At 30 mol % BaO and CaO, it is primarily borate groups with BO_4 tetrahedra that are formed, although it can, however, not be decided what type of borate groups is present in alkaline-earth (Ca and Ba) borate glasses of this composition. Most probably these groups are diborate groups (a_2c_2).

Introduction of Al_2O_3 in borate glasses with up to 30 mol % alkali oxide, clearly leads to a decrease in the number of borate groups containing BO_4 tetrahedra. Boron ions are again primarily present in boroxol groups (a_3) when enough Al_2O_3 is added to remove all the alkali oxide from the borate groups. In borate glasses with a higher alkali-oxide content it is not clear how addition of Al_2O_3 affects the borate network. There is no proof that boroxol groups (a_3) are formed again in this composition area.

The Raman spectra of the borate glasses indicate the presence of boron ions in large borate groups. However, based on the Raman spectra it is also probable that a small part of the boron ions is incorporated in a more random network of "loose" BO_3 triangles (a) and "loose" BO_4 tetrahedra (c) not present in a typical borate ring.

3.4. Raman spectra of silicate glasses

3.4.1. *Experimental results*

The Raman spectra of some vitreous silicates are shown in figures 3.25 to 3.27. Some spectra of potassium-aluminosilicate glasses are shown in fig. 3.28. All Raman spectra were recorded at room temperature, as a linear function of the wavenumber. For excitation the 632·8-nm line of a 6-mW He–Ne laser was used. The band width was always 10 cm^{-1}. For more details about the equipment the reader is referred to sec. 2.2.

Numbers in the Raman spectra close to the peaks show the position of the maxima of these peaks in cm^{-1}. In all spectra the direction of the incident and scattered light is shown, using the symbols explained in sec. 2.2.

3.4.2. *Discussion of results*

Raman spectra of vitreous silica and sodium-silicate glasses have been published by Hass [3–53]) and of lithium-, sodium- and potassium-silicate glasses by Etchepare [3–54]). Therefore only a small number of spectra of silicate glasses were measured by the author.

Hass [3–53]) interpreted the Raman spectrum of vitreous silica as follows. The band observed at about 1055 cm^{-1} is assigned to a vibration in which the

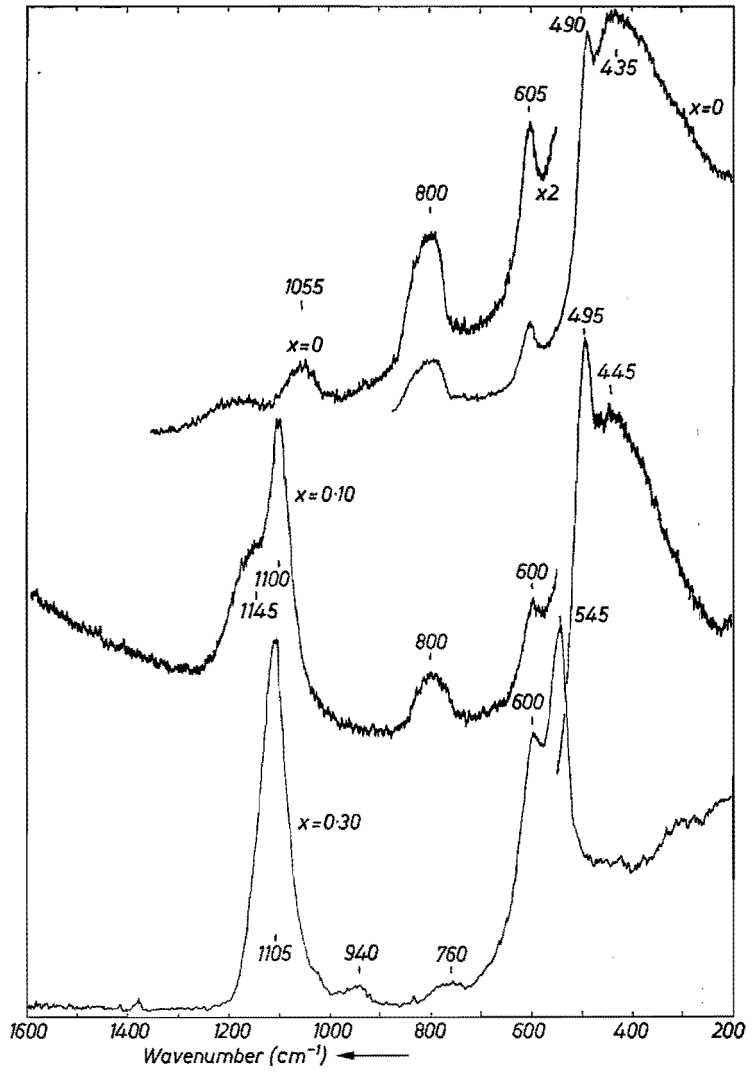

Fig. 3.25. Raman spectra of glasses in the system $x\ K_2O\ .\ (1-x)\ SiO_2$ (direction $x(zz+zx)y$).

bridging oxygen ions move in the opposite direction to their Si neighbours. The band at about 800 cm^{-1} is assigned to a "bond-bending" type of motion in which the oxygen ions move approximately at right angles to the Si–Si lines and in the Si–O–Si planes. At lower frequencies the peaks are not well defined, as the modes are no longer thought to be localized. However, the large peaks at 495 and 435 cm^{-1} may be taken as characteristic of the SiO_4 tetrahedron without non-bridging oxygen ions.

It is interesting to compare the spectra of the silicate glasses with those of the

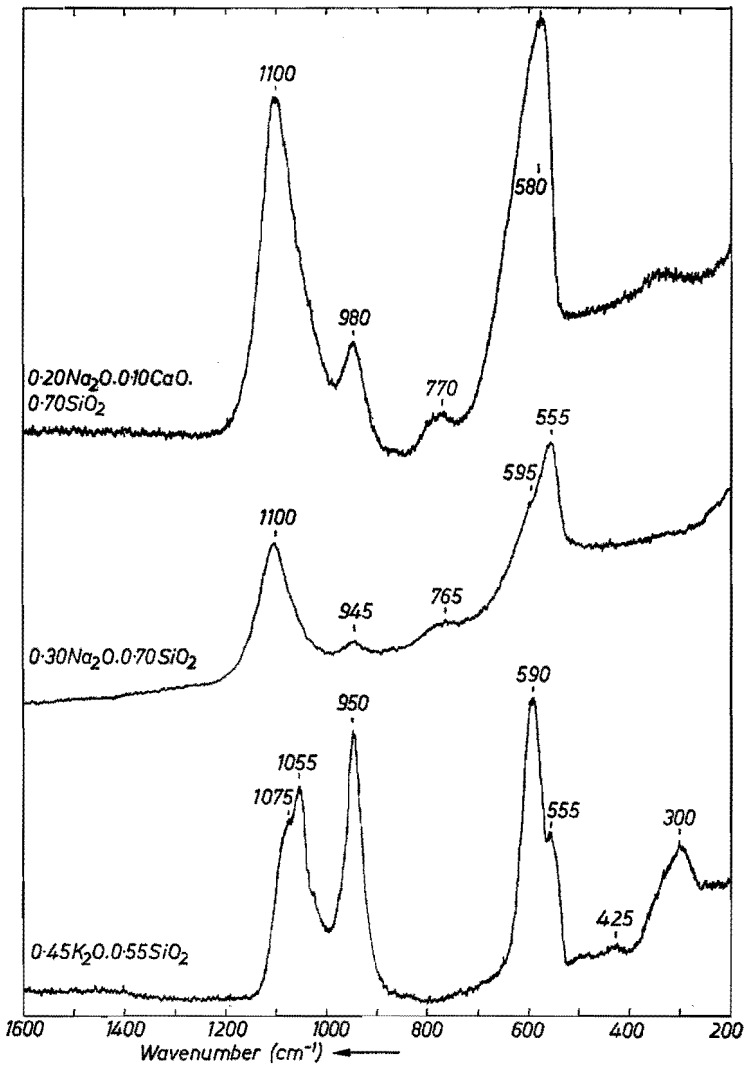

Fig. 3.26. Raman spectra of silicate glasses (direction $x(zz + zx)y$).

silicate compounds. In fig. 3.25 spectra are shown of potassium-silicate glasses. Comparison of the spectrum of the glass of composition 0·30 K_2O . 0·70 SiO_2 with that of the compounds α-Na_2O . 2 SiO_2 and Li_2O . 2 SiO_2 reveals a high degree of similarity (figs 3.25 and 3.10, cf. the large peaks at 530–550 cm^{-1} and at 1080–1100 cm^{-1}). This suggests that glass of composition 0·30 K_2O . 0·70 SiO_2 has primarily structural units similar to those in the disilicate compounds. The spectra of the glasses of composition 0·30 K_2O . 0·70 SiO_2, 0·30 Na_2O . 0·70 SiO_2 and 0·20 Na_2O . 0·10 CaO . 0·70 SiO_2 (figs 3.25 and

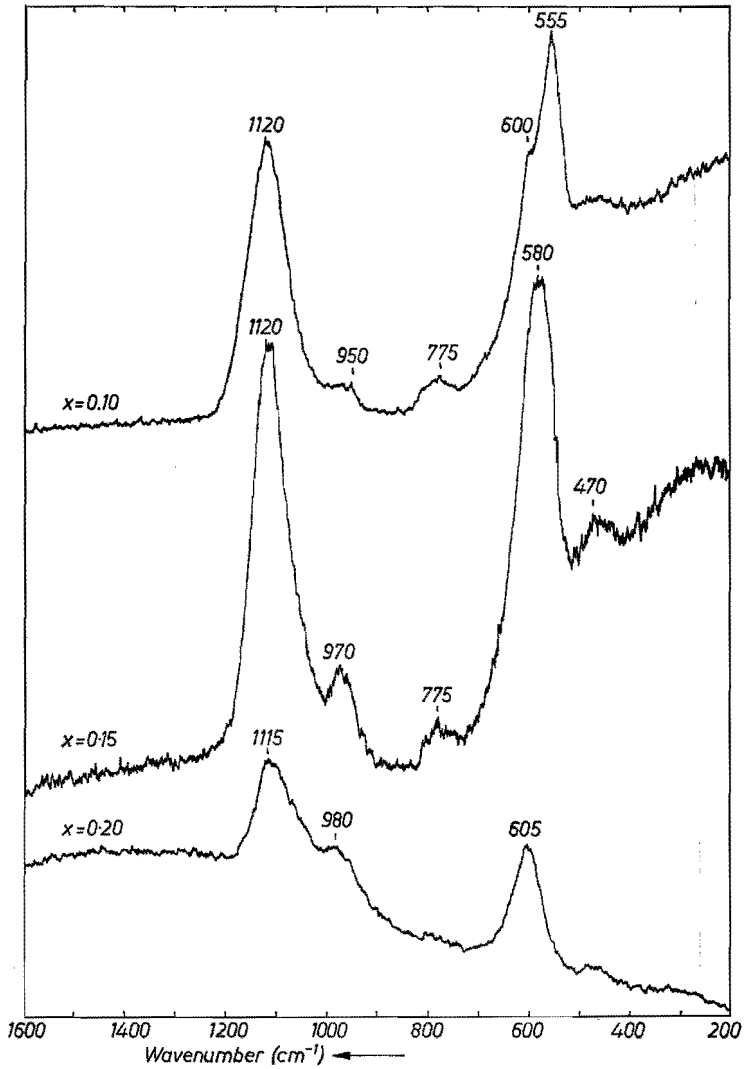

Fig. 3.27. Raman spectra of glasses in the system $0{\cdot}20\,K_2O\,.\,x\,MgO\,.\,(0{\cdot}80-x)\,SiO_2$ (direction $x\,(zz+zx)\,y$).

3.26) are all highly similar, which suggests that in all these glasses the main structural units are similar to those in the disilicate compounds so that primarily SiO_4 tetrahedra with one non-bridging oxygen ion are present in them. The small peak at 950 cm^{-1} in the spectrum of the CaO-containing glass reveals the presence of SiO_4 tetrahedra with two non-bridging oxygen ions.

The spectrum of the glass of composition $0{\cdot}45\,K_2O\,.\,0{\cdot}55\,SiO_2$ shows similarity with the spectra of the metasilicate compounds $Na_2O\,.\,SiO_2$ and

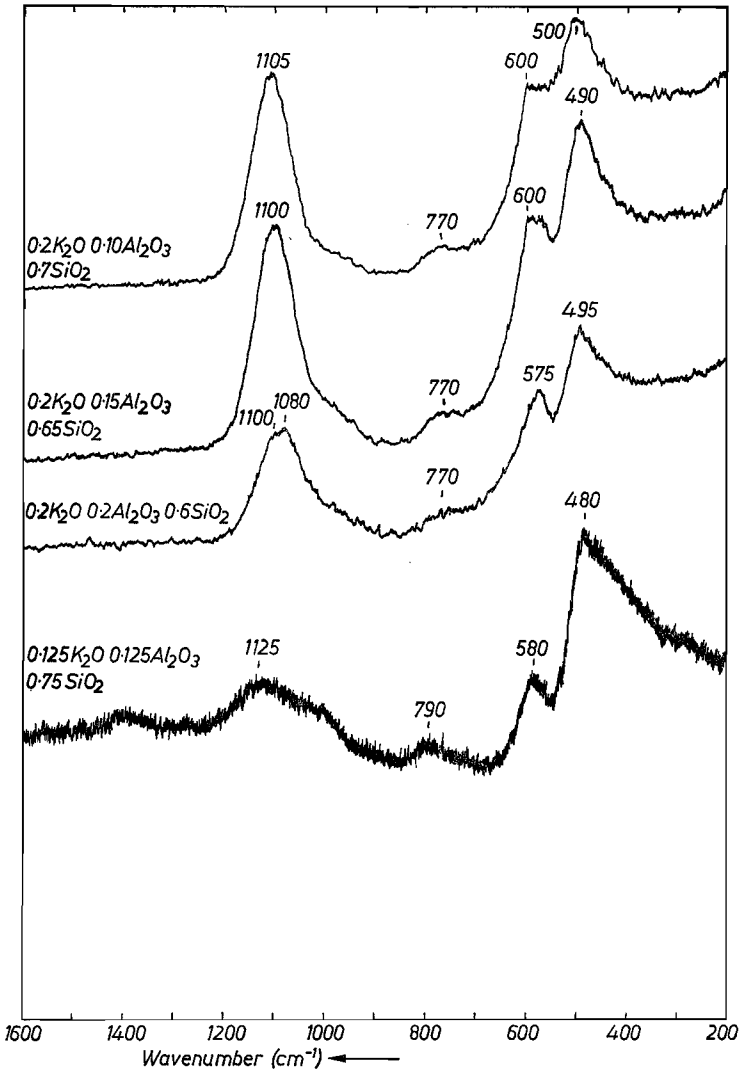

Fig. 3.28. Raman spectra of aluminosilicate glasses (direction $x(zz + zx)y$).

K_2O . SiO_2 (figs 3.26 and 3.10, cf. the large peaks at about 950 cm^{-1} and at 590 cm^{-1}). Thus, the presence of SiO_4 tetrahedra with two non-bridging oxygen ions is indicated. The presence of SiO_4 tetrahedra with one non-bridging oxygen ion is also indicated.

Some spectra of binary barium- and strontium-silicate glasses, published by Etchepare [3–55]) evince a highly similar behaviour compared to those of the alkali-silicate glasses. Again, around 30 mol % BaO the presence of disilicate units is indicated and, with increasing amounts of BaO and SrO, the spectra

acquire characteristics of those of metasilicate compounds. Thus, up to about 30 mol %, mainly SiO_4 tetrahedra with one non-bridging oxygen ion are formed and, from 30 mol % onwards these are gradually replaced by those containing two non-bridging oxygen ions. This behaviour is confirmed for CaO- and MgO-containing glass systems in this thesis (cf. figs 3.26 and 3.27).

From these Raman spectra of the silicate glasses it cannot be decided how far the structure of the disilicate and metasilicate crystals is retained in the glass. So it cannot be decided that in glass around the disilicate composition the rings of SiO_4 tetrahedra are also primarily present as in the compounds, although this may be the case. The spectrum of vitreous SiO_2 shows no unequivocal similarity to that of its polymorphs. Thus it cannot be decided from the Raman spectrum that the types of groups in vitreous SiO_2 are very much like those in one of its crystalline polymorphs.

Mozzi and Warren [3-57]) in their X-ray study on the structure of vitreous SiO_2 have found that most probably the silicon–oxygen–silicon bond angles vary within about 10% of their maximum in the distribution. This distribution of bond angles is wide enough to distinguish the structure from a crystalline arrangement, but is rather narrow compared to a completely random distribution of bond angles. Thus the structure of vitreous silica is quite uniform at short range, although there is no order beyond several layers of tetrahedra, corresponding to 20 to 30 Å. So it is not so strange that the Raman spectrum of vitreous silica is somewhat reminiscent of the spectra of its crystalline polymorphs.

From X-ray analysis the distribution of alkali or alkaline-earth ions in silicate glasses is uncertain. However, there is enough evidence to show that these ions are not uniformly distributed, but that their average nearest-neighbour separation is considerably less than for a uniform distribution. This situation is also found in crystalline $Li_2O \cdot 2\,SiO_2$ and α-$Na_2O \cdot 2\,SiO_2$ where the alkali-ion nearest-neighbour distances are definitely less than if the ions had been distributed uniformly. Thus there may be a tendency in alkali-silicate glasses of roughly disilicate composition to form the same type of structure as in the corresponding crystals. This picture is supported by the Raman spectra.

Some spectra of potassium-aluminosilicate glasses were recorded to investigate a possible similarity in the structure of aluminosilicate and borosilicate glasses (cf. fig. 3.28). A number of Raman spectra of sodium-aluminosilicate glasses were published by DiSalvo et al.[3-56]). In general the Raman spectra of the sodium- and potassium-aluminosilicate glasses show a high degree of similarity for equal alkali-oxide content. The fact that the spectra of the aluminosilicate glasses do not differ very much from those of silicate glasses suggests that the structure of silicate glasses does not change much on the introduction of aluminum ions. This is consistent with general ideas on the structure of aluminosilicate glasses. It is believed that the aluminum ions are tetrahedrally

coordinated by oxygen ions when enough alkali ions are present for charge compensation and that these tetrahedra are situated in the network where the SiO_4 tetrahedra may also be present, in a manner analogous to the structure of many crystalline aluminosilicate compounds.

3.4.3. *Conclusions*

From the Raman spectra of alkali- and alkaline-earth-silicate glasses it becomes clear that the addition of up to about 30 mol % alkali or alkaline-earth oxide to SiO_2 leads to the formation of SiO_4 tetrahedra with one non-bridging oxygen ion. The Raman spectra support X-ray experimental evidence that silicate glasses of roughly disilicate composition also show a somewhat sheet-like structure as in the crystalline disilicate compounds. This means that the structure is more ordered than a random network of SiO_4 tetrahedra suggests.

From about 30 to 45 mol % alkali or alkaline-earth oxide the units with one non-bridging oxygen ion are gradually replaced by those containing two of these oxygen ions. In this case, too, the Raman spectra do not contradict a certain ordering of the SiO_4 tetrahedra, like that found in metasilicate compounds.

3.5. Raman spectra of borosilicate glasses

3.5.1. *Experimental results*

The Raman spectra of a large number of borosilicate glasses are shown in figs 3.29 to 3.65. This concerns borosilicate glasses containing Li_2O, Na_2O, K_2O separately, Na_2O and K_2O mixed, CaO and BaO. In addition a number of spectra of glasses containing Al_2O_3 are shown. All Raman spectra were recorded at room temperature; for more details about the equipment used see sec. 2.2, and for other experimental details sec. 3.3.1.

3.5.2. *Discussion of results*

The discussion of the experimental results will gradually proceed from glasses with a low SiO_2 to those with a higher SiO_2 content.

Borosilicate glasses with 15 *mol* % SiO_2

The first series of spectra that will be discussed are the spectra of glasses with the composition $x\,Na_2O\,.\,(0{\cdot}85-x)\,B_2O_3\,.\,0{\cdot}15\,SiO_2$, $x\,K_2O\,.\,(0{\cdot}85-x)\,B_2O_3\,.\,0{\cdot}15\,SiO_2$, $x\,NaKO\,.\,(0{\cdot}85-x)\,B_2O_3\,.\,0{\cdot}15\,SiO_2$ and $x\,Li_2O\,.\,(0{\cdot}85-x)\,B_2O_3\,.\,0{\cdot}15\,SiO_2$ (cf. figs 3.30 to 3.35). A comparison of the spectra in series $x\,K_2O\,.\,(1-x)\,B_2O_3$ with those of series $x\,K_2O\,.\,(0{\cdot}85-x)\,B_2O_3\,.\,0{\cdot}15\,SiO_2$ (cf. figs 3.15 and 3.16) reveals the same trend in these spectra with increasing K_2O content of the glasses. In the case of the glasses in the series $x\,K_2O\,.\,(0{\cdot}85-x)\,B_2O_3\,.\,0{\cdot}15\,SiO_2$ the decrease of the peak at about 806 cm^{-1}

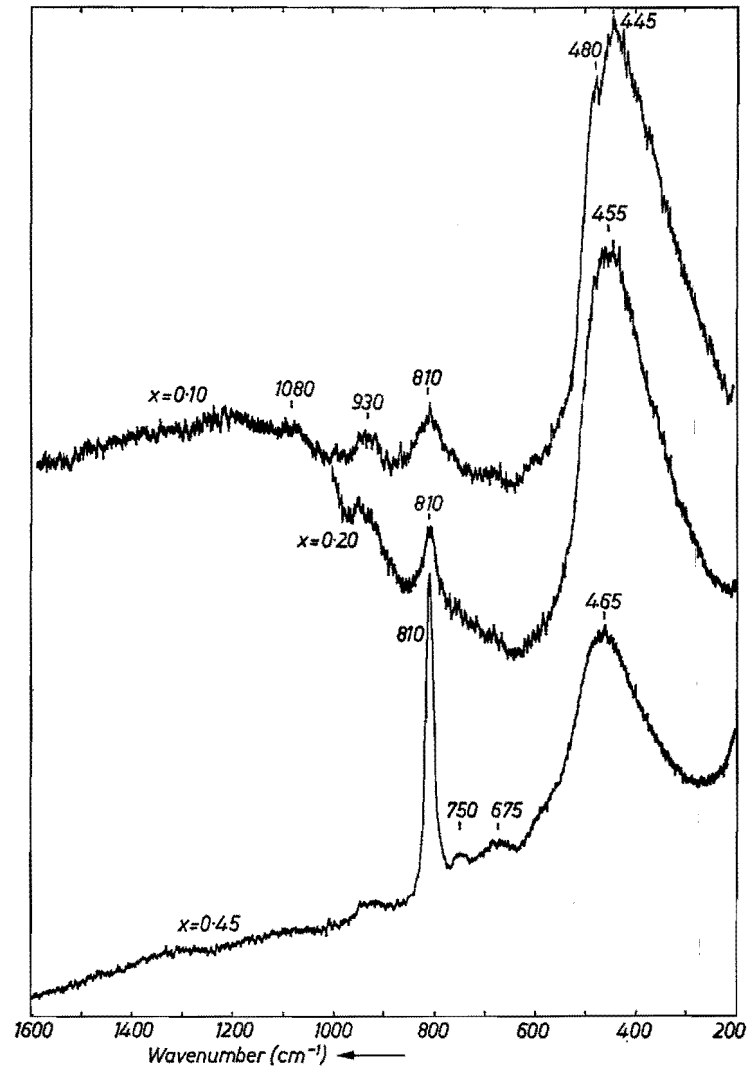

Fig. 3.29. Raman spectra of glasses in the system $x\,B_2O_3\,.\,(1-x)\,SiO_2$ (direction $x(zz+zx)y$).

and the increase of the peak at about 770 cm^{-1} is observed again. The small amount of SiO_2 seems only to have some influence in the spectrum of the glass at $x = 0{\cdot}30$. So it seems probable that most of the alkali oxide in this composition series is used for the formation of borate groups also present in the binary potassium-borate glasses.

One observes that at $x = 0{\cdot}20$ the 806-cm^{-1} peak has completely disappeared, hence there are no boroxol groups (a_3) left in the glass network at this concentration. Probably up to $x = 0{\cdot}20$ just as for the binary borate glass, six-

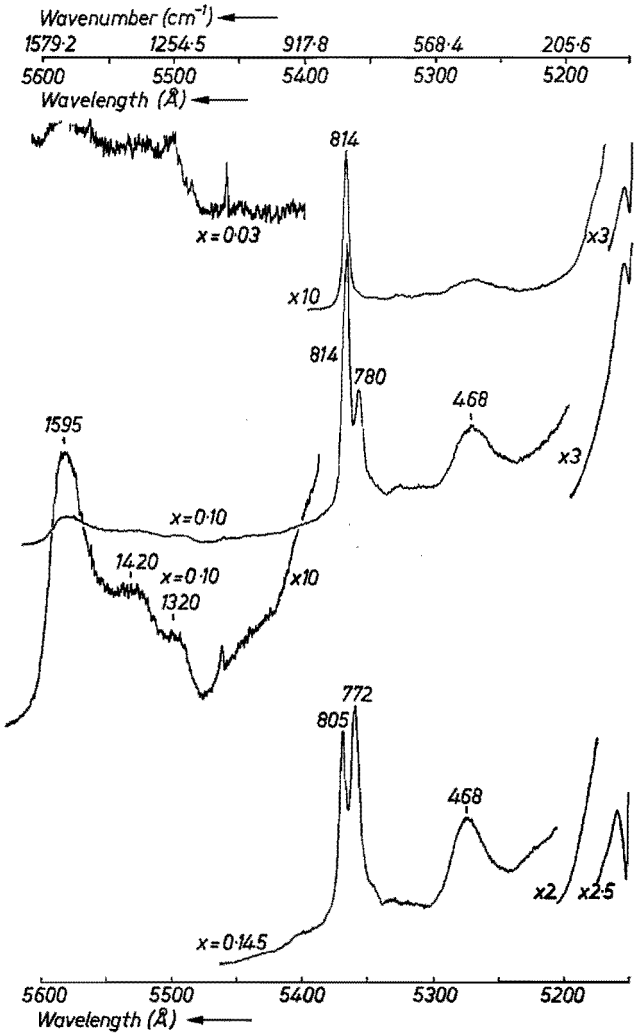

Fig. 3.30. Raman spectra of glasses in the system $x\,K_2O\,.\,(0{\cdot}85 - x)\,B_2O_3\,.\,0{\cdot}15\,SiO_2$ (direction $x(zz + zx)y$).

membered rings with a BO_4 tetrahedron (a_2c) are formed, which to a certain extent form tetraborate groups (a_6c_2). The presence of a small peak at 630 cm^{-1} at $x = 0{\cdot}20$ indicates the presence of ring-type metaborate groups (b_3).

At $x = 0{\cdot}30$ one may observe a band around 1100 cm^{-1} which means that SiO_4 tetrahedra are formed with one non-bridging oxygen ion. It can be observed, too, that the band around 450–500 cm^{-1} has its maximum at 465 cm^{-1} and 468 cm^{-1} respectively for $x = 0{\cdot}20$ and $x = 0{\cdot}30$ in the series with 0·15 SiO_2. In the case of the binary potassium-borate glasses this band is observed at 480 cm^{-1} and 490 cm^{-1} for $x = 0{\cdot}20$ and $x = 0{\cdot}30$ respectively (cf. fig. 3.15). This shift

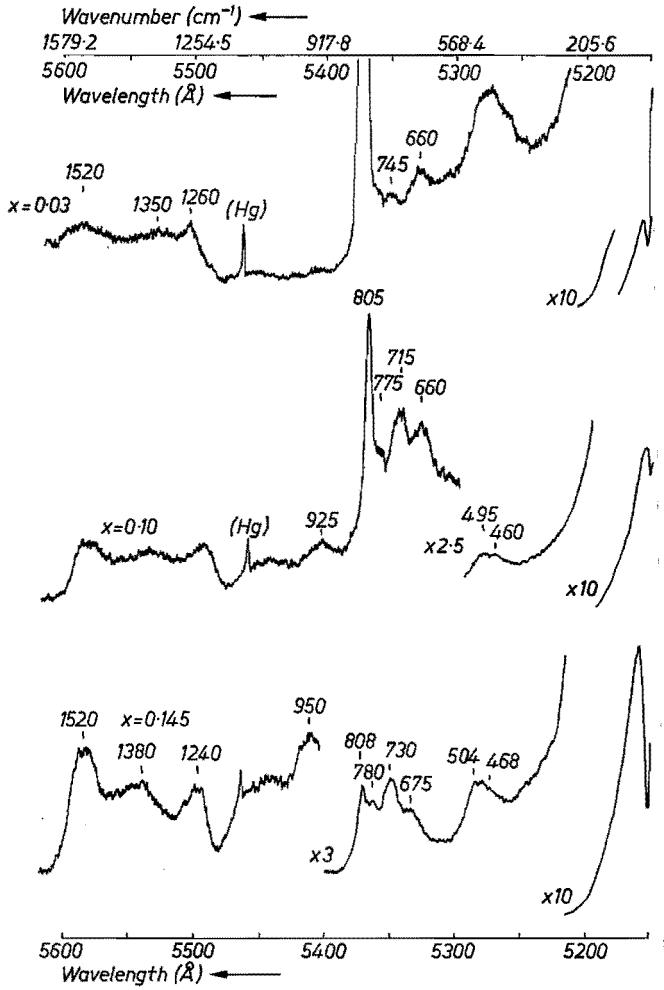

Fig. 3.31. Raman spectra of glasses in the system $x\,K_2O\,.\,(0{\cdot}85 - x)\,B_2O_3\,.\,0{\cdot}15\,SiO_2$ (direction $x(yz + yx)y$).

to lower frequencies in the borosilicate glasses might be explained by taking into consideration that fused-silica or silicate glass with a low alkali-oxide content show Raman spectra with a maximum around 450 cm^{-1}. Therefore SiO_4 units are probably present with very few non-bridging oxygen ions and even in small agglomerates with a structure that resembles vitreous silica.

The glass of composition $0{\cdot}30\,K_2O\,.\,0{\cdot}55\,B_2O_3\,.\,0{\cdot}15\,SiO_2$ contains most probably a major number of diborate groups (a_2c_2), similar to the binary borate glass with roughly the same alkali-to-boron ratio. Ring-type metaborate groups (b_3) are present as indicated by the peak at 635 cm^{-1}. It is interesting to compare this spectrum with the spectrum of the glass of composition

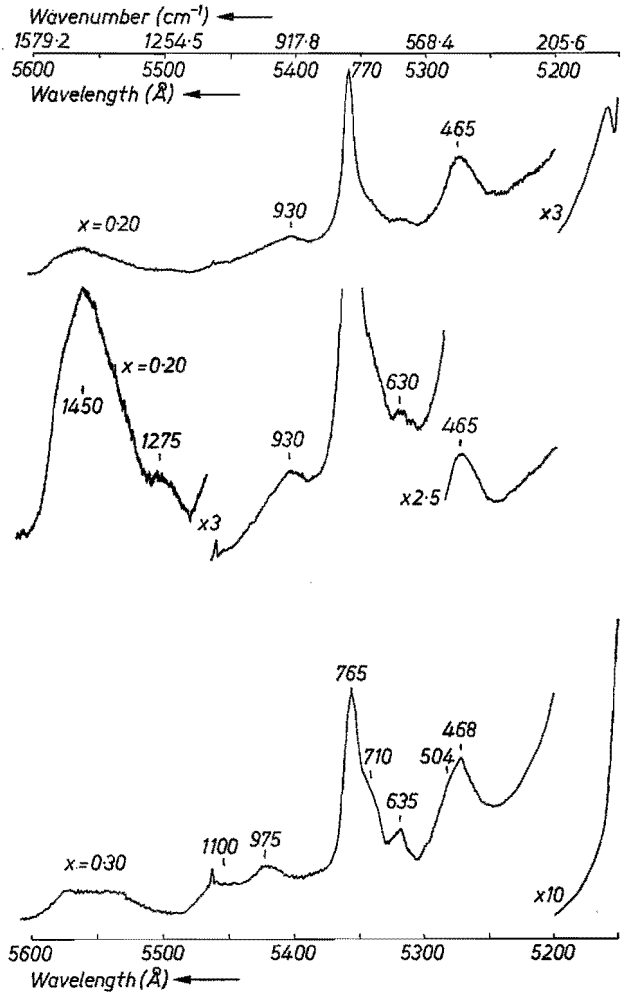

Fig. 3.32. Raman spectra of glasses in the system $x\,K_2O\,.\,(0{\cdot}85 - x)\,B_2O_3\,.\,0{\cdot}15\,SiO_2$ (direction $x(zz + zx)y$).

$0{\cdot}20\,Na_2O\,.\,0{\cdot}20\,K_2O\,.\,0{\cdot}45\,B_2O_3\,.\,0{\cdot}15\,SiO_2$ (cf. fig. 3.36). It seems that there is a tendency with the composition $x = 0{\cdot}30$ that alkali oxide is used for the formation of non-bridging oxygen ions in SiO_4 tetrahedra prior to the formation of diborate (a_2c_2) or di-triborate groups (ac_2), thus to the formation of borate rings with two connected BO_4 tetrahedra.

Comparison of the spectra of glasses containing K_2O with those containing Li_2O, Na_2O or NaKO reveals a high degree of similarity. This suggests that the same types of groups are present as in the corresponding potassium glasses.

It is interesting to note the influence of Al_2O_3 on the presence of certain groups in this concentration area of the alkali-borosilicate glasses. In figs 3.41

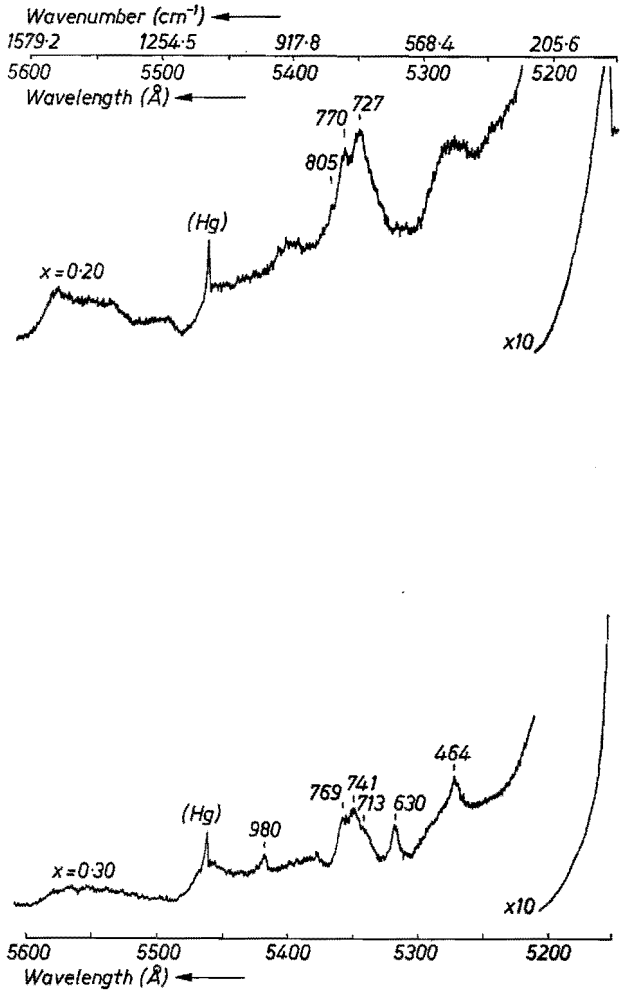

Fig. 3.33. Raman spectra of glasses in the system $x\,K_2O\,.\,(0{\cdot}85-x)\,B_2O_3\,.\,0{\cdot}15\,SiO_2$ (direction $x(yz+yx)\bar{y}$).

and 3.42 we may observe the effect of adding Al_2O_3 to a glass of composition $0{\cdot}10\,K_2O\,.\,0{\cdot}75\,B_2O_3\,.\,0{\cdot}15\,SiO_2$. It can be observed that the addition of Al_2O_3 leads to the disappearance of the peak at about 770 cm^{-1} characteristic of the six-membered ring with a BO_4 tetrahedron and the reoccurrence of the peak at 806 cm^{-1}. This probably means that the alkali ions are attracted by Al_2O_3 to form AlO_4 tetrahedra and consequently boroxol groups (a_3) are formed again. No indications are found of the formation of a new strong peak in the Raman spectra due to the presence of AlO_4 tetrahedra in the glass. It is also interesting to note that the addition of twice as much Al_2O_3 as K_2O neither results in the formation of new peaks nor in the disappearance of others.

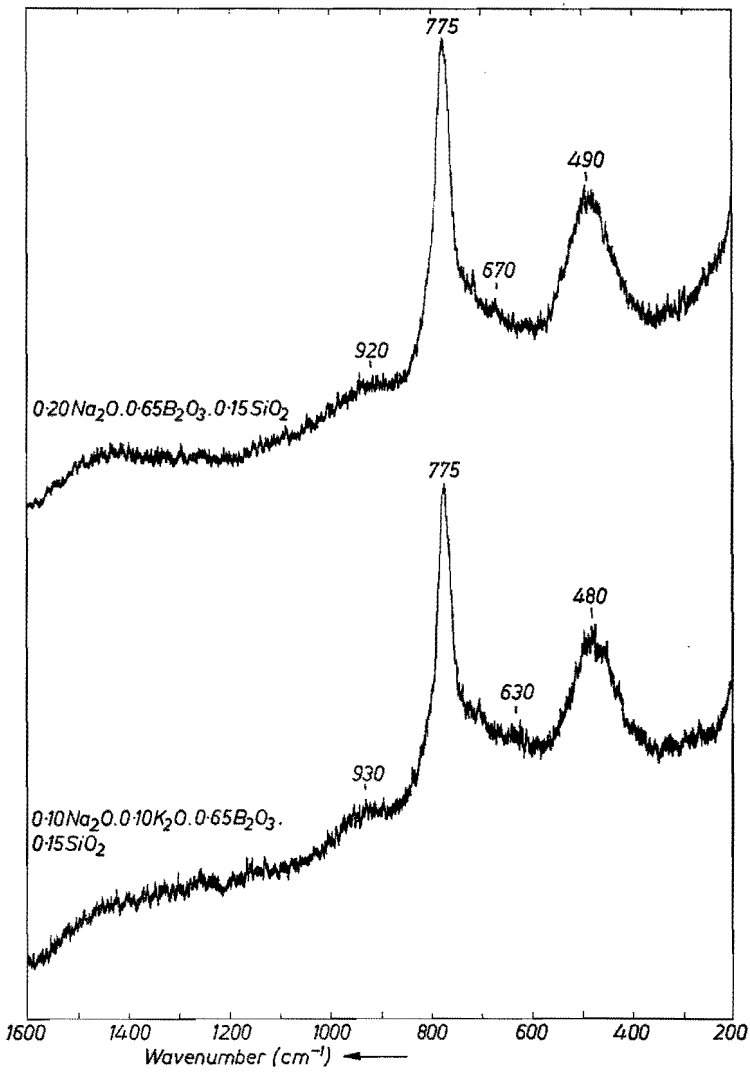

Fig. 3.34. Raman spectra of borosilicate glasses (direction $x(zz + zx)y$).

This probably means that the borate network is not greatly influenced when more Al_2O_3 than K_2O is added.

The same behaviour of Al_2O_3 can be observed in figs 3.43 and 3.44 which show the effect of the addition of Al_2O_3 on the Raman spectra of a glass with composition $0{\cdot}10\ Na_2O\ .\ 0{\cdot}10\ K_2O\ .\ 0{\cdot}65\ B_2O_3\ .\ 0{\cdot}15\ SiO_2$. Again one may observe the gradual disappearance of the peak at 770 cm^{-1} and the gradual rise in intensity of the peak at 806 cm^{-1}. Again it must be concluded that on addition of Al_2O_3 to this glass, BO_4 tetrahedra are replaced by AlO_4 tetrahedra

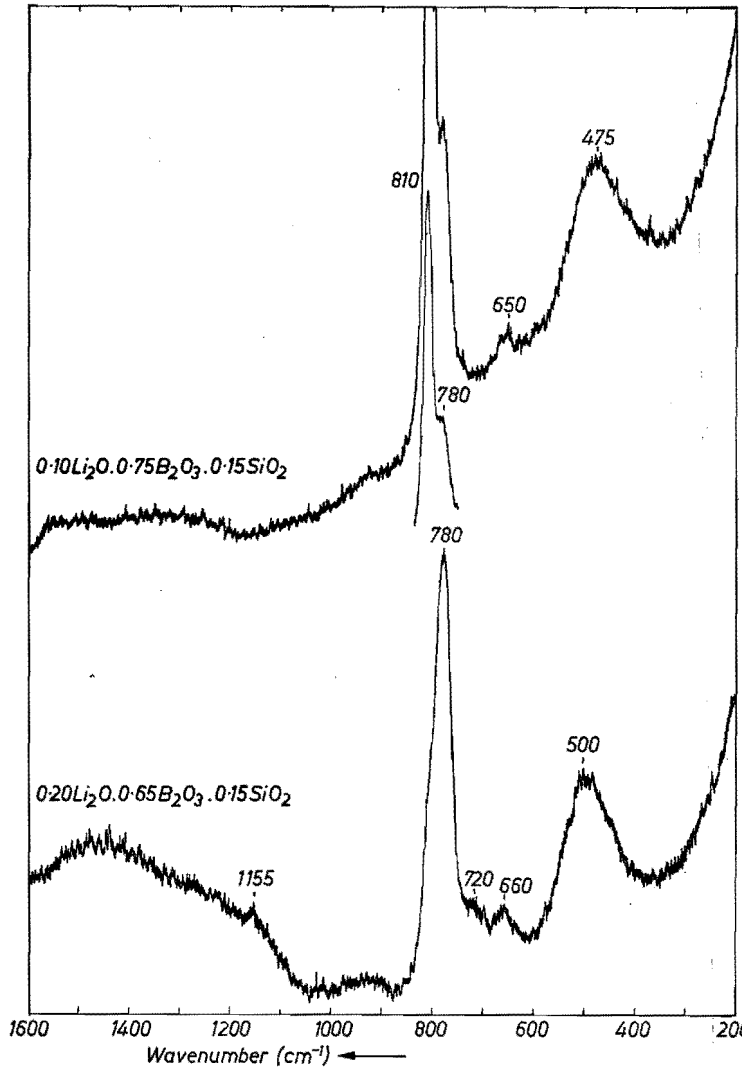

Fig. 3.35. Raman spectra of lithium-borosilicate glasses (direction $x(zz + zx)y$).

and boroxol groups (a_3) are formed again. Once more no peaks are observed that can be attributed to AlO_4 tetrahedra.

The same trend can be observed in the series $x\,K_2O\,.\,(0{\cdot}85 - x)\,B_2O_3\,.\,0{\cdot}15\,SiO_2$ to which $0{\cdot}05\,Al_2O_3$ is added (cf. figs 3.45 and 3.46), except that at $x = 0{\cdot}30$ it cannot be observed that boroxol groups are formed again. In this case one may observe that the peak at 635 cm^{-1} present in the spectrum of the glass without Al_2O_3 (cf. figs 3.32 and 3.33) practically disappears on addition of $0{\cdot}05\,Al_2O_3$ (cf. figs 3.45 and 3.46). This means that ring-type metaborate

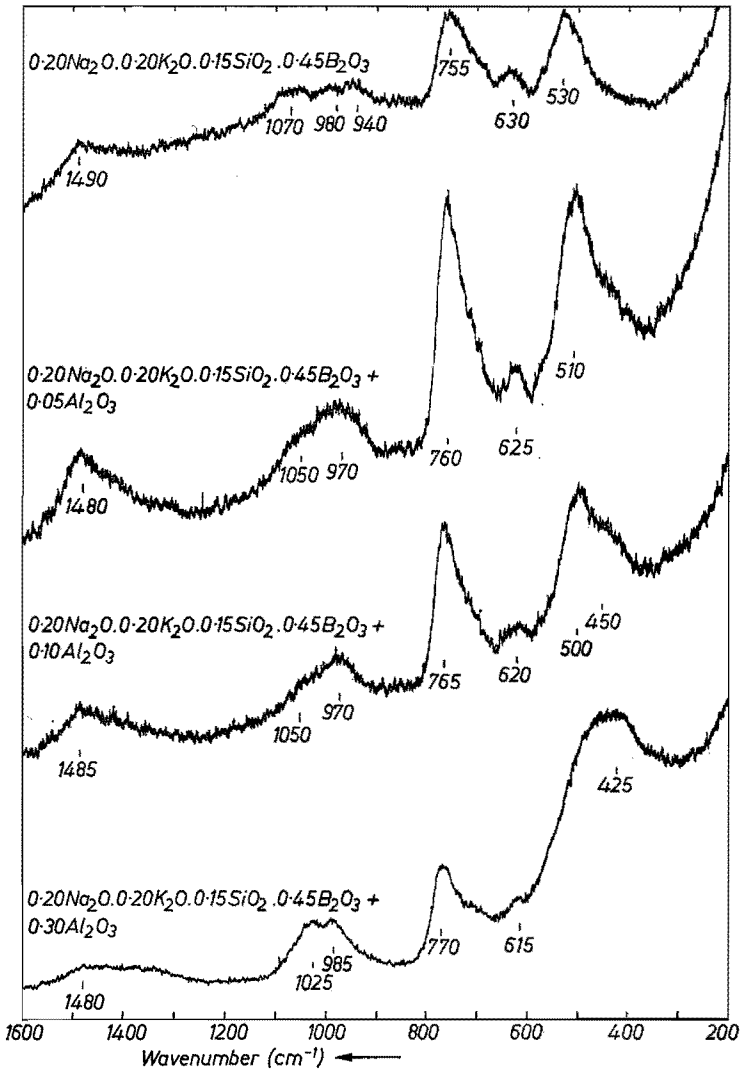

Fig. 3.36. Raman spectra of borosilicate glasses with increasing amounts of Al_2O_3 (direction $x(zz + zx)y$).

groups (b_3) disappear on addition of 0·05 Al_2O_3. The band around 1100 cm^{-1} seems to diminish somewhat too. It would mean that non-bridging oxygen ions connected with SiO_4 tetrahedra are removed.

In fig. 3.36 the influence is demonstrated of addition of Al_2O_3 on glass of composition 0·20 Na_2O . 0·20 K_2O . 0·45 B_2O_3 . 0·15 SiO_2. It can be observed that addition of 0·05 Al_2O_3 more or less leads to a disappearance of the peak at 940 cm^{-1}, which might be attributed to the disappearance of the orthoborate unit BO_3^{3-}. The bands in the area 970–1070 cm^{-1} are probably due to SiO_4

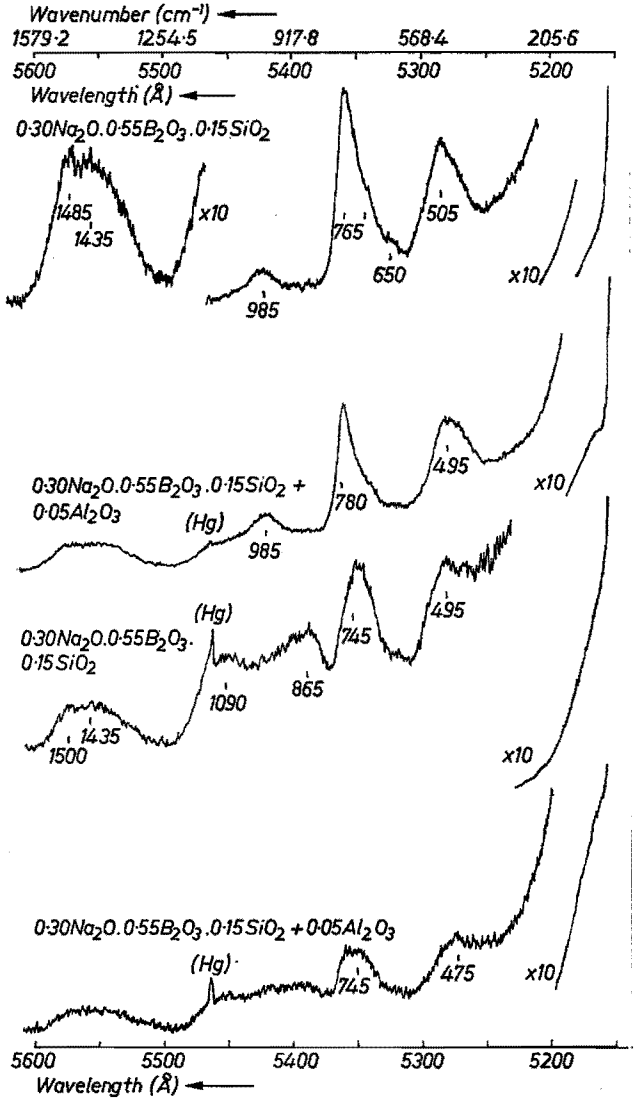

Fig. 3.37. Raman spectra of borosilicate glasses without and with Al_2O_3 (two upper traces: direction $x(zz + zx)y$; two lower traces: direction $x(yz + yx)y$).

units with one and two non-bridging oxygen ions; compare this with the spectrum of the glass of composition 0·45 K_2O . 0·55 SiO_2 in fig. 3.26 and with the Raman spectrum of 0·45 Na_2O . 0·55 SiO_2 published by Etchepare [3-54,55]). The band at about 625 cm^{-1} might be due to ring-type metaborate groups (b_3) that do not disappear on the addition of Al_2O_3. The peak at about 760 cm^{-1} seems to diminish relatively on addition of Al_2O_3, so BO_4 tetrahedra probably do disappear. It is not clear what type of borate group is formed after the dis-

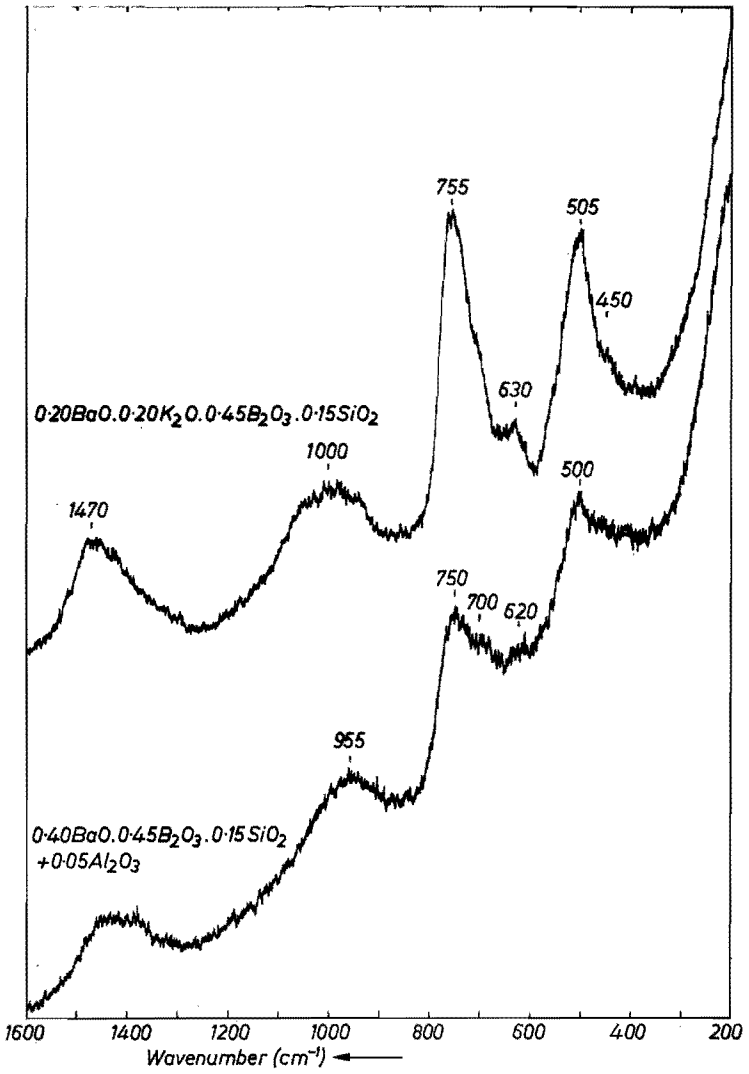

Fig. 3.38. Raman spectra of borosilicate glasses (direction $x(zz + zx)y$).

appearance of the BO_4 tetrahedra as no boroxol groups (a_3) seem to be present to a substantial extent. The fact that the 806-cm^{-1} peak does not appear again does not mean that no boroxol groups (a_3) are formed. It may be that these are indeed formed again but are deformed due to the large number of other borate groups, thus giving rise to a broad Raman band that cannot be distinguished from the noise. It may also be that disordered BO_3 units (a) are formed. It seems that the addition of Al_2O_3 has also influence on the structural units containing silicon ions.

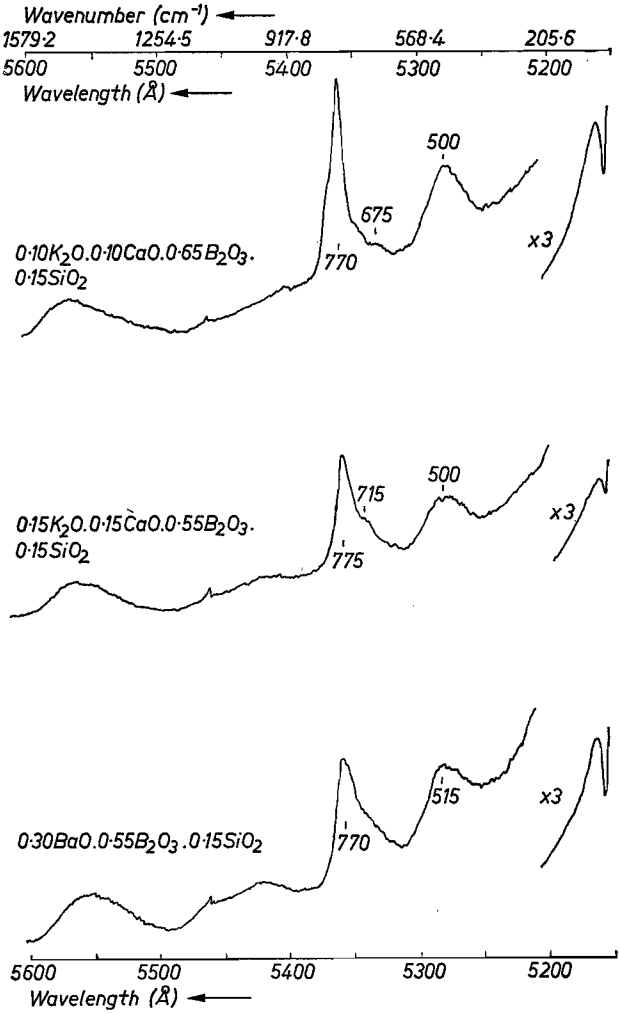

Fig. 3.39. Raman spectra of borosilicate glasses containing alkaline-earth oxides (direction $x(zz + zx)y$).

It can be observed in fig. 3.28, which shows the influence of Al_2O_3 on potassium-silicate glasses, and from the Raman work of DiSalvo et al.[3–56]) on glasses in the composition triangle Na_2O–Al_2O_3–SiO_2 that the band around 500 cm^{-1} rises on increasing the ratio Al/K or Al/Na. It can also be observed that at a ratio Al/K = 1 and Al/Na = 1 the bands around 1000 cm^{-1} have not disappeared, on the contrary they remain rather strong. It can be observed that at Al/Na ratios higher than 1 the bands around 1000–1100 cm^{-1} gradually disappear and that the band at around 500 cm^{-1} moves to around 440 cm^{-1} for a glass of composition 0·7 Na_2O . 1·3 Al_2O_3 . 6 SiO_2 (DiSalvo et al. [3–56])).

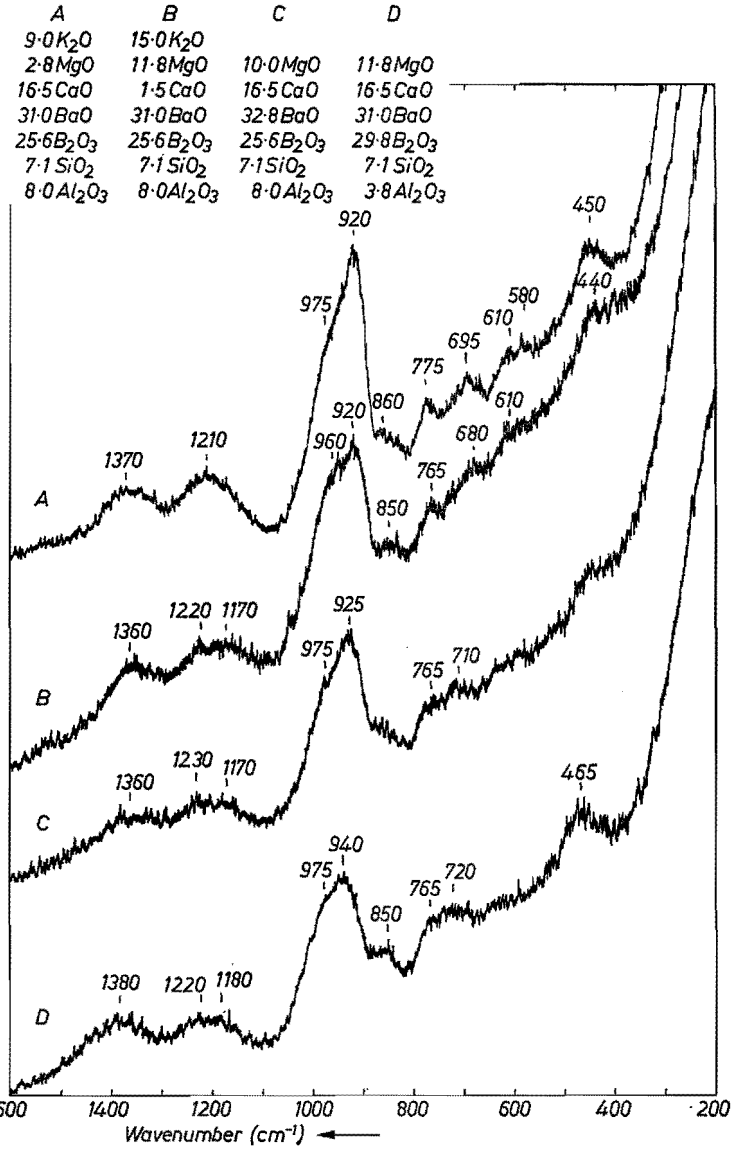

Fig. 3.40. Raman spectra of multicomponent borosilicate glasses (direction $x(zz + zx)y$).

All this information leads to the conclusion that in glass with a composition 0·20 Na_2O . 0·20 K_2O . 0·45 B_2O_3 . 0·15 SiO_2 + 0·30 Al_2O_3 the added Al_2O_3 influences the silicate units appreciably. It is suggested that an aluminosilicate network is formed and that the vitreous-silica-like network disappears.

The influence of alkaline-earth ions on the Raman spectra of glasses in the series with 0·15 SiO_2 is shown in figs 3.38 and 3.39. Comparison of the

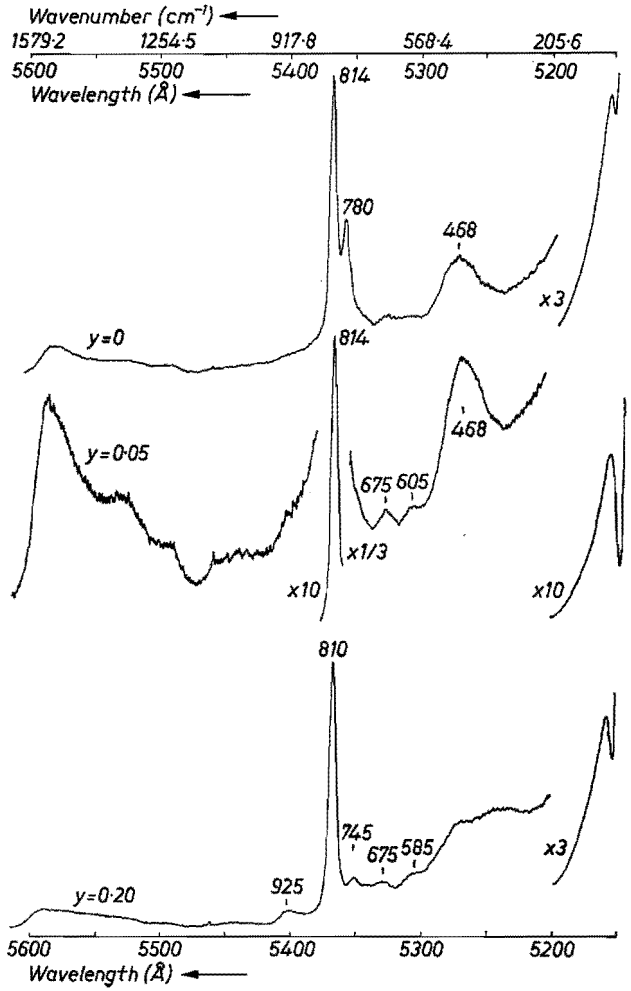

Fig. 3.41. Raman spectra of glasses in the system 0·10 K_2O . 0·75 B_2O_3 . 0·15 SiO_2 + y Al_2O_3 (direction $x(zz + zx)y$).

spectra of the glasses with composition 0·20 K_2O . 0·65 B_2O_3 . 0·15 SiO_2 and 0·10 K_2O . 0·10 CaO . 0·65 B_2O_3 . 0·15 SiO_2 in figs 3.31 and 3.39 reveals the presence of the 806-cm^{-1} peak as a shoulder of the 770-cm^{-1} peak in the spectrum of the glass containing CaO, whereas it is absent in the spectrum of the glass containing only K_2O. This 806-cm^{-1} peak reveals the presence of boroxol groups (a_3). At the same time it may be observed that the peak at 465 cm^{-1} in the spectrum of the glass with K_2O only shifts to 500 cm^{-1} in the case of the CaO-containing glass. Both facts suggest that replacement of K_2O by CaO leads to the formation of pairs of BO_4 tetrahedra as found in the diborate (a_2c_2) and di-triborate groups (ac_2). The suggestion of pair formation of BO_4 tetrahedra

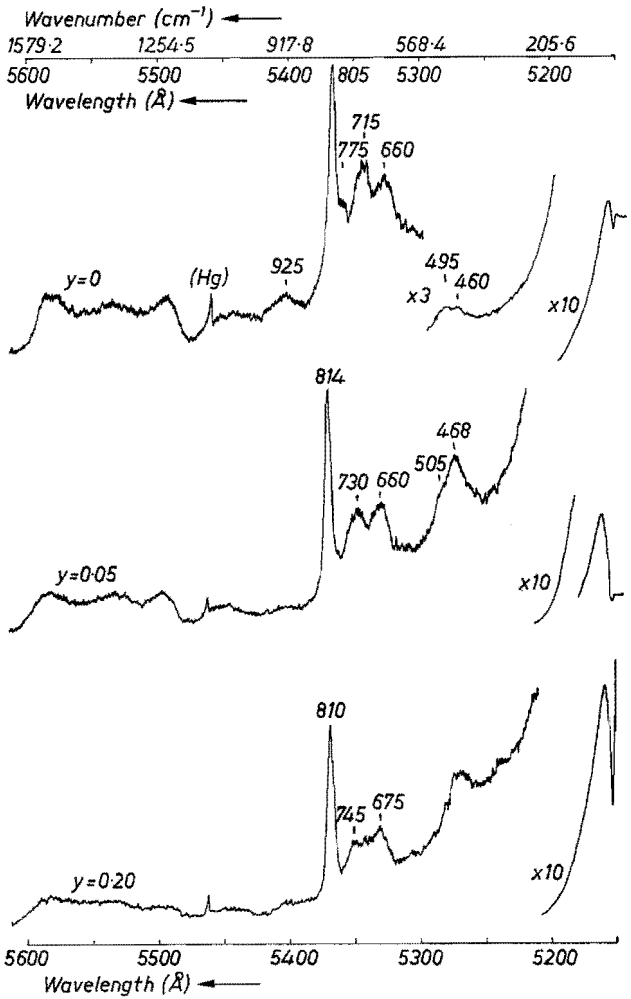

Fig. 3.42. Raman spectra of glasses in the system $0{\cdot}10\,K_2O\,.\,0{\cdot}75\,B_2O_3\,.\,0{\cdot}15\,SiO_2 + y\,Al_2O_3$ (direction $x(yz + yx)y$).

in alkaline-earth-borate glasses was already made earlier by Beekenkamp [3–50]). It can be observed too, that the replacement of K_2O by CaO does not lead to increased formation of non-bridging oxygen ions connected with SiO_4 tetrahedra as may be concluded from the absence of a band at 1100 cm^{-1}.

Comparison of the spectra of the glasses with composition $0{\cdot}30\,K_2O\,.\,0{\cdot}55\,B_2O_3\,.\,0{\cdot}15\,SiO_2$ and $0{\cdot}15\,K_2O\,.\,0{\cdot}15\,CaO\,.\,0{\cdot}55\,B_2O_3\,.\,0{\cdot}15\,SiO_2$ also shows the increase of the peak at about 500 cm^{-1} when K_2O is replaced by CaO. This is also observed for the binary alkaline-earth-borate glasses.

It can also be observed that the replacement of K_2O by CaO leads to the disappearance of the peak at 635 cm^{-1} present in the spectrum of the glass

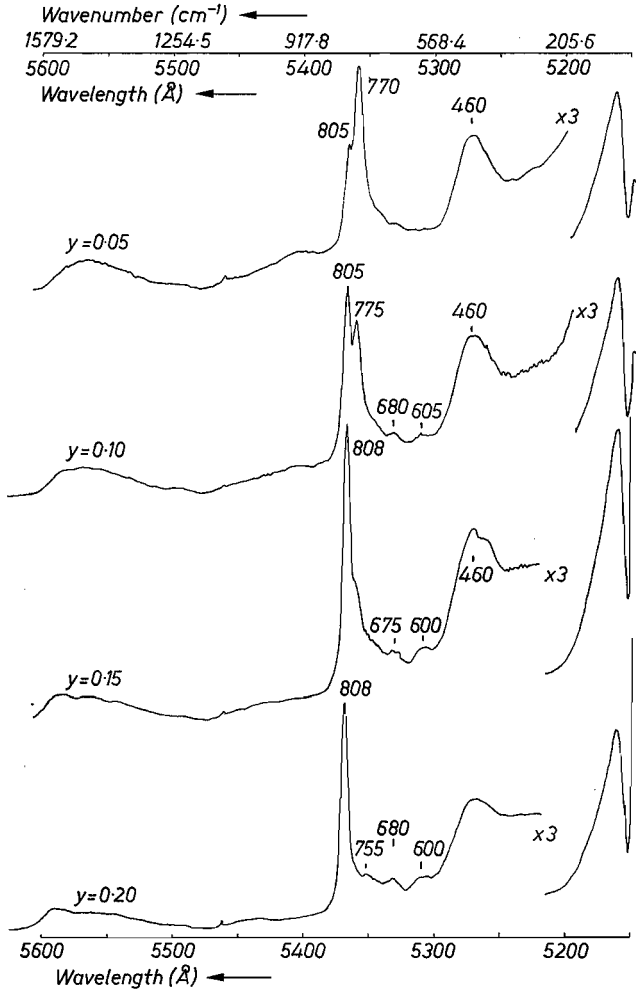

Fig. 3.43. Raman spectra of glasses in the system 0·10 Na_2O . 0·10 K_2O . 0·65 B_2O_3 . 0·15 SiO_2 + y Al_2O_3 (direction $x(zz + zx)y$).

containing only K_2O. This probably means that ring-type metaborate groups (b_3) disappear, though it cannot be decided that chain-type metaborate groups (b_∞) are formed instead. It is recalled that the compound CaO . B_2O_3 contains the chain-type metaborate group and shows the strongest peak in its Raman spectrum at 730 cm^{-1} (cf. fig. 3.4). The Raman spectrum of the glass with composition 0·30 BaO . 0·55 B_2O_3 . 0·15 SiO_2 shows a close similarity to that of the glass of composition 0·30 BaO . 0·70 B_2O_3. This suggests the formation of six-membered rings with two BO_4 tetrahedra.

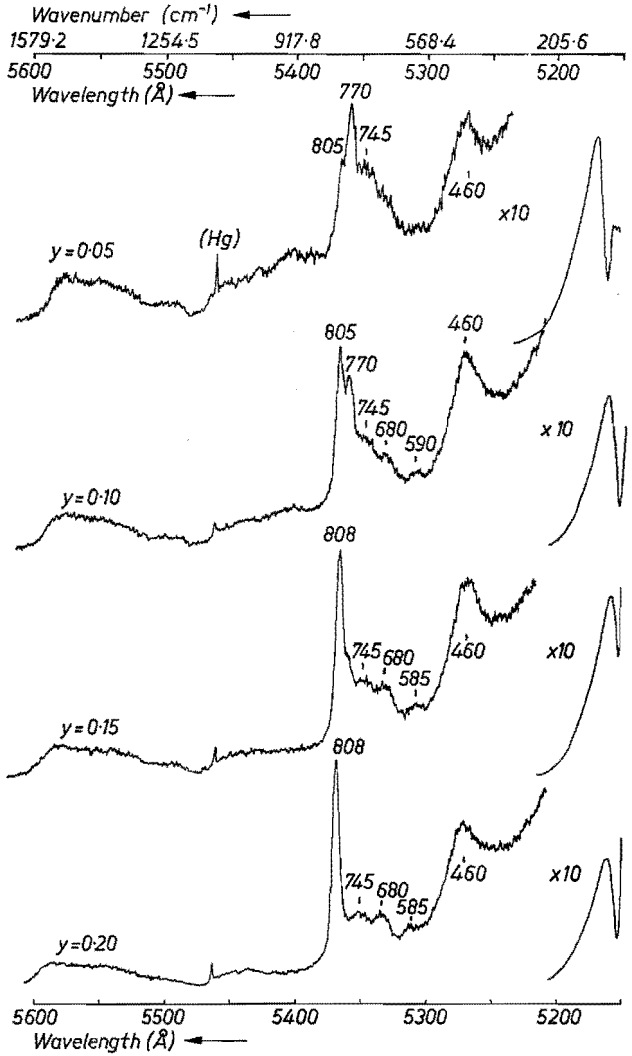

Fig. 3.44. Raman spectra of glasses in the system 0·10 Na_2O . 0·10 K_2O . 0·65 B_2O_3. 0·15 SiO_2 + y Al_2O_3 (direction $x(yz + yx)y$).

From comparison of the spectra of the glasses of composition 0·20 Na_2O . 0·20 K_2O . 0·45 B_2O_3 . 0·15 SiO_2 (fig. 3.36), 0·40 BaO . 0·45 B_2O_3 . 0·15 SiO_2 + 0·05 Al_2O_3 (fig. 3.37), 0·20 BaO . 0·20 K_2O . 0·45 B_2O_3 . 0·15 SiO_2 (fig. 3.37) and the BaO–SiO_2 glasses (Etchepare [3–54,55]) it becomes clear that the band at 955–1000 cm^{-1} present in the glasses of composition 0·40 BaO . 0·45 B_2O_3 . 0·15 SiO_2 + 0·05 Al_2O_3 and 0·20 BaO . 0·20 K_2O . 0·45 B_2O_3 . 0·15 SiO_2 is due to the presence of SiO_4 units with two non-bridging oxygen ions. In general no significant differences can be observed between the spectra of glasses con-

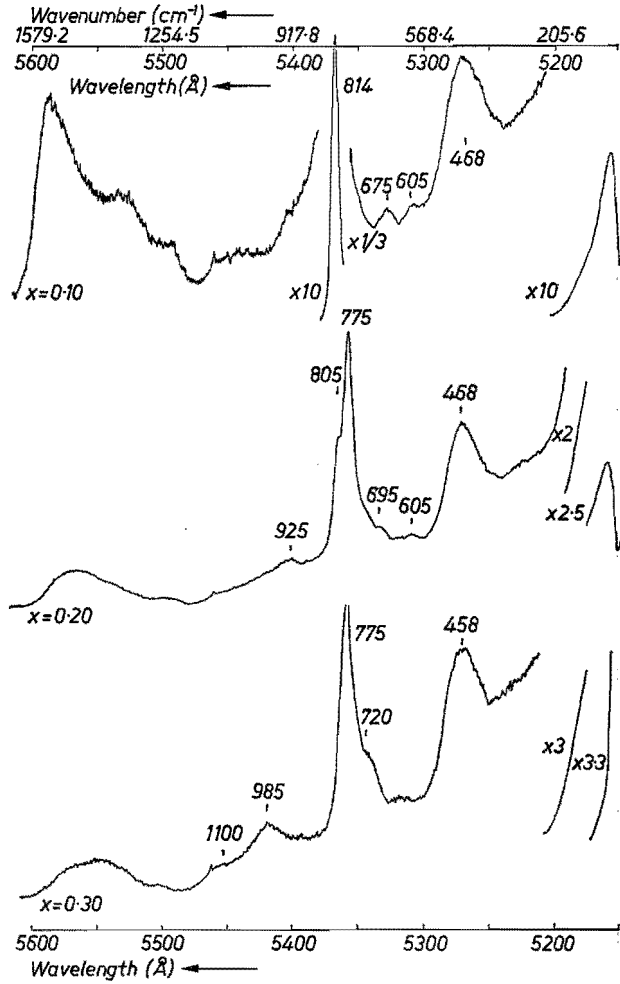

Fig. 3.45. Raman spectra of glasses in the system $x\,K_2O\,.\,(0{\cdot}85-x)\,B_2O_3\,.0{\cdot}15\,SiO_2 + 0{\cdot}05\,Al_2O_3$ (direction $x(zz + zx)y$).

taining 40 mol % alkali oxide, 40 mol % alkaline-earth oxide or 40 mol % mixed alkali–alkaline-earth oxides so that probably more or less the same structural units are present.

It is interesting to look at the spectra of multi-component alkaline-earth-borosilicate glasses shown in fig. 3.40. The composition of one of the glasses is $9{\cdot}0\,K_2O\,.\,2{\cdot}8\,MgO\,.\,16{\cdot}5\,CaO\,.\,31{\cdot}0\,BaO\,.\,25{\cdot}6\,B_2O_3\,.\,7{\cdot}1\,SiO_2\,.\,8{\cdot}0\,Al_2O_3$; in the Raman spectrum of this glass one observes a large number of peaks among which the peak at 920 cm^{-1} and its shoulder at 975 cm^{-1} are the strongest. The peak at 920 cm^{-1} can be attributed to the orthoborate BO_3^{3-} unit, the shoulder at 975 cm^{-1} probably has a connection with SiO_4 units with two non-bridging oxygen ions.

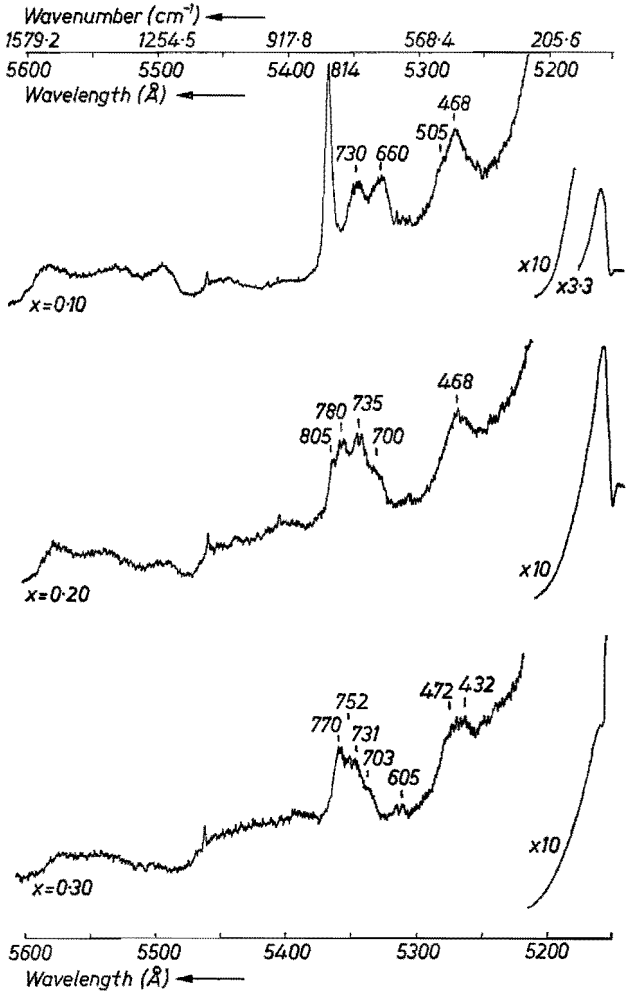

Fig. 3.46. Raman spectra of glasses in the system $x\ K_2O\ .\ (0{\cdot}85 - x)\ B_2O_3\ .\ 0{\cdot}15\ SiO_2 + 0{\cdot}05\ Al_2O_3$ (direction $x(yz + yx)y$).

Borosilicate glasses with 35 *mol* % SiO_2

The discussion on the presence of certain groups will now be shifted to glasses containing an average amount of SiO_2. In figs 3.47 to 3.50 Raman spectra are shown of glasses in the composition series $x\ Na_2O\ .\ (0{\cdot}65 - x)\ B_2O_3\ .\ 0{\cdot}35\ SiO_2$ and $x\ K_2O\ .\ (0{\cdot}65 - x)\ B_2O_3\ .\ 0{\cdot}35\ SiO_2$. At low values of x it can be observed that boroxol groups (a_3) are present as can be concluded from the presence of the characteristic peak at about 806 cm^{-1}. It can be observed too that at a low alkali-oxide concentration ($x \leqslant 0{\cdot}20$) a major amount of the alkali oxide is used to form borate groups with BO_4 tetrahedra in a six-

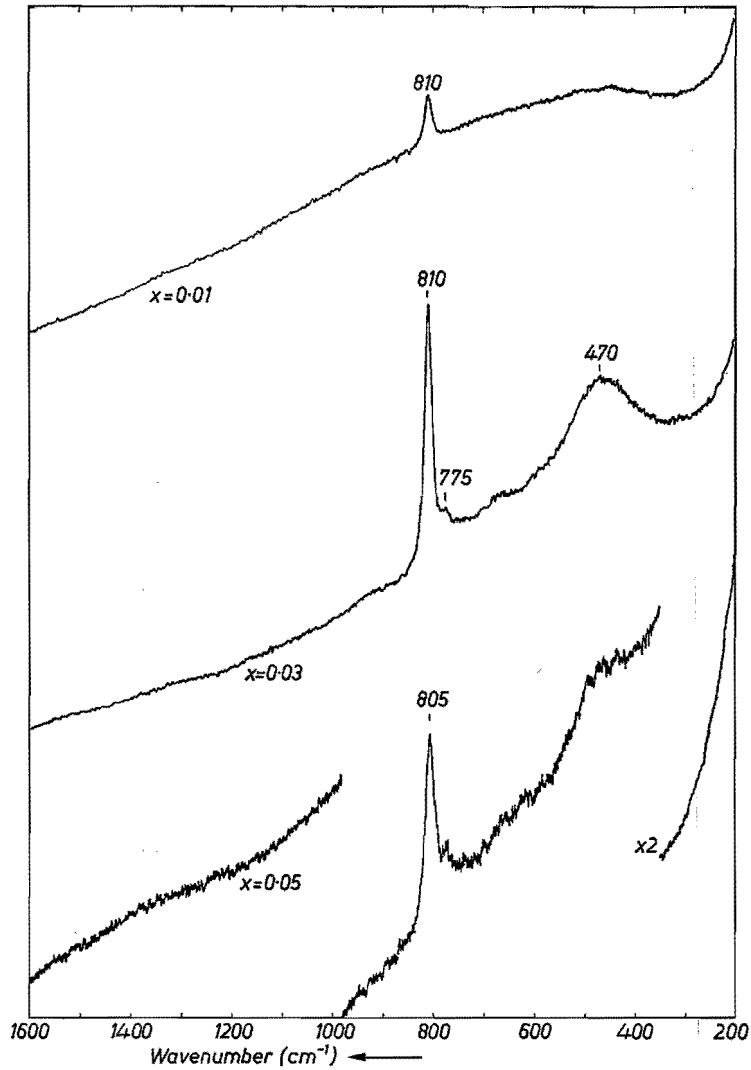

Fig. 3.47. Raman spectra of glasses in the system $x\ Na_2O\ .\ (0{\cdot}65 - x)\ B_2O_3\ .\ 0{\cdot}35\ SiO_2$ (direction $x(zz + zx)y$).

membered ring. As for the binary borate glasses, these rings may be ordered to tetraborate groups (a_6c_2) and diborate groups (a_2c_2). The absence of bands around 1100 cm^{-1} and the presence of a band at 475 cm^{-1} probably means that SiO_2 is present in fused-silica-like structure. It can be observed too that at $x = 0{\cdot}20$ ring-type metaborate groups (b_3) are formed as revealed from the presence of the characteristic peak at 630 cm^{-1}. At values of $x > 0{\cdot}20$ one observes in glasses of composition $0{\cdot}30\ Na_2O\ .\ 0{\cdot}35\ B_2O_3\ .\ 0{\cdot}35\ SiO_2$ (fig. 3.49) and $0{\cdot}40\ K_2O\ .\ 0{\cdot}25\ B_2O_3\ .\ 0{\cdot}35\ SiO_2 + 0{\cdot}05\ Al_2O_3$ (fig. 3.51) the presence of

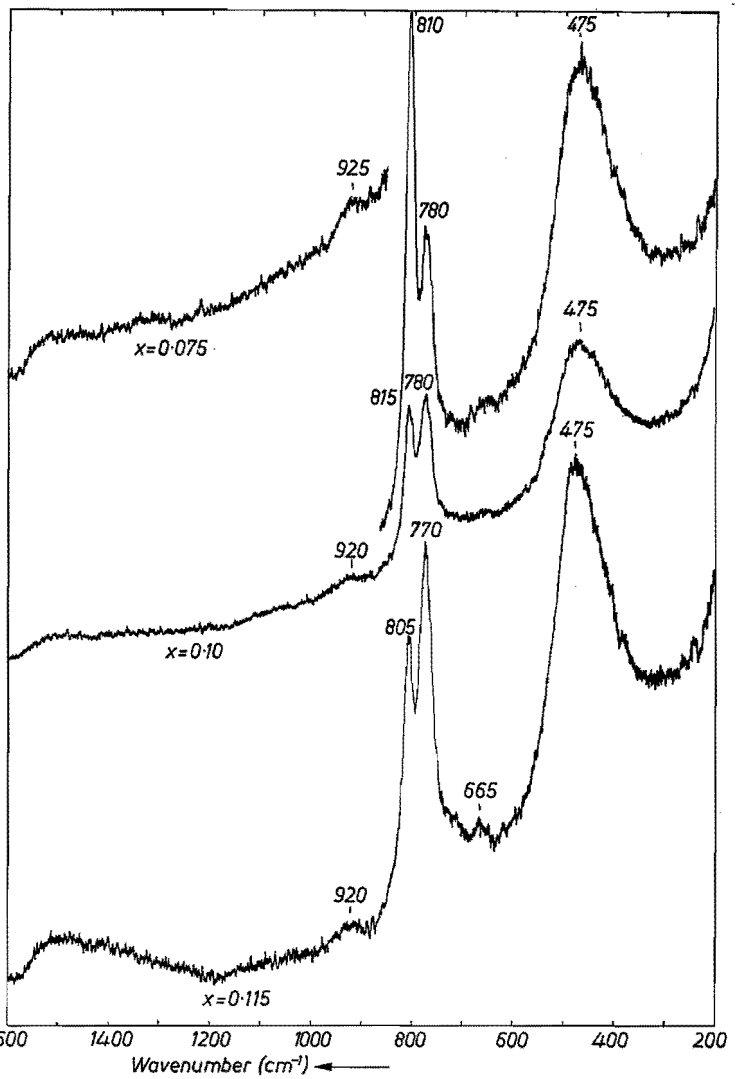

Fig. 3.48. Raman spectra of glasses in the system $x\ Na_2O\ .\ (0{\cdot}65 - x)\ B_2O_3\ .\ 0{\cdot}35\ SiO_2$ (direction $x(zz + zx)y$).

SiO_4 tetrahedra with one non-bridging oxygen ion, as revealed by the fact that a peak is present at about 1070 cm^{-1}. The peak at about 750–770 cm^{-1} decreases relatively in intensity and the peak at 630 cm^{-1} increases. This probably means that more ring-type metaborate groups (b_3) are formed relative to borate groups with BO_4 tetrahedra.

It should be remarked that there seems to be a resistance to the formation of diborate (a_2c_2) and di-triborate groups (ac_2). This is made clear as follows. At $x = 0{\cdot}20$ the Na/B ratio is 0·44, in the diborate compound $Na_2O\ .\ 2\ B_2O_3$

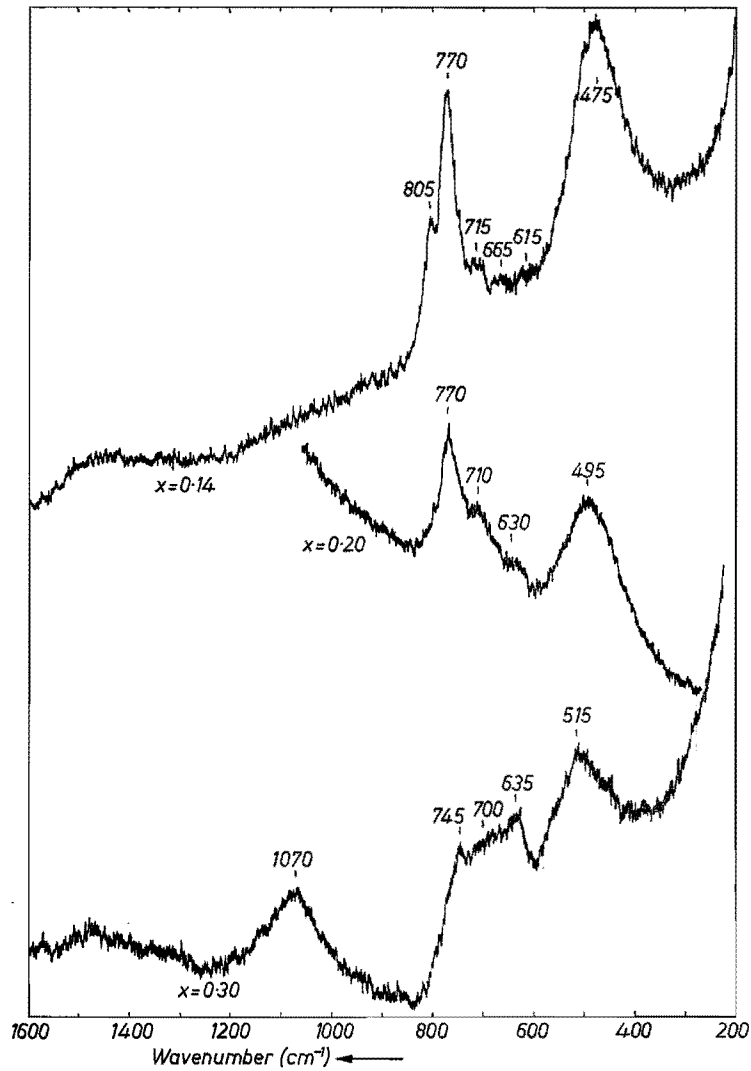

Fig. 3.49. Raman spectra of glasses in the system $x\ Na_2O\ .\ (0{\cdot}65 - x)\ B_2O_3\ .\ 0{\cdot}35\ SiO_2$ (direction $x(zz + zx)y$).

the ratio is 0·5. One observes that at values of $x = 0{\cdot}20$, SiO_4 tetrahedra with one non-bridging oxygen ion are formed and that ring-type metaborate groups too increase in number. Values of $x > 0{\cdot}20$ means that the Na/B ratio in these glasses is $> 0{\cdot}5$ which should necessarily lead to the formation of borate groups with an Na/B of 0·5 or more (on average) if the Na^+ ions are to be absorbed completely by the borate network.

The band around 700 cm^{-1} may be caused by the diborate group (a_2c_2) but

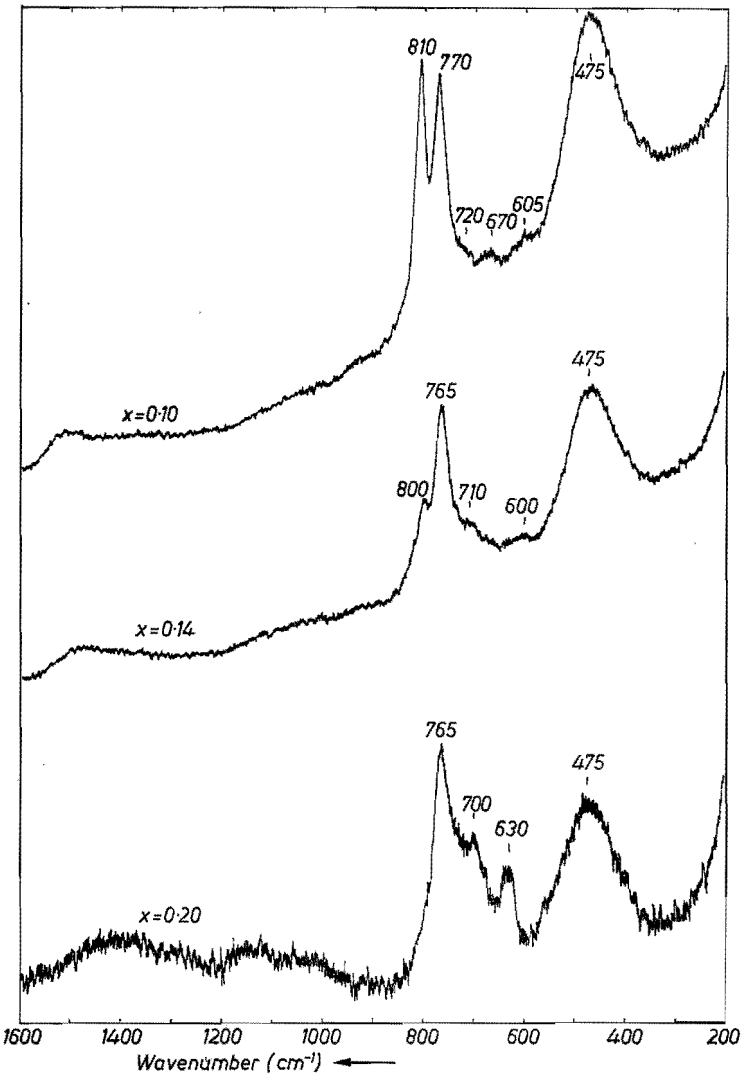

Fig. 3.50. Raman spectra of glasses in the system $x\,K_2O\,.\,(0{\cdot}65 - x)\,B_2O_3\,.\,0{\cdot}35\,SiO_2$ (direction $x(zz + zx)y$).

this is not very evident. This band may be caused too by the presence of chain-type metaborate groups (b_∞) (cf. the spectra of the compounds $Li_2O\,.\,B_2O_3$ and $CaO\,.\,B_2O_3$ in fig. 3.4). This is also not very likely because the spectra of the glasses $0{\cdot}15\,Na_2O\,.\,0{\cdot}15\,Li_2O\,.\,0{\cdot}35\,B_2O_3\,.\,0{\cdot}35\,SiO_2$ and $0{\cdot}15\,Na_2O\,.\,0{\cdot}15\,CaO\,.\,0{\cdot}35\,B_2O_3\,.\,0{\cdot}35\,SiO_2$ (cf. fig. 3.51), only show a decrease in the band at about 700 cm^{-1} compared to the spectrum of the corresponding glass without Li_2O or CaO of composition $0{\cdot}30\,Na_2O\,.\,0{\cdot}35\,B_2O_3\,.\,0{\cdot}35\,SiO_2$ (cf.

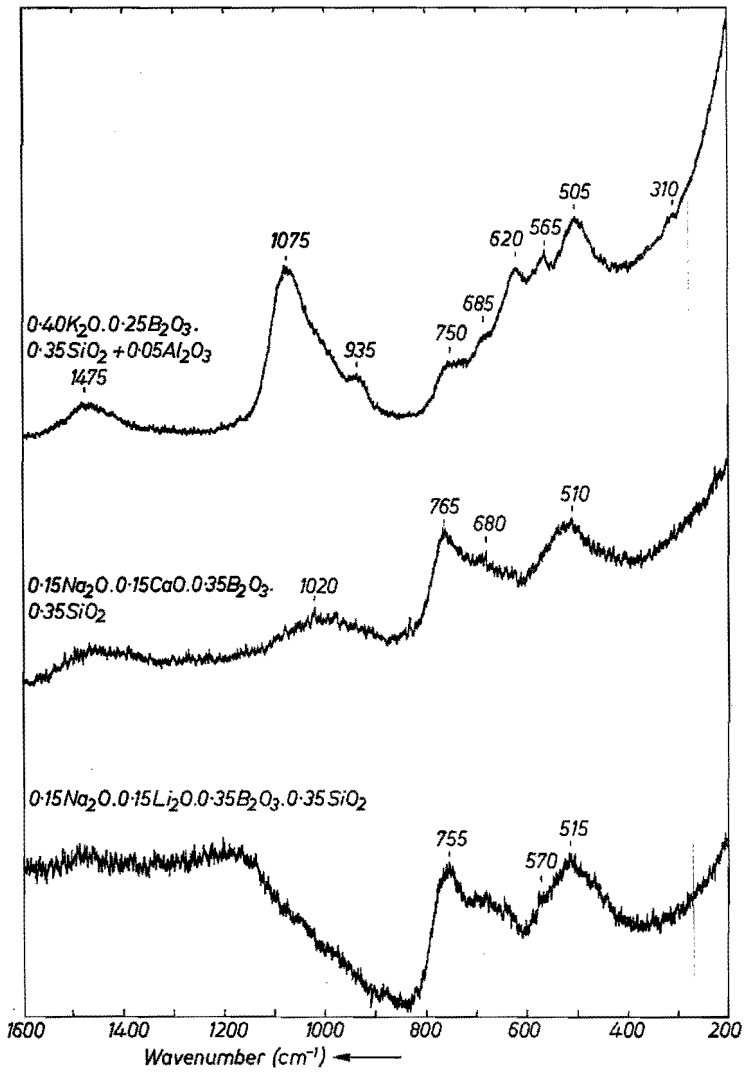

Fig. 3.51. Raman spectra of borosilicate glasses (direction $x(zz + zx)y$).

fig. 3.49). The conclusion may be that the origin of the band at 700 cm^{-1} is not clear.

For the glass of composition 0·115 Na_2O . 0·535 B_2O_3 . 0·35 SiO_2 the influence of phase separation on the Raman spectra was investigated. It was observed that the Raman spectra of a sample prepared by the sol–gel method and water quenched from the melt and a sample that had developed a clearly visible phase separation, were identical. It is known from phase-separation studies of glasses in this composition range that during phase separation a

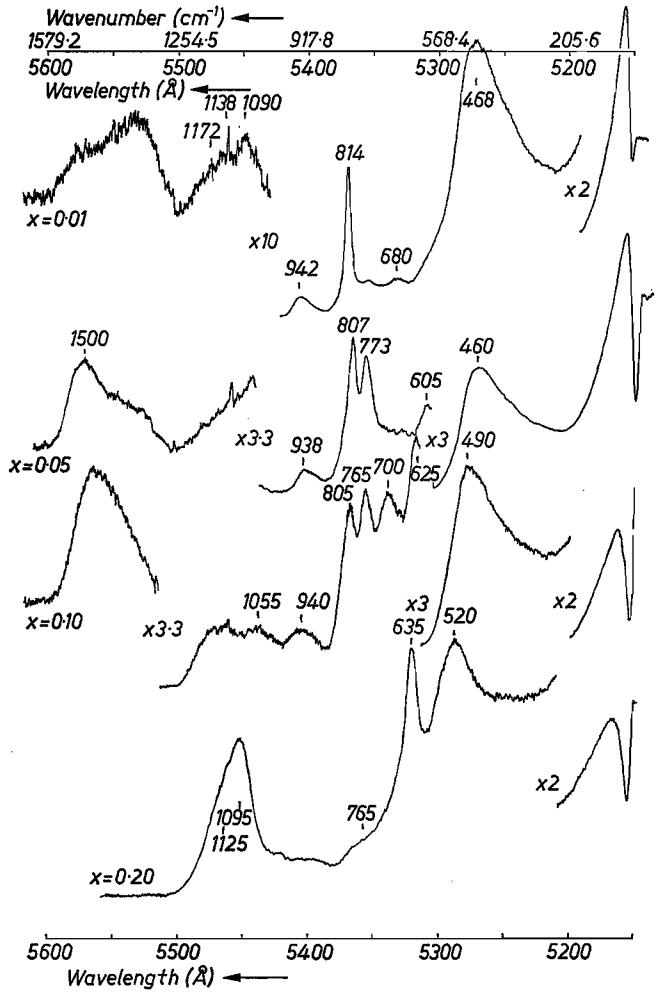

Fig. 3.52. Raman spectra of glasses in the system $x\ K_2O\,.\,(0{\cdot}35-x)\ B_2O_3\,.\,0{\cdot}65\ SiO_2$ (direction $x(zz+zx)y$).

borate- and a silicate-rich phase are developed (cf. sec. 1.3). The Raman spectra now suggest that this phase separation is also present on a very small scale in these borosilicate glasses that are virtually homogeneous.

This is confirmed by electron microscopy of these samples. Although the samples were prepared using wet-chemical techniques and the melt was quenched in water, a phase-separated, irregular structure could nevertheless be observed by electron microscopy. Thus the Raman experiments suggest that the phase separation observed is developed by growth of small areas of different composition in the glass. The composition fluctuations may already be present in the melt.

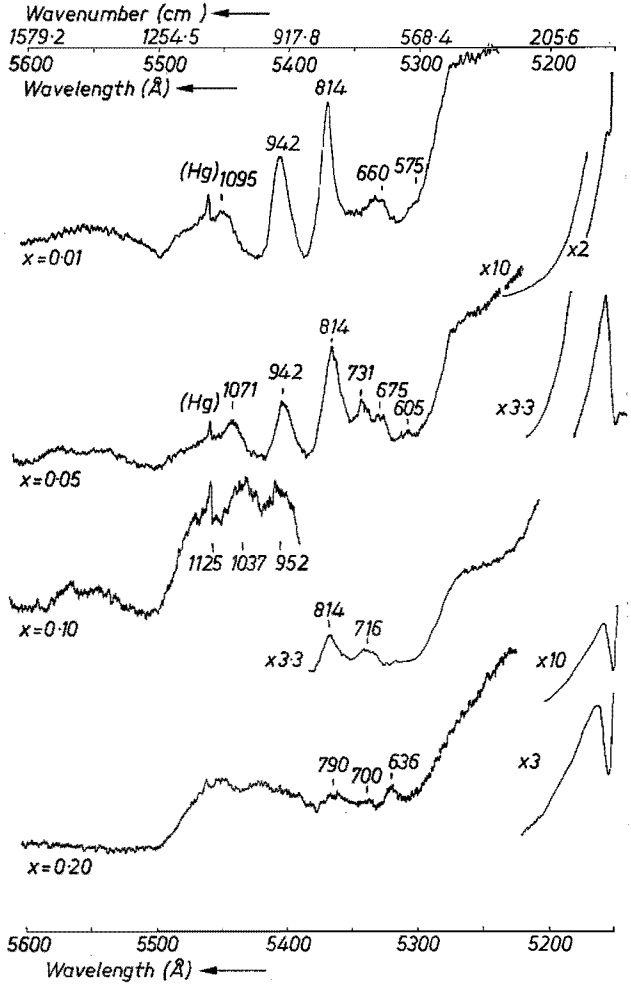

Fig. 3.53. Raman spectra of glasses in the system $x\,K_2O\,.\,(0{\cdot}35 - x)\,B_2O_3\,.\,0{\cdot}65\,SiO_2$ (direction $x(yz + yx)y$).

Borosilicate glasses with 65 *mol* % SiO_2

The Raman spectra of borosilicate glasses with a high amount of SiO_2 are shown in figs 3.52 to 3.65. In the series of glasses of composition $x\,K_2O\,.\,(0{\cdot}35 - x)\,B_2O_3\,.\,0{\cdot}65\,SiO_2$ (figs 3.52 and 3.53) and $x\,K_2O\,.\,(0{\cdot}30 - x)\,B_2O_3\,.\,0{\cdot}70\,SiO_2$ (figs 3.54 and 3.55) one observes that at low K_2O concentration boroxol groups (a_3) are again present as revealed by the presence of the characteristic peak at about 806 cm^{-1}. The high peak at about 470 cm^{-1} suggests that SiO_2 is present in a vitreous-silica-like structure. The glass of composition $0{\cdot}05\,K_2O\,.\,0{\cdot}30\,B_2O_3\,.\,0{\cdot}65\,SiO_2$ shows in its Raman spectrum (cf.

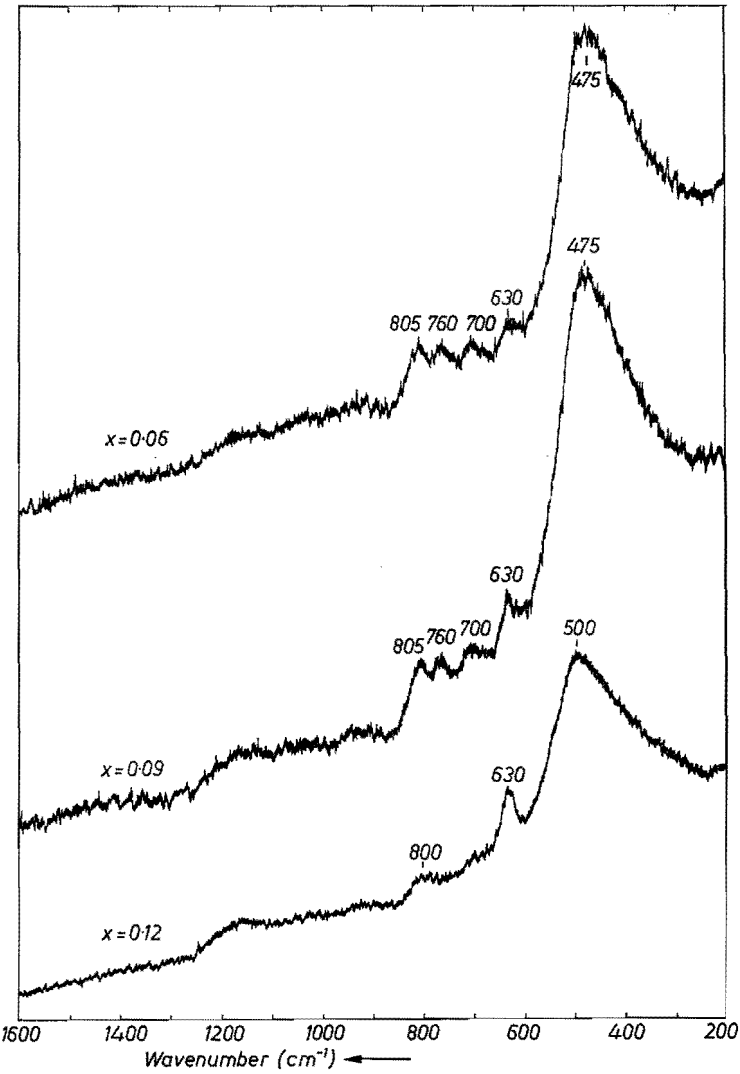

Fig. 3.54. Raman spectra of glasses in the system $x\,K_2O\,.\,(0{\cdot}30-x)\,B_2O_3\,.\,0{\cdot}70\,SiO_2$ (direction $x(zz+zx)y$).

fig. 3.52) the presence of a peak at 770 cm^{-1} which reveals the presence of BO_4 units in six-membered rings.

In the spectrum of the glass with composition $0{\cdot}10\,K_2O\,.\,0{\cdot}25\,B_2O_3\,.\,0{\cdot}65\,SiO_2$ a peak is observed at 805 cm^{-1} due to boroxol groups (a_3), at 765 cm^{-1} due to the six-membered-ring borate groups (a_2c) and at 625 cm^{-1} a small peak due to ring-type metaborate groups (b_3). The shift of the peak at 490 cm^{-1} now reveals that the silica network is attacked by K_2O, compare

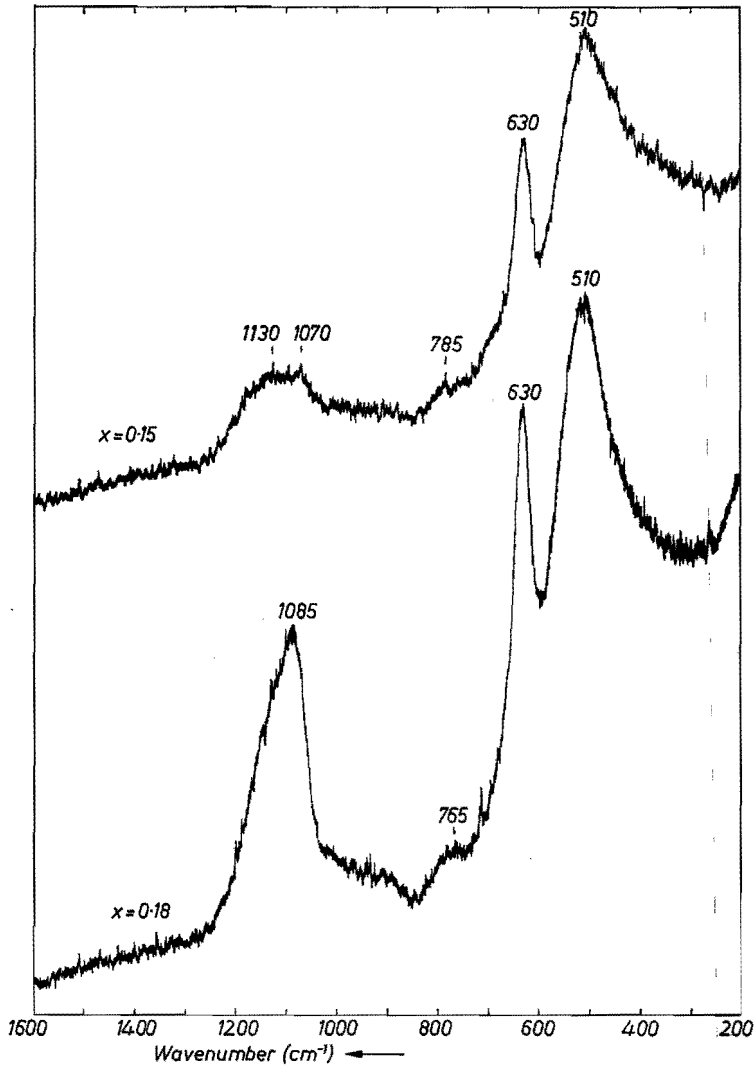

Fig. 3.55. Raman spectra of glasses in the system $x\,K_2O\,.\,(0{\cdot}30-x)\,B_2O_3\,.\,0{\cdot}70\,SiO_2$ (direction $x(zz+zx)y$).

with fig. 3.25 in which the spectra of the K_2O–SiO_2 glasses are shown. It is not clear which unit is responsible for the peak at 700 cm^{-1}. For this composition the K/B ratio is 0·4; it is interesting to note that at this ratio there are still boroxol groups (a_3) present and that part of the alkali ions are bonded to the silicate network.

In the spectrum of the glass with composition $0{\cdot}20\,K_2O\,.\,0{\cdot}15\,B_2O_3\,.\,0{\cdot}65\,SiO_2$ one clearly observes a peak at 635 cm^{-1} due to the ring-type meta-

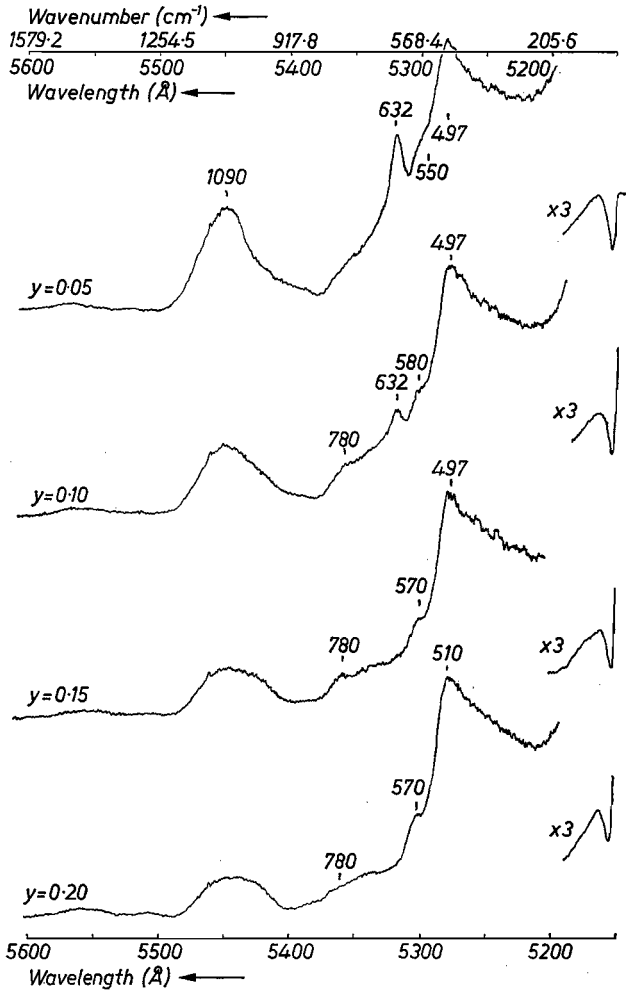

Fig. 3.56. Raman spectra of glasses in the system 0·10 Na_2O . 0·10 K_2O . 0·15 B_2O_3. 0·65 SiO_2 + y Al_2O_3 (direction $x(zz + zx)y$).

borate groups (b_3). The band at 765 cm^{-1} reveals the presence of six-membered-ring borate groups (a_2c).

In the composition series x K_2O . (0·30 — x) B_2O_3 . 0·70 SiO_2 the same type of spectra are observed as in the series x K_2O . (0·35 — x) B_2O_3 . 0·65 SiO_2 (cf. figs 3.54 and 3.55).

The spectra of the glasses in the composition series x K_2O . (0·35 — x) B_2O_3 . 0·65 SiO_2 to which 0·05 Al_2O_3 is added are shown in figs 3.58 and 3.59. On comparing figs 3.58 and 3.52 the influence of Al_2O_3 on the spectra for the direction $x(zz + zx)y$ is evident. It is clear that addition of 0·05 Al_2O_3 to the glass of composition 0·05 K_2O . 0·30 B_2O_3 . 0·65 SiO_2 leads to the dis-

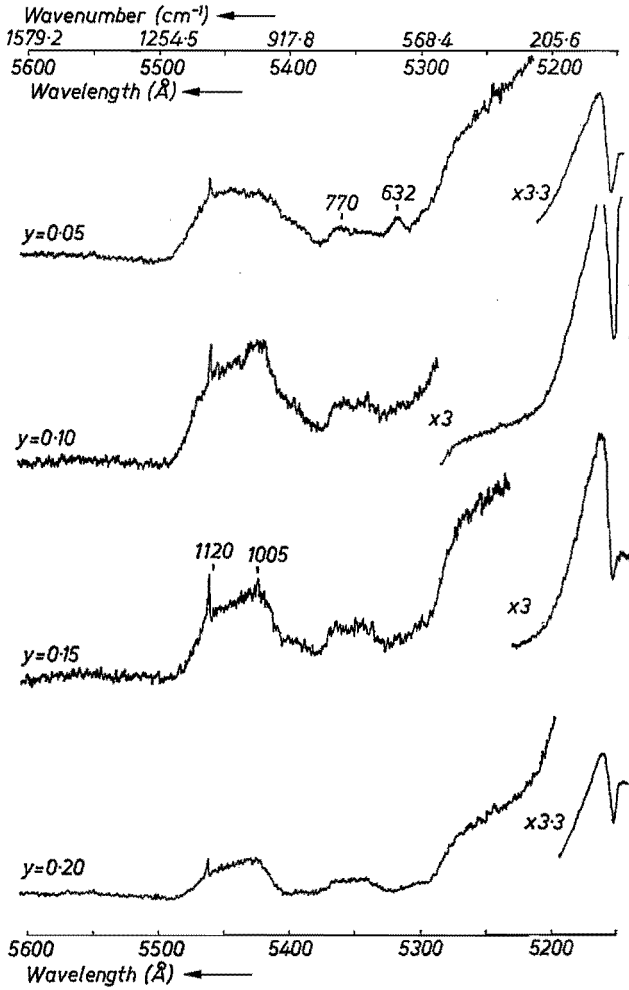

Fig. 3.57. Raman spectra of glasses in the system $0{\cdot}10\ Na_2O\ .\ 0{\cdot}10\ K_2O\ .\ 0{\cdot}15\ B_2O_3\ .\ 0{\cdot}65\ SiO_2 + y\ Al_2O_3$ (direction $x(yz + yx)y$).

appearance of BO_4 tetrahedra in borate groups as evidenced by the disappearance of the characteristic peak at 770 cm^{-1}.

At $x = 0{\cdot}10$ one observes a decrease of the peaks at 770 cm^{-1}, at 700 cm^{-1} and at 630 cm^{-1}. The spectrum that results shows a reasonable similarity with the spectrum of the glass of composition $x = 0{\cdot}05$ with no Al_2O_3 present. This makes it clear that Al takes away the necessary K ions from borate groups to form probably AlO_4 tetrahedra.

The glass of composition $0{\cdot}20\ K_2O\ .\ 0{\cdot}15\ B_2O_3\ .\ 0{\cdot}65\ SiO_2 + 0{\cdot}05\ Al_2O_3$ has probably a decreased content of ring-type metaborate groups (b_3) compared to the glass without Al_2O_3.

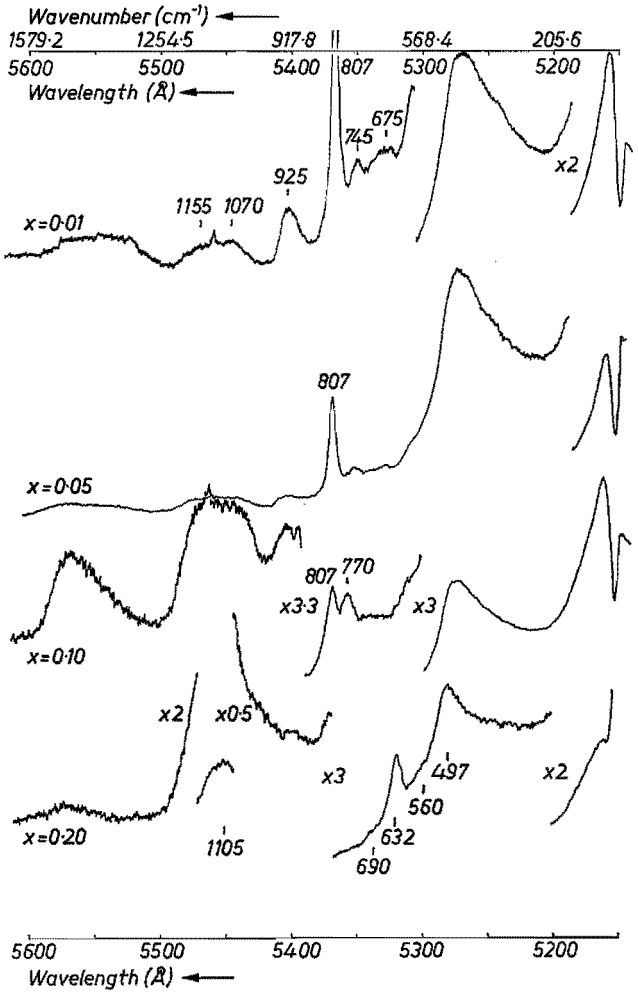

Fig. 3.58. Raman spectra of glasses in the system $x\ K_2O\ .\ (0{\cdot}35 - x)\ B_2O_3\ .\ 0{\cdot}65\ SiO_2 + 0{\cdot}05\ Al_2O_3$ (direction $x(zz + zx)y$).

In the spectra of the composition series $0{\cdot}10\ Na_2O\ .\ 0{\cdot}10\ K_2O\ .\ 0{\cdot}15\ B_2O_3\ .\ 0{\cdot}65\ SiO_2 + y\ Al_2O_3$ the effect can be observed of increasing amounts of Al_2O_3 (cf. figs 3.56 and 3.57). From fig. 3.56 it becomes clear that increasing the amount of Al_2O_3 leads to a disappearance of the ring-type metaborate groups (b_3) at about $y = 0{\cdot}15$. The spectrum of the glass with $y = 0{\cdot}15$ is very similar to the spectrum of the glass of composition $0{\cdot}20\ K_2O\ .\ 0{\cdot}20\ Al_2O_3\ .\ 0{\cdot}60\ SiO_2$ (fig. 3.28), which probably means that Al ions are present practically only in AlO_4 tetrahedra. The small amount of K_2O left is probably used for BO_4 tetrahedra in six-membered borate rings as indicated by the presence of a band at 780 cm^{-1}. Addition of more Al_2O_3 diminishes this band further, see

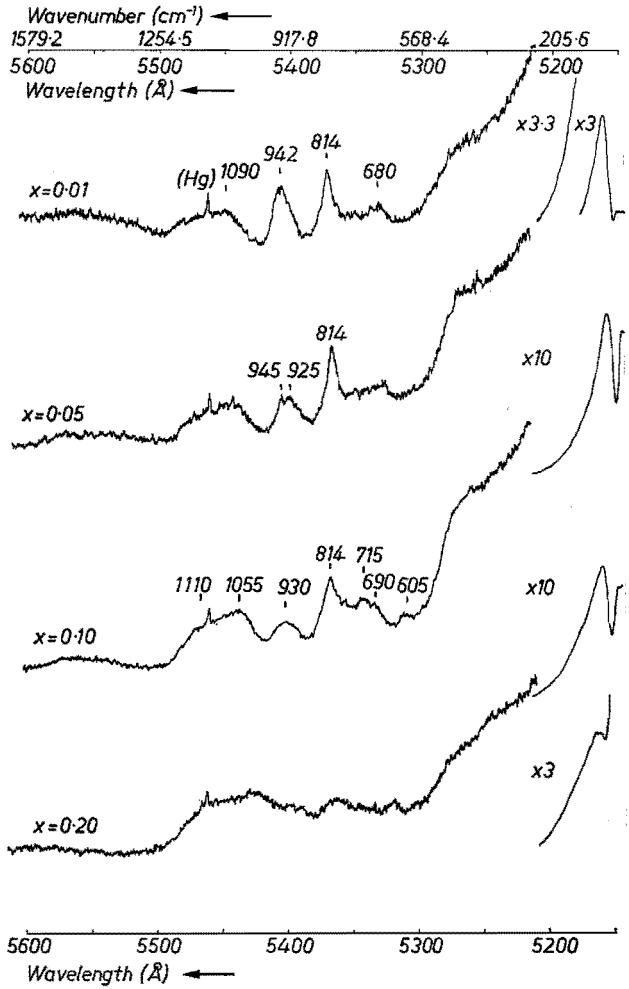

Fig. 3.59. Raman spectra of glasses in the system $x\,K_2O\,.\,(0{\cdot}35 - x)\,B_2O_3\,.\,0{\cdot}65\,SiO_2 + 0{\cdot}05\,Al_2O_3$ (direction $x(yz + yx)y$).

the spectrum of the glass of composition $0{\cdot}10\,Na_2O\,.\,0{\cdot}10\,K_2O\,.\,0{\cdot}15\,B_2O_3\,.\,0{\cdot}65\,SiO_2 + 0{\cdot}20\,Al_2O_3$. In this spectrum one cannot observe peaks that are characteristic of certain borate groups, hence the impression arises that boron is present in BO_3 triangles randomly distributed in the network.

The conclusion from the spectra of the glasses containing increasing amounts of Al_2O_3 can be that in the base glass of composition $0{\cdot}10\,Na_2O\,.\,0{\cdot}10\,K_2O\,.\,0{\cdot}15\,B_2O_3\,.\,0{\cdot}65\,SiO_2$ between 10 and 15 mol % of the alkali oxide is used for the formation of ring-type metaborate groups (b_3). The rest of the alkali oxide is probably used for the formation of ring-type six-membered borate groups with a BO_4 tetrahedron (a_pc_q) and SiO_4 tetrahedra with a non-bridging

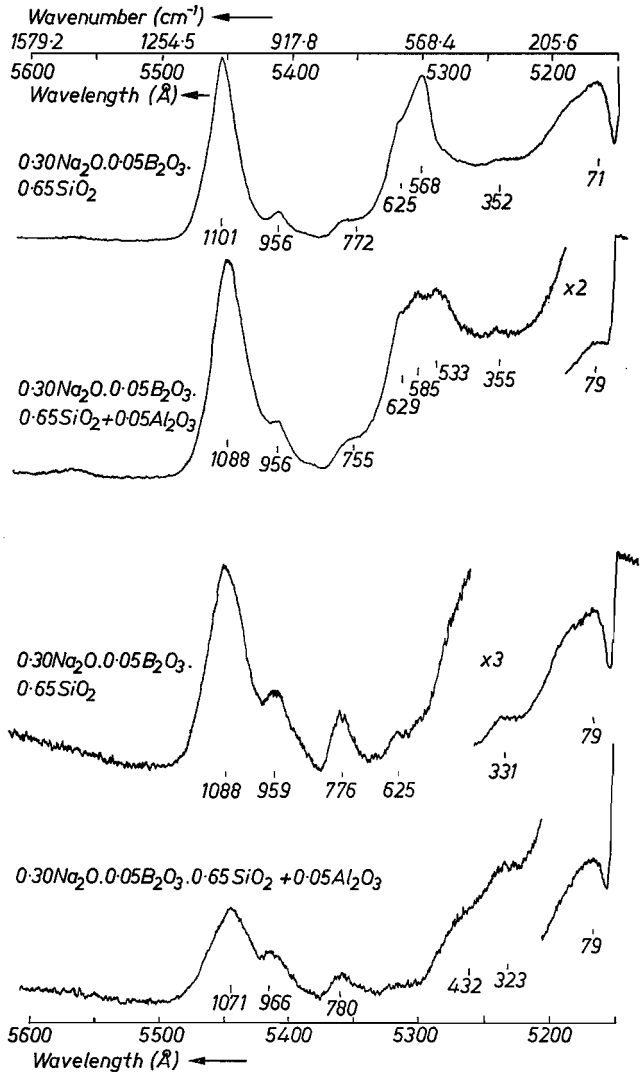

Fig. 3.60. Raman spectra of borosilicate glasses (two upper traces: direction $x(zz + zx)y$; two lower traces: direction $x(yz + yx)y$).

oxygen ion. Electron microscopy of this glass suggests an irregular phase-separated structure. The composition fluctuations seem to extend over a few hundred Ångstrom. This may suggest that the metaborate groups are agglomerated to some extent. Independent of the extent to which the borate groups are agglomerated the conclusion can be drawn that the tendency to phase separation extends to a larger area of the sodium-borosilicate system than is described in sec. 1.3. Another conclusion that can be drawn is that boron ions

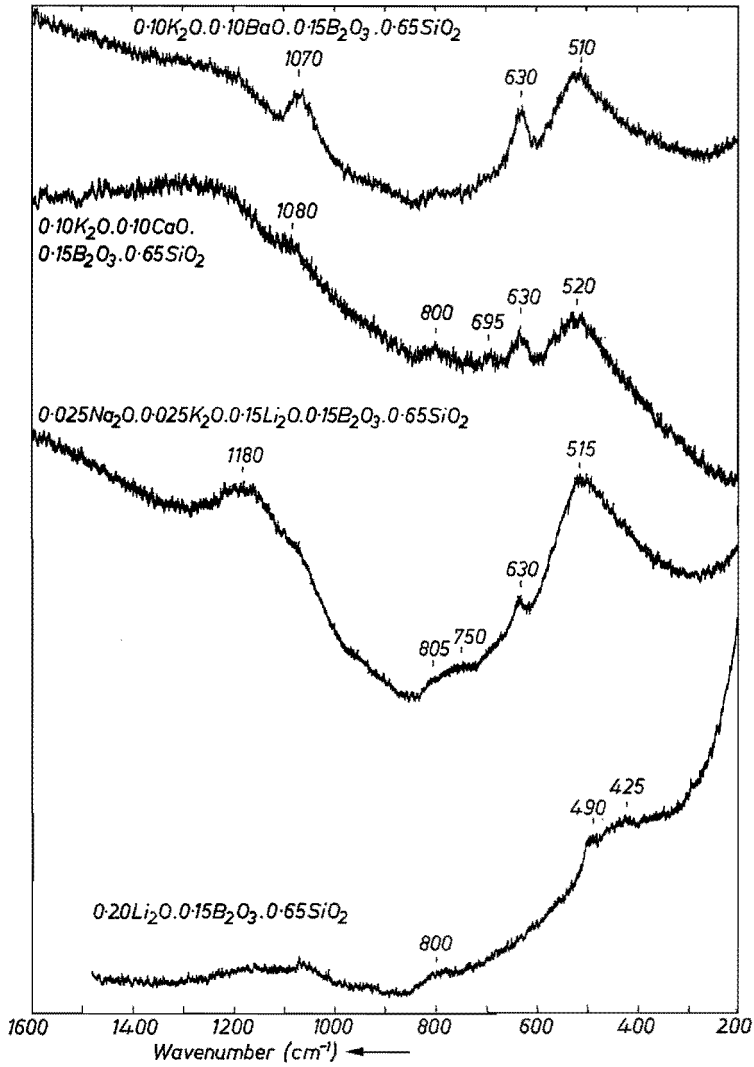

Fig. 3.61. Raman spectra of borosilicate glasses (direction $x(zz + zx)\bar{y}$).

are not incorporated on a large scale in the silicate network in a way analogous to the aluminum ion. This is not so strange, as at atmospheric pressure no crystalline alkali borosilicates could be prepared up to now.

Boron analogues of albite (reedmergnerite, $NaBSi_3O_8$) and potassium feldspar ($KBSi_3O_8$) have been hydrothermally prepared by Eugster and McIver [3–58]), reedmergnerite, NaB Si_3O_8 also by Appleman and Clark [3–59]). Both alkali-borosilicate compounds melt incongruently to quartz and glass (Eugster and McIver [3–58])). In fig. 3.65 the Raman spectra are shown of the correspond-

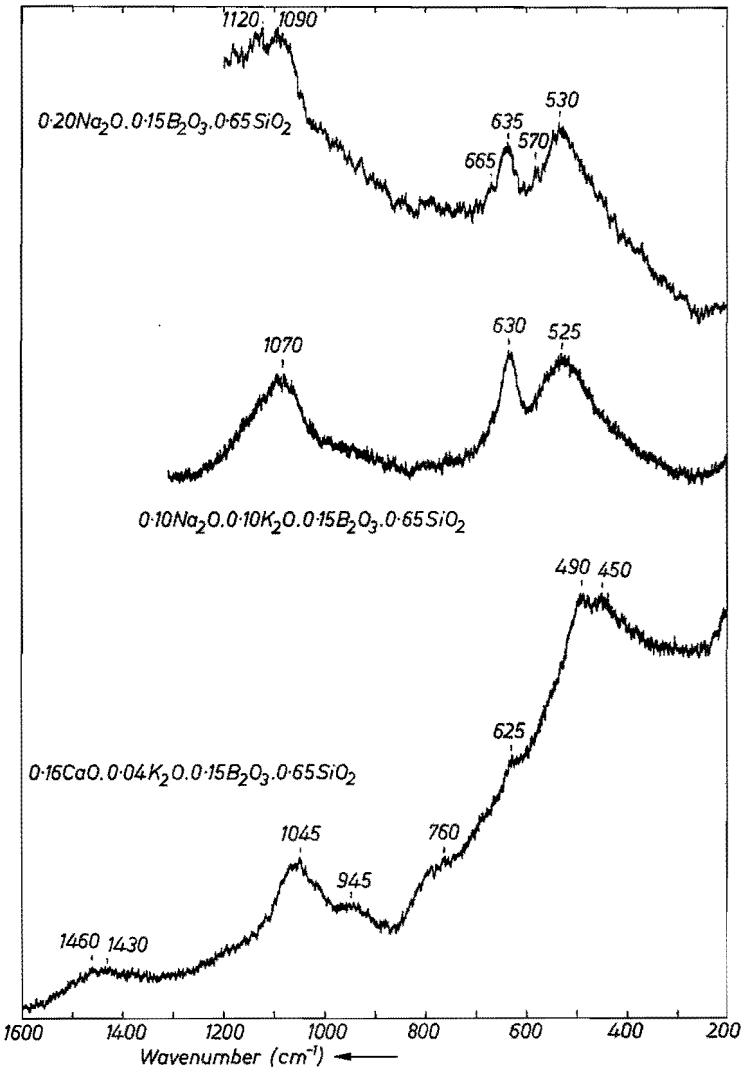

Fig. 3.62. Raman spectra of borosilicate glasses (direction $x(zz + zx)y$).

ing alkali-borosilicate glasses (0·125 R_2O . 0·125 B_2O_3 . 0·75 SiO_2) which confirm that no BO_4 units are incorporated in the silicate network but that primarily ring-type metaborate groups (b_3) are formed instead. Eugster and McIver also synthesized the boron analogue of the compound kalsilite (KB SiO_4). The Raman spectrum of a glass of like composition is shown in fig. 3.65 and again reveals that BO_4 is not primarily taken up in the silicate network.

The results of the Raman spectra in the high-silica range are reasonably

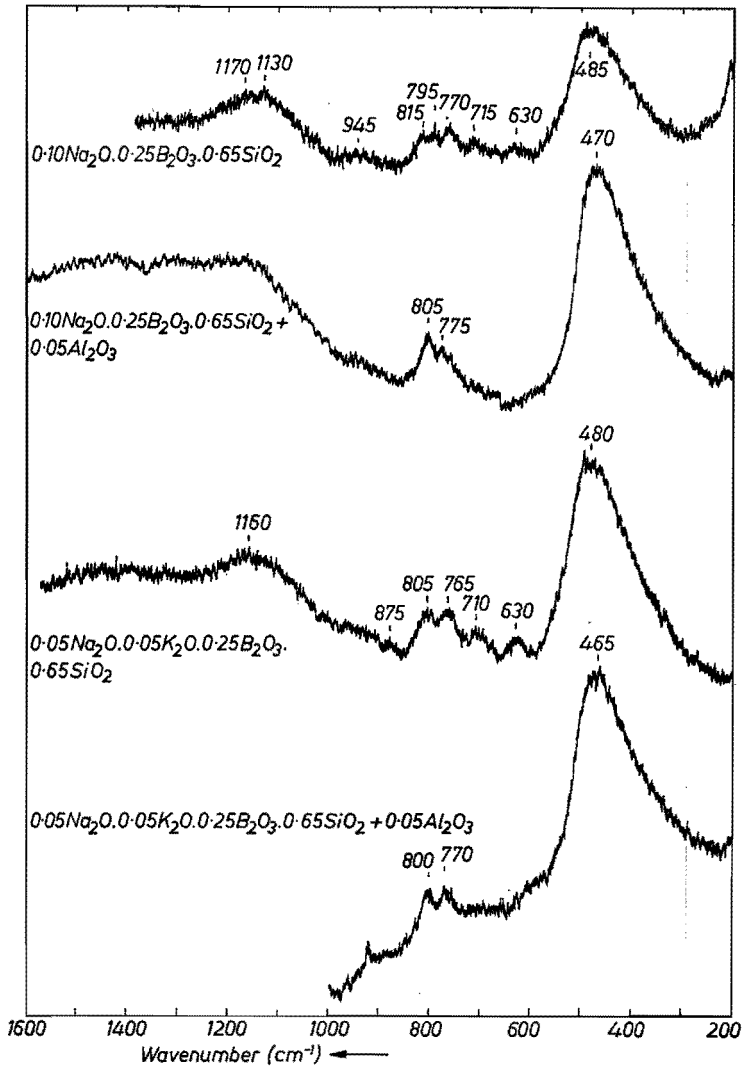

Fig. 3.63. Raman spectra of borosilicate glasses (direction $x(zz + zx)y$.

consistent with the experimental n.m.r. results on borosilicate glasses of Scheerer et al.[3-60]) and Milberg et al.[3-61]). They concluded from their ^{11}B n.m.r. measurements that the alkali oxide is primarily attracted by the borate units. The measured maximum relative number of boron ions in tetrahedral coordination N_4 increases with increasing SiO_2 content at constant alkali-to-boron ratio when this ratio is above 0·5. At lower ratios all alkali is used for the formation of BO_4 tetrahedra, which is consistent with the Raman spectra in this thesis. The N_4 values measured by Scheerer et al.[3-60]) seem somewhat

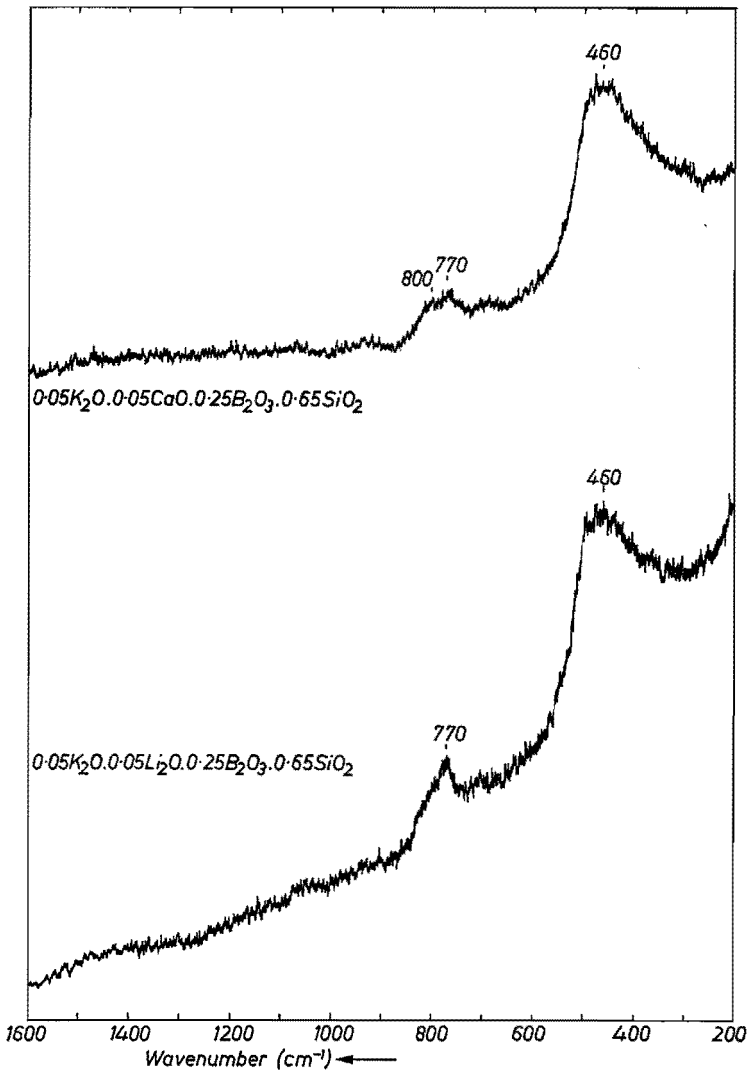

Fig. 3.64. Raman spectra of borosilicate glasses (direction $x(zz + zx)y$).

too high, anyway three of the measured N_4 values are higher than the theoretical maximum values.

The decrease in line width of the ^{11}B resonance with increasing silica content is related by Scheerer et al. to a statistical distribution of the boron and silicon polyhedra. The latter statement is doubted somewhat because the Raman spectra do indicate a preference of the boron ions for borate grouping. It can be observed that the decrease in line width is the greater the more alkali oxide is present in the glass. This may also be explained by assuming that in borosilicate

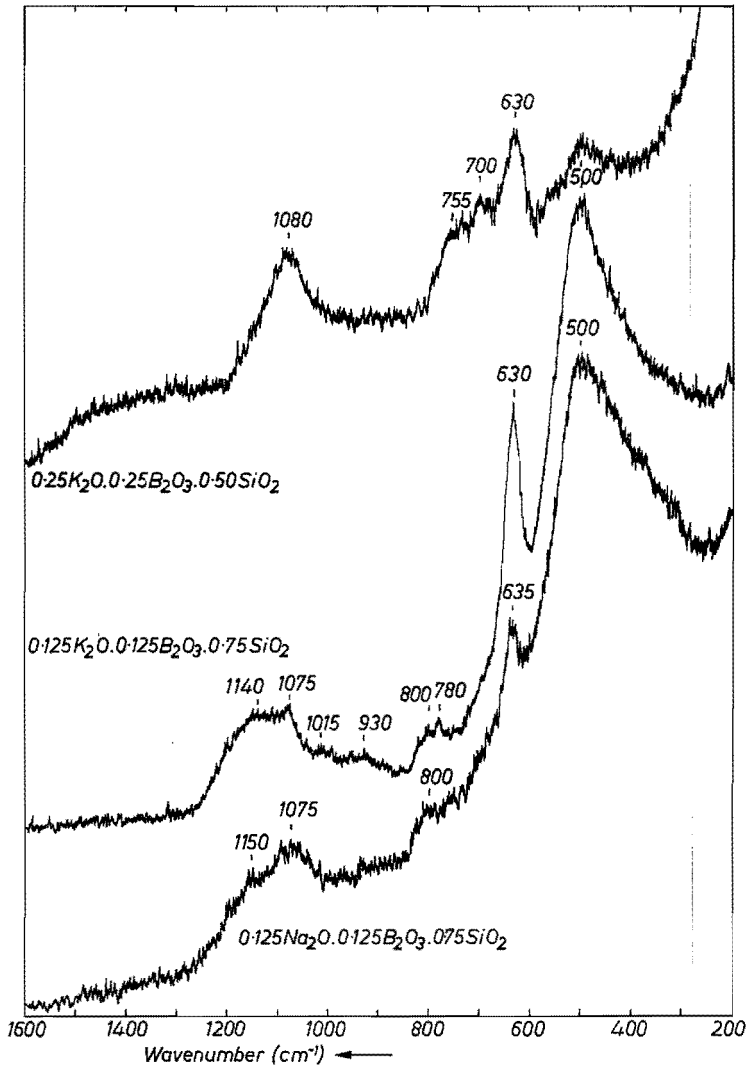

Fig. 3.65. Raman spectra of borosilicate glasses (direction $x(zz + zx)y$).

glasses there is less tendency to form six-membered borate rings with two BO_4 tetrahedra. When BO_4 tetrahedra are separated from each other the dipole–dipole interaction becomes less and consequently the line width of the ^{11}B resonance decreases. This latter explanation of the n.m.r. results of Scheerer et al. is consistent with the Raman spectra referred to in this chapter.

It can be observed that there is no significant difference between the spectra of sodium-, potassium- and mixed Na–K-borosilicate glasses of equal alkali-oxide content. Introduction of Al_2O_3 into these borosilicate glasses, with

65 mol % SiO_2 also gives the same type of spectra for sodium- and potassium-borosilicate glasses.

Replacement of sodium and potassium oxide in a glass of composition 0·20 R_2O . 0·15 B_2O_3 . 0·65 SiO_2 by Li_2O clearly results in different spectra (cf. fig. 3.61). The peak at about 630 cm^{-1} decreases and ultimately vanishes at 0·20 Li_2O . So the ring-type metaborate groups (b_3) are replaced by other borate groups. Crystalline Li_2O . B_2O_3 is not built up of ring-type metaborate groups (b_3) but of chain-type groups (b_∞) with one non-bridging oxygen ion per BO_3 triangle. The spectra of the lithium-borosilicate glasses, however, cannot be reconciled with the presence of chain-type metaborate groups (b_∞), although this cannot be altogether excluded.

Substitution of potassium oxide in the same base glass as above by CaO and BaO shows the same tendency in the Raman spectra as Li_2O (cf. figs 3.61 and 3.62). The introduction of CaO seems to diminish the amount of ring-type metaborate groups (b_3) as could be expected because crystalline CaO . B_2O_3 like Li_2O . B_2O_3, is built up of chain-type metaborate groups (b_∞). The Raman spectrum of a glass of composition 0·16 CaO . 0·04 K_2O . 0·15 B_2O_3 . 0·65 SiO_2 (fig. 3.62) does not suggest that chain-type metaborate groups (b_∞) are formed although this cannot be excluded. As indicated by the rise of the peak at about 945 cm^{-1} it is suggested that some SiO_4 tetrahedra with two non-bridging oxygen ions are present in this glass. In the glasses of composition 0·05 K_2O . 0·05 CaO . 0·25 B_2O_3 . 0·65 SiO_2 and 0·05 K_2O . 0·05 Li_2O . 0·25 B_2O_3 . 0·65 SiO_2 the Raman spectra (fig. 3.64) show that probably fewer ring-type metaborate groups (b_3) are present there than in the corresponding glass with 10 mol % K_2O. There seems to be a tendency to form more six-membered borate rings with a BO_4 unit (a_2c) but this is not very clearly visible in the spectra.

3.5.3. *Conclusions*

In table 3-II the results are summarized for the three series of glasses with different SiO_2 contents. The Raman spectra of the borosilicate glasses indicate that below alkali-to-boron ratios of 0·5, all or nearly all alkali ions are used to form primarily ring-type six-membered borate groups with one or two BO_4 groups (a_pc_q) that to a certain extent may be ordered to form tetraborate (a_6c_2) or diborate groups (a_2c_2). There seems to be some resistance to the formation of six-membered borate rings with two BO_4 tetrahedra (ac_2). On increase of the alkali-to-boron ratio above 0·5 non-bridging oxygen ions connected to SiO_4 tetrahedra are formed in a possibly disilicate-like structure, below this ratio SiO_2 seems only to be present in a vitreous-silica-like structure. At alkali-to-boron ratios above 0·5 significant amounts of ring-type metaborate (b_3), pyroborate (b_2'') groups and orthoborate units (b''') are also formed as in binary alkali-borate glasses. At alkali-to-boron ratios of about unity there seems to be

TABLE 3-II

Borate and silicate groups present in alkali-borosilicate glasses

	alkali/boron ratio $< 0{\cdot}5$	alkali/boron ratio $> 0{\cdot}5$
15 mol % SiO_2	boroxol (a_3) tetraborate (a_6c_2) diborate (a_2c_2) SiO_4 (four bridging oxygen ions)	diborate (a_2c_2) SiO_4 (four bridging oxygen ions) SiO_4^- (one non-bridging oxygen ion)
35 mol % SiO_2	boroxol (a_3) tetraborate (a_6c_2) diborate (a_2c_2) SiO_4 (four bridging oxygen ions)	diborate (a_2c_2) metaborate (b_3) SiO_4 (four bridging oxygen ions) SiO_4^- (one non-bridging oxygen ion)
65 mol % SiO_2	boroxol (a_3) tetraborate (a_6c_2) diborate (a_2c_2) metaborate (b_3) SiO_4 (four bridging oxygen ions)	metaborate (b_3) SiO_4 (four bridging oxygen ions) SiO_4^- (one non-bridging oxygen ion)

an increase in the formation of ring-type metaborate groups (b_3) for the sodium- and potassium-borosilicate glasses on increase of the SiO_2 content. There is no indication that BO_4 units are incorporated in the silicate network in the same way as AlO_4 units.

Part of the boron ions is not present in typical borate rings but as "loose" BO_3 triangles and "loose" BO_4 tetrahedra, analogous to the binary borate glasses. The Raman spectra of the borosilicate glasses suggest a certain phase-separated structure of these glasses on a very small scale extending beyond the usually indicated borders of subliquidus phase separation in these systems. At low SiO_2 content the molecules seem to be agglomerated to a vitreous-silica-like structure. At higher SiO_2 and Na_2O or K_2O concentrations the structure of the continuous phase resembles that of silicate glasses; in these same concentration regions the metaborate groups (b_3) seem to be agglomerated too, as suggested by electron microscopy.

The introduction of Al_2O_3 leads to a decrease of borate units with alkali ions and the probable formation of AlO_4 tetrahedra. At low alkali-to-boron ratios the introduction of Al_2O_3 clearly leads to the re-formation of boroxol groups (a_3). At higher ratios it is not clear how boron is incorporated in the structure; it may be that boron is present in a random structure of BO_3 units (a) more or less dispersed over the silicate network. The AlO_4 tetrahedra seem to be incorporated in the silicate network.

The presence of SiO_4 tetrahedra with two non-bridging oxygen ions is observed in borosilicate glasses containing a fair amount of alkaline-earth oxides.

REFERENCES

3-1) R. Shuker and R. W. Gamon, in M. Balkanski (ed.), Proc. 2nd international conference on lightscattering in solids, Flammarion Sciences, Paris, 1971, p. 334.
3-2) N. Neuroth, in H. Volkmann (ed.), Handbuch der Infra-rot Spektroskopie, Verlag Chemie, Weinheim, 1972, Ch. 10.
3-3) J. Wong and C. A. Angell, Appl. Spectr. Rev. **4**, 155, 1971.
3-4) I. Simon, in J. D. Mackenzie (ed.), Modern aspects of the vitreous state, Butterworth, London, 1960, p. 120.
3-5) V. A. Maroni and E. J. Cairns, J. chem. Phys. **52**, 4915, 1970.
3-6) T. W. Bril, Thesis, Technological University Eindhoven, The Netherlands, 1975.
3-7) S. Pinchas and J. Shamir, J. chem. Phys. **56**, 2017, 1972.
3-8) K. Frey and E. Funck, Z. Naturforsch. **27b**, 101, 1972.
3-9) J. B. Bates, A. S. Quist and G. E. Boyd, J. chem. Phys. **54**, 124, 1971.
3-10) J. L. Parsons, J. chem. Phys. **33**, 1860, 1960.
3-11) J. Krogh-Moe, Phys. Chem. Glasses **6**, 46, 1965.
3-12) W. H. Zachariasen, Acta cryst. **17**, 749, 1964.
3-13) M. Marezio, H. A. Plettinger and W. H. Zachariasen, Acta cryst. **16**, 390, 1963.
3-14) M. Marezio, H. A. Plettinger and W. H. Zachariasen, Acta cryst. **16**, 594, 1963.
3-15) W. Schneider and G. B. Carpenter, Acta cryst. **B26**, 1189, 1970.
3-16) J. Krogh-Moe, Acta cryst. **15**, 190, 1962.
3-17) J. Krogh-Moe, Acta cryst. **B24**, 179, 1968.
3-18) J. Krogh-Moe, Acta cryst. **B30**, 578, 1974.
3-19) J. Krogh-Moe, Acta cryst. **B28**, 3089, 1972.
3-20) M. Martinez-Ripoll, S. Martinez-Carrera and S. Garcia-Blanco, Acta cryst. **B27**, 672, 1970.
3-21) S. Block and A. Perloff, Acta cryst. **19**, 297, 1965.
3-22) J. Krogh-Moe, Acta chem. Scand. **18**, 2055, 1964.
3-23) J. Krogh-Moe, Acta cryst. **13**, 889, 1960.
3-24) J. Krogh-Moe, Acta cryst. **B28**, 1571, 1972.
3-25) J. Krogh-Moe, Acta cryst. **B30**, 747, 1974.
3-26) A. Hyman, A. Perloff, F. Mauer and S. Block, Acta cryst. **22**, 815, 1967.
3-27) J. Krogh-Moe, Acta cryst. **18**, 1088, 1965.
3-28) J. Krogh-Moe, Acta cryst. **B28**, 168, 1972.
3-29) J. F. Scott and S. P. S. Porto, Phys. Rev. **161**, 903, 1967.
3-30) J. B. Bates and A. S. Quist, J. chem. Phys. **56**, 1528, 1971.
3-31) J. B. Bates, J. chem. Phys. **57**, 4042, 1972.
3-32) F. Liebau, Acta cryst. **14**, 389, 1961.
3-33) F. Liebau, Acta cryst. **14**, 395, 1961.
3-34) A. K. Pant and D. W. J. Cruickshank, Acta cryst. **B24**, 13, 1968.
3-35) A. N. Lazarev, Vibrational spectra and structure of silicates, Consultants Bureau New York-London, 1972.
3-36) W. S. McDonald and D. W. J. Cruickshank, Acta cryst. **22**, 37, 1967.
3-37) R. L. Mozzi and B. E. Warren, J. appl. Cryst. **3**, 251, 1970.
3-38) J. Goubeau and H. Keller, Z. anorg. Chem. **272**, 363, 1953.
3-39) L. A. Kristiansen and J. Krogh-Moe, Phys. Chem. Glasses **9**, 96, 1968.

3–40) J. Krogh-Moe, J. non-cryst. Solids **1**, 269, 1969.
3–41) M. Coenen, Glastechn. Ber. **35**, 14, 1962.
3–42) C. Rhee, J. Korean phys. Soc. **4**, 51, 1971.
3–43) J. Krogh-Moe, Phys. Chem. Glasses **3**, 101, 1962.
3–44) S. Kumar, Phys. Chem. Glasses **4**, 106, 1963.
3–45) S. R. Nagel and C. G. Bergeron, J. Am. ceram. Soc. **57**, 129, 1974.
3–46) P. J. Bray and J. G. O'Keefe, Phys. Chem. Glasses **4**, 37, 1963.
3–47) J. Krogh-Moe, Phys. Chem. Glasses **3**, 1, 1962.
3–48) S. Block and G. J. Piermarini, Phys. Chem. Glasses **5**, 138, 1964.
3–49) J. Krogh-Moe, Phys. Chem. Glasses **3**, 208, 1962.
3–50) P. Beekenkamp, Philips Res. Repts Suppl. 1966, No. 4.
3–51) G. M. Willis and F. L. Hennessy, J. Metals **5**, 1367, 1953.
3–52) J. Krogh-Moe, Ark. Kemi **14**, 451, 1959.
3–53) M. Hass, J. Phys. Chem. Solids **31**, 415, 1970.
3–54) J. Etchepare, J. chem. Phys. **67**, 890, 1970.
3–55) J. Etchepare, Spectrochim. Acta **26A**, 2147, 1970.
3–56) R. DiSalvo, W. B. White, G. E. Rindone, G. J. McCarthy and S. Brawer, Laser Raman spectra and structure of glasses in the system Na_2O–Al_2O_3–SiO_2, Presented at the 75th annual meeting of the American Ceramic Society, Cincinnati, Ohio, U.S.A., May 1973.
3–57) R. L. Mozzi and B. E. Warren, J. appl. Cryst. **2**, 164, 1969.
3–58) H. P. Eugster and N. L. McIver, Bull. geol. Soc. Amer. **70**, 1598, 1959.
3–59) D. E. Appleman and J. R. Clark, Am. Mineral. **50**, 1827, 1965.
3–60) J. Scheerer, W. Müller-Warmuth and H. Dutz, Glastechn. Ber. **46**, 109, 1973.
3–61) M. E. Milberg, J. G. O'Keefe, R. A. Verhelst and H. O. Hooper, Phys. Chem. Glasses **13**, 79, 1972.
3–62) J. Krogh-Moe, Acta cryst. **B30**, 1178, 1974.
3–63) J. Krogh-Moe, Acta cryst. **B30**, 1827, 1974.
3–64) J. Etchepare, M. Merian and L. Smetankine, J. chem. Phys. **60**, 1873, 1974.
3–65) C. Rhee and P. J. Bray, Phys. Chem. Glasses **12**, 165, 1971.

4. INFRARED SPECTRA OF BORATE, SILICATE AND BOROSILICATE GLASSES

4.1. Introduction

No theory of vibrations is available for the interpretation of infrared spectra of glasses, which do not possess long-range order. Therefore a definite interpretation of the spectra of borate, silicate and borosilicate glasses cannot be given. Although the feasibility of an interpretation of the spectra is low, some authors have attempted by simple approaches to correlate certain absorption bands with the presence of certain structural units in glass. For a recent review of the infrared spectra of glasses the reader is referred to the work of Neuroth [4–1]).

The infrared spectra of a large number of crystalline inorganic borates were published by Weir and Schroeder [4–2]). Borates with complex ring-type groups generally exhibited spectra of such complexity that only a superficial discussion was attempted by the authors mentioned. Recently, Frey and Funck [4–3]) successfully applied the concept of group-frequency analysis to the interpretation of some hydrated pentaborate spectra. Up to now this is the only thorough interpretation of the infrared spectrum of an inorganic crystalline borate available. The same situation applies to the complex inorganic silicates.

As already stated, the infrared spectra of many borate compounds were already published by Weir and Schroeder [4–2]) but these spectra do not show the 3000–4000 cm^{-1} area in which hydroxyl groups have their characteristic vibrations. These hydroxyl groups also show their influence in the 400–1600 cm^{-1} area where the borate vibrations are situated. It is therefore absolutely necessary to study the complete spectra from 400 to 4000 cm^{-1} if one wishes to give a critical interpretation of these spectra. A second reason for republishing these spectra in this thesis is that the spectra of Weir and Schroeder [4–2]) and those given here of the same compounds are not always the same. A third reason is that in the last decennium the crystal structure of a number of borates was revealed and in these cases the samples were checked by X-ray analysis and found to be the same as the ones described. A final reason for republishing the spectra is that in this thesis the Raman spectra of the same samples are also published, hence the comparison of these spectra is not devalued by the fact that the latter are spectra of different samples.

No attempt will be made to interpret the spectra of the crystalline borates due to the great number of peaks and the complex structure of the borates. It will only be attempted by comparing the spectra of the glasses with the corresponding crystalline compounds, to postulate the presence of the same type of groups in the glasses as are present in the crystalline compounds. By this method

Krogh-Moe [4–4]) has found indications of the presence of certain borate groups in the glass that are also present in the crystalline borates.

With the silicates the situation is analogous to that of the borates. In this case too the spectra of the crystalline compounds will be used to discuss the presence of certain units in the silicate and borosilicate glasses.

4.2. Infrared spectra of polycrystalline borates and silicates

4.2.1. *Experimental results*

The infrared spectra of the crystalline borates are shown in figs 4.1 to 4.8. The spectra of crystalline silicates are shown in fig. 4.9. All spectra are recorded at room temperature using the KBr technique. All samples are the same as those used for the Raman investigations. In the tables 1-I and 1-II the crystal struc-

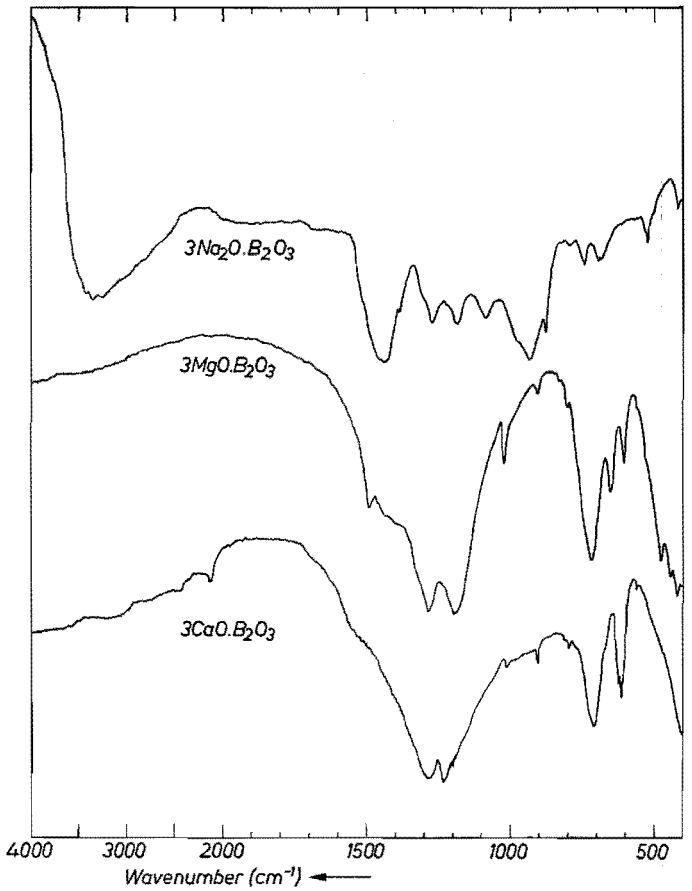

Fig. 4.1. Infrared spectra of polycrystalline orthoborates.

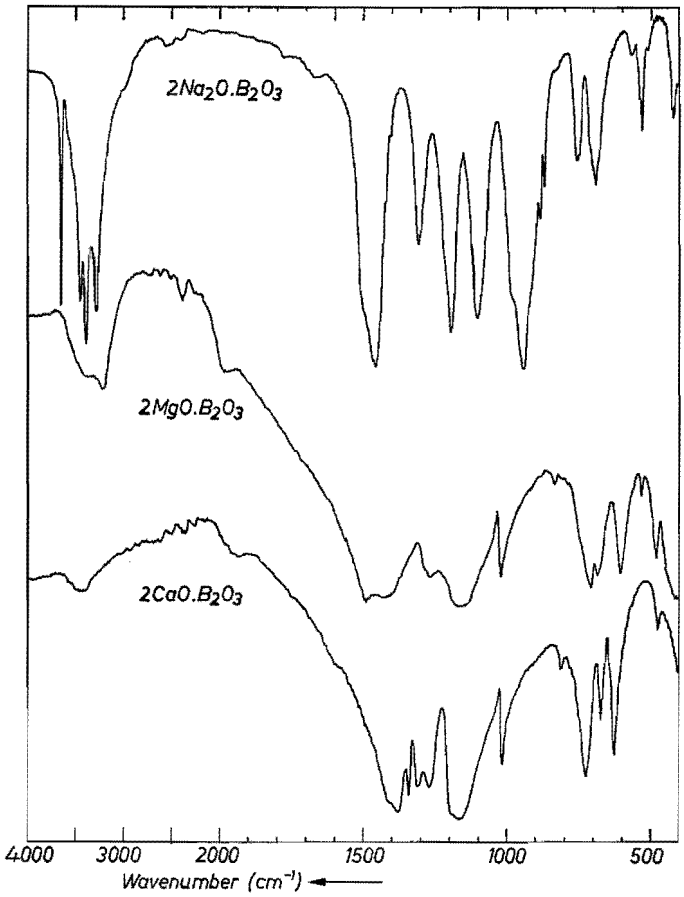

Fig. 4.2. Infrared spectra of polycrystalline pyroborates.

ture of the compounds is indicated. For information on the experimental equipment, see sec. 2.2.

4.2.2. *Discussion of results*

The infrared spectra of many borate compounds were already published by Weir and Schroeder [4–2]) but a number of them are republished for reasons mentioned in sec. 4.1. Earlier, Hart and Smallwood [4–5]) published a number of spectra of primarily alkaline-earth-borate compounds. The spectra of a number of crystalline borates with varying amounts of the isotopes ^{10}B and ^{11}B are published by Bril [4–6]).

The spectra of the polymorphs of crystalline SiO_2 are discussed in a review by Wong and Angell [4–7]). The infrared spectra of crystalline silicate compounds are widely scattered in the literature; spectra and further references can be found

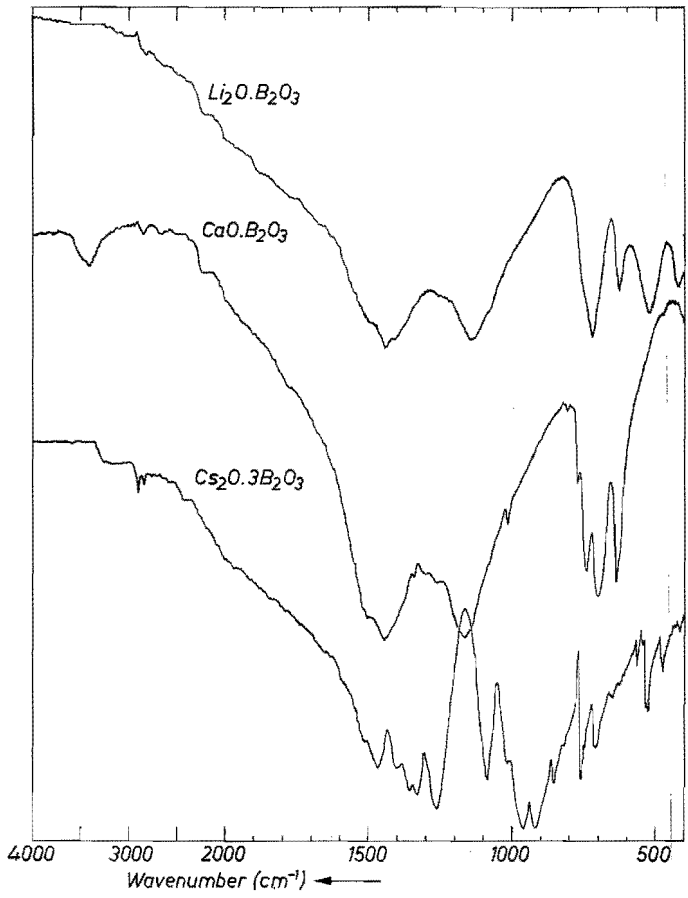

Fig. 4.3. Infrared spectra of polycrystalline borates.

in the work of Wong and Angell [4–7]), Dutova [4–8]), Cherneva and Florinskaya [4–9]), and Dutz [4–10]).

In the literature there are few attempts to give an interpretation of the spectra of crystalline borates. Exceptions are the work of Weir and Schroeder [4–2]), Frey and Funck [4–3]) and Gaskell [4–11]), see also the review by Wong and Angell [4–7]). The work of Bril [4–6]) also is of interest because, in this case, the Raman and infrared spectra of borate compounds with varying amounts of ^{10}B and ^{11}B are discussed. From the large number of peaks that are observed in these spectra it is clear that they are characteristic of large borate groups, such as, for instance, the metaborate ring (b_3). From comparison of the spectra of the crystalline borates it becomes clear that they may well serve as a fingerprint to reveal the presence of the same type of groups in the glasses as in the compounds.

Lazarev [4–13]) has given an interpretation of the spectra of crystalline silicates.

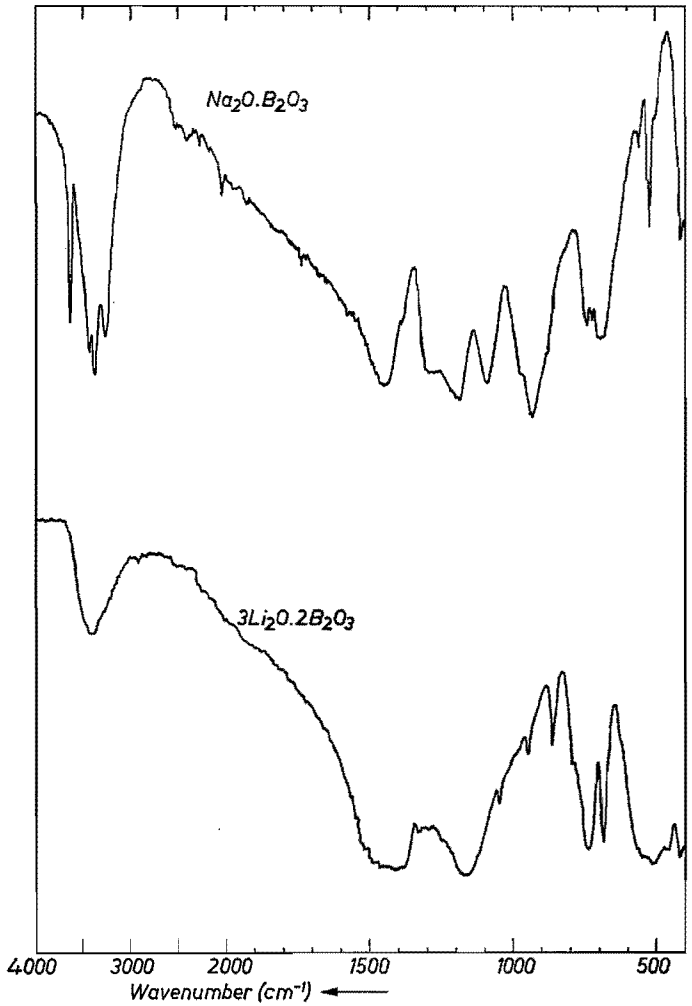

Fig. 4.4. Infrared spectra of polycrystalline borates.

The peaks are generally assigned to vibrations of small units. Due to the differences in the spectra of SiO_2, disilicate and metasilicate compounds they may serve well as a fingerprint to reveal the presence of SiO_4 units with no, one or two non-bridging oxygen ions.

The work of Iiishi, Tomisaka, Kato and Umegaki [4–12]) on potassium feldspar is also worth mentioning here.

4.2.3. *Conclusion*

Due to the large number of peaks that are observed in the spectra of the crystalline borates they cannot simply be ascribed to a BO_3 triangle or BO_4 tetra-

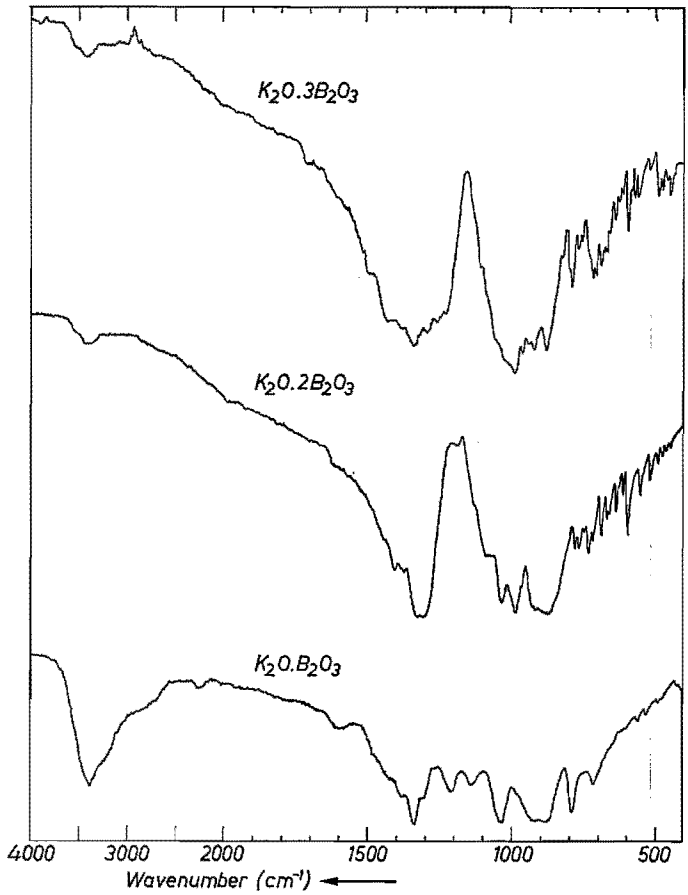

Fig. 4.5. Infrared spectra of polycrystalline potassium borates.

hedron. The spectra make it clear that they are characteristic of the presence of larger groups than these simple units, for example the six-membered borate group with a BO_4 tetrahedron (a_2c), the ring-type metaborate group (b_3), or of these groups influenced by their surroundings. Due to the large number of peaks, comparison with the spectra of the glasses can only be qualitative.

The spectra of the crystalline silicates are generally interpreted by assigning the peaks to small vibrating units, for instance Si–O–Si bridges. Thus these spectra cannot be taken as characteristic of larger groups, so that in comparison with the spectra of the glasses the interpretation, in terms of structural units present, cannot go beyond these small units. Due to the observed differences in the spectra, they may serve well to reveal the presence of SiO_4 tetrahedra with no, one or two non-bridging oxygen ions.

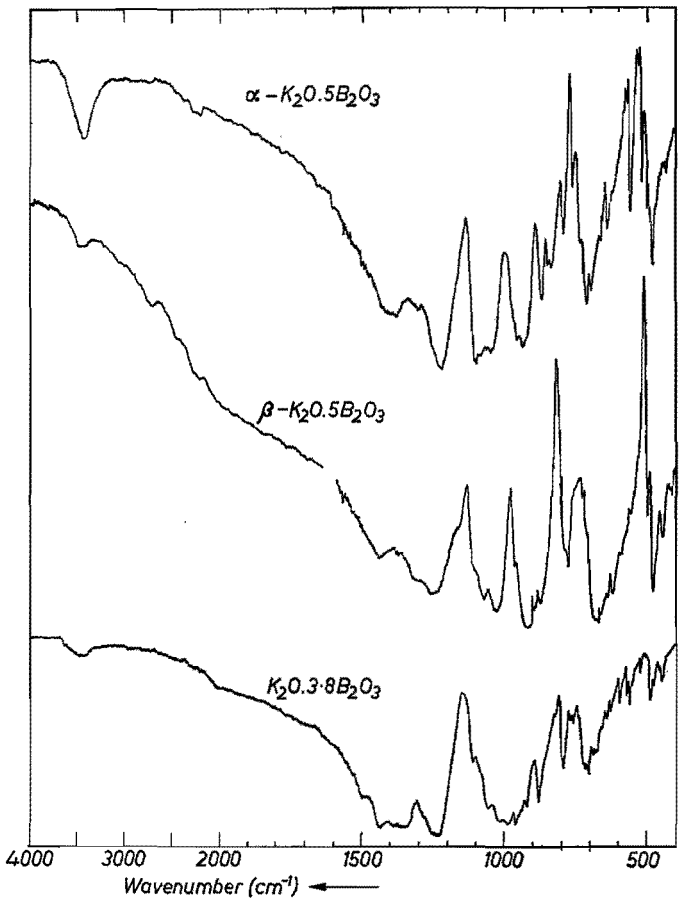

Fig. 4.6. Infrared spectra of polycrystalline potassium borates.

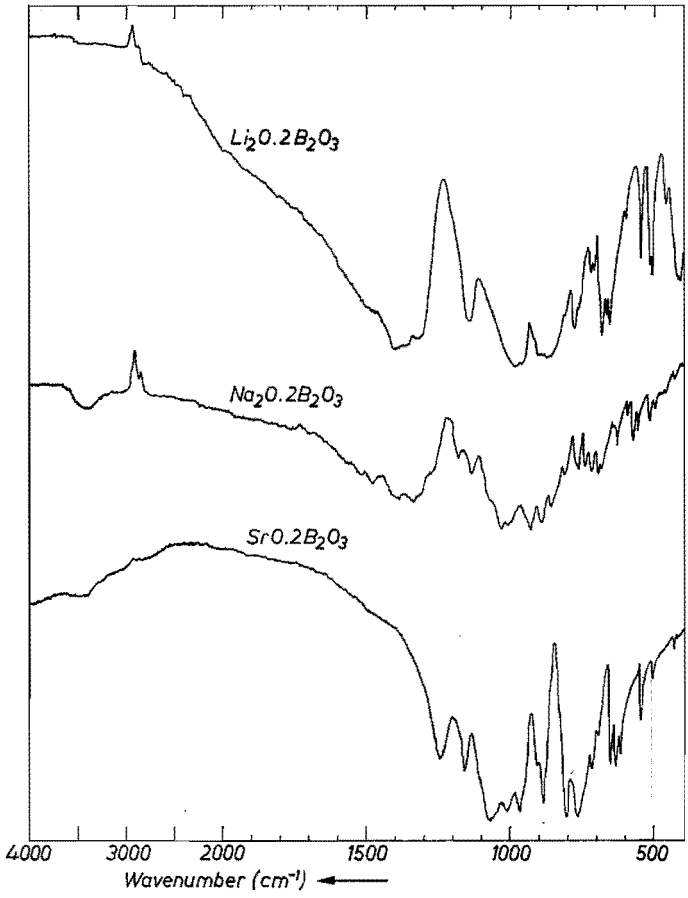

Fig. 4.7. Infrared spectra of polycrystalline borates.

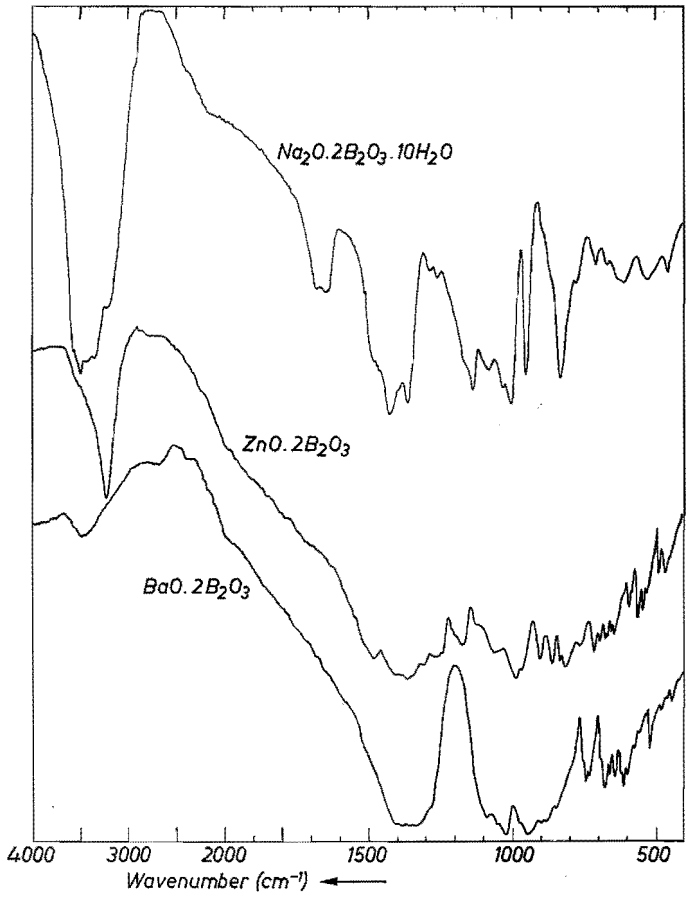

Fig. 4.8. Infrared spectra of polycrystalline borates.

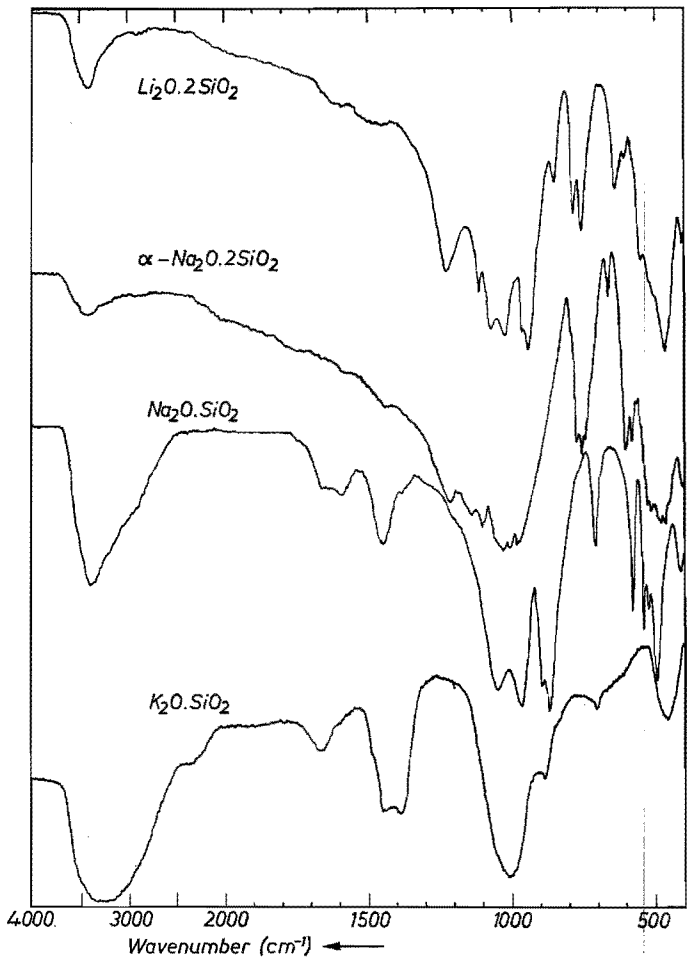

Fig. 4.9. Infrared spectra of polycrystalline silicates.

4.3. Infrared spectra of borate glasses

4.3.1. *Experimental results*

The infrared spectra of alkali-borate glasses are shown in figs 4.10, 4.11 and 4.12. Spectra of glasses containing alkaline-earth oxides are shown in figs 4.13 and 4.14. The effect of Al_2O_3 on the infrared spectra of borate glasses is shown in figs 4.15 and 4.16.

The spectra of the glasses were obtained from thin films, a few microns thick. The glasses were measured in vacuum and near liquid-nitrogen temperatures. This last improved the resolution of the spectra somewhat in the wavenumber range 400–1000 cm^{-1} compared to spectra recorded at room temperature. Cooling to about 20 K did not further improve this resolution.

For more information on the experimental conditions the reader is referred to sec. 2.2.

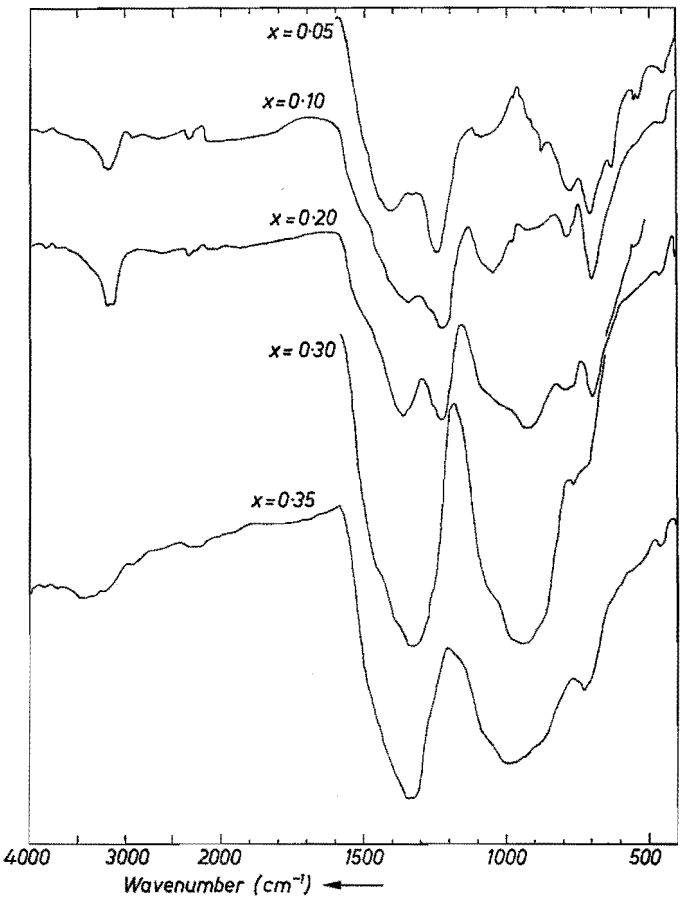

Fig. 4.10. Infrared spectra of glasses in the system $x\ Na_2O\ .\ (1-x)\ B_2O_3$.

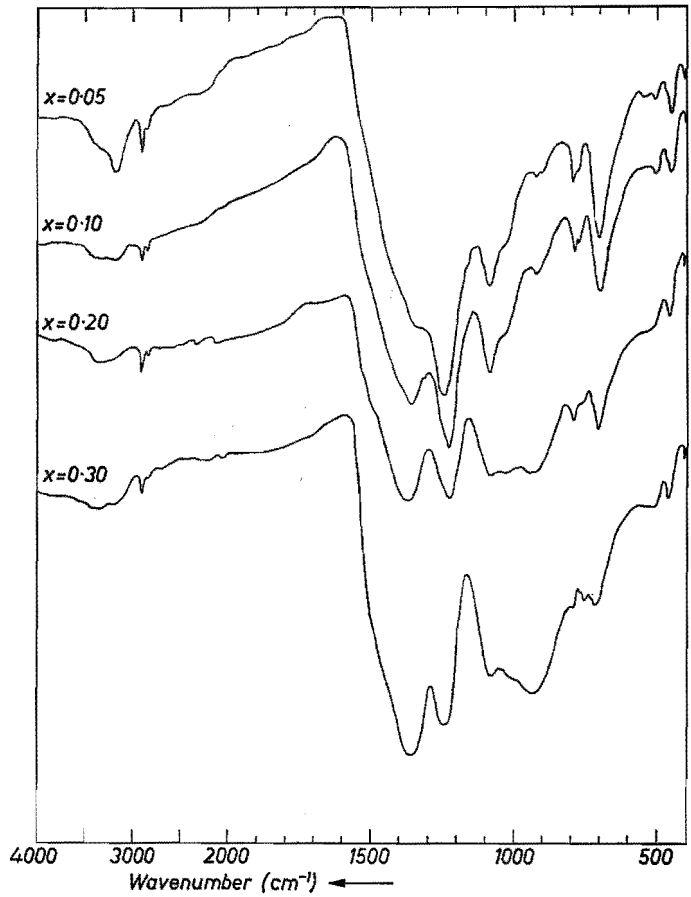

Fig. 4.11. Infrared spectra of glasses in the system $x\ K_2O\ .\ (1-x)\ B_2O_3$.

4.3.2. *Discussion of results*

Borate glasses with 0–20 *mol % alkali oxide*

The infrared spectrum of vitreous boron oxide was not recorded by the present author. The room-temperature spectrum of vapour-deposited B_2O_3 glass was published by Tenney and Wong [4–15]). This spectrum shows a strong absorption band at 1265 cm^{-1} and small bands at 720 cm^{-1} and at about 1400 cm^{-1} as a shoulder of the 1265-cm^{-1} band. In the area 800–1200 cm^{-1} no absorption bands were recorded.

The strongest absorption band at 1265 cm^{-1} in the B_2O_3 spectrum has been assigned to the bond-stretching vibration of the B–O bond. The weak shoulder at about 1400 cm^{-1} has been assigned by Krogh-Moe [4–4]) to the ring-stretching

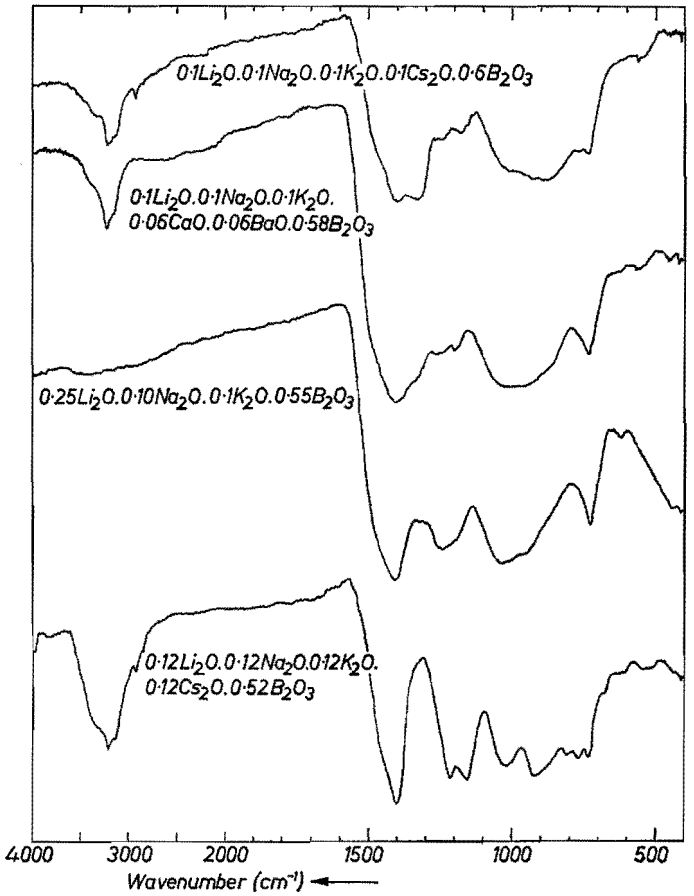

Fig. 4.12. Infrared spectra of borate glasses.

vibration of the boroxol ring. The weaker band at 720 cm^{-1} arises from a bond-bending motion of the B–O–B groups within the network.

In the spectra of the sodium- and potassium-borate glasses (figs 4.10 and 4.11) it may be observed that absorption bands arise in the range 800–1100 cm^{-1} and around 1350 cm^{-1} on increase of the alkali-oxide concentration of the glass. Beginning at 20 mol % alkali-oxide sodium- and potassium-borate glasses show slightly different spectra.

The infrared spectra of the compounds K_2O . 3·8 B_2O_3 (this thesis) and Na_2O . 4 B_2O_3 (Weir and Schroeder [4–2]) also show differences. This is not at all strange because the structure of the compound Na_2O . 4 B_2O_3 is built up of paired pentaborate (a_4c) and triborate groups (a_2c), called tetraborate groups (a_6c_2). In the compound K_2O . 3·8 B_2O_3 pentaborate (a_4c), triborate groups (a_2c) and "loose" BO_3 (a) and BO_4 (c) units are present.

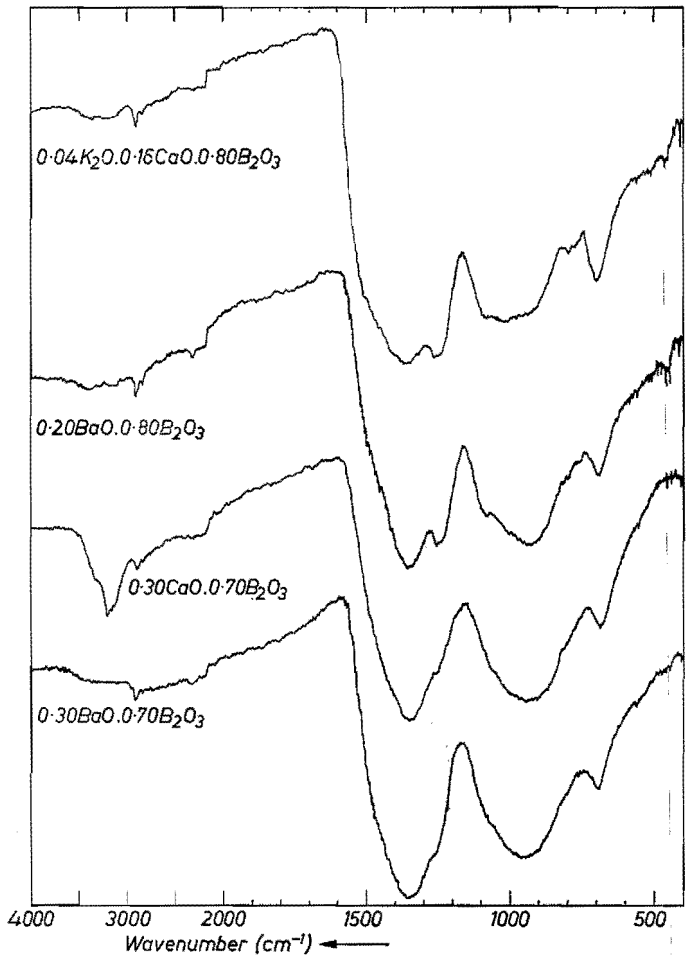

Fig. 4.13. Infrared spectra of borate glasses.

There is close similarity between the spectra of the glass of composition 0·20 Na_2O . 0·80 B_2O_3 (fig. 4.10) and the compound Na_2O . $4B_2O_3$ (Weir and Schroeder [4–2]). This suggests a structural similarity between the glass and the crystal, thus, most probably tetraborate groups (a_6c_2) are formed.

In the Raman spectrum of the glass of composition 0·20 K_2O . 0·80 B_2O_3 the presence of boroxol groups (a_3) is clearly indicated. Thereabove a close similarity can be observed between the infrared spectra of the glass of composition 0·20 K_2O . 0·80 B_2O_3 and the compound K_2O . 3·8 B_2O_3. This suggests that the same types of groups are formed in both cases, thus pentaborate (a_4c), triborate groups (a_2c), and BO_3 (a) and BO_4 units (c).

All this information suggests that up to 20 *mol % alkali oxide primarily tetraborate groups* (a_6c_2) *are formed and boroxol groups removed. The slight dif-*

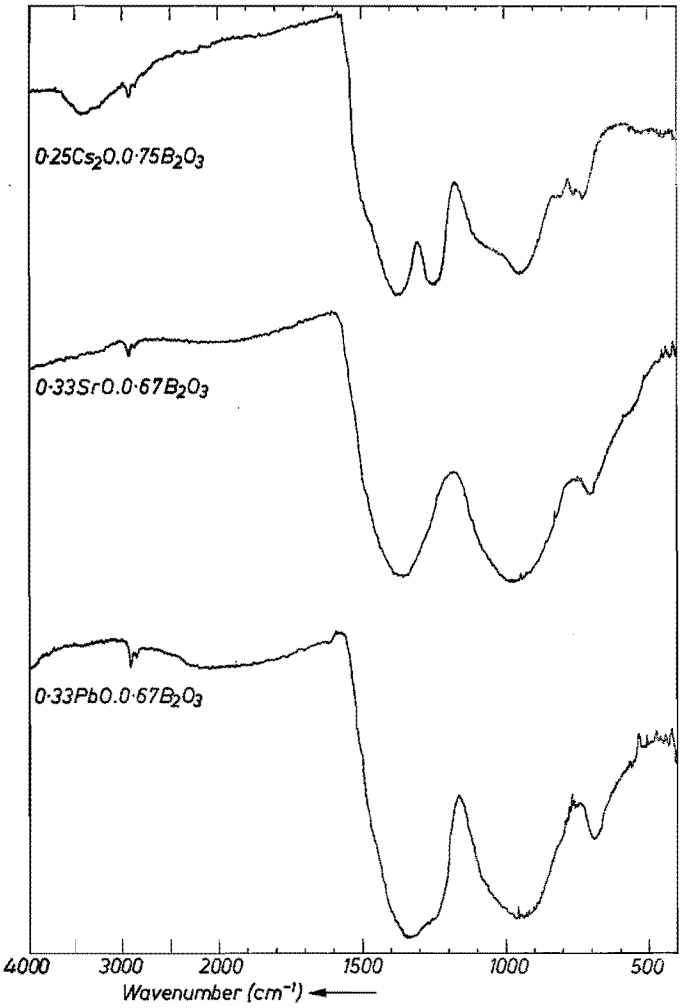

Fig. 4.14. Infrared spectra of borate glasses.

ferences between the spectra of the glasses with 20 *mol* % Na_2O *and* K_2O *reflect the tendency to the formation of compounds at the tetraborate composition with slightly different structures.*

Borate glasses with 20–35 *mol* % *alkali oxide*

From comparison of the infrared spectra of the potassium-borate glasses with 20 and 30 mol % K_2O (fig. 4.11) with the spectrum of the compound K_2O . 3 B_2O_3 (fig. 4.5) it is clear that other borate groups are most probably present in the glasses mentioned than in the compound K_2O . 3 B_2O_3. Structural analogy with the compound K_2O . 3 B_2O_3 is not very probable either, be-

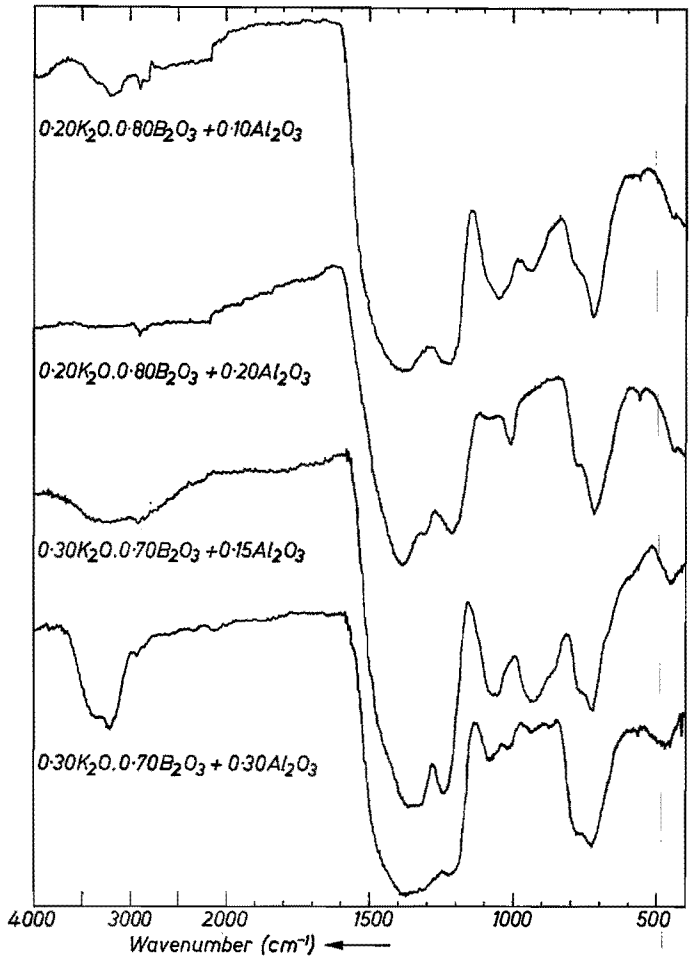

Fig. 4.15. Infrared spectra of aluminoborate glasses.

cause this compound has an incongruent melting point. For the corresponding sodium-borate glass the situation seems to be analogous.

At $x = 0{\cdot}30$ there is a slight difference between the spectra of the sodium- and potassium-borate glasses (figs 3.10 and 3.11). Unfortunately, due to crystallization, no thin film could be made of a glass of composition $0{\cdot}33\ Li_2O\ .\ 0{\cdot}67\ B_2O_3$, so that no infrared spectrum could be obtained of this glass. The increased tendency to crystallization of vitreous $0{\cdot}33\ Li_2O\ .\ 0{\cdot}67\ B_2O_3$ compared to the corresponding sodium- and potassium-borate glasses may suggest a closer structural similarity of vitreous $0{\cdot}33\ Li_2O\ .\ 0{\cdot}67\ B_2O_3$ to the corresponding compound than in the case of the sodium- and potassium-borate

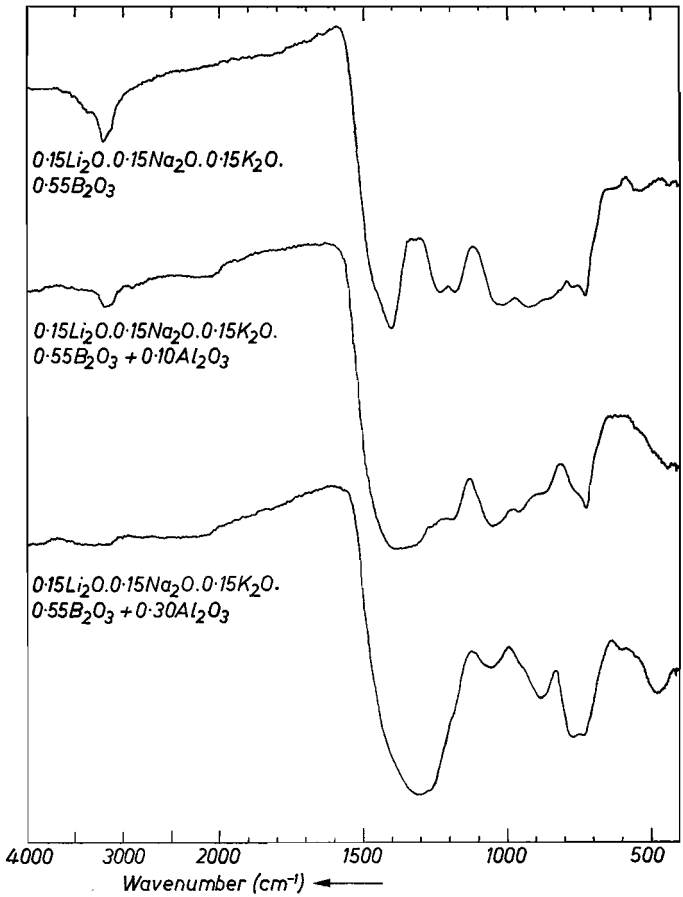

Fig. 4.16. Infrared spectra of aluminoborate glasses.

glasses. This would then mean that vitreous 0·33 Li_2O . 0·67 B_2O_3 contains a major number of diborate groups (a_2c_2). This is not contradicted by the density difference between vitreous and crystalline 0·33 Li_2O . 0·67 B_2O_3.

Vitreous 0·33 Na_2O . 0·67 B_2O_3 shows a higher density than the corresponding crystalline compound which suggests a structural dissimilarity, so that it is improbable that a major amount of the dipentaborate group (a_3c_2) and the triborate group with a non-bridging oxygen (*abc*) is present in this glass. The similarity to the lithium-borosilicate glasses may suggest that in vitreous 0·33 Na_2O . 0·67 B_2O_3 a major number of diborate groups (a_2c_2) is present. A certain similarity to the spectrum of the compound Li_2O . 2 B_2O_3 (fig. 4.7) may also be observed, again indicating the presence of diborate groups (a_2c_2). Other evidence, mentioned in chapter 3, goes in the same direction.

The potassium-borate glass with 30 mol % K_2O shows an infrared spectrum

that slightly differs from that of the corresponding sodium-borate glass. There is a clear difference in the spectra of vitreous 0·30 K_2O . 0·70 B_2O_3 and crystalline K_2O . 2 B_2O_3. The slight difference between the spectra of sodium- and potassium-borate glasses seems not significant. Thus, probably a major number of the boron ions is present in diborate groups (a_2c_2).

The spectrum of vitreous 0·25 Cs_2O . 0·75 B_2O_3 shows no close similarity to that of the corresponding crystalline compound (figs 4.14 and 4.3). This suggests that the glass is not primarily built up of triborate groups (a_2c). The spectrum of the glass shows a strong resemblance to that of the glass 0·20 Na_2O . 0·80 B_2O_3. This suggests that in the caesium-borate glass mainly tetraborate groups (a_6c_2) are formed. This is consistent with the results of the Raman spectrum and n.m.r. measurements discussed in chapter 3.

The results of the infrared spectra of the glasses in the composition range 20–35 *mol % alkali oxide are consistent with the results of the Raman spectra. It is indicated that on increase of the alkali-oxide content the tetraborate groups* (a_6c_2) *are gradually replaced by diborate groups* (a_2c_2).

Borate glasses with 35–50 *mol % alkali oxide*

Figures 4.12 and 4.15 show spectra of borate glasses containing 40–48 mol % mixed alkali oxides. Due to the relatively large amount of OH^- ions in these glasses and in the corresponding metaborate compounds, a comparison of their infrared spectra with the aim of drawing conclusions as to the presence of certain groups in the glasses is thought to be inappropriate. However, it may be concluded that in the area around 50 mol % alkali oxide there is no special tendency to the formation of ring- or chain-type metaborate groups (b_3 or b_∞).

Borate glasses with alkaline-earth oxides

Some spectra of glasses containing alkaline-earth oxides are shown in figs 4.13 and 4.14. The spectra of the glasses of composition 0·04 K_2O . 0·16 CaO . 0·80 B_2O_3 and 0·20 BaO . 0·80 B_2O_3 show slight differences. It may be that this difference is due to the 4 mol % K_2O present in the first glass and that the alkaline-earth calcium- and barium-borate glasses fundamentally have the same structure. The spectrum of the barium-borate glass is very similar to that of the corresponding sodium-borate glass, so probably tetraborate groups (a_6c_2) are formed similar to those in the compound Na_2O . 4 B_2O_3.

The spectrum of the glass of composition 0·04 K_2O . 0·16 CaO . 0·80 B_2O_3 is closer in similarity to the spectrum of the corresponding potassium-borate glass, which probably means that it contains groups similar to those of the compound K_2O . 3·8 B_2O_3 and that the network structure is somewhat different from that of the compound Na_2O . 4 B_2O_3.

At 30 mol % CaO and BaO the infrared spectra are very similar and show a strong resemblance to the spectrum of the borate glass containing 30 mol %

Na_2O (figs 4.10 and 4.13), which probably means that diborate groups (a_2c_2) are formed.

It is interesting to note the similarity of the spectra of the borate glasses containing 30 mol % CaO or BaO and 33 mol % SrO. The spectrum of vitreous 0·33 SrO . 0·67 B_2O_3 differs greatly from that of the compound SrO . 2 B_2O_3 (figs 4.14 and 4.7). This indicates that vitreous 0·33 SrO . 0·67 B_2O_3 contains no structural units that are found in the compound SrO . 2 B_2O_3, which has a deviating kind of borate network.

Finally the lead-borate glass of composition 0·33 PbO . 0·67 B_2O_3 shows an infrared spectrum very similar to that of the calcium-, strontium- and barium-borate glasses of roughly this composition. This suggests that all these glasses have primarily the same structure, most probably built up of diborate groups (a_2c_2).

Influence of Al_2O_3 *on the structure of borate glasses*

The influence of increasing amounts of Al_2O_3 on the infrared spectra of alkali-borate glasses is shown in figs 4.15 and 4.16. For glass of composition 0·20 K_2O . 0·80 B_2O_3 one may observe that increasing the amounts of Al_2O_3 up to 20 mol % leads to a decrease of the absorption bands in the area 900–1100 cm^{-1}, showing the disappearance of BO_4 units. This is consistent with the result of the Raman spectroscopy of these glasses which has shown that boroxol groups are formed again.

The behaviour of glass of composition 0·30 K_2O . 0·70 B_2O_3 is analogous; in this case too it is clear that the number of borate groups with BO_4 tetrahedra which have absorption bands in the area 900–1100 cm^{-1} diminish on addition of Al_2O_3 to the glass. Without further analysis the strong absorption band at about 1380 cm^{-1} cannot be assigned.

For the mixed alkali glass of composition 0·15 Li_2O . 0·15 Na_2O . 0·15 K_2O . 0·55 B_2O_3 one may observe that addition of Al_2O_3 leads to a decrease of the absorption bands in the infrared spectra in the area 900–1100 cm^{-1} (fig. 4.16). This also suggests that borate groups with alkali ions are replaced by AlO_4 tetrahedra with a charge-compensating alkali ion and borate groups without alkali ions or a lower alkali-to-boron ratio.

4.3.3. *Conclusions*

The infrared spectra suggest that in Na- and K-borate glasses with up to about 20 mol % alkali oxide primarily tetraborate groups (a_6c_2) are formed. At about 30 mol % alkali oxide the infrared spectra suggest the presence of diborate groups (a_2c_2). At 50 mol % mixed alkali-borate glasses no special tendency to the formation of ring- or chain-type metaborate groups is found, which is confirmed by the results of the Raman spectra.

The spectra of the alkaline-earth-borate glasses show a high degree of similar-

ity to those of the corresponding sodium-borate glasses, suggesting that the same type of borate groups are present.

Addition of Al_2O_3 to alkali-borate glasses clearly leads to a decrease in the relative number of groups containing BO_4 tetrahedra. The infrared spectra are consistent with the Raman spectra in that probably boroxol groups are formed again in these glasses up to about 30 mol % alkali oxide. When more alkali oxide is present it is not clear which type of borate group is formed on addition of Al_2O_3.

The increase in the line width in the spectra of the glasses clearly indicates that the units are deformed to some extent. Notwithstanding the lower resolution of the spectra of the glasses the conclusion may be that the same type of borate rings are generally present in the borate glasses as in the corresponding borate compounds. An exception to this is vitreous 0·33 SrO . 0·67 B_2O_3.

4.4. Infrared spectra of silicate glasses

4.4.1. *Experimental results*

Due to the fact that infrared spectra of many vitreous silicates are available from the literature only a few spectra are shown in figs 4.17 and 4.18. The spectra of some alkali-aluminosilicate glasses are shown in fig. 4.19.

The spectra of thin films of these glasses were recorded at room temperature and in air. Cooling to liquid-nitrogen temperature has no influence on the resolution. For more information on the equipment used, see sec. 2.2.

4.4.2. *Discussion of results*

The spectra of silicate glasses have often been discussed in the literature. For a review the reader is referred to the work of Wong and Angell [4–7]).

The spectra of some glasses were recorded to check our experimental technique and to facilitate comparison with the spectra of the borosilicate glasses. All the spectra shown in this thesis fit in very well with other infrared studies on silicate glasses. The spectra of some aluminosilicates were recorded to see whether Al and B ions are taken up in the silicate network in a similar way.

The spectra of the glasses of composition 0·30 Na_2O . 0·70 SiO_2 and 0·30 K_2O . 0·70 SiO_2 are fairly similar to those of the compounds Li_2O . 2 SiO_2 and α-Na_2O . 2 SiO_2 (figs 4.17 and 4.9). The band at about 1210 cm^{-1} in the crystalline compounds, however, is absent in these glasses. Due to the large number of peaks in the spectra of the crystalline disilicates it is supposed that the spectra are due to complex silicate groups of low symmetry. The complexity of the structure is confirmed by X-ray analysis. The infrared spectra of the glasses suggest that this complexity is retained in the structure of the glasses and even increased somewhat by the irregular deformation of these groups that has taken place. Thus it is suggested that in these glasses a layer-like structure

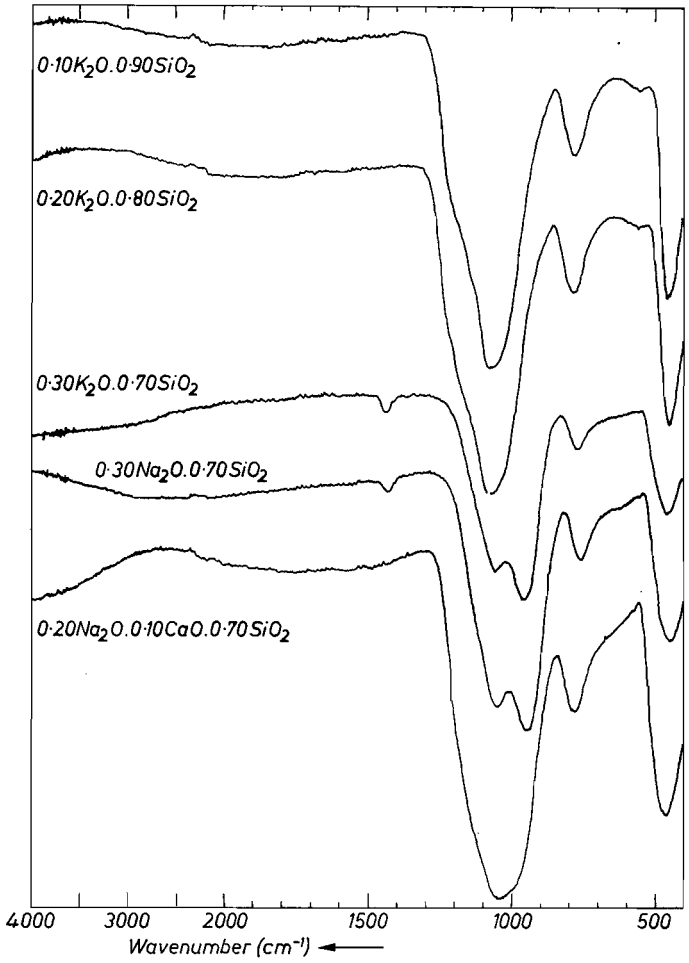

Fig. 4.17. Infrared spectra of silicate glasses.

is also present on a small scale. This is consistent with the X-ray results on these glasses obtained by Mozzi and Warren [4–16]) and the Raman results in chapter 3. The presence of SiO_4 units with no, one or two non-bridging oxygen ions can easily be reconciled by comparison of the spectra of vitreous and crystalline silicates.

As can be observed from fig. 4.19 the introduction of Al_2O_3 in silicate glasses does not lead to drastically changing spectra, which confirms the expected general structural similarity of silicate and aluminosilicate glasses.

4.4.3. *Conclusions*

In general the spectra of the silicate glasses show a fair similarity to the spectra of the corresponding compounds, so probably the same structural units

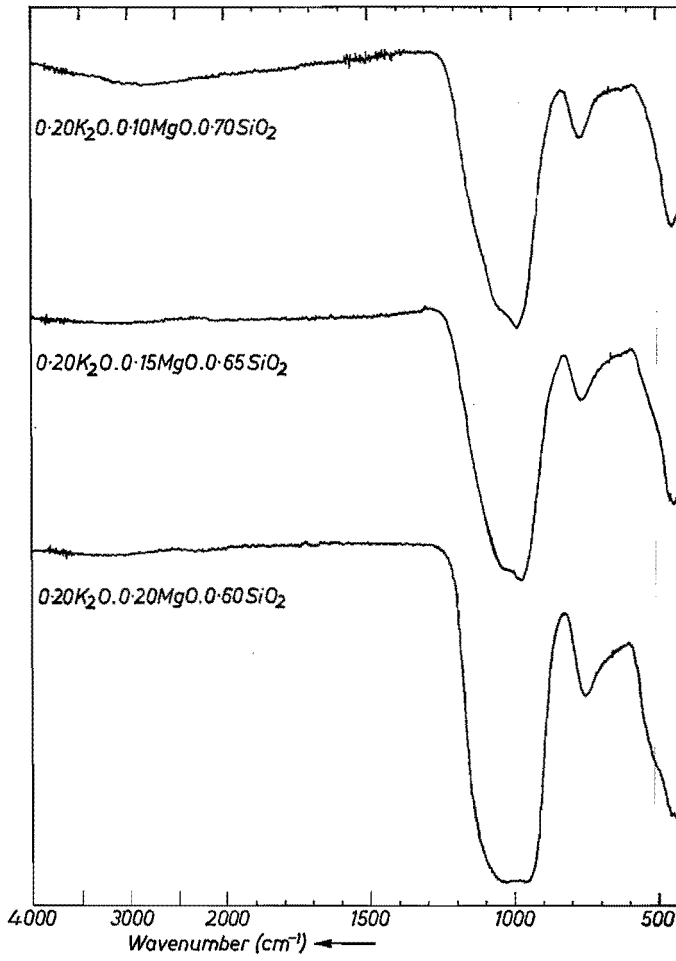

Fig. 4.18. Infrared spectra of silicate glasses.

are present in the glasses as in the corresponding crystalline compounds. At least it is clear that up to 30 mol % alkali oxide primarily SiO_4 tetrahedra with only one non-bridging oxygen ion are formed.

When the amount of Al_2O_3 in alkali-aluminosilicate glasses does not exceed that of alkali oxide then the silicate and aluminosilicate glasses show a great structural similarity.

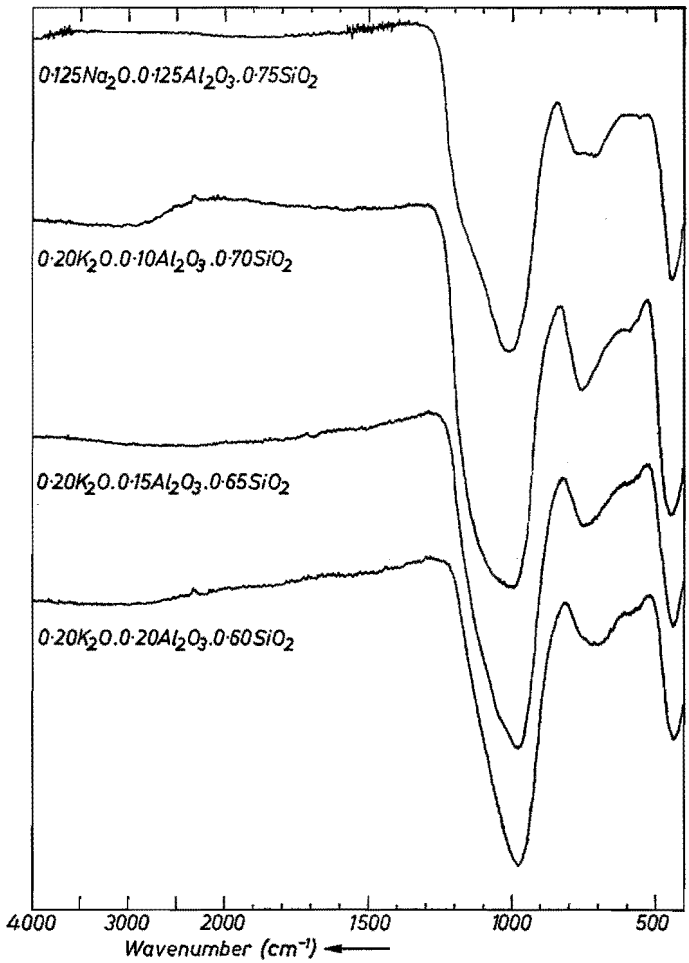

Fig. 4.19. Infrared spectra of aluminosilicate glasses.

4.5. Infrared spectra of borosilicate glasses

4.5.1. *Experimental results*

The infrared spectra of a large number of borosilicate glasses are shown in figs 4.20 to 4.42. All spectra were recorded at liquid-N_2 temperatures in vacuum, using thin films of the samples. All samples are the same as those used for the Raman experiments.

A number of spectra of borosilicate glasses are found in the literature. For spectra in the system B_2O_3–SiO_2 the reader is referred to the work of Taft [4–17]) and Tenney and Wong [4–15]). Some spectra of sodium-borosilicate glasses were published by Jellyman and Procter [4–18]) and republished by Neuroth [4–1]).

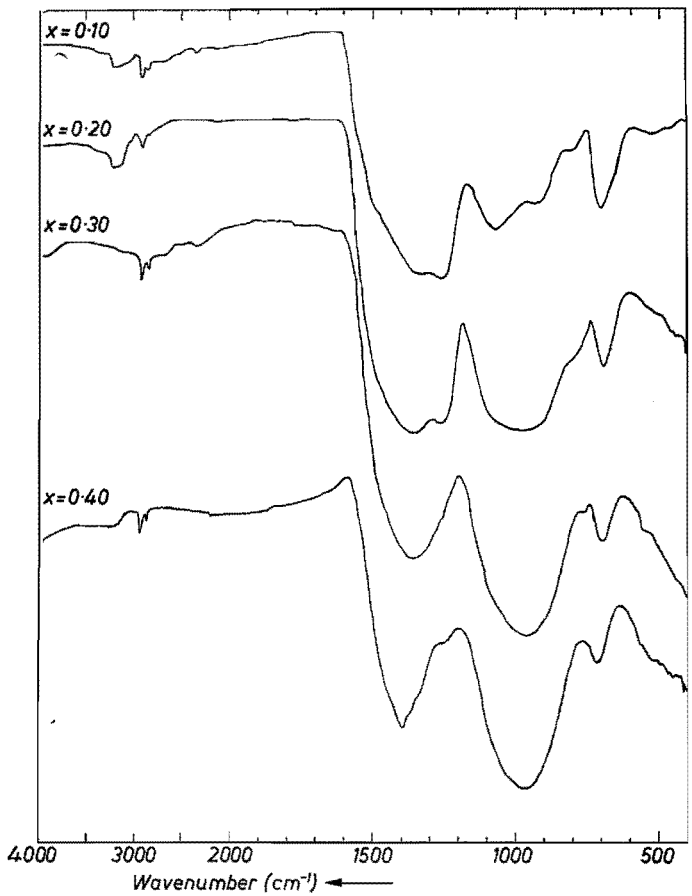

Fig. 4.20. Infrared spectra of glasses in the system $x\,Li_2O\,.\,(0{\cdot}85 - x)\,B_2O_3\,.\,0{\cdot}15\,SiO_2$.

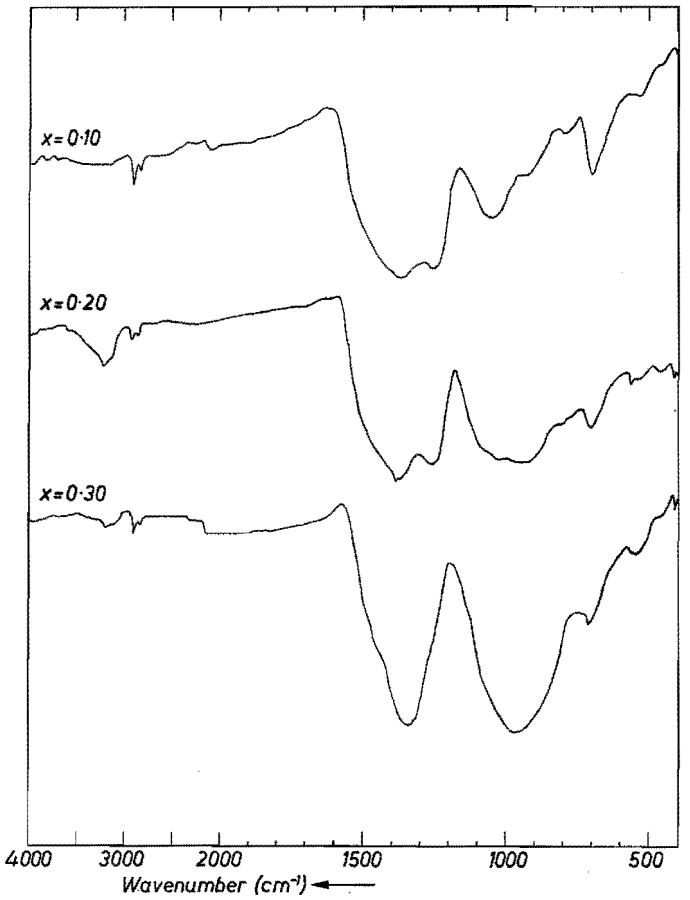

Fig. 4.21. Infrared spectra of glasses in the system $x\,Na_2O\,.\,(0{\cdot}85-x)\,B_2O_3\,.\,0{\cdot}15\,SiO_2$.

4.5.2. *Discussion of results*

Borosilicate glasses with 15 *mol* % SiO_2

A comparison of the spectra of the glasses in the series $x\,Na_2O\,.\,(0{\cdot}85-x)\,B_2O_3\,.\,0{\cdot}15\,SiO_2$ with those of the glasses in the series $x\,Na_2O\,.\,(1-x)\,B_2O_3$ (cf. figs 4.21 and 4.10) reveals the close similarity to the spectra of the glass with the same amount of Na_2O. This suggests that Na_2O in the composition series $x\,Na_2O\,.\,(0{\cdot}85-x)\,B_2O_3\cdot 0{\cdot}15\,SiO_2$ is used to form the same type of borate groups as in the comparable binary sodium-borate glasses and that no significant amount of Na_2O is used to form non-bridging oxygen ions as part of SiO_4 tetrahedra. The way in which SiO_2 is present in these glasses is not elucidated by these infrared spectra due to the small amount present and the overlap with the strong absorption bands of the borate groups. The slight

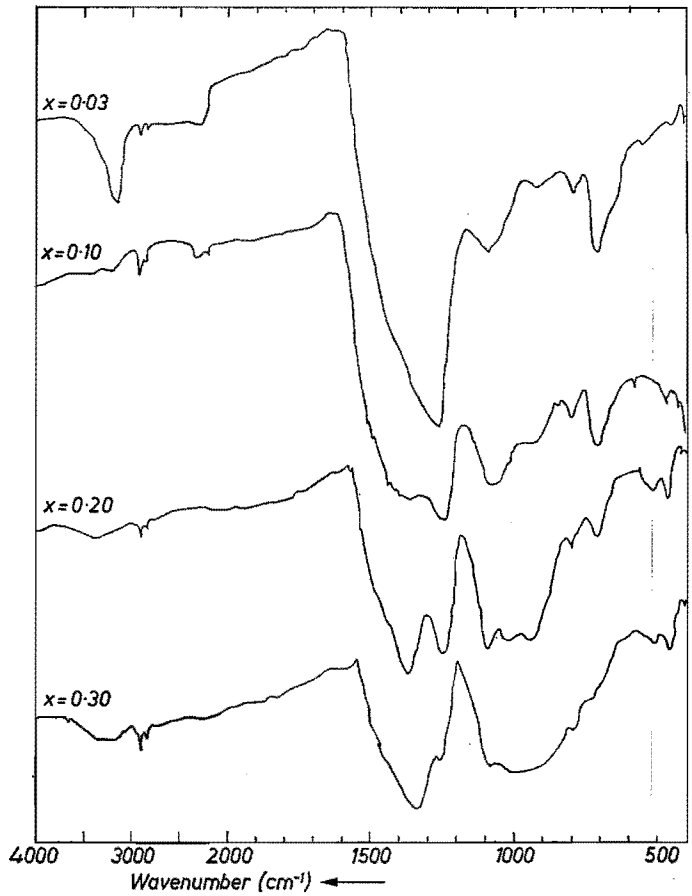

Fig. 4.22. Infrared spectra of glasses in the system $x\,K_2O\,.\,(0{\cdot}85-x)\,B_2O_3\,.\,0{\cdot}15\,SiO_2$.

differences that are observed between the spectra of glasses with the same mole fraction of Na_2O, but with or without SiO_2, are too small for discussion in terms of significant quantitative differences in the structure of these glasses. So the conclusion can be that once again tetraborate groups (a_6c_2) are formed below 20 mol % Na_2O, while at higher Na_2O concentration diborate groups (a_2c_2) are gradually formed.

A comparison of the spectra of the glasses in the series $x\,K_2O\,.\,(0{\cdot}85-x)\,B_2O_3\,.\,0{\cdot}15\,SiO_2$ with those of the glasses in the series $x\,K_2O\,.\,(1-x)\,B_2O_3$ reveals the analogy with the sodium-containing glasses described above. Some differences between the spectra of glasses containing an equal mole fraction K_2O, but with or without SiO_2, are a bit more detailed (cf. figs 4.22 and 4.11). In this case too, practically all the potassium oxide is used for the formation of borate groups that are also present in the comparable binary borate

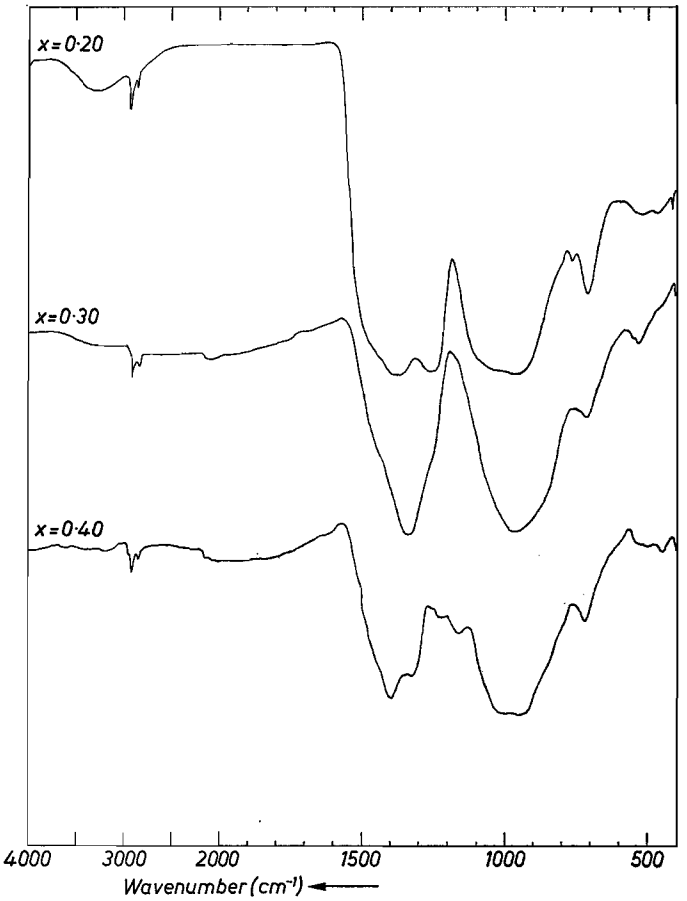

Fig. 4.23. Infrared spectra of glasses in the system x NaKO . $(0{\cdot}85 - x)$ B_2O_3 . 0·15 SiO_2.

glasses. Only a minor number of SiO_4 tetrahedra with a non-bridging oxygen ion is formed.

The spectra of the glasses in the series x NaKO . $(0{\cdot}85 - x)$ B_2O_3 . 0·15 SiO_2 show close similarity to those of the glasses in the Na_2O series (cf. figs 4.23 and 4.21). This suggests a structural similarity between the sodium- and mixed sodium–potassium-borosilicate glasses.

The spectra of the glasses in the series x Li_2O . $(0{\cdot}85 - x)$ B_2O_3 . 0·15 SiO_2 show at $x = 0{\cdot}10$ and $x = 0{\cdot}20$ a high degree of similarity to the corresponding Na_2O-containing glasses (cf. figs 4.20 and 4.21). This suggests that primarily the same groups are formed in the Li_2O-containing glasses as in the Na_2O-containing glasses at $x = 0{\cdot}10$ and $x = 0{\cdot}20$.

At $x = 0{\cdot}30$ Li_2O, the spectrum is somewhat different from the one at $x = 0{\cdot}30$ Na_2O as shown by the relatively stronger band at 1000 cm^{-1}. This

does not correspond to the spectrum of crystalline $Li_2O \cdot 2\,B_2O_3$ (cf. fig. 4.7) or crystalline $Li_2O \cdot B_2O_3$ (cf. fig. 4.3). In this case it may be suggested that more SiO_4 tetrahedra with non-bridging oxygen ions are formed, giving rise to the relative increase in intensity of the band at 1000 cm^{-1}. At $x = 0{\cdot}40$ Li_2O the same arguments seem to apply. The rise of the band between 400 and 500 cm^{-1} suggests the same. Compare this with the infrared spectra of the compounds $Li_2O \cdot 2\,SiO_2$ and α-$Na_2O \cdot 2\,SiO_2$ (fig. 4.9) and the glasses $0{\cdot}30\,Na_2O \cdot 0{\cdot}70\,SiO_2$ and $0{\cdot}30\,K_2O \cdot 0{\cdot}70\,SiO_2$ (fig. 4.17).

Krogh-Moe [4–19]) suggested that in this composition area cross-linking of borate polymer chains takes place by means of SiO_4 tetrahedra. This was based on the fact that crystalline $Li_2O \cdot B_2O_3$ precipitates from melts of $Li_2O \cdot B_2O_3$ with up to 10 mol % SiO_2, with SiO_2 in solid solution. This conclusion was based on the X-ray powder pattern. Because of this information Krogh-Moe put forward that SiO_4 tetrahedra with one non-bridging oxygen ion are formed, giving rise to a structure reproduced in fig. 4.24.

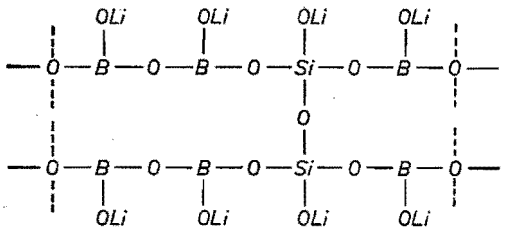

Fig. 4.24. Cross-linking of borate polymer chains by means of SiO_4 tetrahedra according to Krogh-Moe [4–19]).

If this type of cross-linking also takes place in the glass at $x = 0{\cdot}30$ and $x = 0{\cdot}40$ Li_2O then at $x = 0{\cdot}40$ Li_2O for instance 0·075 Li_2O would be bonded to SiO_4 tetrahedra, 0·125 Li_2O to chain-type metaborate groups (b_∞) and 0·20 Li_2O to diborate groups (a_2c_2). This quantitative distribution of groups is not contradicted by the infrared spectrum of the glass at 0·40 Li_2O but other distributions might as well lead to the same spectrum. Unfortunately, Raman spectroscopy gives no solution because of luminescence.

Infrared spectra of glasses in the composition series $0{\cdot}5\,x\,(K_2O + CaO) \cdot (0{\cdot}85 - x)\,B_2O_3 \cdot 0{\cdot}15\,SiO_2$ and x BaO . $(0{\cdot}85 - x)\,B_2O_3 \cdot 0{\cdot}15\,SiO_2$ are shown in figs 4.25 and 4.26. The spectra of the glasses in the mixed K–Ca series show a strong resemblance to the spectra of the corresponding K_2O glasses (fig. 4.22). At $x = 0{\cdot}30$ a difference may be observed. The rise of the bands at about 1000 cm^{-1} and about 460 cm^{-1} is analogous to the spectra of Li_2O-containing glasses at $x = 0{\cdot}30$ and $x = 0{\cdot}40$ (cf. fig. 4.20). This suggests that in the K–Ca glass at $x = 0{\cdot}30$, chain-type metaborate groups (b_∞) are formed with SiO_4 tetrahedra having one non-bridging oxygen ion, so that again a certain cross-linking takes place, analogous to what Krogh-Moe suggested for the lithium-

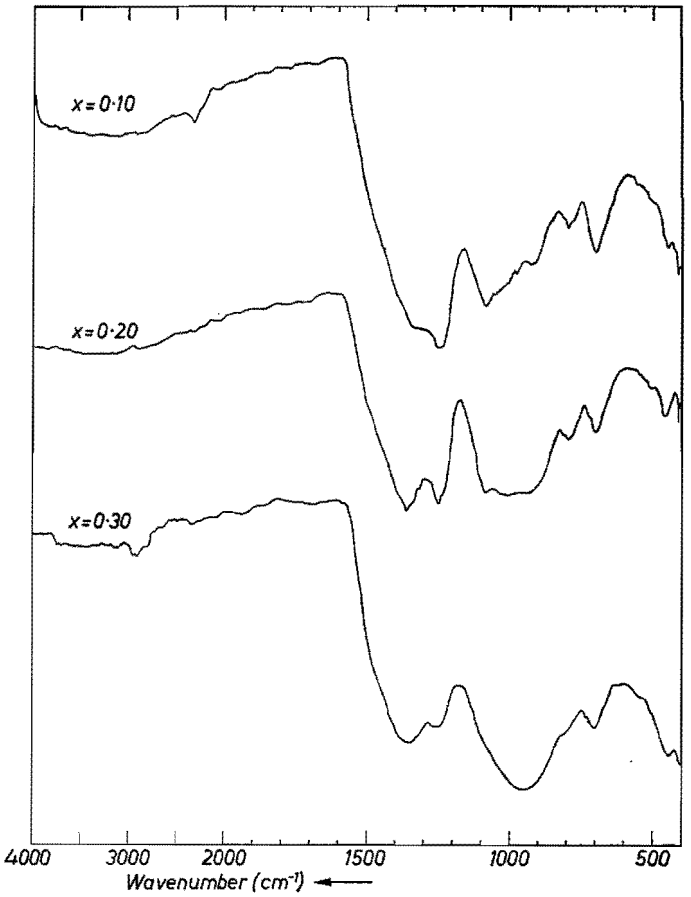

Fig. 4.25. Infrared spectra of glasses in the system $0{\cdot}5\,x\,(K_2O + CaO)\,.\,(0{\cdot}85 - x)\,B_2O_3\,.\,0{\cdot}15\,SiO_2$.

containing systems. This explanation also fits in with the Raman spectra of these glasses.

The spectra of the glasses of the composition x BaO . $(0{\cdot}85 - x)\,B_2O_3$. $0{\cdot}15\,SiO_2$ are fairly similar at $x = 0{\cdot}20$ and $x = 0{\cdot}30$ to the corresponding sodium-borosilicate glasses (cf. figs 4.26 and 4.21).

At $x = 0{\cdot}40$ the spectrum of the glass shows the same characteristics as that of the corresponding lithium-borosilicate glass. This may indicate that in this barium-borosilicate glass there is also a tendency to the formation of chain-type metaborate groups (b_∞) with SiO_4 units in these chains.

Influence of Al_2O_3 *on borosilicate glasses with* 15 *mol* % SiO_2

The influence of increasing amounts of Al_2O_3 on a borosilicate glass of composition $0{\cdot}10\,Na_2O\,.\,0{\cdot}10\,K_2O\,.\,0{\cdot}65\,B_2O_3\,.\,0{\cdot}15\,SiO_2$ is shown in fig. 4.27.

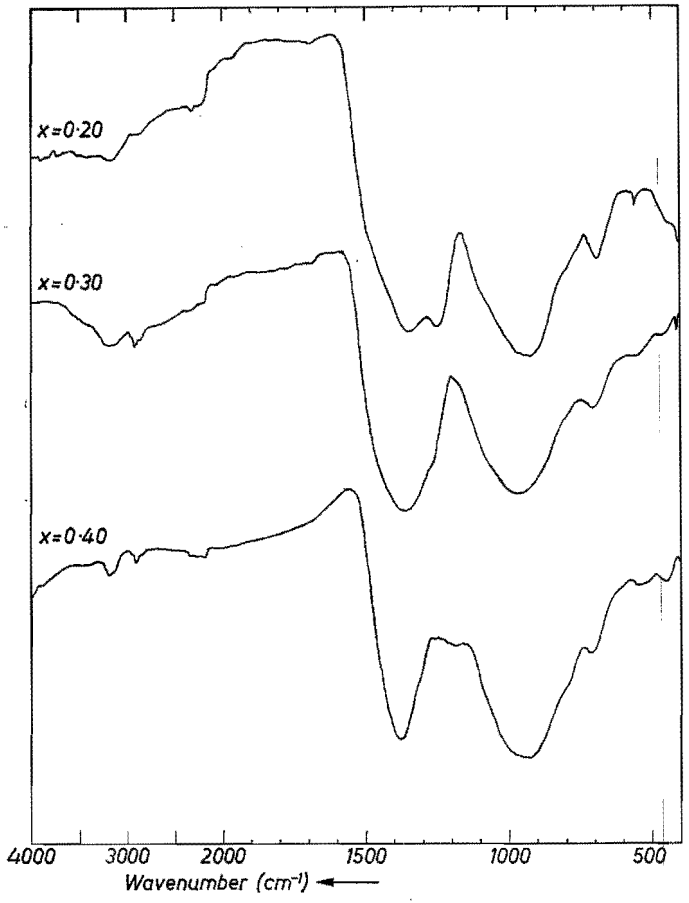

Fig. 4.26. Infrared spectra of glasses in the system x BaO . (0·85 — x) B_2O_3 . 0·15 SiO_2.

This influence is fairly analogous to that observed in the spectra of some boroaluminate glasses shown in fig. 4.15. The conclusion may be that borate groups with a BO_4 unit (a_2c) are replaced by AlO_4 tetrahedra and borate groups without an alkali ion.

The fact that the bands in the area 1000–1100 cm^{-1} remain more tense in the borosilicate glasses may be caused by the absorption bands of SiO_4 tetrahedra without non-bridging oxygen ions. This influence of Al_2O_3 again shows that the alkali ions are primarily bonded to borate groups at this concentration.

The spectra of the glasses in the series x Na_2O . (0·85 — x) B_2O_3 . 0·15 SiO_2 + 0·05 Al_2O_3 and x K_2O . (0·85 — x) B_2O_3 . 0·15 SiO_2 + 0·05 Al_2O_3 show a good similarity (figs 4.28 and 4.29). In the glasses without 5 mol % Al_2O_3 this similarity is slightly less. The introduction of 5 mol % Al_2O_3 to the

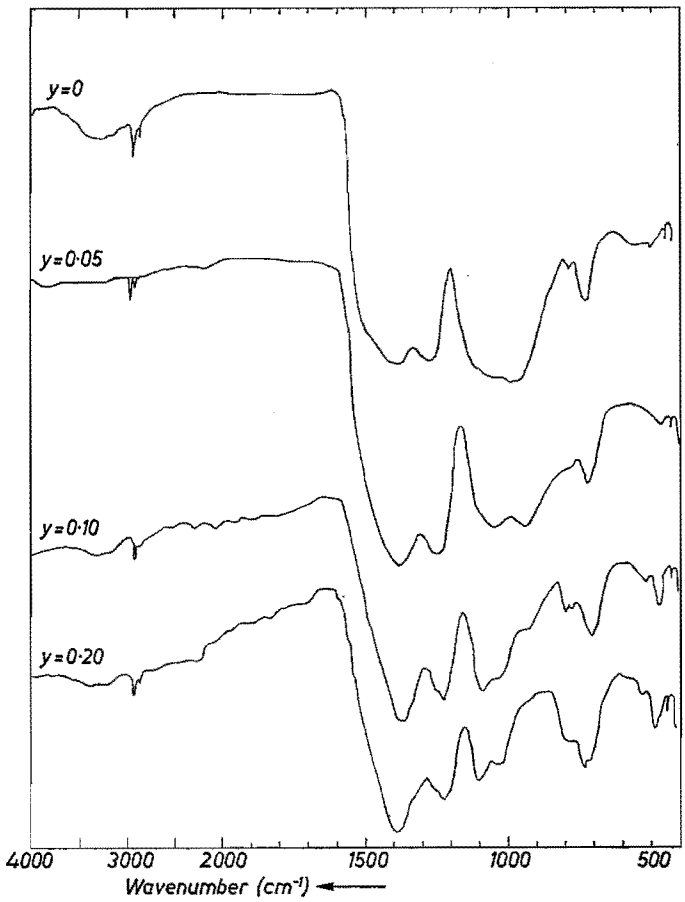

Fig. 4.27. Infrared spectra of glasses in the system 0·10 Na_2O . 0·10 K_2O . 0·65 B_2O_3 . 0·15 SiO_2 + y Al_2O_3.

sodium-borosilicate glasses is enough to change the borate network slightly to that of potassium-borosilicate glasses with 15 mol % SiO_2.

The influence of the addition of 5 mol % Al_2O_3 to some barium-borosilicate glasses with 15 mol % SiO_2 is shown in fig. 4.30. At 20 mol % BaO one may observe, on comparison with the spectrum of the glass without Al_2O_3 (fig. 4.26), that the addition of 5 mol % Al_2O_3 leads to a lowering of the absorption band in the area 900–1000 cm^{-1}. This indicates the disappearance of the BO_4 tetrahedra. At 40 mol % BaO the introduction of 5 mol % Al_2O_3 is probably too slight to result in a significant difference in the spectra of the glasses either with or without Al_2O_3.

In fig. 4.31 spectra are shown of boroaluminosilicate glasses containing large amounts of alkaline-earth oxides. These spectra confirm the Raman-spectra

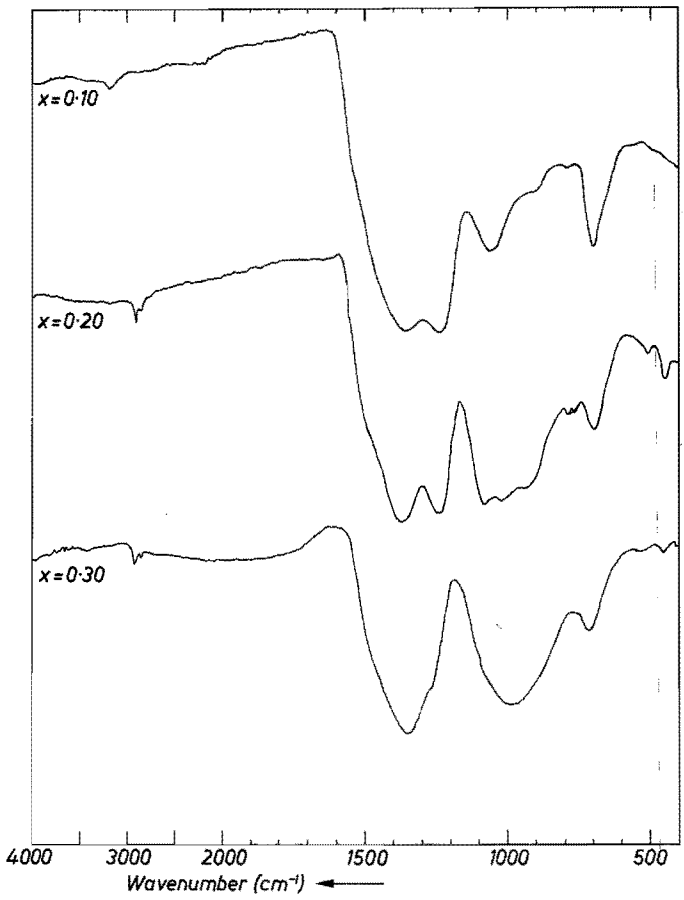

Fig. 4.28. Infrared spectra of glasses in the system $x\ Na_2O\ .\ (0{\cdot}85 - x)\ B_2O_3\ .\ 0{\cdot}15\ SiO_2 + 0{\cdot}05\ Al_2O_3$.

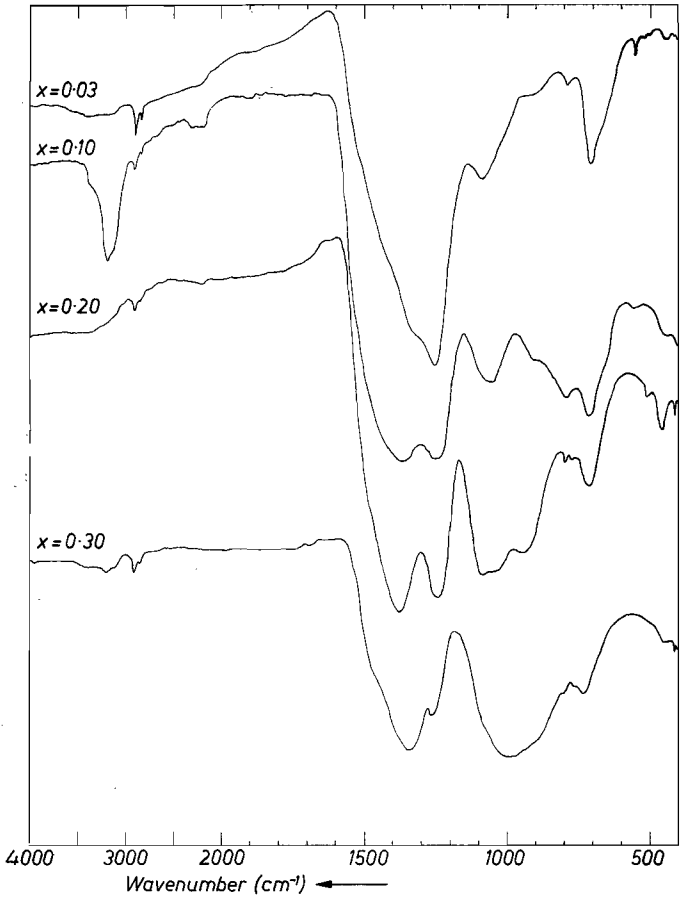

Fig. 4.29. Infrared spectra of glasses in the system $x\,K_2O\,.\,(0{\cdot}85 - x)\,B_2O_3\,.\,0{\cdot}15\,SiO_2 + 0{\cdot}05\,Al_2O_3$.

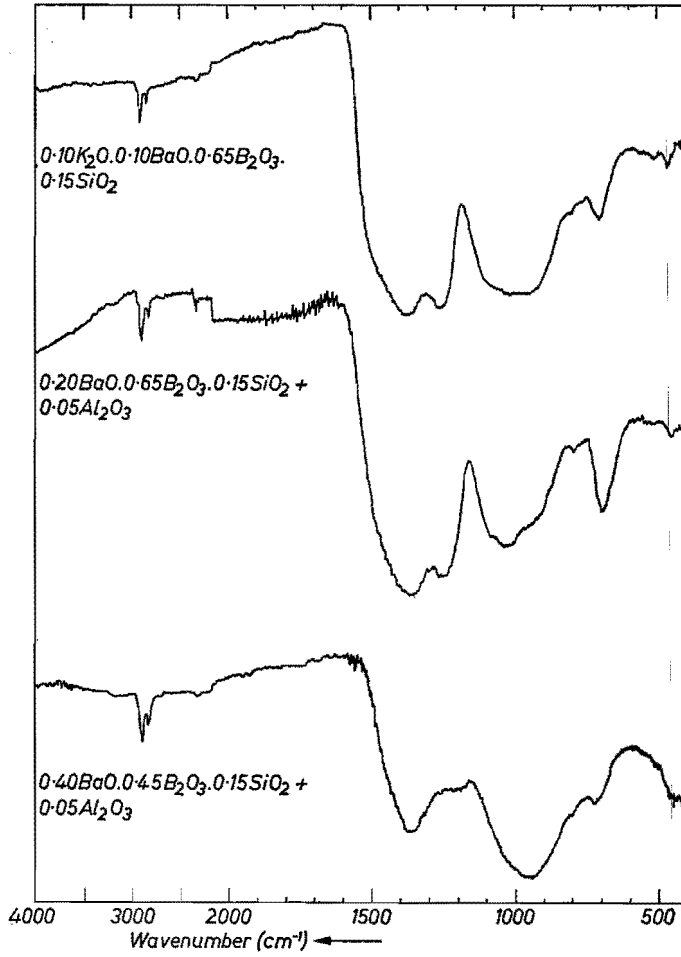

Fig. 4.30. Infrared spectra of borosilicate glasses.

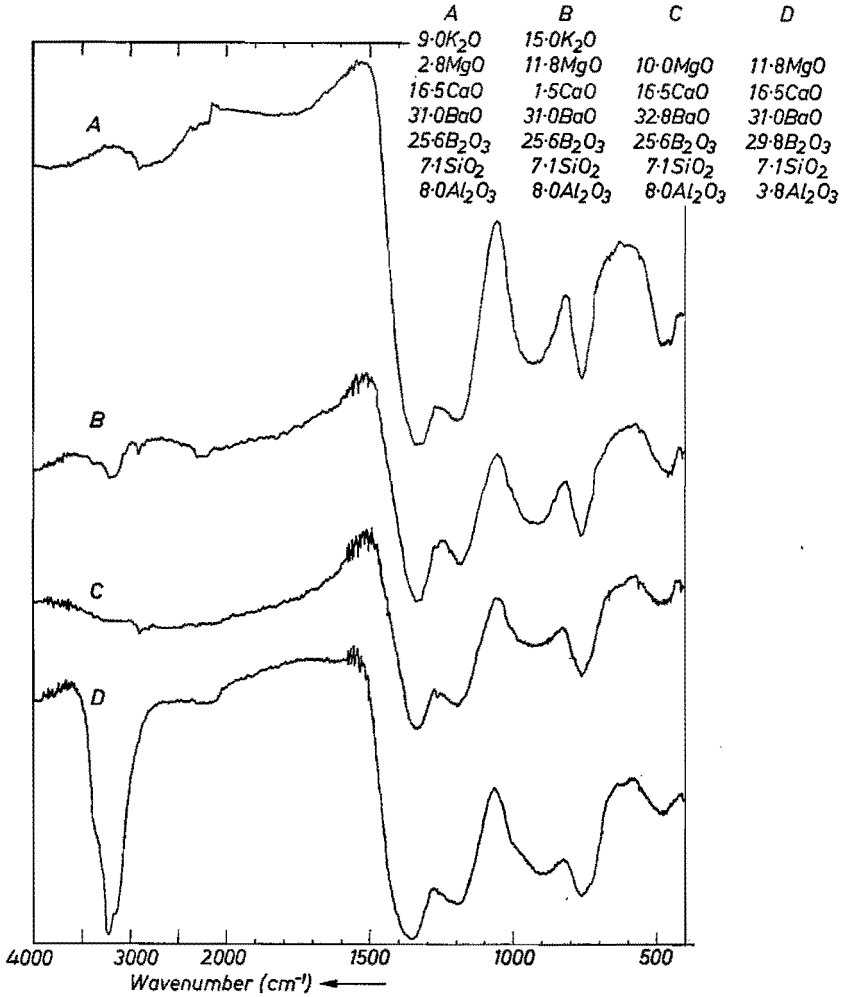

Fig. 4.31. Infrared spectra of multicomponent borosilicate glasses.

results indicating the presence of orthoborate (b'''), pyroborate (b_2''), metaborate groups (b_3) and groups with a BO_4 tetrahedron.

Borosilicate glasses with 65 mol % SiO_2

In fig. 4.32 the infrared spectra are shown of glasses in the series $x\,K_2O\,.\,(0{\cdot}35 - x)\,B_2O_3\,.\,0{\cdot}65\,SiO_2$. At $x = 0{\cdot}01$ the spectrum shows peaks at the same wavenumbers as found by Tenney and Wong [4–15]) for the binary borosilicate glass $0{\cdot}36\,B_2O_3\,.\,0{\cdot}64\,SiO_2$, produced by vapour-deposition techniques. Here also peaks are observed at about 670 cm^{-1} and 930 cm^{-1} which are absent in the unmixed B_2O_3 and SiO_2 glasses. On increasing the potassium-oxide concentration the band at about 1400 cm^{-1} gradually diminishes in intensity, like the bands at 670 cm^{-1} and 930 cm^{-1}. At $x = 0{\cdot}30$ the

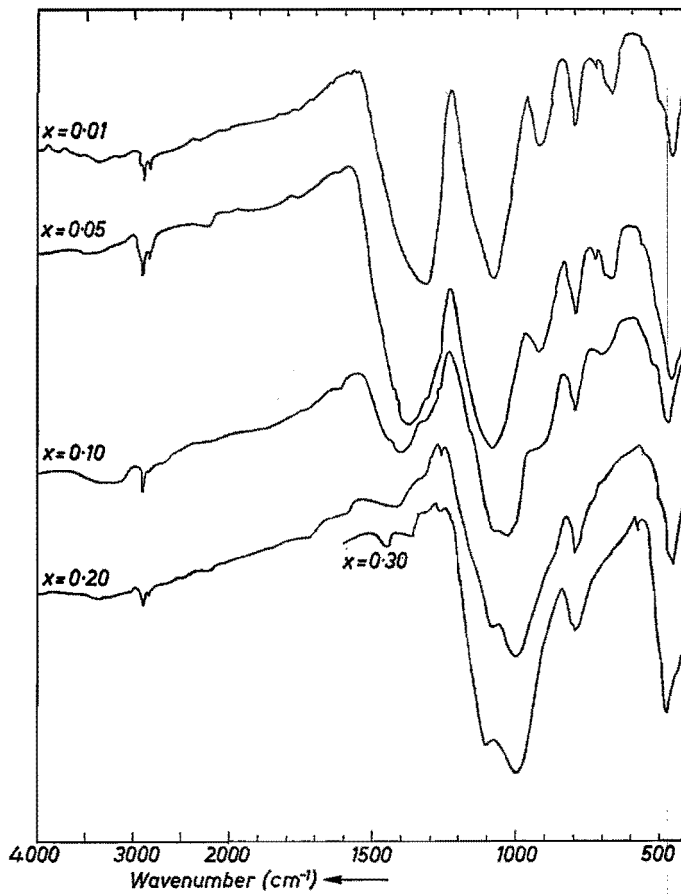

Fig. 4.32. Infrared spectra of glasses in the system $x\,K_2O\,.\,(0{\cdot}35 - x)\,B_2O_3\,.\,0{\cdot}65\,SiO_2$.

spectrum is very similar to that of the glasses with composition 0·30 K_2O . 0·70 SiO_2 and 0·30 Na_2O . 0·70 SiO_2. At this concentration no influence can be observed of the presence of 5 mol % B_2O_3. At $x = 0{\cdot}20$ the presence of ring-type metaborate groups (b_3) is not evidenced by the infrared spectrum, in contrast to the Raman spectrum of the same glass. At $x = 0{\cdot}05$ and $x = 0{\cdot}10$ the presence of a number of borate groups is not revealed, again in contrast to the Raman spectra.

The spectra of the glasses in the series $x\ K_2O$. $(0{\cdot}30 - x)\ B_2O_3$. 0·70 SiO_2 show the same behaviour with composition as do those of the series with 65 mol % SiO_2 discussed above (fig. 4.33).

At $x = 0{\cdot}05$ some difference may be observed in the relative height of the

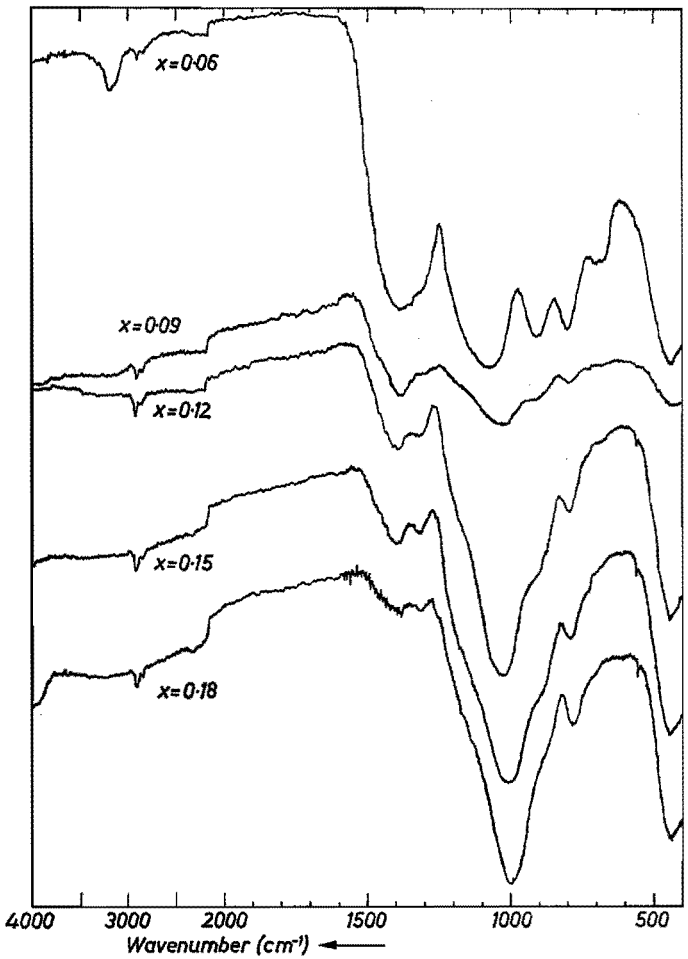

Fig. 4.33. Infrared spectra of glasses in the system $x\ K_2O$. $(0{\cdot}30 - x)\ B_2O_3$. 0·70 SiO_2.

peaks in the spectra of the Na_2O-, NaKO- and K_2O-containing glasses. These differences are too small to be discussed in terms of differences in the structure (figs 4.34 and 4.32). At $x = 0{\cdot}10$ the spectra of the glasses in the Na_2O, NaKO and K_2O series are practically identical, suggesting that the structures of these glasses are very similar (figs 4.35 and 4.32). The same holds for the spectra at $x = 0{\cdot}20$ and $x = 0{\cdot}30$ (figs 4.36 and 4.37).

Some spectra of borosilicate glasses containing CaO and BaO are shown in fig. 4.37. These spectra all show a high degree of similarity to those of glasses containing only an equivalent amount of alkali oxide. These infrared spectra suggest that the same structural units are present in the glasses containing 20 or 30 mol % mixed alkaline earth/alkali oxide or only alkali oxide. Glass of composition $0{\cdot}05\ K_2O\ .\ 0{\cdot}05\ CaO\ .\ 0{\cdot}25\ B_2O_3\ .\ 0{\cdot}65\ SiO_2$ shows an infrared spec-

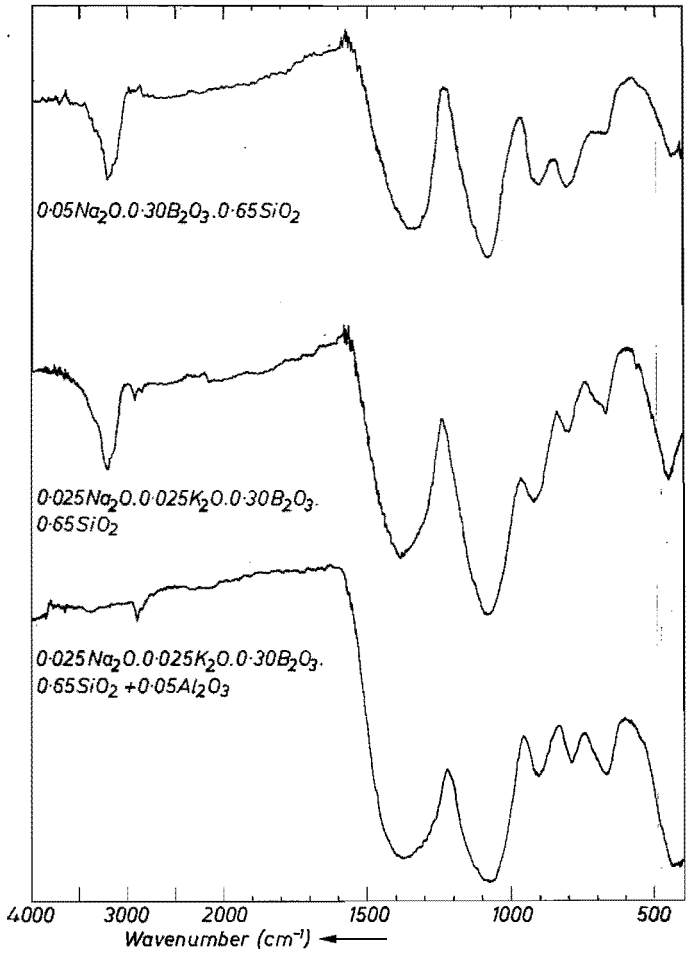

Fig. 4.34. Infrared spectra of borosilicate glasses.

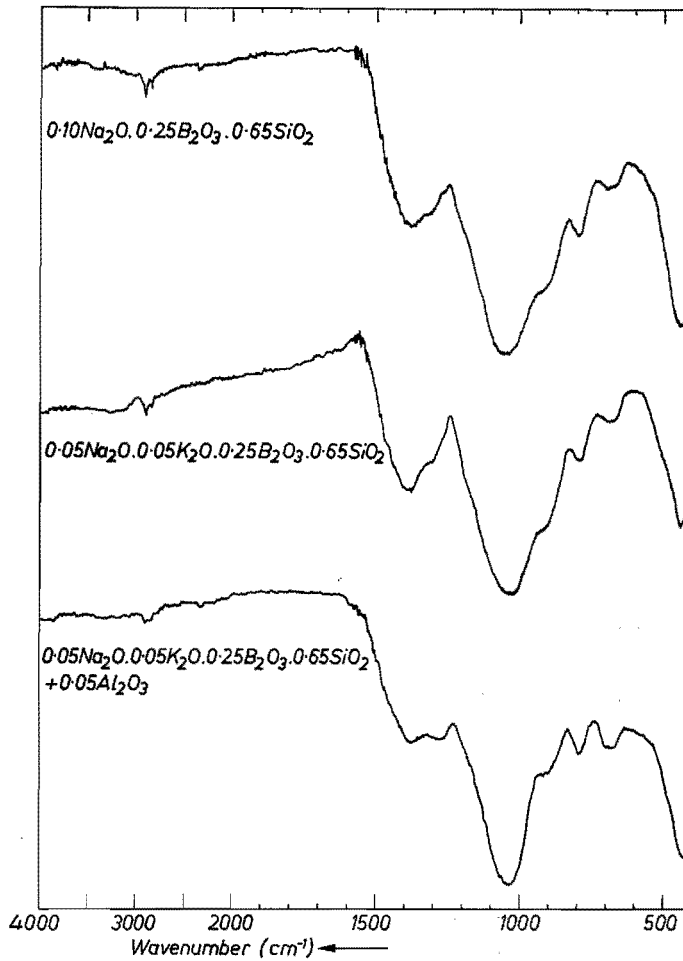

Fig. 4.35. Infrared spectra of borosilicate glasses.

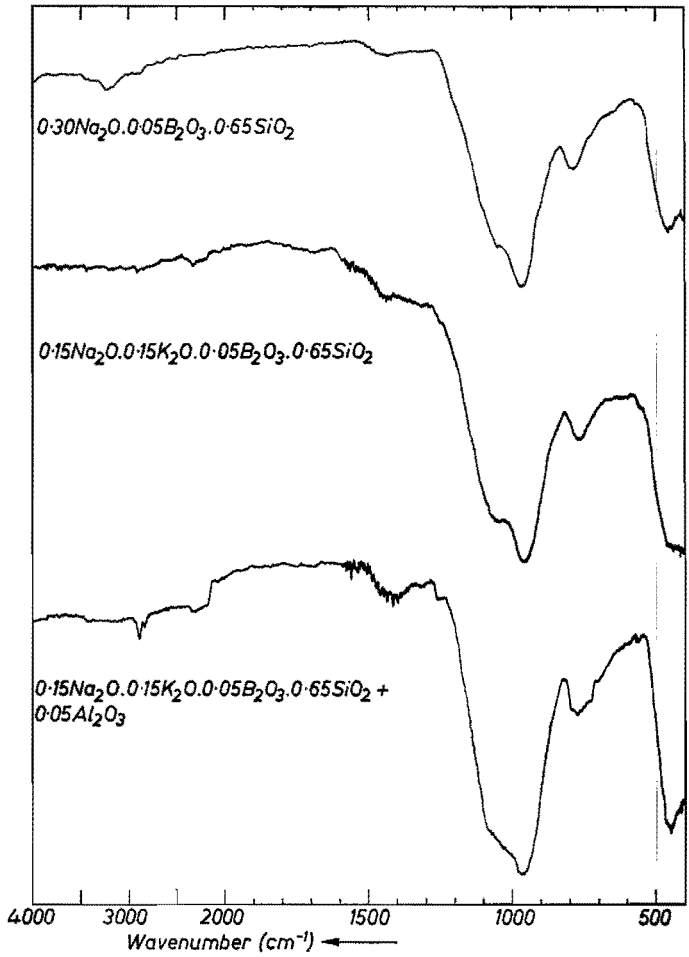

Fig. 4.36. Infrared spectra of borosilicate glasses.

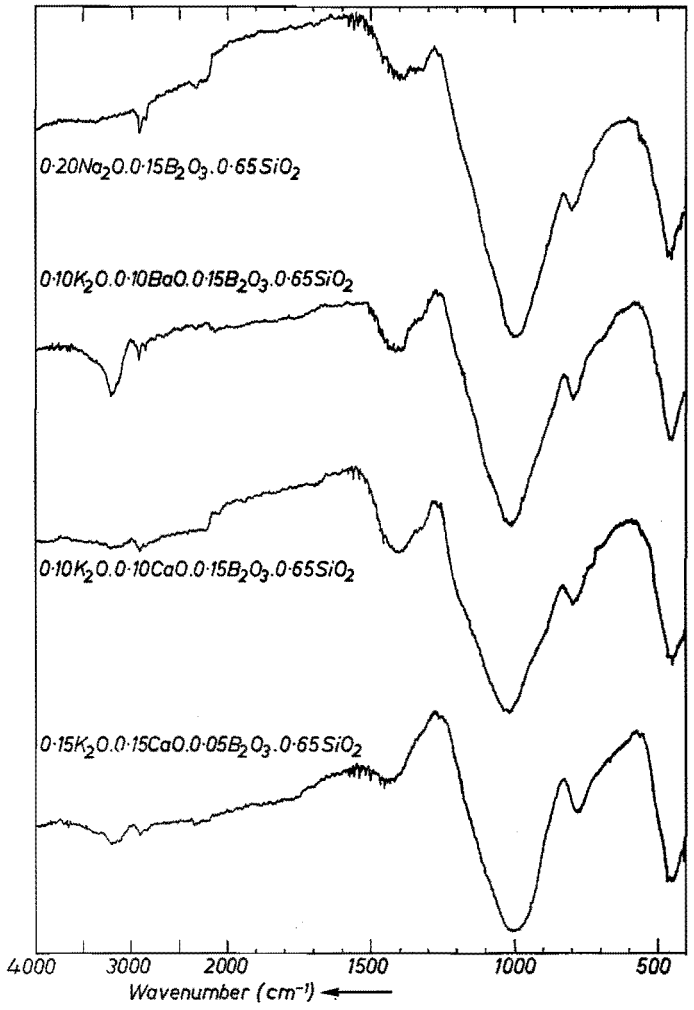

Fig. 4.37. Infrared spectra of borosilicate glasses.

trum similar to the spectra of the glasses 0·10 K_2O . 0·25 B_2O_3 . 0·65 SiO_2 and 0·05 Li_2O . 0·05 K_2O . 0·25 B_2O_3 . 0·65 SiO_2. So the introduction of Ca and Li does not result in a clearly different structure of these glasses (figs 4.41 and 4.32).

The general conclusion may be that in the borosilicate glasses with 65 and 70 mol % SiO_2 the boron ions primarily take up the alkali oxide and that SiO_2 is primarily present in a vitreous-silica-like structure that, on increase of the alkali-oxide content and decrease of the boron-oxide content, gradually changes into a disilicate-like structure.

The effect of increasing amounts of Al_2O_3 on the infrared spectra of the glass

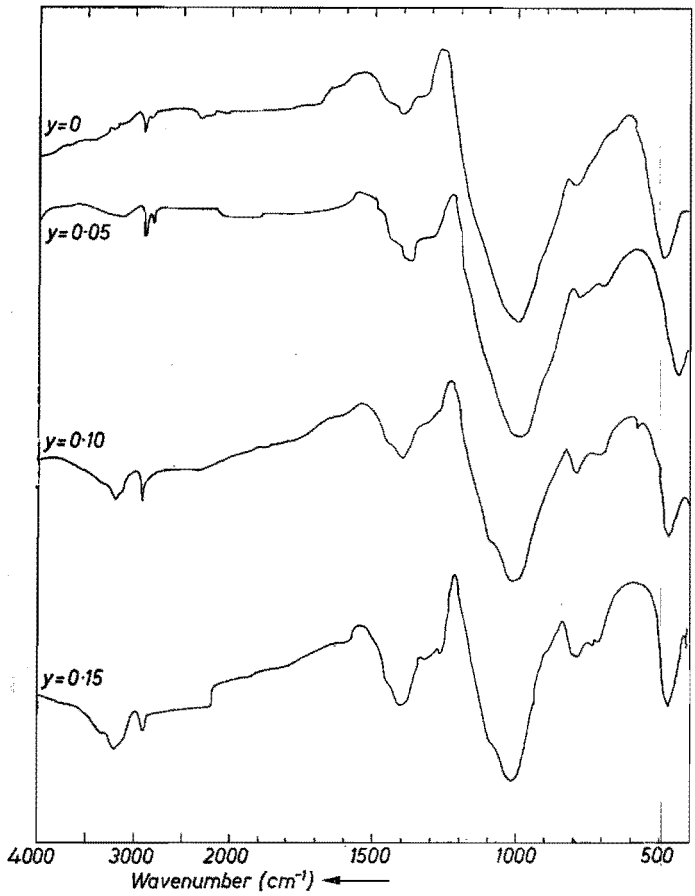

Fig. 4.38. Infrared spectra of glasses in the system $0{\cdot}10\,Na_2O\,.\,0{\cdot}10\,K_2O\,.\,0{\cdot}15\,B_2O_3\,.\,0{\cdot}65\,SiO_2 + y\,Al_2O_3$.

of composition $0{\cdot}10\,Na_2O\,.\,0{\cdot}10\,K_2O\,.\,0{\cdot}15\,B_2O_3\,.\,0{\cdot}65\,SiO_2$ is shown in fig. 4.38. The differences, however, are too small to be discussed in terms of a change of the structure.

The addition of 5 mol % Al_2O_3 to the borosilicate glasses has in general only a slight influence on the infrared spectra (cf. figs 3.39 and 3.40). This slight difference cannot be discussed in terms of structural units. In general the spectra of the borosilicate and aluminosilicate glasses show differences in the infrared spectra (cf. e.g. figs 4.42 and 4.19). This suggests that boron ions are not incorporated in the silicate network in a way analogous to the aluminum ions.

4.5.3. *Conclusions*

The infrared spectra of the borosilicate glasses show that alkali oxide is

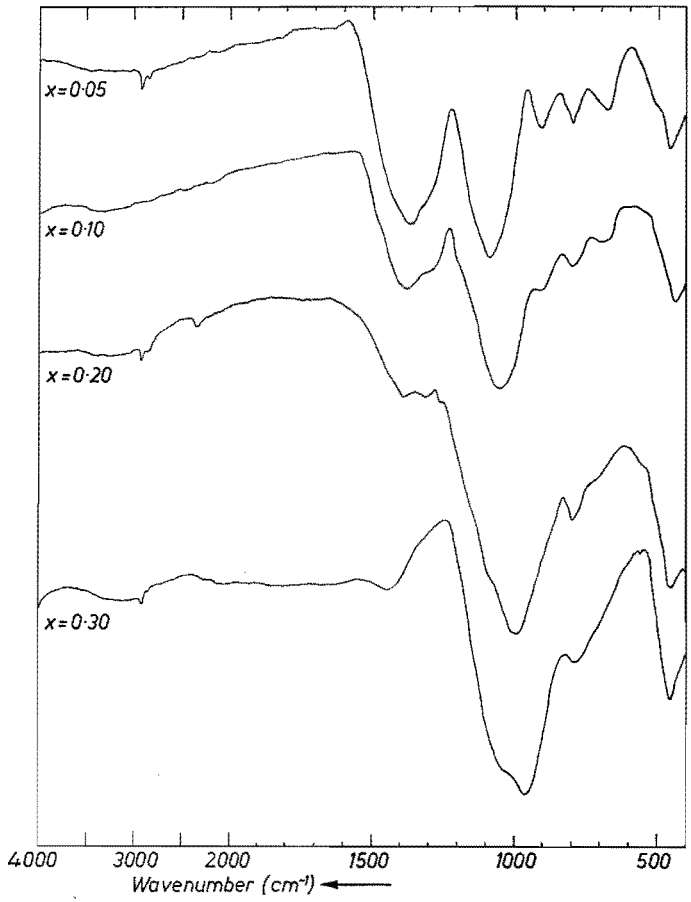

Fig. 4.39. Infrared spectra of glasses in the system $x\ Na_2O\ .\ (0{\cdot}35 - x)\ B_2O_3\ .\ 0{\cdot}65\ SiO_2 + 0{\cdot}05\ Al_2O_3$.

primarily incorporated in the glass to form borate groups that are also present in the binary borates.

Glasses with 15 *mol* % SiO_2

At 15 mol % SiO_2 content, silica seems primarily to be present in SiO_4 units with no non-bridging oxygen ions, while SiO_4 units with a non-bridging oxygen ion are formed only at alkali-oxide concentrations of about 40 mol %. In these composition series the sodium-borosilicate glasses are very similar in structure to the binary sodium-borate glasses. This holds good also for the potassium-borosilicate systems. This means that at low alkali-oxide concentrations tetraborate groups (a_6c_2) are formed which are gradually replaced by diborate groups (a_2c_2) at alkali-to-boron ratios above 0·25. The formation of chain-type metaborate groups (b_∞) is indicated in Li_2O-containing systems with a lithium-

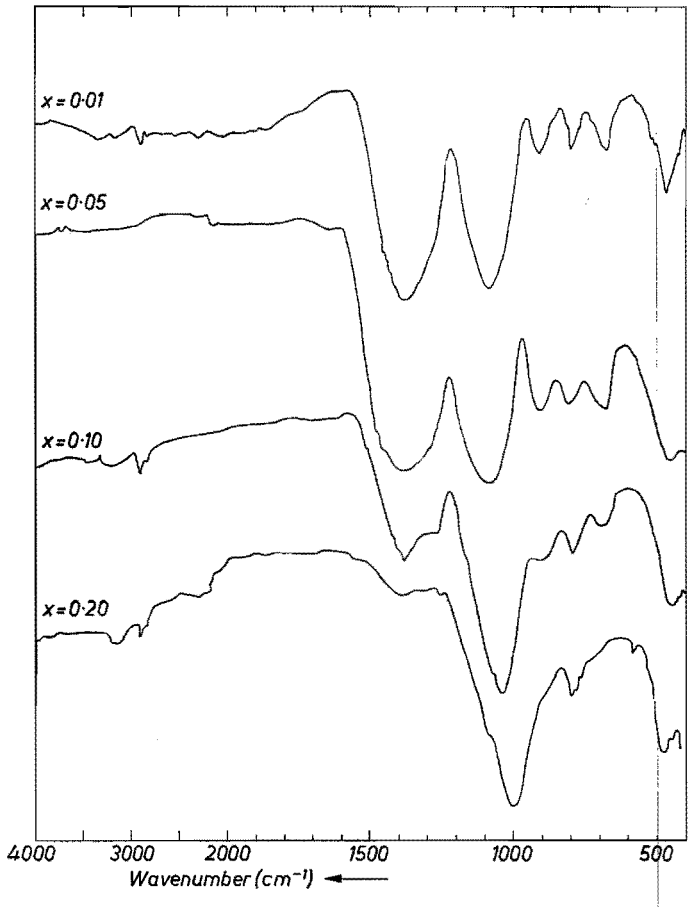

Fig. 4.40. Infrared spectra of glasses in the system $x\,K_2O\,.\,(0{\cdot}35 - x)\,B_2O_3\,.\,0{\cdot}65\,SiO_2 + 0{\cdot}05\,Al_2O_3$.

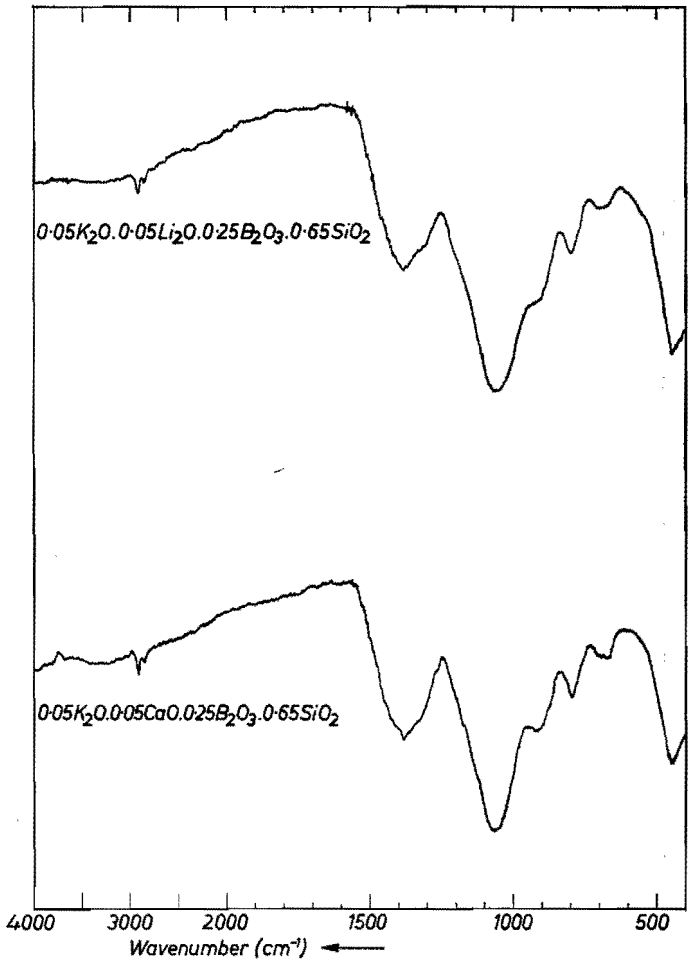

Fig. 4.41. Infrared spectra of borosilicate glasses.

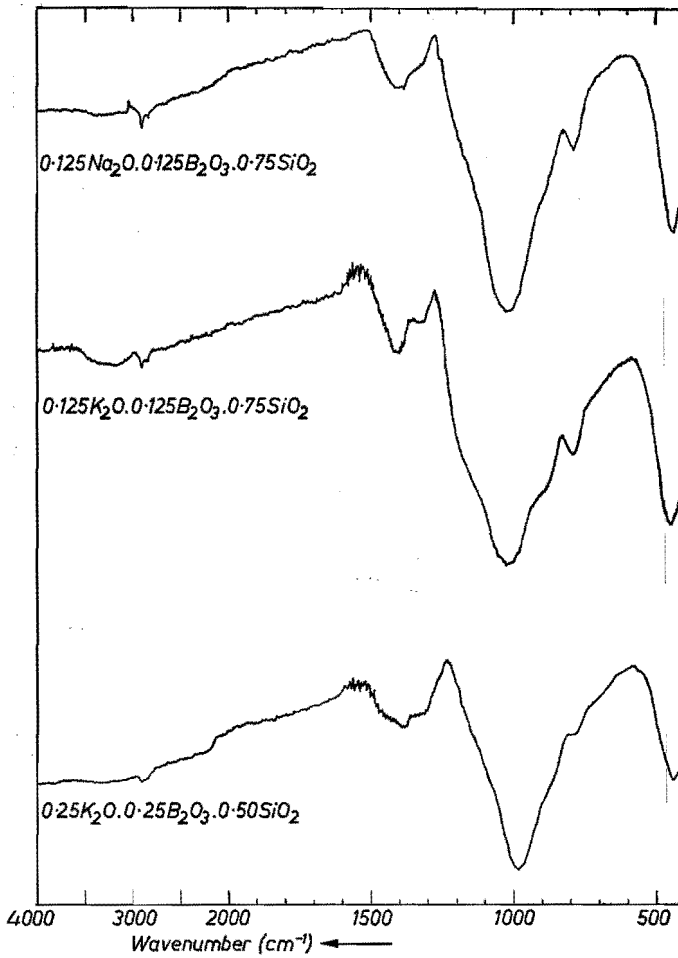

Fig. 4.42. Infrared spectra of borosilicate glasses.

to-boron ratio near to unity. Introduction of Al_2O_3 clearly leads to the disappearance of BO_4 tetrahedra in this composition series.

The borosilicate glasses containing alkaline-earth oxide generally exhibit spectra similar to those of the alkali-borosilicate glasses. This suggests a close structural similarity.

Glasses with 65 mol % SiO_2

At compositions with 65 (and 70) mol % SiO_2 it may be observed that boron again primarily consumes the alkali ions to form borate groups. The type of borate group is not evident from the spectra. SiO_2 seems primarily to be present in SiO_4 units with no non-bridging oxygen ions which are gradually replaced by SiO_4 units with a non-bridging oxygen ion on the replacement of B_2O_3 by alkali oxide. The influence of Al_2O_3 on the borosilicate glasses with 65 mol % SiO_2 is not very clear from the infrared spectra. This again suggests that, primarily, the small number of borate groups is attacked and that the silicate network is preserved. The infrared spectra suggest also that boron ions are incorporated in the silicate-glass network in a different way than the aluminum ions.

REFERENCES

4–1) N. Neuroth, in H. Volkmann (ed.), Handbuch der Infrarot-Spektroskopie, Verlag Chemie, Weinheim, 1972, Ch. 10.
4–2) C. E. Weir and R. A. Schroeder, J. Res. natl Bur. Standards **68A**, 465, 1964.
4–3) K. Frey and E. Funck, Z. Naturforsch. **27b**, 101, 1972.
4–4) J. Krogh-Moe, Phys. Chem. Glasses **6**, 46, 1965.
4–5) P. B. Hart and S. E. F. Smallwood, J. inorg. nucl. Chem. **24**, 1047, 1962.
4–6) T. W. Bril, Thesis, Technological University Eindhoven, The Netherlands, 1975.
4–7) J. Wong and C. A. Angell, Appl. Spectr. Rev. **4**, 55, 1971.
4–8) K. P. Dutova, Inorg. Mater. **4**, 1136, 1968.
4–9) E. F. Cherneva and V. A. Florinskaya, Inorg. Mater. **5**, 1831, 1969.
4–10) H. Dutz, Ber. dtsch. keram. Ges. **46**, 75, 1969.
4–11) P. H. Gaskell, Trans. Far. Soc. **62**, 1493, 1966.
4–12) K. Iiishi, T. Tomisaka, T. Kato and Y. Umegaki, Z. Kristall. **85**, 425, 1971.
4–13) A. N. Lazarev, Vibrational spectra and structure of silicates, Consultants Bureau, New York-London, 1972.
4–14) N. F. Borrelli, B. D. McSwain and G. J. Su, Phys. Chem. Glasses **4**, 11, 1963.
4–15) A. S. Tenney and J. Wong, J. chem. Phys. **56**, 5516, 1972.
4–16) R. L. Mozzi and B. E. Warren, J. appl. Cryst. **2**, 164, 1969.
4–17) E. A. Taft, J. electrochem. Soc. **118**, 1985, 1971.
4–18) P. E. Jellyman and P. J. Procter, J. Glass Techn. **39**, 173, 1955.
4–19) J. Krogh-Moe, J. Am. ceram. Soc. **47**, 307, 1964.

5. VISCOSITY OF BOROSILICATE GLASSES

5.1. Introduction

The study of the viscosity can be of great help in understanding the structure of borosilicate glasses. This is based on the fact that the viscosity properties of glass are generally very sensitive to composition differences. Usually the viscosity–temperature dependence of glass is characterized by some reference points. The reference points that will be made use of are the annealing temperature and the softening temperature. The annealing temperature is defined as the temperature where the viscosity of the glass is 10^{13} poise. The softening temperature is defined as the temperature where the viscosity is $10^{7{\cdot}6}$ poise.

Because the viscosity of the borosilicate glasses was measured by the fibre-elongation method between 10^7 and 10^{12} poise the temperature at which the viscosity is 10^{12} poise will be taken to characterize the viscosity near the transformation range.

It is logical to assume that introduction of non-bridging oxygen ions decreases the coherency of the network and consequently lowers the viscosity. Therefore an increase in the relative number of non-bridging oxygen ions in a glass will lead to lower annealing and softening temperatures. In this thesis the change in the annealing and softening temperatures with composition will be adduced in discussing the presence of non-bridging oxygen ions in borosilicate glasses.

5.2. Experimental results

The viscosity–temperature relationship was measured by the fibre-elongation method in the range $\eta = 10^7$ poise to $\eta = 10^{12}$ poise. Details on the equipment and method used can be found in sec. 2.3. For the viscosity measurements of a sample 5 to 6 measuring points were taken at different temperatures in the viscosity range mentioned. In practically all cases a linear relationship between $\log \eta$ and $1/T$ could be observed, so that this relationship follows the equation

$$\log_{10} \eta = A + \frac{E_\eta}{4{\cdot}57\, T}$$

in which η is the viscosity in poises and E_η the activation energy in kcal/mol. For a more extensive discussion of this equation the reader is referred to elementary books on glass science.

The tables in the appendix show the values of A and E_η for all glasses studied. The values of $T(\log \eta = 7{\cdot}6)$ and $T(\log \eta = 12)$ are also given; these values can be calculated from the equation after obtaining the optimal values of A and E_η from the experimental measurements. For selected composition series the results of $T(\log \eta = 12)$ and $T(\log \eta = 7{\cdot}6)$ versus composition are shown

graphically in figs 5.1 to 5.12. This was done for a number of composition series in the systems Na_2O–B_2O_3–SiO_2, K_2O–B_2O_3–SiO_2, $NaKO$–B_2O_3–SiO_2 and Li_2O–B_2O_3–SiO_2. In some figures the influence of the addition of 5 mol % Al_2O_3 to the glass on the reference points is shown. The influence of up to 20 mol % Al_2O_3 on two glass compositions is shown in table 5-I.

TABLE 5-I

Influence of Al_2O_3 on the reference temperatures of two borosilicate glasses

glass composition		T (log η = 7·6) (°C)	T (log η = 12) (°C)
$0{\cdot}10Na_2O\,.\,0{\cdot}10K_2O\,.\,0{\cdot}65B_2O_3\,.\,0{\cdot}15SiO_2$		544	459
,,	$+0{\cdot}05Al_2O_3$	541	454
,,	$+0{\cdot}10Al_2O_3$	532	440
,,	$+0{\cdot}15Al_2O_3$	535	435
,,	$+0{\cdot}20Al_2O_3$	545	450
$0{\cdot}10Na_2O\,.\,0{\cdot}10K_2O\,.\,0{\cdot}15B_2O_3\,.\,0{\cdot}65SiO_2$		665	563
,,	$+0{\cdot}05Al_2O_3$	683	562
,,	$+0{\cdot}10Al_2O_3$	703	568
,,	$+0{\cdot}15Al_2O_3$	704	576
,,	$+0{\cdot}20Al_2O_3$	777	612

Abe [5-1]) described an area in which a delayed viscosity effect was observed. This area coincides fairly well with the area in which phase separation can be expected. For compositions in this area care was taken that the measurements were done as rapidly as possible after the glass fibre had attained the appropriate temperature. To obtain reproducible viscosity results the wet-chemical preparation methods described elsewhere (Konijnendijk, Van Duuren and Groenendijk [5-2])), were found to be indispensable. The influence of small amounts of water on the viscosity results was reduced by remelting all samples in vacuum (see also sec. 2.1). The error in the reference temperatures is about 5 °C maximally.

5.3. Discussion of results

From figs 5.1 to 5.5, showing the relation between the temperature T at which $\log_{10}\eta = 12$ and the glass composition it is clear that replacement of B_2O_3 by alkali oxide in B_2O_3 and B_2O_3–SiO_2 glass results in more-viscous glasses up to a certain mol % alkali oxide. After a maximum is reached the viscosity

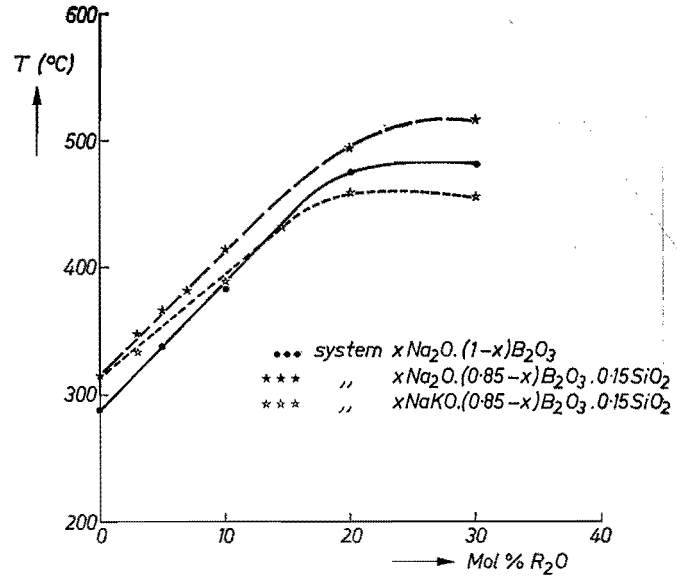

Fig. 5.1. Temperature T at which $\log_{10}\eta = 12$ versus mol % Na_2O or NaKO.

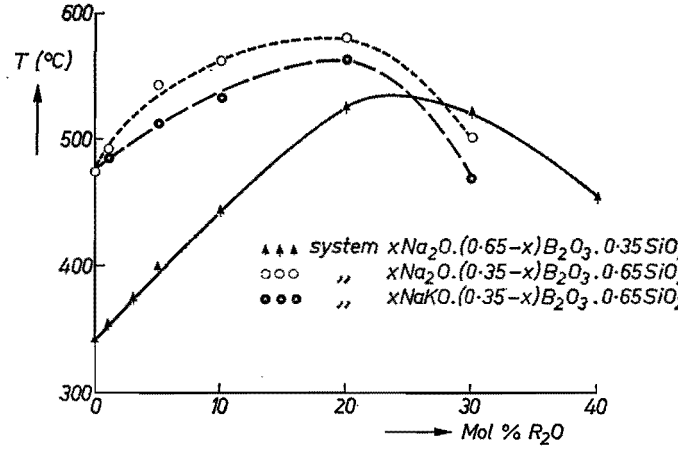

Fig. 5.2. Temperature T at which $\log_{10}\eta = 12$ versus mol % Na_2O or NaKO.

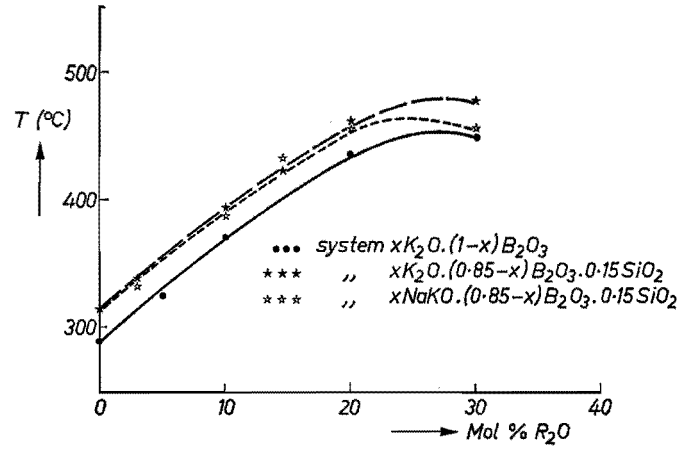

Fig. 5.3. Temperature T at which $\log_{10}\eta = 12$ versus mol % K_2O or NaKO.

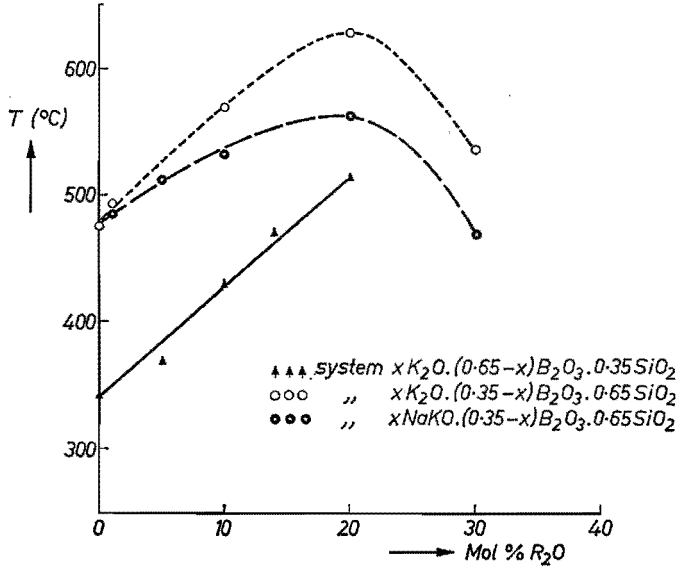

Fig. 5.4. Temperature T at which $\log_{10}\eta = 12$ versus mol % K_2O or NaKO.

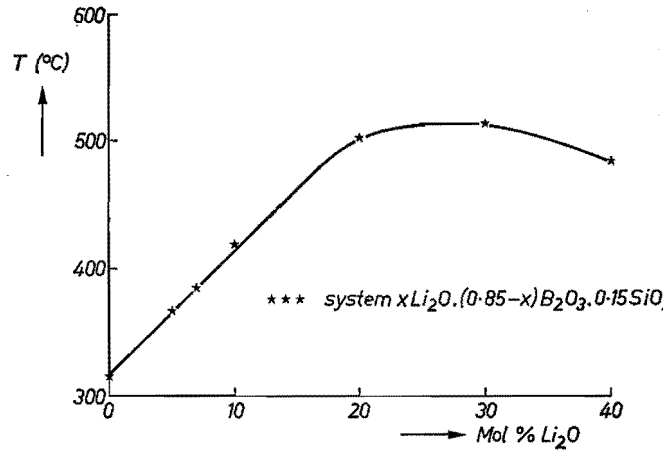

Fig. 5.5. Temperature T at which $\log_{10}\eta = 12$ versus mol % Li_2O. System $x\,LiO_2 . (0{\cdot}85 - x)\,B_2O_3 . 0{\cdot}15\,SiO_2$.

decreases again on replacement of more B_2O_3 by alkali oxide. The maximum is found at about the same alkali-oxide concentration with increasing SiO_2 content.

Glasses with 15 *mol* % SiO_2 *content*

The results suggest that the replacement of B_2O_3 by alkali oxide at first increases the coherency of the network and then, after a certain maximum is reached, decreases it. The increase in the coherency is usually explained by an increase in the oxygen coordination of the boron ions in the glass from 3 to 4. At higher alkali-oxide concentrations sufficient non-bridging oxygen ions are formed, giving rise to a decrease in coherency and consequently in viscosity.

Glasses with 65 *mol* % SiO_2 *content*

The fact that at constant alkali-oxide content the viscosity increases with increasing SiO_2 content suggests that SiO_2 is incorporated in the structure with only a limited number of non-bridging oxygen ions in those composition areas where enough boron is available to take up the alkali oxide.

The Raman data (cf. chapter 3) suggest that where the maximum can be observed in the viscosity as a function of alkali-oxide content, the number of non-bridging oxygen ions connected to ring-type metaborate groups (b_3) increases considerably with increasing SiO_2 content. This means that an increase of the relative amount of boron ions in four-coordination cannot be responsible for the increase of the viscosity on increase of the SiO_2 content, but that gradually a vitreous silica-like glass structure becomes the continuous phase and is an important viscosity-determining factor.

Influence of the type of alkali ion

Comparing the $T(\log \eta = 12)$ values for the systems $x\ Na_2O\ .\ (1-x)\ B_2O_3$ and $x\ K_2O\ .\ (1-x)\ B_2O_3$ one observes that the sodium-oxide systems are more viscous than the corresponding potassium-oxide systems. For the composition series with 15 mol % SiO_2 one may observe that the Li_2O and Na_2O glasses show an almost identical composition–viscosity relationship and that the corresponding K_2O glasses again show a lower viscosity. On addition of more SiO_2 the difference between the Na_2O and K_2O systems reverses, so that at 65 mol % SiO_2 the viscosity of the K_2O systems is equal to the corresponding Na_2O systems or higher. This suggests structural and/or bonding differences between the Na_2O- or K_2O-containing borosilicate glasses. It may be that since the field strength of Na^+ is higher than of K^+ the attraction forces between the sodium and the oxygen ions are higher and thus the viscosity of the sodium glasses with low SiO_2 content is higher. It was put forward by Stevels [5–3]) that in silicate glasses at low alkali-oxide content the bonding forces between silicon and oxygen ions practically determine the viscosity. From the Raman spectra it becomes clear that the continuous phase in the borosilicate glasses with 65 mol % SiO_2 is a silicate glass with a low alkali-oxide content. The Na^+ ions exert a stronger polarizing effect on the oxygen ions than the K^+ ions, so the bonding between silicon and oxygen is weaker in case of the sodium-borosilicate glasses, giving rise to a lower viscosity than the corresponding potassium-borosilicate glasses.

Mixed NaK *systems*

For the mixed NaK-borate glasses it was shown by Visser [5–4]) that the $T(\log \eta = 12)$ values of the systems $x\ NaKO\ .\ (1-x)\ B_2O_3$ and $x\ K_2O\ .\ (1-x)\ B_2O_3$ are almost equal. The mixed NaK systems have a significantly lower viscosity than the corresponding sodium-borate glasses. The systems in the composition series with 15 mol % SiO_2 show the same behaviour. The mixed NaK systems with 65 mol % SiO_2 show a significantly decreased viscosity compared both to the unmixed Na- and K-containing glasses, as is generally observed in mixed alkali-silicate glasses (Stevels [5–3]), Poole [5–5]), Isard [5–6])). The extent to which the viscosity decreases is also near the values observed in mixed NaK-silicate glasses. If it is assumed, according to Stevels [5–7]), that in mixed alkali glasses, ions of different size can be incorporated in the structure more easily than ions which are all of one size, this decreased viscosity can be explained qualitatively. The improved geometrical fit gives rise to better bonding of the alkali ions to the network, thus weakening the Si–O bonding and leading to a decreased viscosity for the glass systems with 65 mol % SiO_2. This explanation does not hold good for the systems with 0 and 15 mol % SiO_2 because the viscosity of the mixed NaK systems is almost equal to that of the corresponding K systems.

The explanations given above for the mixed-alkali effect and for the order of the viscosity of corresponding Li, Na and K systems are not very firm. It is difficult to discuss the viscosity results in the absence of a generally agreed theory of the processes which govern viscous flow in glass. The explanations given above are only qualitative.

Influence of Al_2O_3 *on glasses with* 15 *mol* % SiO_2

The addition of 5 mol % Al_2O_3 to the glasses in the composition series $x\ Na_2O\ .\ (0{\cdot}85 - x)\ B_2O_3\ .\ 0{\cdot}15\ SiO_2$ leads to a decrease in viscosity when the concentration of Na_2O is higher than that of Al_2O_3 (cf. fig. 5.6). The Raman data in chapter 3 suggest that in the glasses of this series only a very limited number of non-bridging oxygen ions is present and that the addition of 5 mol % Al_2O_3 generally leads to a decrease in the number of BO_4 tetrahedra and the formation of boroxol groups (a_3). Al_2O_3 is most probably taken up in the network in the form of AlO_4 tetrahedra. So an increase in viscosity on adding Al_2O_3 cannot be expected.

For the corresponding potassium glasses it may be observed that the addition of 5 mol % Al_2O_3 has a negligible influence (cf. fig. 5.7) on the viscosity. For the corresponding mixed NaK glasses it may be observed that the curves vary in a similar way as the unmixed Na and K glasses (cf. fig. 5.8).

It is difficult to explain the observed results on a structural basis. From the Raman and infrared spectra of these glasses it is not clear how the AlO_4 tetrahedra are distributed over the borate network.

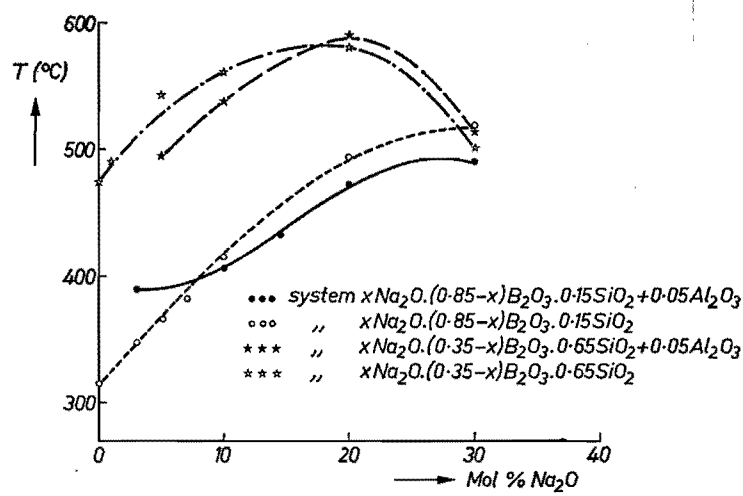

Fig. 5.6. Temperature T at which $\log_{10} \eta = 12$ versus mol % Na_2O.

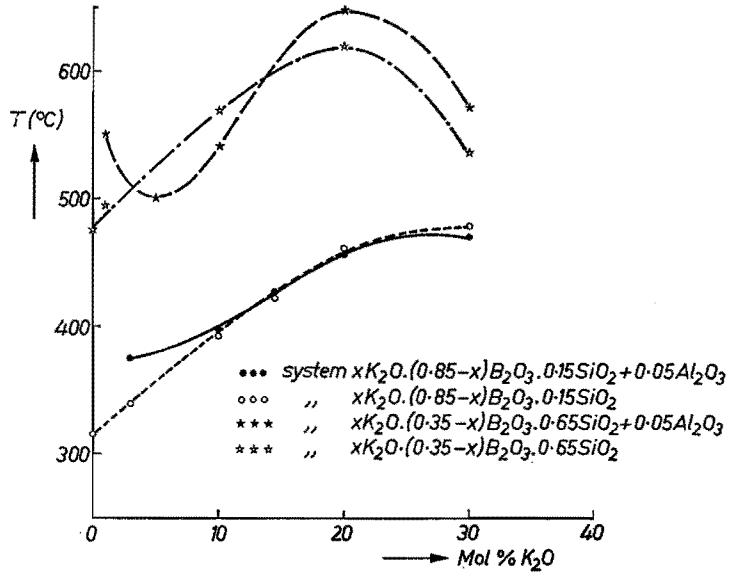

Fig. 5.7. Temperature T at which $\log_{10}\eta = 12$ versus mol % K_2O.

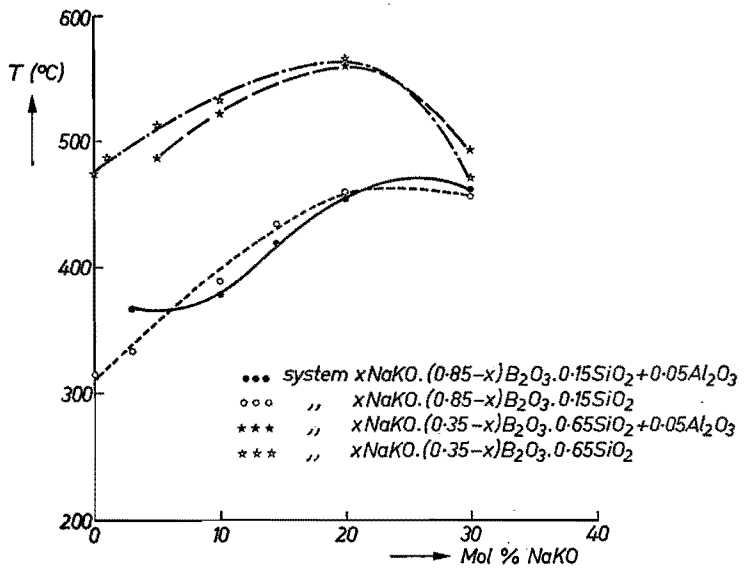

Fig. 5.8. Temperature T at which $\log_{10}\eta = 12$ versus mol % NaKO.

Influence of Al_2O_3 *on glasses with* 65 *mol* % SiO_2

For the systems with 65 mol % SiO_2 one may observe that the addition of 5 mol % Al_2O_3 to the glasses with 5 and 10 mol % Na_2O, K_2O and NaKO leads to a decrease in the viscosity. In a given composition series one may observe that the addition of 5 mol % Al_2O_3 to the glasses with 20 and 30 mol % alkali oxide leads to an increase in the viscosity, for the mixed NaK systems at 20 mol % the viscosity does not change significantly and at 30 mol % there is an increase.

From the Raman spectra it became clear that the addition of 5 mol % Al_2O_3 to the glasses with 5 and 10 mol % alkali oxide primarily results in a decrease in the number of BO_4 tetrahedra and an increase in that of boroxol groups (a_3). Probably Al_2O_3 is incorporated in the structure as AlO_4 tetrahedra. The decrease in viscosity may be explained by the decrease in the coherency of the network. It is doubted that this explanation is altogether correct because the role of phase separation in this region is not yet fully understood. The increase in viscosity for the compositions with 20 and 30 mol % Na_2O and K_2O can be explained by a decrease in the amount of non-bridging oxygen ions as was revealed by the Raman spectra.

Influence of larger amounts of Al_2O_3

From table 5-I it may be observed that the addition of up to 20 mol % Al_2O_3 to a glass of composition 0·10 Na_2O . 0·10 K_2O . 0·65 B_2O_3 . 0·15 SiO_2 has no significant influence on the viscosity. As only a small amount of non-bridging oxygen ions can be expected in the base-glass composition this result is not very strange.

Addition of up to 20 mol % Al_2O_3 to a glass of composition 0·10 Na_2O . 0·10 K_2O . 0·15 B_2O_3 . 0·65 SiO_2 leads to a significant increase in the viscosity. Especially the viscosity difference between the glasses to which 15 and 20 mol % Al_2O_3 are added is striking. From the Raman spectra it became clear that addition of Al_2O_3 to the base glass first leads to a decrease in the ring-type metaborate groups (b_3). At higher concentrations of Al_2O_3 the non-bridging oxygen ions connected to SiO_4 tetrahedra also disappear. This result, together with the accelerated viscosity increase with the ultimate addition of Al_2O_3, suggests that the base glass is built up of a silica-glass-like structure with only a minor amount of non-bridging oxygen ions and that the ring-type metaborate groups (b_3) are isolated in this silicate-network structure, probably as small islands. This explains the slighter increase in viscosity on the addition of the first amounts of Al_2O_3 which attacks the islands of metaborate groups (b_3) and leaves the silicate network unchanged, and the subsequent higher increase in viscosity when Al_2O_3 causes the decrease of the number of non-bridging oxygen ions of the silicate network.

Influence of composition on the transition temperature

Figures 5.9 to 5.12 showing the relation between the temperature T at which $\log \eta = 7{\cdot}6$ and the composition of the glasses, reveal that the maxima in the viscosity move to somewhat lower alkali-oxide content and become less pronounced the more SiO_2 is present in the glass, compared to the figures showing the behaviour of T ($\log \eta = 12$) with composition. Visser [5–4]), basing himself on the work of Beekenkamp [5–8]) on borate glasses, has explained this effect by postulating that at higher temperatures more non-bridging oxygen ions are formed at the expense of BO_4 tetrahedra, resulting in a less coherent network and thus a less pronounced viscosity increase.

However, Raman spectra of glasses cooled from different temperatures and at different velocities did not show any difference. This result does suggest that there is no coordination change of the boron ions from tetrahedral to triangular coordination on increasing the temperature. Also, the work of Riebling [5–9]) on volume relations in Na_2O–B_2O_3 and Na_2O–B_2O_3–SiO_2 melts at 1300 °C, shows that BO_4 tetrahedra appear to be quite stable at high temperatures. Due to the absence of a generally agreed theory of the processes which govern viscous flow no attempt will be made to give an explanation for the differences in the viscosity results at T ($\log \eta = 12$) and T ($\log \eta = 7{\cdot}6$).

5.4. Conclusions

The composition–viscosity relationship measured for borosilicate glasses is consistent with other experimental evidence in this thesis when these have to be interpreted in terms of structure of the glasses.

The results show that at *low* SiO_2 content the borate phase is continuous and

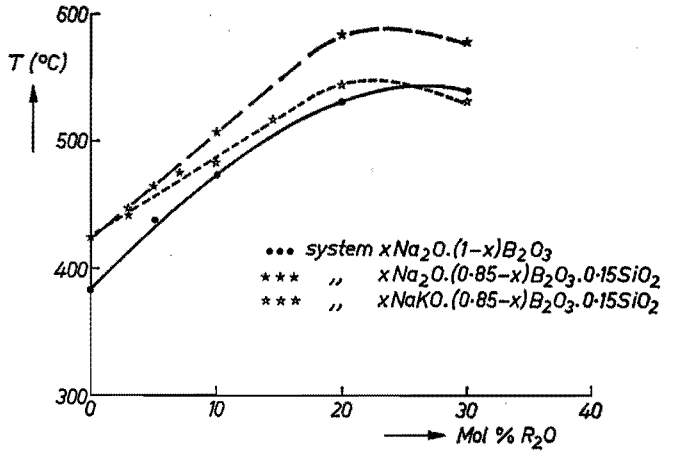

Fig. 5.9. Temperature T at which $\log_{10} \eta = 7{\cdot}6$ versus mol % Na_2O or NaKO.

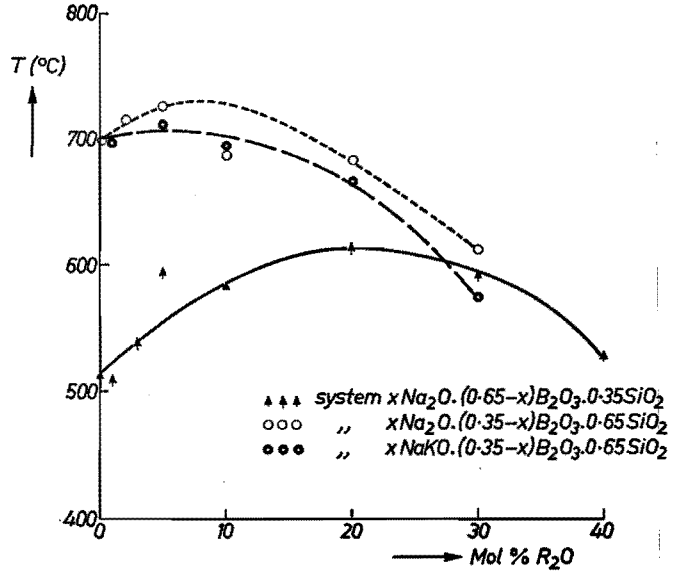

Fig. 5.10. Temperature T at which $\log_{10} \eta = 7{\cdot}6$ versus mol % Na_2O or NaKO.

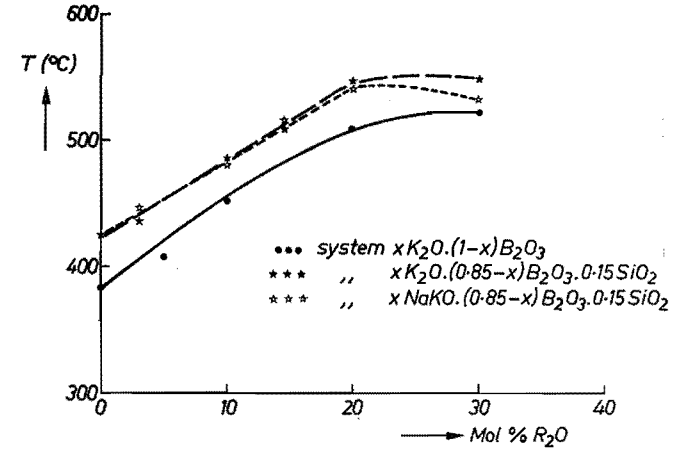

Fig. 5.11. Temperature T at which $\log_{10} \eta = 7{\cdot}6$ versus mol % K_2O or NaKO.

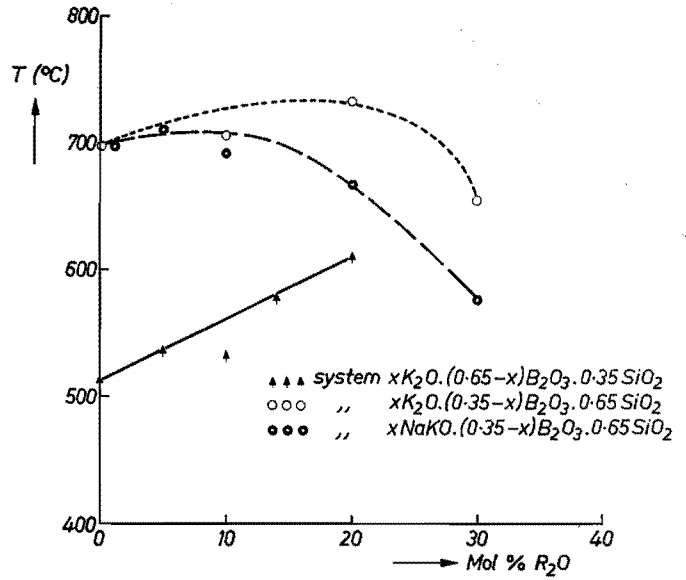

Fig. 5.12. Temperature T at which $\log_{10} \eta = 7{\cdot}6$ versus mol % K_2O or NaKO.

is the primary viscosity-determining factor. Nearly all the alkali ions are incorporated into the borate network to form BO_4 tetrahedra. At alkali-to-boron ratios of about 0·5 the presence of non-bridging oxygen ions is indicated by the decline of the increase in viscosity with addition of alkali oxide. SiO_2 seems to be present in a vitreous silica-like structure most probably agglomerated into islands; at alkali-to-boron ratios of about 0·5 the presence of non-bridging oxygen ions connected to SiO_4 tetrahedra cannot be excluded.

At relatively *high* SiO_2 content of the borosilicate glasses a similar behaviour may be observed although less clearly than when the SiO_2 content is lower. This means that borate groups with BO_4 tetrahedra are again formed at low alkali-oxide content and that only a minor number of alkali ions is incorporated in the glass network directly connected to SiO_4 tetrahedra.

REFERENCES

5–1) T. Abe, J. Am. ceram. Soc. **35**, 284, 1952.
5–2) W. L. Konijnendijk, M. van Duuren and H. Groenendijk, Verres Réfract. **27**, 11, 1973.
5–3) J. M. Stevels, The structure and physical properties of glass, in S. Flügge (ed.), Handbuch der Physik, Vol. 13, 1962.
5–4) Th. J. M. Visser, Thesis, Technological University Eindhoven, The Netherlands, 1971.
5–5) J. P. Poole, J. Am. ceram. Soc. **32**, 230, 1949.
5–6) J. O. Isard, J. non-cryst. Solids **1**, 235, 1969.
5–7) J. M. Stevels, The electrical properties of glass, in S. Flügge (ed.), Handbuch der Physik, Vol. 20, 1957.
5–8) P. Beekenkamp, Philips Res. Repts Suppl. 1966, No. 4.
5–9) E. F. Riebling, J. Am. ceram. Soc. **50**, 46, 1967.

6. ELECTRICAL CONDUCTION OF BOROSILICATE GLASSES

6.1. Introduction

It is generally accepted that in many glasses alkali ions move under the influence of an electric field. Therefore, glasses such as alkali silicate, alkali borate and alkali borosilicate show ionic conduction.

The conductivity σ of a glass containing only one type of charge carrier, for instance an alkali ion, can in general be described by the equation

$$\sigma = \sigma_0 \exp(-E/RT)$$

where σ_0 is a pre-exponential factor, E the activation energy, R the gas constant and T the absolute temperature. The logarithmic version of this expression is usually referred to as the Rasch-and-Hinrichsen equation [6–1]). In most glasses a linear relationship can be observed between $\log \sigma$ and the reciprocal of the absolute temperature, with the result that the Rasch-and-Hinrichsen equation has come into common use. A break can generally be observed in the relation of the logarithm of electrical conduction and the reciprocal of the absolute temperature near the transition temperature. As the temperature approaches the range where structural rearrangements become possible, the conductivity increases more rapidly with increasing temperature, usually leading to a second region where the Rasch-and-Hinrichsen equation applies with a higher activation energy.

The dependence of the activation energy of the electrical conduction on the composition of the glass is discussed by Stevels [6–10]). This author suggests that the activation energy is determined by the average height of potential barriers. In this way one may explain the higher activation energy for K^+ ions in potassium-silicate glasses compared to the activation energy for Na^+ ions in sodium-silicate glasses up to a certain amount of alkali oxide. At higher alkali-oxide concentration the glass structure becomes less dense, the larger K^+ ions may now move more easily than the smaller Na^+ ions because the latter are bonded more strongly to the network. For a more extensive introduction to the mechanism of ionic conductivity the reader is referred to the reviews by Hench and Schaake [6–2]) and Stevels [6–10]).

There have been relatively few attempts to get information on the molecular structure of oxide glasses from electrical-conduction measurements. Beekenkamp [6–3]), for instance, used electrical-conduction measurements to study the structure of glasses in the system K_2O–B_2O_3–Al_2O_3. Electrical conductivity in alkali-silicate glasses has been studied extensively. In general a rapid increase of the conductivity is observed on addition of alkali oxide to vitreous silica up to about 20–30 mol % alkali oxide, at higher concentrations the increase is less pronounced. This increase in conductivity can be directly related to the mobile alkali ions.

It is also known that thermal treatments in the annealing-transformation range have a significant influence on the electrical conduction of many glasses. As an example the work of Charles [6–4]) on lithium-silicate glasses may be quoted. This shows the influence of phase separation or stress in the glass on the electrical conduction of glasses.

The effect of the water content on the electrical conduction of sodium-silicate glass was studied by Martinsen and McGee [6–5]). It was established that small numbers of hydroxyl ions increased the electrical conduction of the silicate glasses remarkably. Scholze and Mulfinger [6–6]), on the basis of diffusion experiments, proposed that H^+ ions jump from OH^- ions to a neighbouring non-bridging oxygen ion and that the electrical charges are neutralized by simultaneous diffusion of OH^- ions. Such a reaction may also take place in the presence of an electric field giving rise to an increase in the conduction as suggested by Martinsen and McGee [6–5]).

Electrical conduction in alkali-borate melts was studied by Müller [6–7,8]). This author showed that the electrical conduction in alkali-borate melts increased rapidly in the 15 to 50 mol % alkali-oxide range measured at the same temperature. The presence of small units in borate melts is not confirmed by these measurements.

Electrical conduction in sodium- and lithium-borosilicate glasses was measured by Otto [6–9]). The temperature dependence of the electrical conductivity was found to follow the Rasch-and-Hinrichsen [6–1]) equation up to the softening range. The conductivity was increased by raising the alkali-oxide content, or, if the mole fraction of alkali oxide was kept constant, by increasing the concentration of SiO_2. According to Otto three concentration regions could be distinguished for the description of the activation energies. A rather steep but linear decrease was observed from 0 to 25 mol % alkali oxide at a constant mol % SiO_2. An abrupt change was observed at 25 mol % alkali oxide, the activation energy still decreased linearly with increasing alkali-oxide content but the proportionality constant is only about one fourth the value at lower concentrations. Raising the alkali concentration above 50 mol % does not lower the activation energy any further. This behaviour is not explained by the author.

6.2. Experimental results

The direct-current resistivity, which is the reciprocal of the conductivity σ, has been measured as a function of temperature in the range $\varrho = 10^5$ to 10^8 ohm cm, for a large number of compositions in the Li-, Na-, K- and mixed Na–K-borosilicate glasses. As already explained in sec. 2.1, it was essential to prepare the samples by wet-chemical techniques followed by vacuum melting for a certain period, so as to obtain reproducible results. In most cases a linear relationship between $\log \varrho$ and $1/T$ could be observed, where ϱ is the specific

resistance, so that the resistivity seems to obey the Rasch-and-Hinrichsen relation

$$\log \varrho = A + \frac{E}{RT},$$

where $-A$ is the logarithm of the pre-exponential factor and E the activation energy. In a number of cases the relationship showed a bend near the transformation range but on both sides of this bend a linear relationship could be observed.

Figures 6.1. to 6.8 show the relation between the values of the activation energy E_ϱ and the composition of the glass for certain composition series. Figures 6.9 to 6.16 show the relation between the temperature T at which $\log_{10} \varrho = 7$ and the composition for the same series. The measured values of E_ϱ that are encircled in figs 6.1 to 6.8 at low alkali concentration, are values of E_ϱ above the transformation range. The tables in the appendix show the values of A and E_ϱ for every composition measured, together with the appropriate temperature range for the values measured.

For each composition the specific resistance was measured on two samples and at least ten temperatures. The experimental error in determining the activation energy is below 0·04 eV, the error in the temperature at which $\log_{10} \varrho = 7$ is below 5 °C in comparison with all the compositions studies; there may be an absolute error of 10 °C maximally which is the same for all compositions.

All samples were cooled directly from the melting temperature to room temperature in air and not annealed. For some compositions in the series with 35 mol % SiO_2 the influence of phase separation on the E_ϱ and T ($\log \varrho = 7$) values was studied. Compared to the unannealed glasses, the glasses with a clearly visible developed phase separation did not show significant differences in the values of E_ϱ and T ($\log \varrho = 7$).

The influence of hydroxyl ions on E_ϱ and T ($\log \varrho = 7$) was evident. Especially those values of E_ϱ, which were measured above the transition range are susceptible to small numbers of hydroxyl ions. From infrared measurements in the range around 3600 cm^{-1} where the hydroxyl ions show their characteristic absorption it was established that an increase in the number of hydroxyl ions means a significant decrease in the activation energy. For a glass of composition 0·65 B_2O_3 . 0·35 SiO_2, E_ϱ was 1·66 eV when this glass contained about 300 ppm H_2O, decreasing to 1·54 eV at about 400 ppm H_2O. The values of E_ϱ measured below the transition range are much less susceptible to small variations in the water content, thereabove the amount of hydroxyl ions in the glass decreases with increasing alkali-oxide content down to values of about 30 ppm H_2O (or less) at 30 mol % alkali oxide.

The influence of increasing amounts of Al_2O_3 on E_ϱ and T (log $\varrho = 7$) of two borosilicate glass compositions is shown in table 6-I.

TABLE 6-I

The influence of Al_2O_3 on E_ϱ and T (log $\varrho = 7$) of two borosilicate glasses

glass composition	E_ϱ (eV)	T (log $\varrho = 7$) (°C)
0·1 Na_2O . 0·1 K_2O . 0·65 B_2O_3 . 0·15 SiO_2	1·23	375
,, + 0·05 Al_2O_3	1·09	363
,, + 0·10 Al_2O_3	1·19	368
,, + 0·15 Al_2O_3	1·13	369
,, + 0·20 Al_2O_3	1·09	364
0·1 Na_2O . 0·1 K_2O . 0·15 B_2O_3 . 0·65 SiO_2	1·05	306
,, + 0·05 Al_2O_3	1·04	306
,, + 0·10 Al_2O_3	1·02	300
,, + 0·15 Al_2O_3	0·96	274
,, + 0·20 Al_2O_3	0·92	245

6.3. Discussion of results

Discussion on E_ϱ

It may be observed in figs 6.1 to 6.8 that the first additions of alkali oxide to borosilicate glasses bring about a rise in the value of E_ϱ, measured at temperatures above the transformation range. After a maximum is reached, the value of E_ϱ decreases. This behaviour can hardly be explained in terms of structural units in the borosilicate glasses because of the influence of hydroxyl ions in this range. By longer vacuum melting the values of E_ϱ did not rise further, nor does the hydroxyl content decrease.

Otto [6–9]) who measured E_ϱ at temperatures below the transition range in the systems Na_2O–B_2O_3–SiO_2 and Li_2O–B_2O_3–SiO_2 found a linear decrease of the activation energy with increasing alkali-oxide content neglecting any influence of hydroxyl ions. In this thesis it is found that this influence below the transition range is less.

The decrease in the activation energy below T_g with increasing alkali-oxide content is also observed in this thesis, although here the observed decrease is not linear with composition as in the measurements carried out by Otto [6–9]).

For the lithium-, sodium- and potassium-borosilicate glasses in the composition series with 15 mol % SiO_2 about the same values of E_ϱ at compositions

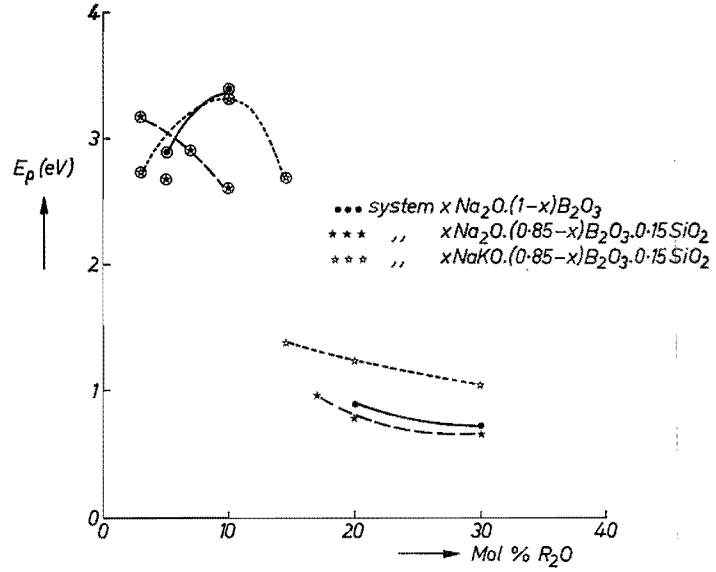

Fig. 6.1. Activation energy of electrical conduction E_e versus mol % Na_2O or NaKO.

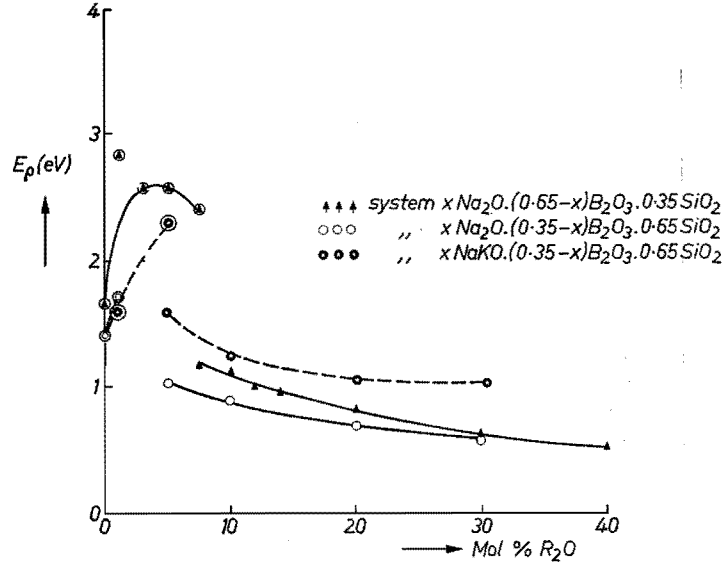

Fig. 6.2. Activation energy of electrical conduction E_e versus mol % Na_2O or NaKO.

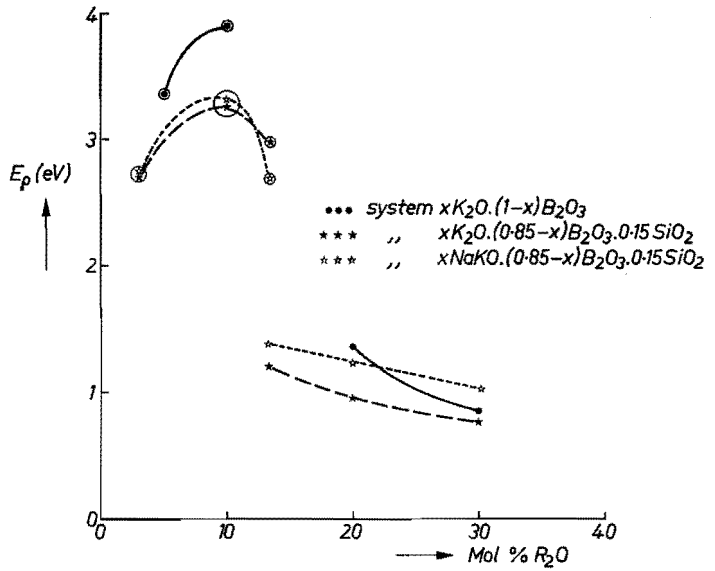

Fig. 6.3. Activation energy of electrical conduction E_e versus mol % K_2O or NaKO.

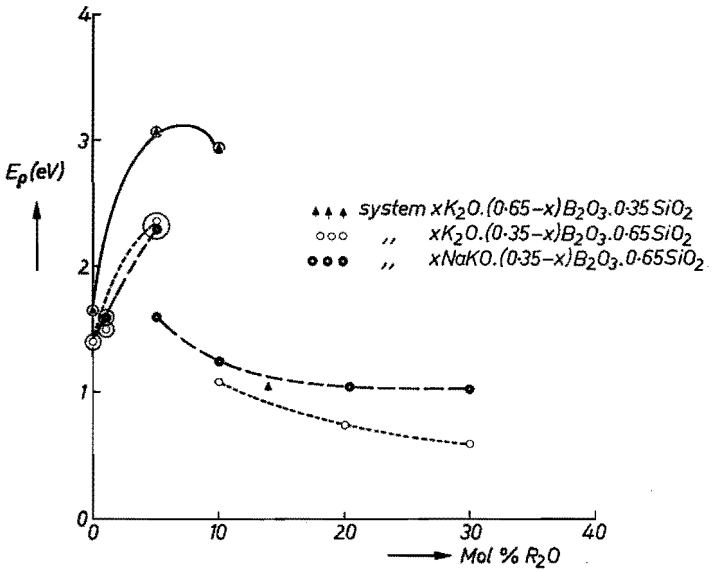

Fig. 6.4. Activation energy of electrical conduction E_e versus mol % K_2O or NaKO.

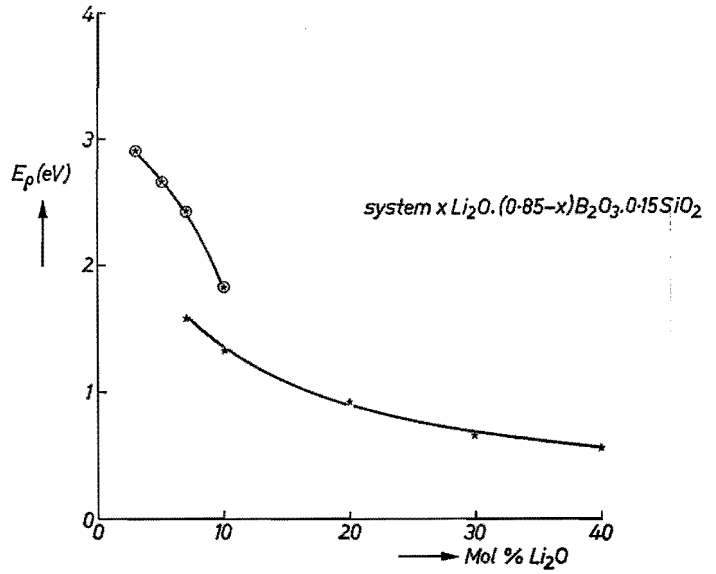

Fig. 6.5. Activation energy of electrical conduction E_e in the system $x\ Li_2O\ .\ (0{\cdot}85 - x)\ B_2O_3 .\ 0{\cdot}15\ SiO_2$.

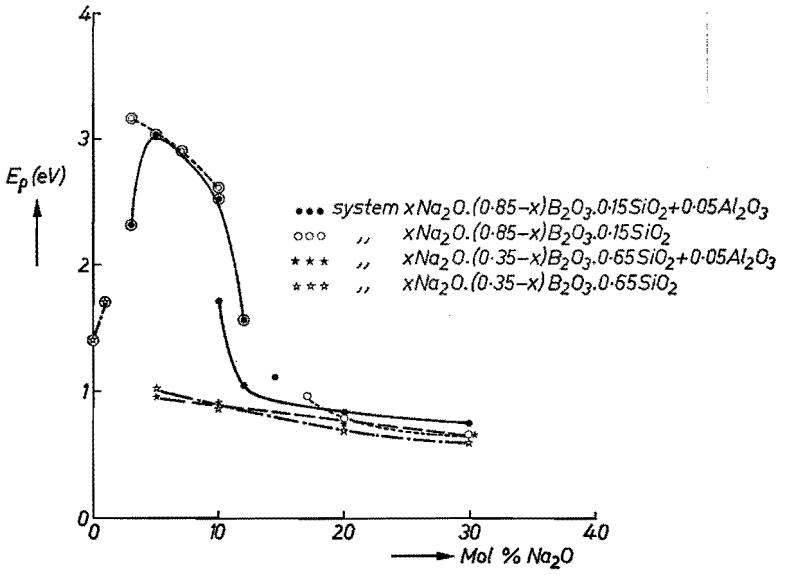

Fig. 6.6. Activation energy of electrical conduction E_e versus mol % Na_2O.

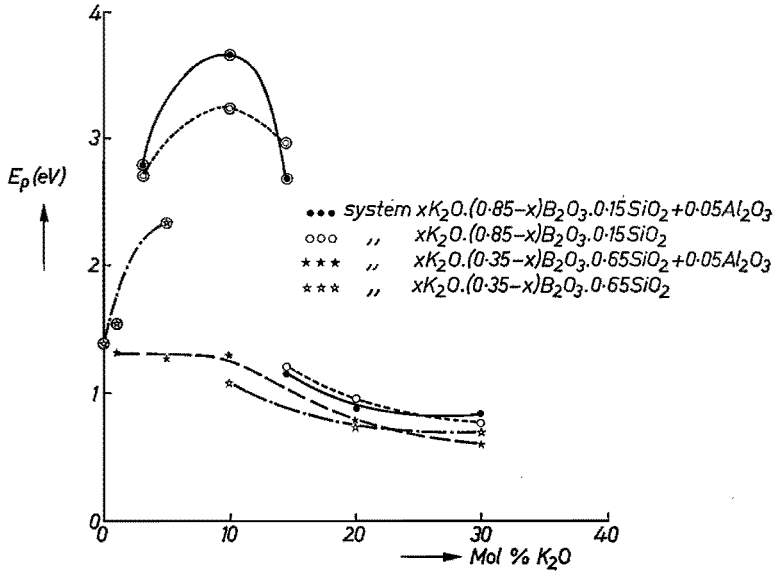

Fig. 6.7. Activation energy of electrical conduction E_ϱ versus mol % K_2O.

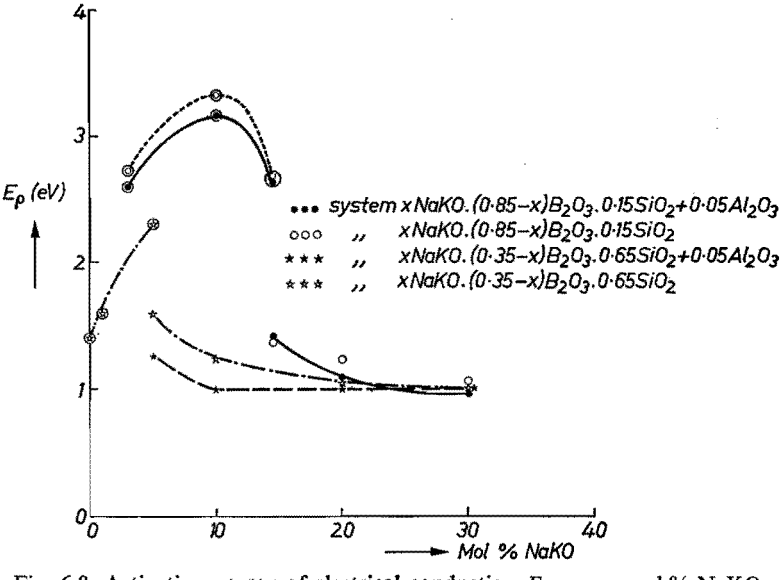

Fig. 6.8. Activation energy of electrical conduction E_ϱ versus mol % NaKO.

of equal alkali-oxide content is observed (range below T_g). At 65 mol % SiO_2 the values of E_ϱ for the potassium-borosilicate glasses are somewhat higher than for the sodium-borosilicate glasses. It can be observed that the values of E_ϱ for mixed Na–K-borosilicate glasses are higher than the corresponding values for the unmixed systems. This is usually observed in mixed alkali glasses (mixed-alkali effect). For an explanation of this see the work of Stevels [6–10].

The influence of Al_2O_3

The influence of the addition of 5 mol % Al_2O_3 on E_ϱ for certain composition series is shown in figs 6.6, 6.7 and 6.8. It may be observed that the added 5 mol % Al_2O_3 exert some slight influences on E_ϱ. Again the slight differences that are observed are too small to be discussed in terms of certain structural units.

The introduction of increasing amounts of Al_2O_3 up to 20 mol % in a glass of composition 0·1 Na_2O . 0·1 K_2O . 0·65 B_2O_3 . 0·15 SiO_2 gradually lowers the activation energy somewhat (cf. table 6-I); this is difficult to explain in terms of structural units. It does however not contradict the observation made by Raman spectroscopy which suggests that alkali-borate groups are gradually replaced by AlO_4 tetrahedra and boroxol groups.

For glass of compositition 0·1 Na_2O . 0·1 K_2O . 0·15 B_2O_3 . 0·65 SiO_2 increasing amounts of Al_2O_3 lead to a decrease in the activation energy (cf. table 6-I). This is also observed in silicate glasses. The aluminum-oxygen tetrahedron has a larger effective anionic radius than the silicon-oxygen tetrahedron since the negative charge is effectively spread over the aluminum-oxygen tetrahedron. Thus the alkali ions are bonded less tightly to this aluminum-oxygen tetrahedron and the activation energy for electrical conduction is lowered.

This explanation suggests too that in the base glass (without Al_2O_3) the small number of alkali ions in the continuous silicate phase primarily takes part in the conduction process.

Discussion on T ($\log \varrho = 7$)

From figs 6.9 to 6.16 it may be observed that in general the T ($\log \varrho = 7$) decreases on increase of the alkali-oxide content in certain series with a constant mole fraction of SiO_2. The values obtained above T_g are encircled in the figures. The values are again susceptible to hydroxyl ions in the glass, the resistance being lowered in general on increase of the hydroxyl content.

The observed lowering of the resistance on increase of the alkali-oxide content is consistent with the theory that alkali ions are the most mobile charge-conduction species. The resistance of the potassium-borosilicate glasses below T_g is generally somewhat higher than that of the sodium-borosilicate glasses which may be explained by the difference in the radii of these ions, although other factors may also be involved. The mixed Na–K-borosilicate glasses in general

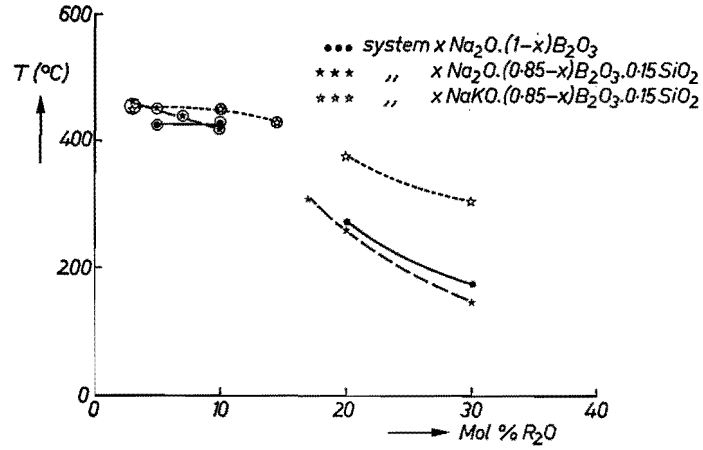

Fig. 6.9. Temperature T at which $\log_{10} \varrho = 7$ versus mol % Na_2O or NaKO.

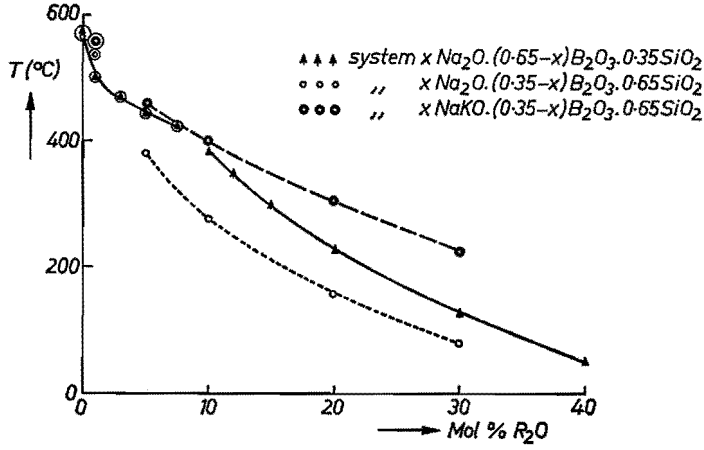

Fig. 6.10. Temperature T at which $\log_{10} \varrho = 7$ versus mol % Na_2O or NaKO.

show a higher resistance than the unmixed systems at equal alkali-oxide content (mixed-alkali effect).

Introduction of 5 mol % Al_2O_3 in borosilicate glasses of certain composition series does not alter the resistance significantly at compositions with a relatively high alkali-oxide content. For the compositions with 65 mol % SiO_2 it may be observed that at lower alkali-oxide content the resistivity is decreased somewhat. This is consistent with the Raman data which show a decrease of alkali-borate groups on the introduction of Al_2O_3 and a possibly more uniform distribution of the alkali ions over the complete glass network.

The influence of higher amounts of Al_2O_3 on the resistivity of glass of composition 0·1 Na_2O . 0·1 K_2O . 0·65 B_2O_3 . 0·15 SiO_2 is negligible (cf. table 6-I).

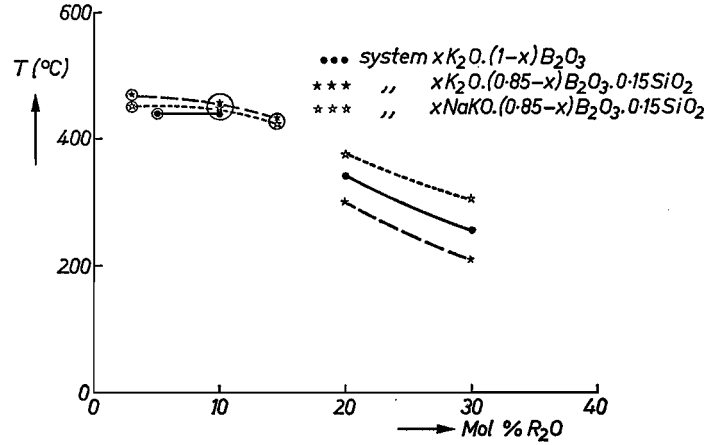

Fig. 6.11. Temperature T at which $\log_{10} \varrho = 7$ versus mol % K_2O or NaKO.

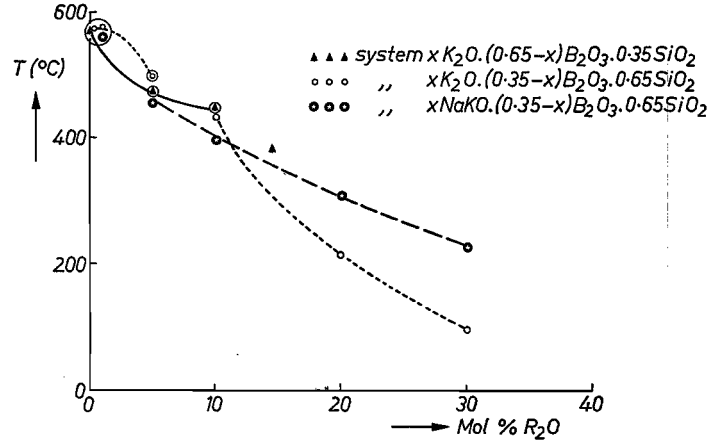

Fig. 6.12. Temperature T at which $\log_{10} \varrho = 7$ versus mol % K_2O or NaKO.

This is consistent with the results of the Raman spectra of these glasses, which suggest that SiO_2 is dispersed in an alkali-borate network and that the introduction of Al_2O_3 does not alter the distribution of the alkali ions in the borate network to such an extent that significant differences in the resistivity may be expected. So the AlO_4 groups seem to be distributed over the boroxol network and not agglomerated in small islands thus giving rise to a low-conducting, continuous boroxol network.

For the composition 0·1 Na_2O . 0·1 K_2O . 0·15 B_2O_3 . 0·65 SiO_2 a significant decrease in resistivity may be observed on increase of the Al_2O_3 content. This is consistent with the results of the Raman spectra of these glasses and suggests that on the introduction of Al_2O_3 in this glass the alkali ions are taken away

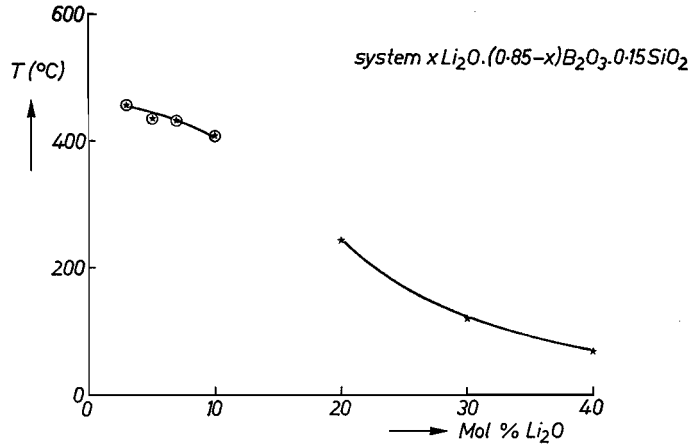

Fig. 6.13. Temperature T at which $\log_{10} \varrho = 7$ in the system $x\,Li_2O\,.\,(0{\cdot}85 - x)\,B_2O_3\,.\,0{\cdot}15\,SiO_2$.

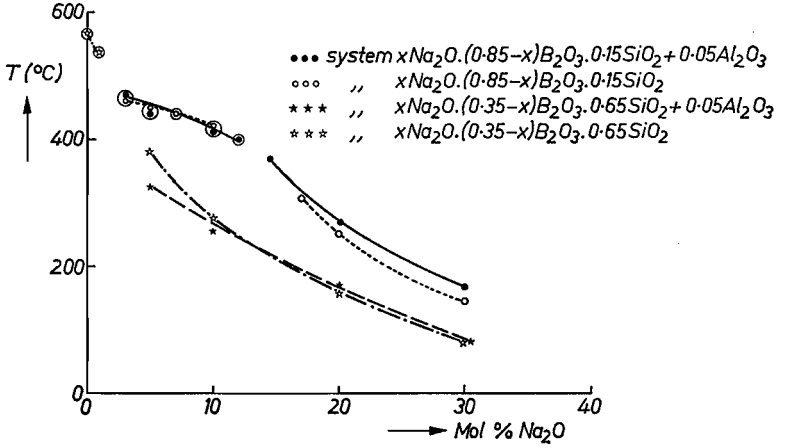

Fig. 6.14. Temperature T at which $\log_{10} \varrho = 7$ versus mol % Na_2O.

from the metaborate groups, most probably grouped together in small agglomerates to form a more uniform distribution over the aluminum-silicate network, thus increasing the number of charge carriers in the continuous phase.

6.4. Conclusions

The electrical-conduction behaviour of borosilicate glasses confirms the generally accepted view that alkali ions are the primary charge carriers below T_g. Above T_g it cannot be excluded that small numbers of hydroxyl ions and/or protons take part in the conduction process, so that an interpretation in terms of structural units is impossible.

There is a negligible influence on the electrical resistivity of annealing and thus induced visible phase separation in the samples. Thus, the annealing proc-

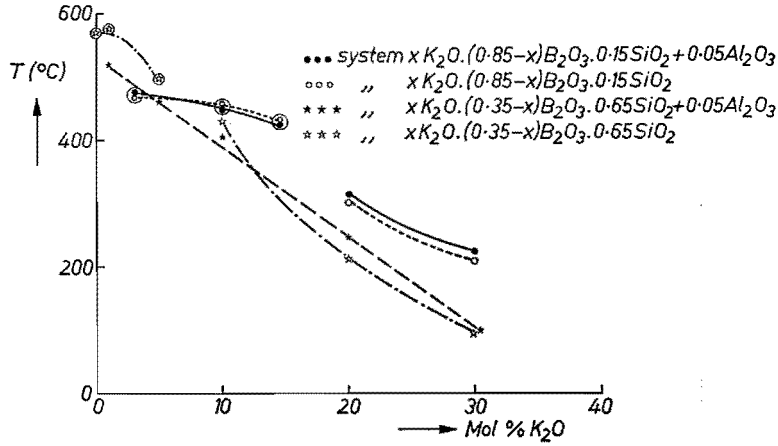

Fig. 6.15. Temperature T at which $\log_{10} \varrho = 7$ versus mol % K_2O.

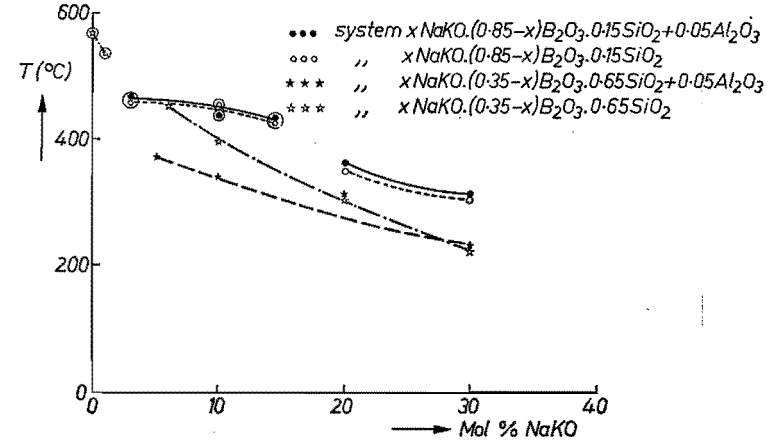

Fig. 6.16. Temperature T at which $\log_{10} \varrho = 7$ versus mol % NaKO.

ess does not significantly influence the mobility of the alkali ions in the conducting continuous phase. This is consistent with the results of the Raman spectra which showed that even in the unannealed samples an invisible phase separation is present.

Interpretation of the results in terms of structural units in borosilicate glasses is very difficult. The introduction of increasing amounts of Al_2O_3 in two borosilicate glasses influences the E_ϱ and T ($\log \varrho = 7$) in a way that is consistent with the results of the Raman spectra. At low SiO_2 concentration the AlO_4 tetrahedra seem to be distributed uniformly over the boroxol network and not agglomerated into islands of enriched aluminum content. At relatively high SiO_2 concentration the AlO_4 tetrahedra seem to be distributed uniformly over the silicate network.

REFERENCES

6–1) E. Rasch and F. W. Hinrichsen, Z. Electrochem. **14**, 41, 1908.
6–2) L. L. Hench and H. F. Schaake, Electrical properties of glass, in L. D. Pye, H. J. Stevens and W. C. LaCourse (eds), Introduction to glass science, Plenum Press, 1972.
6–3) P. Beekenkamp, Phys. Chem. Glasses **9**, 14, 1968.
6–4) R. J. Charles, J. Am. ceram. Soc. **48**, 432, 1963.
6–5) W. E. Martinsen and T. D. McGee, J. Am. ceram. Soc. **54**, 175, 1971.
6–6) H. Scholze and H. O. Mulfinger, Glastechn. Ber. **32**, 381, 1959.
6–7) K. P. Müller, Glastechn. Ber. **42**, 1, 1969.
6–8) K. P. Müller, Glastechn. Ber. **42**, 44, 1969.
6–9) K. Otto, Phys. Chem. Glasses **7**, 29, 1966.
6–10) J. M. Stevels, The electrical properties of glass, in S. Flügge (ed.), Handbuch der Physik, Band XX, Springer-Verlag, 1957.

7. LINEAR THERMAL EXPANSION OF BOROSILICATE GLASSES

7.1. Introduction

The purpose of the measurement of the linear-thermal- expansion coefficient of borosilicate glasses is to obtain some more qualitative information on their structure. The coefficient of linear thermal expansion generally depends on the temperature, composition and thermal history of the glass. The composition of a glass influences its structure, hence by comparison of the expansion coefficient of glasses of different composition, information can be obtained on the differences of their structure. In general the presence of more-asymmetrical units in the glass will lead to an increase in the thermal-expansion coefficient because the thermal expansion is caused by anharmonic vibrations, on the other hand a more coherent network will lead to a decrease in the expansion coefficient.

The influence of the thermal history is diminished extensively by using wet-chemical preparation methods as explained elsewhere (Konijnendijk, Van Duuren and Groenendijk [7-1]).

7.2. Experimental results

The linear thermal expansion (deg^{-1}) was measured from 30 °C to 300 °C for a large number of compositions. All measurements were done on two samples both during a heating-up period and during a cooling-down period immediately afterwards. The error in the measurement of the expansion coefficients is below 2%. The expansion coefficients at 200, 250 and 300 °C are given in the tables in the appendix.

For selected composition series the results are shown graphically in figs 7.1 to 7.5. These figures show the change in the expansion coefficient at constant SiO_2 content and increasing alkali-oxide content. In these figures only the expansion coefficients at 200 °C during the cooling period are presented. Together with these, figures of a normalized expansion coefficient are also shown. By this is meant the ratio

$$\alpha([R_2O] = x)/\alpha([R_2O] = 0).$$

These values are plotted versus mol % alkali oxide in figs 7.9 and 7.10. This is done to get a better insight in the influence of SiO_2 on the expansion behaviour.

The influence of an addition of 5 mol % Al_2O_3 to the glass on the expansion coefficient is shown in figs 7.6, 7.7 and 7.8. The influence of the addition of more Al_2O_3 is shown in table 7-I for two glasses. In all these figures the points represent the average of two experimental values.

For some compositions the influence of phase separation on the thermal-expansion coefficient was measured. The results are shown in table 7-II. The

TABLE 7-I

Influence of increasing amounts of Al_2O_3 on the expansion coefficient at 200 °C of two borosilicate glasses

glass composition		$\alpha \cdot 10^7$	
0·10 Na_2O . 0·10 K_2O . 0·65 B_2O_3 . 0·15 SiO_2		105	101
„	+0·05 Al_2O_3	106	105
„	+0·10 Al_2O_3	108	108
„	+0·15 Al_2O_3	108	107
„	+0·20 Al_2O_3	107	105
0·10 Na_2O . 0·10 K_2O . 0·15 B_2O_3 . 0·65 SiO_2		105	104
„	+0·05 Al_2O_3	96·9	96·7
„	+0·10 Al_2O_3	94·6	93·1
„	+0·15 Al_2O_3	95·0	94·9
„	+0·20 Al_2O_3	99·6	99·5

TABLE 7-II

Influence of annealing at 600 °C for 4 hours on the expansion coefficient of some borosilicate glasses apt to phase separation (in all specimens a clearly visible phase separation had developed except in the specimen with 0·20 Na_2O)

glass composition	$\alpha \cdot 10^7$ not annealed		$\alpha \cdot 10^7$ annealed	
0·075 Na_2O . 0·575 B_2O_3 . 0·35 SiO_2	76·7	75·3	71·5	70·2
0·115 Na_2O . 0·535 B_2O_3 . 0·35 SiO_2	78·7	77·6	73·2	71·9
0·14 Na_2O . 0·51 B_2O_3 . 0·35 SiO_2	83·3	79·5	78·8	72·8
0·20 Na_2O . 0·45 B_2O_3 . 0·35 SiO_2	99·3	98·6	91·5	90·6

glasses were annealed at 600 °C for 4 hours, giving rise in most cases to a visible phase separation.

Borosilicate glasses with alkaline-earth ions generally show small glass-forming areas, so it is impossible to measure the expansion coefficient of alkaline-earth-borosilicate glasses in the same composition series as the alkali-oxide-containing glasses. The results of some measurements of, in most cases mixed alkaline-earth- and alkali-borosilicate glasses, are shown in table 7-III.

TABLE 7-III

Expansion coefficient of alkaline-earth-oxide-containing borosilicate glasses. For comparison some values of mixed sodium- and-potassium-borosilicate glasses are shown

composition	$\alpha \cdot 10^7$		$\alpha \cdot 10^7$ of NaKO glasses	
0·015 K_2O . 0·015 CaO . 0·82 B_2O_3 . 0·15 SiO_2	90·4	88·0	103	103
0·05 K_2O . 0·05 CaO . 0·75 B_2O_3 . 0·15 SiO_2	80·8	80·6	94·0	93·6
0·10 K_2O . 0·10 CaO . 0·65 B_2O_3 . 0·15 SiO_2	80·5	80·1	105	101
0·15 K_2O . 0·15 CaO . 0·55 B_2O_3 . 0·15 SiO_2	92·4	91·2	121	118
0·10 K_2O . 0·10 CaO . 0·15 B_2O_3 . 0·65 SiO_2	75·4	75·3	105	104
0·15 K_2O . 0·15 CaO . 0·05 B_2O_3 . 0·65 SiO_2	97·3	93·9	157	156
0·10 K_2O . 0·10 BaO . 0·65 B_2O_3 . 0·15 SiO_2	81·2	79·8	105	101
0·10 K_2O . 0·10 BaO . 0·15 B_2O_3 . 0·65 SiO_2	76·3	75·4	105	104
0·20 BaO . 0·65 B_2O_3 . 0·15 SiO_2	67·3	67·2		
0·30 BaO . 0·55 B_2O_3 . 0·15 SiO_2	80·6			
0·20 BaO . 0·65 B_2O_3 . 0·15 SiO_2 + 0·05 Al_2O_3	68·1			
0·40 BaO . 0·45 B_2O_3 . 0·15 SiO_2 + 0·05 Al_2O_3	93·2			

Varying numbers of hydroxyl ions, at the level discussed in sec. 2.1 on the preparation of the samples, did not show a significant influence on the expansion coefficient. The wet-chemical preparation method of borosilicate glasses generally results in reproducible results, as has been discussed elsewhere (Konijnendijk, Van Duuren and Groenendijk [7–1]). Literature data on the expansion coefficient of alkali-borate glasses were published by many authors, most recently by Uhlmann [7–2]. Literature data on borosilicate glasses were published by Abe [7–3]. Some data on volume relations in Na_2O–B_2O_3 and Na_2O–B_2O_3–SiO_2 melts at 1300 °C were published by Riebling [7–4].

7.3. Discussion of results

Figures 7.1 to 7.5 show a minimum in the linear-expansion coefficient of borate and borosilicate glasses as a function of alkali-oxide content. This minimum becomes less pronounced if more SiO_2 is incorporated in the glass. This means that adding alkali oxide to vitreous B_2O_3 or B_2O_3–SiO_2 systems at first leads to a more coherent network, this effect becoming less pronounced the higher the SiO_2 content of the glass. After a certain maximum in the coherency of the network has been reached, this coherency decreases when more alkali oxide is added to the glass.

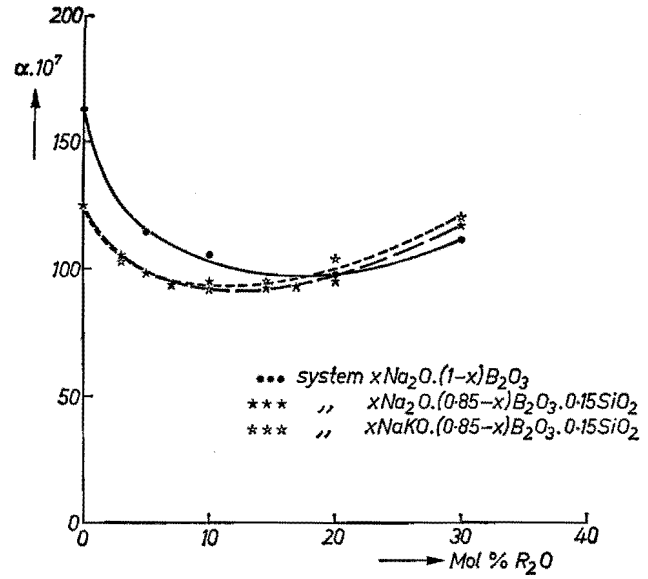

Fig. 7.1. Linear-thermal-expansion coefficient $\alpha \cdot 10^7$ at 200 °C versus mol % Na_2O or NaKO.

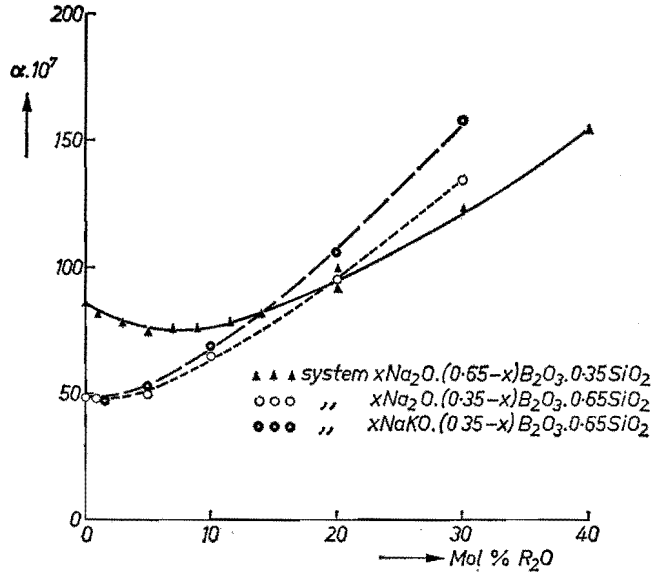

Fig. 7.2. Linear-thermal-expansion coefficient $\alpha \cdot 10^7$ at 200 °C versus mol % Na_2O or NaKO.

The increase in coherency can be explained by the mechanism of conversion of triangularly coordinated boron ions to tetrahedrally coordinated ions. Beyond a certain alkali-oxide content enough non-bridging oxygen ions are

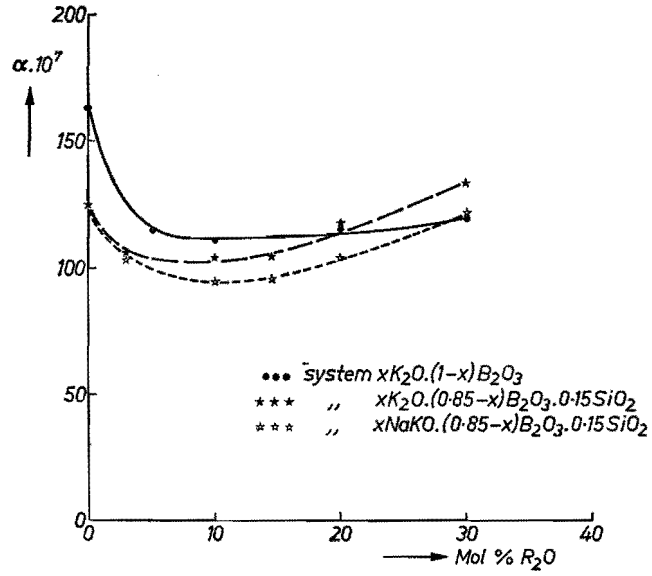

Fig. 7.3. Linear-thermal-expansion coefficient $\alpha \cdot 10^7$ at 200 °C versus mol % K_2O or NaKO.

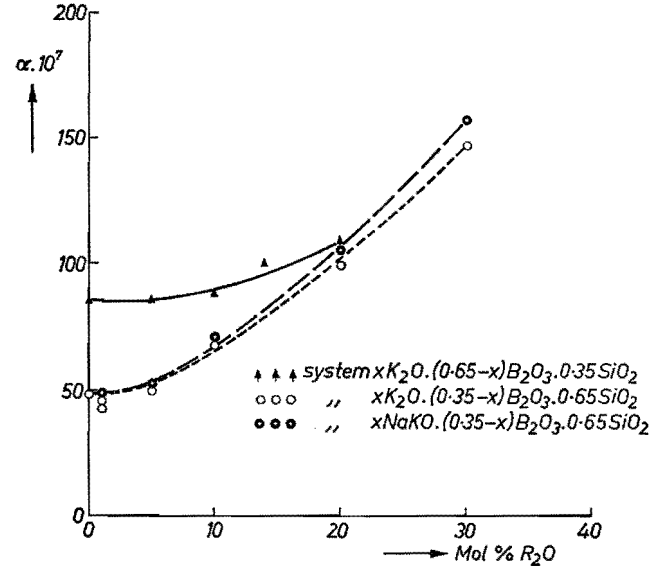

Fig. 7.4. Linear-thermal-expansion coefficient $\alpha \cdot 10^7$ at 200 °C versus mol % K_2O or NaKO.

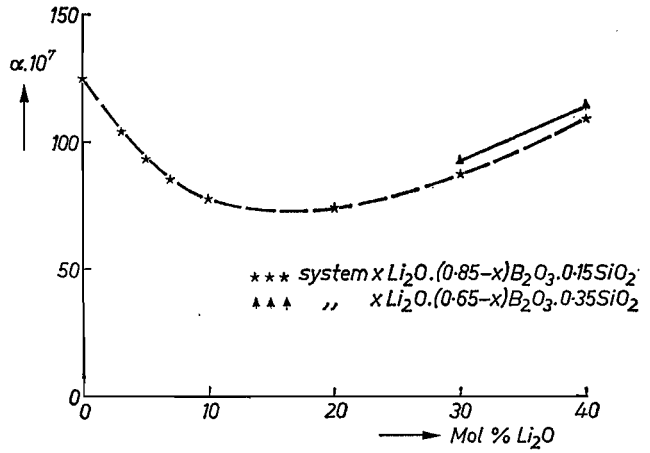

Fig. 7.5. Linear-thermal-expansion coefficient $\alpha \cdot 10^7$ at 200 °C versus mol % Li_2O.

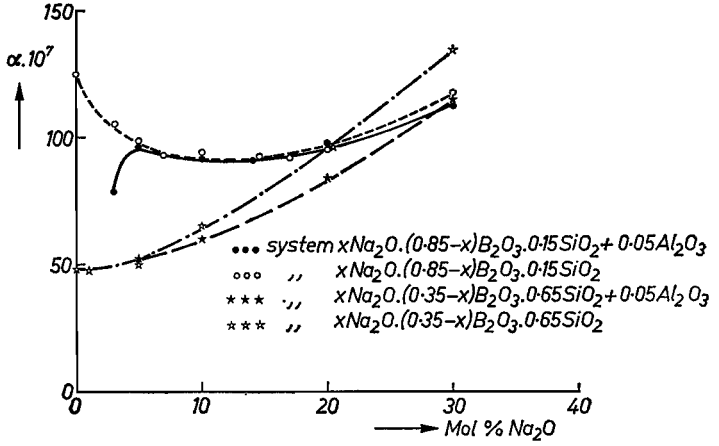

Fig. 7.6. Linear-thermal-expansion coefficient $\alpha \cdot 10^7$ at 200 °C versus mol % Na_2O.

formed, giving rise to a less coherent network and subsequently a higher expansion coefficient. In this way one can qualitatively explain the existence of the minima. The fact that these minima are less pronounced when the SiO_2 content is increased, can be explained by taking into account that the relative increase in the coherency due to the formation of BO_4 tetrahedra will be less as relatively more SiO_4 tetrahedra with bridging oxygen ions are present.

The place of the minimum shifts to lower alkali-oxide concentrations with increasing SiO_2 content. It is observed every time at roughly the same alkali-to-boron ratio of 1/7 to 1/8, suggesting that this ratio is an important determining factor for the presence of certain structural units in borosilicate glasses. This picture could also be developed from the Raman, infrared and viscosity data-

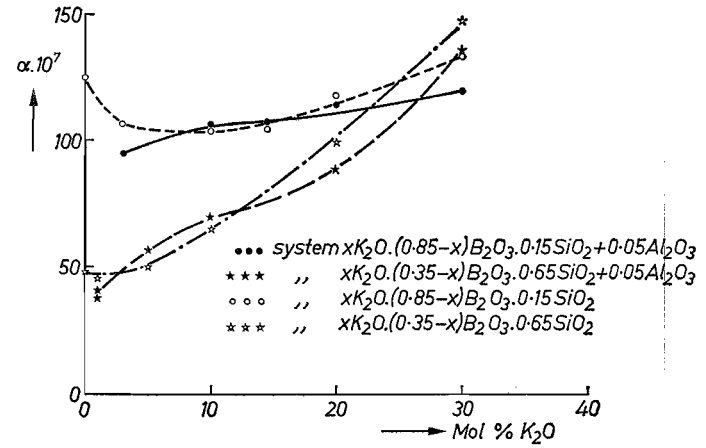

Fig. 7.7. Linear-thermal-expansion coefficient $\alpha \cdot 10^7$ at 200 °C versus mol % K_2O.

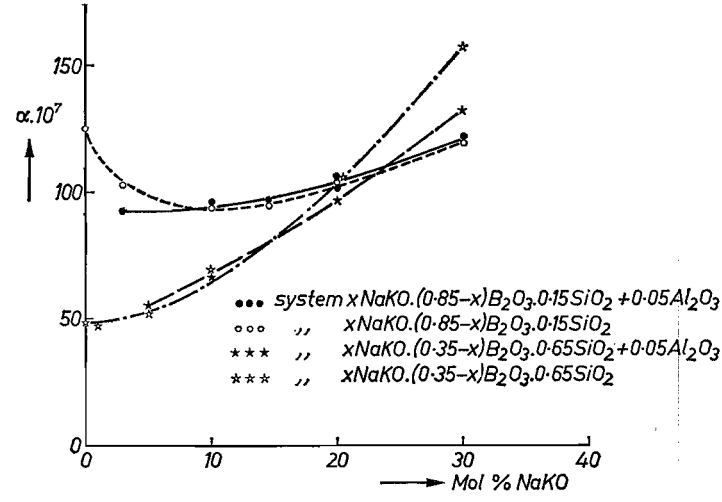

Fig. 7.8. Linear-thermal-expansion coefficient $\alpha \cdot 10^7$ at 200 °C versus mol % NaKO.

The effect of the shift of the minimum to lower alkali-oxide concentration at higher SiO_2 content and the effect that the minima become less pronounced at higher SiO_2 content are more clearly shown in figs 7.9 and 7.10. In these figures the relative thermal expansion coefficient

$$\alpha_{rel} = \alpha([R_2O] = x)/\alpha([R_2O] = 0)$$

at constant SiO_2 content is shown as a function of alkali-oxide content.

More quantitative information on the presence of certain structural units cannot be obtained from these expansion data. It cannot be decided which type of borate group with a BO_4 tetrahedron is formed nor whether the non-bridging

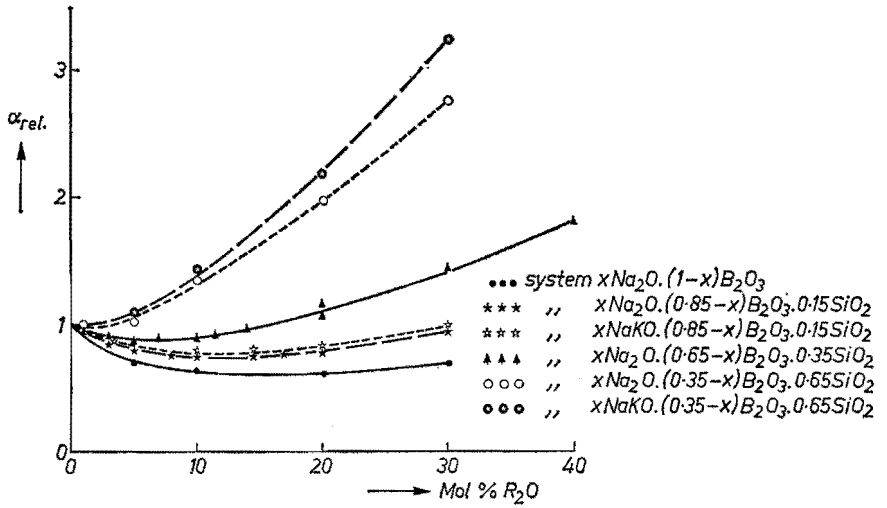

Fig. 7.9. Relative linear-thermal-expansion coefficient $\alpha_{x=x}/\alpha_{x=0}$ versus mol % Na_2O or NaKO.

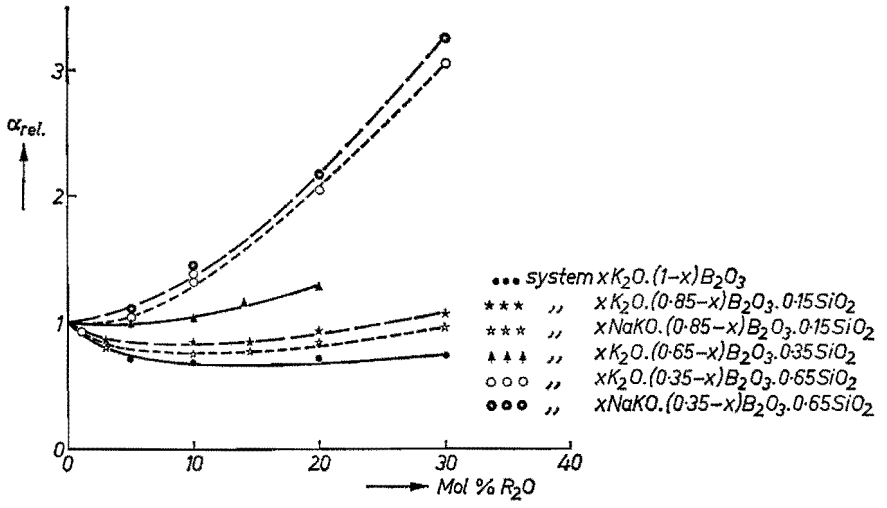

Fig. 7.10. Relative linear-thermal-expansion coefficient $\alpha_{x=x}/\alpha_{x=0}$ versus mol % K_2O or NaKO.

oxygen ions are primarily connected to B or Si. Nor is it possible to conclude from these data at what concentration of alkali oxide the formation of non-bridging oxygen ions becomes significant, since the tendency to increase the expansion coefficient is also caused by the formation of less-symmetrical units, actually taking place on the formation of pentaborate, triborate groups, etc., as becomes clear from Raman and infrared data.

Up to now exact knowledge about the location and environments of alkali ions in glass is lacking. This makes it difficult to explain the differences in properties between the glasses with different types of alkali ions. For properties that greatly depend on the coherency of the network such as the thermal expansion the alkali ion with the highest ionic radius seems to produce the least coherent structures. This is generally explained as follows. If a cation is relatively large, its bonding to the network will be relatively small, leading to vibrations with larger amplitudes, therefore, these vibrations have less resemblance with harmonic oscillators. The increased anharmonicity of the vibrations leads to higher expansion coefficients. In this way it can be explained that the Li_2O-containing borosilicate glasses show a lower expansion coefficient than the corresponding sodium-borosilicate glasses and these latter a smaller expansion coefficient than the corresponding potassium-borosilicate systems.

It has been stated by Isard [7–5]), in a review article, that most workers found that the expansion coefficient in mixed alkali-silicate glasses shows a small positive departure from linearity which may give rise to a maximum. For the systems $x\ Na_2O\ .\ (0{\cdot}85 - x)\ B_2O_3\ .\ 0{\cdot}15\ SiO_2$ and $x\ K_2O\ .\ (0{\cdot}85 - x)\ B_2O_3\ .\ 0{\cdot}15\ SiO_2$ compared to x NaKO . $(0{\cdot}85 - x)\ B_2O_3\ .\ 0{\cdot}15\ SiO_2$ a negative departure from linearity can be observed. The mixed Na–K systems show an expansion coefficient slightly larger than the unmixed Na systems but a clearly smaller expansion coefficient than the unmixed K systems, so the departure from linearity is negative (cf. figs 7.1 and 7.3).

In the borosilicate glasses with 65 mol % SiO_2 a clear positive departure is observed and the presence of a maximum is indicated for the mixed Na–K systems (cf. figs 7.2 and 7.4). The presence of a maximum is indicated because the expansion coefficient of the mixed Na–K systems is higher than those of the unmixed Na and K systems.

Both effects are hard to explain due to the generally poor understanding of the mixed-alkali effect in glass. It should be remarked that the measurement of the expansion coefficient took place at 200 °C which is closer to T_g for the glasses with 15 mol % SiO_2 than with 65 mol % SiO_2. This may interfere with the rule of the positive departure from linearity, observed for silicate glasses.

Influence of Al_2O_3

The influence of the addition of 5 mol % Al_2O_3 on the expansion coefficient of the sodium-borosilicate glasses seems to be in accordance with other experimental data (cf. fig. 7.6). It can be observed that the addition of 5 mol % Al_2O_3 to the glasses in the series $x\ Na_2O\ .\ (0{\cdot}85 - x)\ B_2O_3\ .\ 0{\cdot}15\ SiO_2$ has a negligible influence on the expansion coefficient. This suggests that the coherency is not changed very much by the addition of 5 mol % Al_2O_3, so in the glasses of the series $x\ Na_2O\ .\ (0{\cdot}85 - x)\ B_2O_3\ .\ 0{\cdot}15\ SiO_2$ up to $x = 0{\cdot}30$ probably only a small amount of non-bridging oxygen ions is present.

The influence of the addition of 5 mol % Al_2O_3 to the glasses in the series $x\ Na_2O\ .\ (0{\cdot}35 - x)\ B_2O_3\ .\ \underline{0{\cdot}65\ SiO_2}$ is that the expansion coefficient is significantly lowered the more Na_2O is present in the glass. This suggests that from $x = 0{\cdot}10$ on in this composition series non-bridging oxygen ions are converted into bridging ones by the addition of Al_2O_3, giving rise to a lowering of the linear expansion. This picture of the influence of the addition of Al_2O_3 to these sodium-borosilicate glasses is completely confirmed by the Raman, infrared and viscosity data.

The similar potassium-borosilicate glasses behave somewhat irregularly compared to the sodium-containing glasses (cf. fig. 7.7). For the composition serie $x\ K_2O\ .\ (0{\cdot}85 - x)\ B_2O_3\ .\ \underline{0{\cdot}15\ SiO_2}$ one may observe that the influence of the addition of Al_2O_3 to the glasses at $x = 0{\cdot}10$, $x = 0{\cdot}145$ and $x = 0{\cdot}20$ is small but is significant at $x = 0{\cdot}30$. Probably the potassium-containing glass at $x = 0{\cdot}30$ has more non-bridging oxygen ions than the corresponding sodium-containing glass.

In the potassium-borosilicate glasses with $\underline{65\ \text{mol}\%\ SiO_2}$ one may observe that the addition of 5 mol % Al_2O_3 to the glasses at $x = 0{\cdot}05$ and $x = 0{\cdot}10$ gives rise to an increase in the expansion coefficient and at $x = 0{\cdot}20$ and $x = 0{\cdot}30$ to a decrease. The decrease can be explained by the transformation of non-bridging oxygen ions into bridging ones, which is confirmed by other data. However, the increase in the expansion coefficient at $x = 0{\cdot}05$ and $0{\cdot}10$ is difficult to explain in terms of a change of the structural groups present. It may be that in the sodium- and potassium-borosilicate glasses the Al ions are distributed differently, for instance that the AlO_4 tetrahedra show a tendency to form part of the silicate network in the case of the glasses with potassium, a tendency that might be less in the glasses with sodium. By introducing Al in the silica network the asymmetry is increased and consequently the expansion coefficient increased, but this is only a tentative explanation.

The influence of the addition of 5 mol % Al_2O_3 to the mixed Na–K-borosilicate glasses is more or less in between the two unmixed systems. Again it may be observed that addition of Al_2O_3 to the glasses in the composition series $x\ NaKO\ .\ (0{\cdot}85 - x)\ B_2O_3\ .\ \underline{0{\cdot}15\ SiO_2}$ has a negligible influence on the expansion coefficient for values of x higher than about 0·05. This probably means that no significant amount of non-bridging oxygen ions is present in the glasses of this series.

For the glasses with $\underline{65\ \text{mol}\%\ SiO_2}$ one may observe that the addition of Al_2O_3 leads to a decrease of the expansion coefficient at $x = 0{\cdot}20$ and $x = 0{\cdot}30$, probably caused by the disappearance of non-bridging oxygen ions. At $x = 0{\cdot}10$ certainly non-bridging oxygen ions are present connected with ring-type metaborate groups as was revealed by the Raman spectra. However, the addition of Al_2O_3 does not reveal this in the expansion behaviour. Again, as in the unmixed potassium system, a counteracting mechanism may be responsible for the

absence of the decrease in the expansion coefficient with this composition.

The influence on the expansion coefficient of the addition of up to 20 mol % Al_2O_3 to a glass of composition 0·10 Na_2O . 0·10 K_2O . 0·65 B_2O_3 . 0·15 SiO_2 is negligible (cf. table 7-I). From Raman spectra it became clear that this glass has almost no non-bridging oxygen ions, so that a spectacular decrease in the expansion coefficient is not very likely to occur, as evidenced by the experimental data. On the glass of composition 0·10 Na_2O . 0·10 K_2O . 0·15 B_2O_3 . 0·65 SiO_2 the influence of the addition of up to 20 mol % Al_2O_3 is different (cf. table 7-I). One observes a decrease in the expansion coefficient up to 10 to 15 mol % Al_2O_3 and thereafter an increase. Raman data suggest that in the glass without Al_2O_3 10 to 15 mol % of the alkali oxide is bonded to non-bridging oxygen ions of the ring-type metaborate group. This explains the decrease in the expansion coefficient up to 10 to 15 mol % Al_2O_3. The increase of the expansion coefficient may be caused by the incorporation of AlO_4 tetrahedra in the silicate structure giving rise to more asymmetry and consequently a higher expansion coefficient as suggested earlier.

The influence of alkaline-earth oxides on the expansion coefficient of some borosilicate glasses is shown in table 7-III. The expansion coefficient of the mixed K–Ca and K–Ba glasses is definitely lower than those of the mixed Na–K glasses. This suggests that the coherency of the network has increased by the introduction of alkaline-earth ions. This can be explained by taking into account that one alkaline-earth ion compensates the negative charge of two BO_4 tetrahedra or two non-bridging oxygen ions. Thus the coherency of the network is increased. Also, the unmixed barium-borosilicate glasses show an expansion coefficient much below the values of the unmixed sodium- and potassium-borosilicate glasses. The explanation for this is the same as above.

7.4. Conclusions

The results of the linear-thermal-expansion-coefficient measurements are in agreement with other experimental evidence in this work when these results have to be interpreted in terms of structure of the borosilicate glasses.

At low SiO_2 content the alkali ions are primarily bonded to the borate network to form BO_4 tetrahedra. Increase in the alkali-oxide content generally results in a gradual, relative increase of the amount of non-bridging oxygen ions.

The relative amount of non-bridging oxygen ions also increases with increasing SiO_2 content. It cannot be concluded as to whether these non-bridging oxygen ions are bonded to the borate or the silicate network.

Addition of Al_2O_3 leads to a decrease in the expansion coefficients in those composition ranges of the borosilicate system where significant amounts of non-bridging oxygen ions are present.

REFERENCES

[7-1]) W. L. Konijnendijk, M. van Duuren and H. Groenendijk, Verres Réfract. **27**, 11, 1973.
[7-2]) D. R. Uhlmann, J. non-cryst. Solids **1**, 347, 1969.
[7-3]) T. Abe, J. Am. ceram. Soc. **35**, 284, 1952.
[7-4]) E. F. Riebling, J. Am. ceram. Soc. **50**, 46, 1967.
[7-5]) J. O. Isard, J. non-cryst. Solids **1**, 235, 1969.

8. INTERNAL FRICTION OF BOROSILICATES GLASSES

8.1. Introduction

In oxide glasses a variety of mobile ions is present which may exhibit mechanical relaxation phenomena. These ions are able to react to an external alternating mechanical stress with a certain delay. Due to this delayed relaxation, phenomena may be observed which are accompanied by the absorption of energy. In the case of mechanical relaxation, the quantity tan δ is proportional to the energy dissipation. Usually tan δ is given by the factor Q^{-1} which is known as the internal friction.

It is well known that one of the processes that causes the mechanical losses in glasses is related to the relaxation of the alkali ions in the network, which jump from interstice to interstice as a result of the deformation caused by the mechanical forces applied (Stevels [8–1])). For sodium ions the activation energy of this mechanical relaxation process has been found to be of the order of 0·7 eV, a value that is consistent with other experimental data, such as electrical-conduction and diffusion processes.

This mechanical relaxation process may be observed at frequencies from about 1 to 10 Hz around room temperature and shifts to higher temperatures as the frequency is increased. For a more extensive theory of the processes underlying the mechanical relaxation phenomena in glasses, the reader is for instance referred to the work of Stevels [8–1]) or De Waal [8–2]).

As was remarked by Eckstein [8–3]) the existence of internal-friction peaks in glass is not consistent with the structural model of glasses put forward by Zachariasen in his random-network model. In a completely random network all relaxation times must have the same probability and the internal friction may only be observed as a continuous flat spectrum. In view of this it has been suggested that a certain short-range order exists in glass, by which is meant that the environment of the sodium ions cannot all be completely different from another. However, no internal-friction peak can be produced when the sodium ions jump from and to equal sites. That is to say, the sites must be different with respect to the direction of the macroscopic stress.

8.2. Experimental results

All glasses were prepared using the sol–gel technique described in sec. 2.1. After melting, the glasses were remelted under vacuum. From these samples fibres, about 100 mm long and 0·6 mm thick, were drawn. All these fibres were annealed for about half an hour at the temperature at which $\log \eta = 14$ and thereafter cooled to room temperature in the same electric furnace.

The internal-friction measurements were done with a torsion pendulum*),

*) This torsion pendulum is present at the Technological University Eindhoven, The Netherlands.

described by Van Ass and Stevels [8–4]). The measurements were done as a function of the temperature and the composition of the glass at a frequency of about 0·7 Hz and at pressure below 0·05 torr. The temperature range was from —90 °C to 400 °C. The internal friction was calculated from the decay rate of the torsional vibrations.

The torsion pendulum, primarily constructed by De Waal [8–2]) and modified by Van Ass and Stevels [8–4]) is built up as follows. An inertia member is attached to a glass fibre which is positioned inside the controlled zone of an electric furnace. The system is set in torsional vibration by means of a pair of electromagnets located closely to the steel ends of the inertia member. The oscillation of the system is followed by means of an optical electronic detector which essentially determines the angular velocity of the pendulum when it passes through its rest position. The whole system is contained in a vacuum enclosure and is provided with a double-walled glass bell jar as used for liquid-nitrogen cooling.

For selected composition series the results of the tan δ measurements are shown in figs 8.1 to 8.4. The measuring points are deleted from these figures, but these were taken about every 8–10 °C.

8.3. Discussion of results

Figure 8.1 shows that on increase of the Na_2O content in glasses in the series $x\ Na_2O\ .\ (0{\cdot}85 - x)\ B_2O_3\ .\ 0{\cdot}15\ SiO_2$ the maximum of the low-temperature peak shifts to lower temperatures and increases in height. Introduction of 5 mol % Al_2O_3 generally increases the "peak temperature" somewhat and lowers the height.

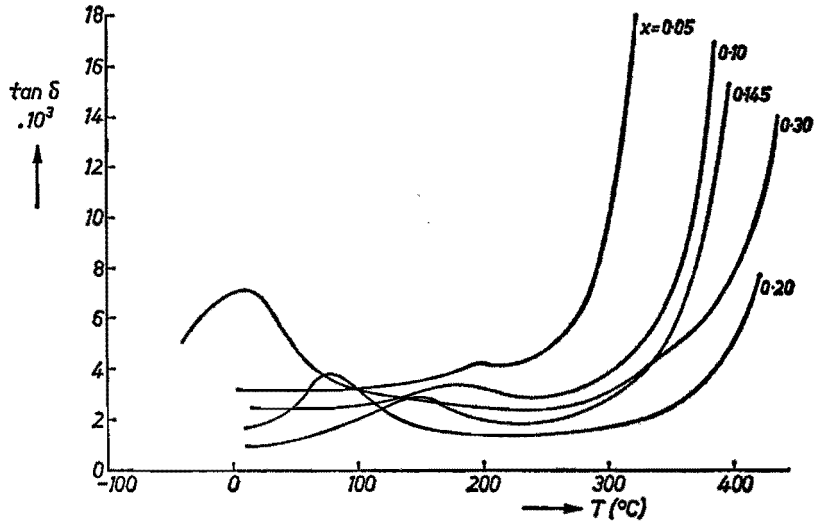

Fig. 8.1. Internal friction of glasses in the system $x\ Na_2O\ .\ (0{\cdot}85 - x)\ B_2O_3\ .\ 0{\cdot}15\ SiO_2$.

Compared to the internal-friction measurements of De Waal [8–2]) in the binary system $x\,Na_2O\,.\,(1-x)\,B_2O_3$, the peak temperature is lowered somewhat by the introduction of 15 mol % SiO_2 at equal x. This alkali relaxation peak is also observed at lower values of x. Introduction of a small amount of Al_2O_3 in the binary system $x\,Na_2O\,.\,(1-x)\,B_2O_3$ has a similar influence, as was shown by De Waal [8–2]).

The increase in height of the sodium relaxation peak on increase of the alkali-oxide content may be caused by the following relevant factors:

— the distribution of the relaxation times changes,

— the number of ions taking part in the relaxation process increases,

— the number and distribution of sites changes.

From fig. 8.1 it becomes clear that there is no drastic change of the half width of the peaks, so it is not suggested that a change in the distribution times is responsible for the rise of the peak. It is suggested that the second and third factors mentioned are primarily responsible for the rise of this peak.

The system $x\,Na_2O\,.\,(1-x)\,B_2O_3$ may be discussed for values $x > 0{\cdot}15$. At lower values of x no alkali relaxation peak was observed by De Waal [8–2]). As was mentioned by De Waal it is absolutely necessary that the sites are unequally modified by a macroscopic stress if an internal-friction peak is to be observed. It is obvious that the presence of non-bridging oxygen ions introduces a great asymmetry in the network. De Waal [8–2]) pointed out that the presence of two types of oxygen ions, viz. the bridging and the non-bridging oxygen ions introduces a certain asymmetry in the distribution of the bonding forces between a sodium ion and its surroundings and this favours the occurrence of an internal-friction peak. This occurrence of an internal-friction peak at 15 mol % Na_2O fits in with other experimental evidence that at about this concentration the first detectable amount of non-bridging oxygen ions is formed (Beekenkamp [8–5])).

Glasses with 15 *mol* % SiO_2

Because the internal-friction peak may already be observed at $x = 0{\cdot}05$ for glasses in the composition series $x\,Na_2O\,.\,(0{\cdot}85-x)\,B_2O_3\,.\,0{\cdot}15\,SiO_2$ the conclusion can be drawn that the introduction of SiO_2 leads to an increase in the formation of non-bridging oxygen ions compared to the binary sodium-borate glasses. This is consistent with other experimental evidence in this thesis.

The decrease of the peak temperature generally suggests that the activation energy is lowered, but in fact this can only be proved by measuring tan δ at another frequency also. However, the lowering of the activation energy is consistent with the decrease in activation energy of electrical conduction in these glasses (cf. chapter 6). The introduction of 5 mol % Al_2O_3 generally lowers the peak height of the losses and increases the peak temperature somewhat. The first effect may be explained by assuming that Al_2O_3 primarily takes away non-

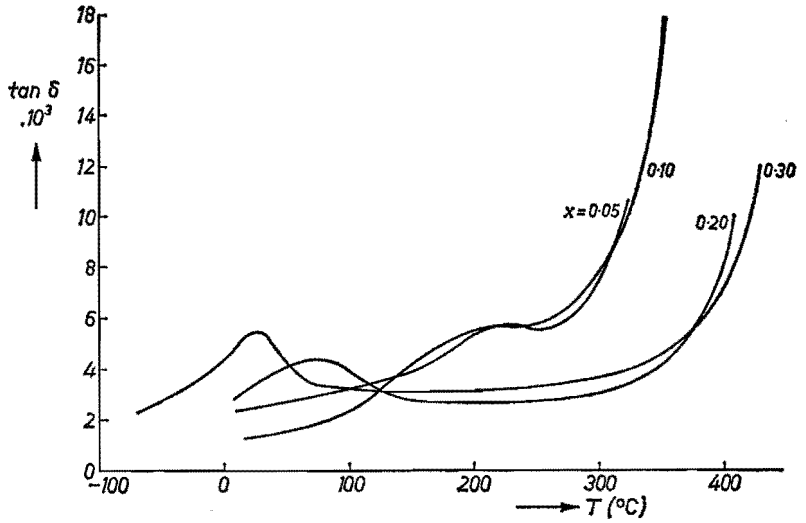

Fig. 8.2. Internal friction of glasses in the system $x\ Na_2O\ .\ (0{\cdot}85 - x)\ B_2O_3\ .\ 0{\cdot}15\ SiO_2 + 0{\cdot}05\ Al_2O_3$.

bridging oxygen ions, thus decreasing the sites that may give rise to an internal-friction peak.

Glasses with 65 *mol* % SiO_2

For glasses with 65 mol % SiO_2 it may be observed in fig. 8.3 that the low-temperature loss peaks due to relaxation of the alkali ions are only somewhat higher or about equal as compared to those of glasses with 15 mol % SiO_2 and equal Na_2O content. From the Raman spectra of the glasses in both composition series it follows that in the glasses with 65 mol % SiO_2 relatively more non-bridging oxygen ions are present. However, the internal-friction peak is not higher. This suggests that in the case of glasses with 65 mol % SiO_2 about the same amount of sodium ions takes part in the relaxation process as in glasses with 15 mol % SiO_2.

A similar effect is observed on addition of Al_2O_3. The influence on the internal-friction peak of the introduction of 5 mol % Al_2O_3 is generally small on glasses with 65 mol % SiO_2 (fig. 8.4). At $x = 0{\cdot}10$ and 0·20 the peak height is about equal, at $x = 0{\cdot}30$ it decreases somewhat. The peak temperature increases somewhat at $x = 0{\cdot}20$ and 0·30 but this is not very significant. From the Raman spectra it is clear that the introduction of Al_2O_3 into the glass at $x = 0{\cdot}20$ primarily leads to a decrease in the amount of ring-type metaborate groups and thus to a decrease of the amount of non-bridging oxygen ions. This decrease of the amount of non-bridging oxygen ions has no significant influence on the peak height of the alkali internal-friction peak.

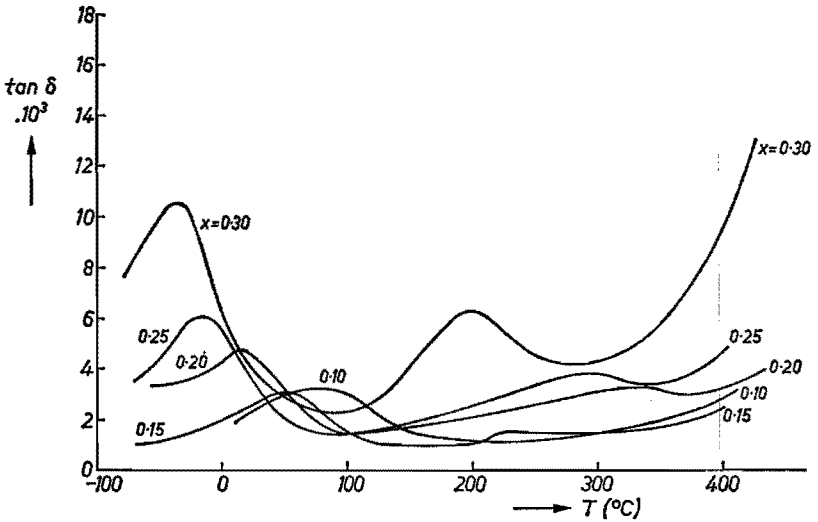

Fig. 8.3. Internal friction of glasses in the system $x\ Na_2O\ .\ (0{\cdot}35 - x)\ B_2O_3\ .\ 0{\cdot}65\ SiO_2$.

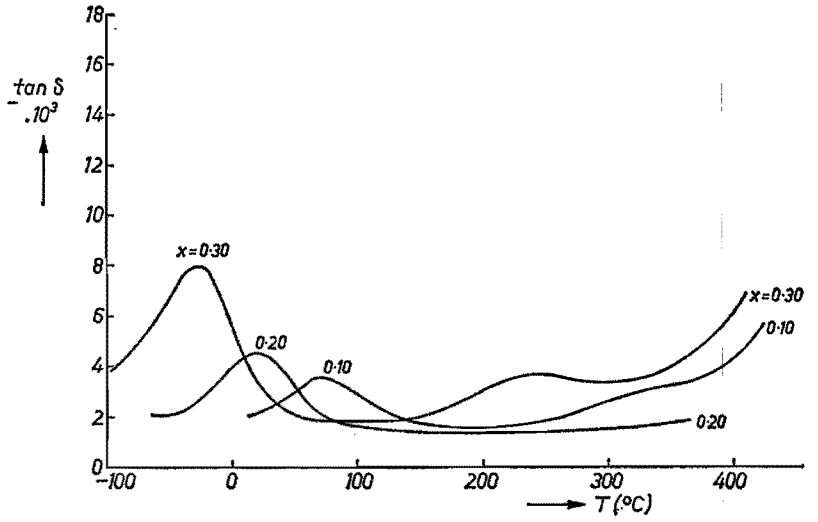

Fig. 8.4. Internal friction of glasses in the system $x\ Na_2O\ .\ (0{\cdot}35 - x)\ B_2O_3\ .\ 0{\cdot}65\ SiO_2 + 0{\cdot}05\ Al_2O_3$.

The high-temperature peak in figs 8.3 and 8.4 will not be discussed in this context since it must be attributed to the cooperative movement of a sodium ion and a neighbouring proton as was proved by Day and Stevels [8–6]).

8.4. Conclusions

The internal-friction measurements suggest that in the borosilicate glasses with 15 mol % SiO_2, more non-bridging oxygen ions are present than in the binary sodium-borate glasses. Increase of the Na_2O content leads to more non-bridging oxygen ions.

For the borosilicate glasses with 65 mol % SiO_2 it may be observed that increase in the alkali-oxide content leads to an increase of the internal-friction-peak height. Although, in this case, more non-bridging oxygen ions are formed than for the glasses with 15 mol % SiO_2 the sodium-loss peaks have nearly the same height when the alkali concentration is equal. This suggests that a certain amount of non-bridging oxygen ions has to be available for an internal-friction peak to be observed but that the height of the peak is primarily determined by the number of sodium ions.

REFERENCES

[8–1]) J. M. Stevels, The structure and physical properties of glass, in S. Flügge (ed.), Handbuch der Physik, Vol. 13, 1957.
[8–2]) H. de Waal, Thesis, Delft University of Technology, Delft, The Netherlands, 1967.
[8–3]) B. Eckstein, Kolloid-Z. **194**, 34, 1963.
[8–4]) H. M. J. M. van Ass and J. M. Stevels, J. non-cryst. Solids **15**, 215, 1974.
[8–5]) P. Beekenkamp, Philips Res. Repts Suppl. 1966, No. 4.
[8–6]) D. E. Day and J. M. Stevels, J. non-cryst. Solids **14**, 165, 1974.

9. DENSITY AND REFRACTIVE INDEX OF BOROSILICATE GLASSES

9.1. Introduction

Measurement of the density of glasses as a function of their composition usually gives little information on the structure of these glasses. Irregularities may sometimes be observed in the density versus composition relation which is used by some authors to explain said irregularities in terms of change of the structure (Coenen [9–1]) and Eversteijn, Stevels and Waterman [9–2]).

Measurements of the refractive index as a function of the composition of glasses can give some qualitative information on the presence of non-bridging oxygen ions, when the density of the glasses is measured at the same time. The non-bridging oxygen ions have a higher polarizability than the bridging ones, which gives rise to an increase in the refractive index of glasses when these non-bridging oxygen ions are formed. However, a rise in the refractive index may also be caused by an increase in the density, hence discussion of measurements of the refractive index may be hampered when these measurements have to be interpreted in terms of structural units.

As all samples had been prepared primarily for other measurements, it was fairly easy to determine the density and refractive index of these samples also.

9.2. Experimental results

All samples were prepared using the sol–gel method described in sec. 2.2. The glasses were melted and remelted in vacuum, the melt being cooled afterwards to room temperature without annealing. Samples were obtained for the measurements by sawing and polishing. The density (g/cm^3) of the glasses was calculated from the difference in weight of the samples in air and water at 24 °C. There are more-accurate methods for measuring the density but the one applied here is sufficiently so to allow use of the results for conclusions as to the structural changes of borosilicate glasses in some composition series.

The measurements of the refractive index were done with an Abbe refractometer.

For some selected composition series the results are shown graphically in figs 9.1 to 9.4. The tables in the appendix show the numerical values of the density and refractive index of these glasses.

9.3. Discussion of results

In fig. 9.1, which shows the density for some sodium- and potassium-borosilicate glasses in the composition series with 15 mol % SiO_2, it may be observed that the sodium- and potassium-borosilicate glasses have practically the same density up to 30 mol % alkali oxide. The binary sodium- and potassium-borate

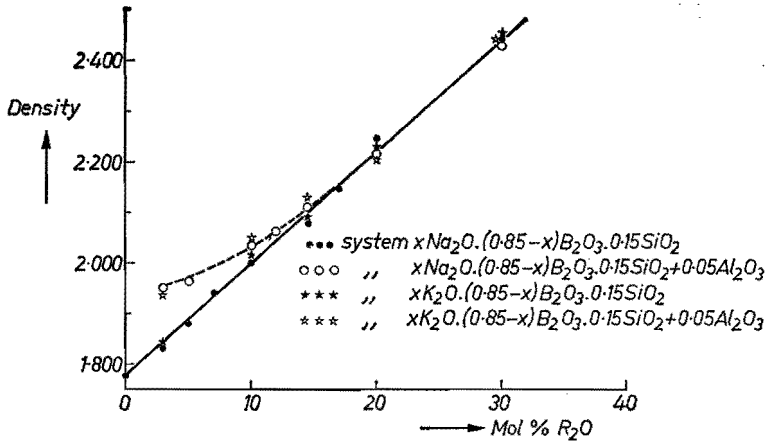

Fig. 9.1. Density of borosilicate glasses.

glasses also show a practically identical density at equal alkali-oxide content (Coenen [9-1]). The glasses in the composition series with 15 mol % Sio_2 have a somewhat lower density than the binary borate glasses. No breaks can be observed in the density versus composition behaviour of these borosilicate glasses.

It may be observed that the introduction of 5 mol % Al_2O_3 in the borosilicate glasses with 15 mol % SiO_2 increases the density somewhat at lower alkali-oxide content, but gradually the difference disappears.

The absence of breaks in the density versus composition relation suggests that there are no sudden structural changes in these glasses at a certain composition.

The general lower density of the borosilicate glasses with 15 mol % SiO_2 at low alkali-oxide content is consistent with the results of other measurements given in this thesis showing that SiO_2 is primarily present in a vitreous silica-like structure.

For the glasses with 65 mol % SiO_2 it may be observed that the increase in the density on increase of the alkali-oxide content gradually diminishes the higher the alkali-oxide content (fig. 9.2). This may be explained by assuming that the tendency to formation of BO_4 units becomes less the more alkali oxide is present, and that the contraction of the network is counteracted in this way. Other slight differences that may be observed can hardley be used for conclusions about the structure of these glasses.

The relationship between the refractive index and the composition of the sodium- and potassium-borosilicate glasses with 15 mol % SiO_2 is shown in fig. 9.3. Here too, no sudden breaks can be observed in the refractive-index–composition relationship so that no sudden structural changes are indicated in these glasses.

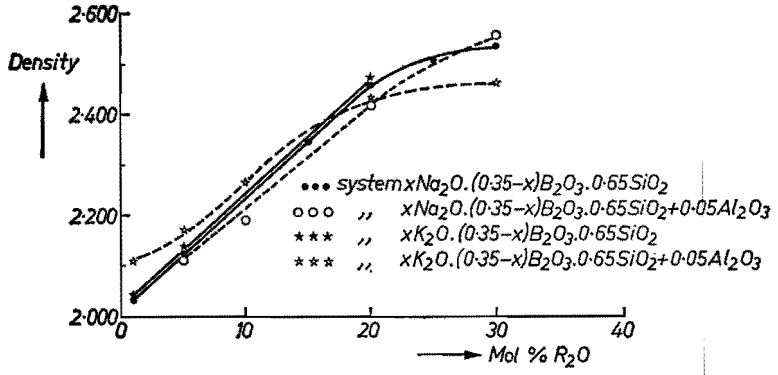

Fig. 9.2. Density of borosilicate glasses.

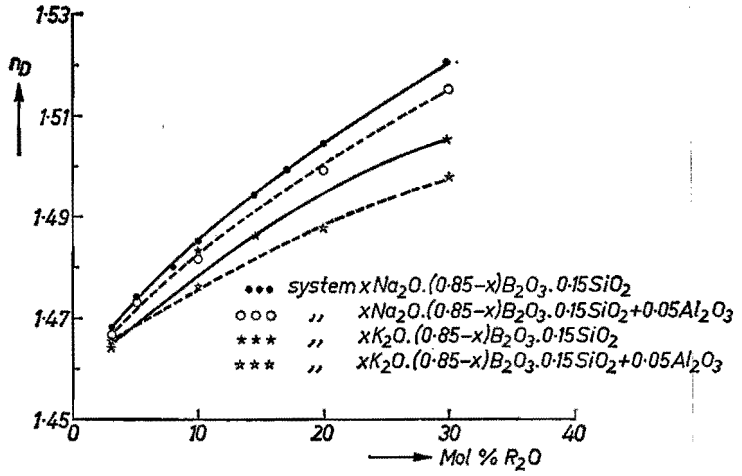

Fig. 9.3. Refractive index of borosilicate glasses.

The refractive index of the potassium-borosilicate glasses is somewhat lower than those of the corresponding sodium glasses, which is also observed for the binary borate glasses. From the density and refractive-index values the molar refraction can be calculated, using the equation

$$R_M = \frac{n^2 - 1}{n^2 + 2} \frac{\bar{M}}{d}$$

where R_M is the molar refraction, n the index of refraction, $\bar{M}$ the average molar weight and d the density. The molar refractions are usually additively built up of the contributions of the various ions, the ionic refraction, which is proportional to the polarizibility of the ion in question. Thus from the values of the molar refraction the values of the ionic refraction of the oxygen ions can

be calculated when the values of the cations are known. As can be expected the ionic refraction of the non-bridging oxygen ion is higher than that of the bridging one. Using the ionic-refraction values of the cations quoted by Scholze [9–3]) the values for the average ionic refraction of the oxygen ions were calculated in the composition series with 15 mol % SiO_2. These values decreased on increase of the sodium and potassium contents. This suggests that no large numbers of non-bridging oxygen ions are formed in the glasses with 15 mol % SiO_2 up to 30 mol % alkali oxide.

For the composition series with 65 mol % SiO_2 the average ionic refraction increases on increase of the alkali-oxide content. The gradual increase of the average ionic refraction of the oxygen ions in the series with 65 mol % SiO_2 may be explained by an increase in the number of the more-polarizable non-bridging oxygen ions.

The introduction of 5 mol % Al_2O_3 into the glasses of the composition series with 15 and 65 mol % SiO_2 leads to a slight increase in the average ionic refraction of the oxygen ions. This does not suggest that the number of non-bridging oxygen ions is decreased in the series with 65 mol % SiO_2, as suggested from other measurements. However, the ionic refraction of oxygen in aluminosilicates is relatively high (Fajans and Kreidl [9–4]). Thus, removing a non-bridging oxygen ion and formation of an AlO_4 tetrahedron does not necessarily have to lead to a decrease in the average ionic refraction of the oxygen ions.

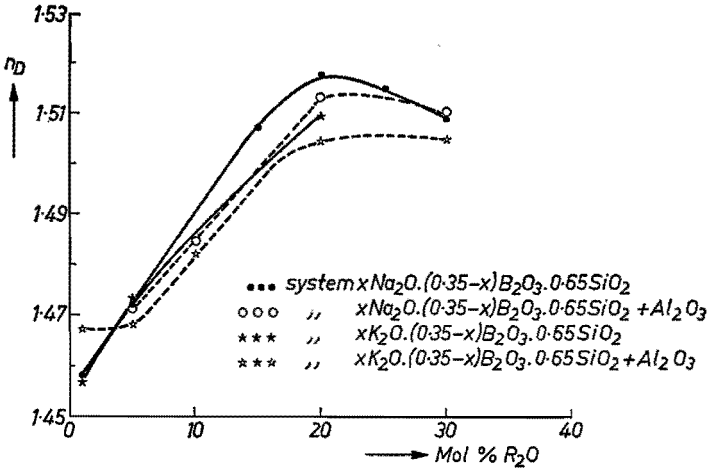

Fig. 9.4. Refractive index of borosilicate glasses.

9.4. Conclusions

The results of the density and refractive-index measurements are consistent with the other results given in this thesis. It is again indicated that at low SiO_2 content the alkali ions are primarily bonded to the borate network and that only a small number of non-bridging oxygen ions is present. At higher SiO_2 content the replacement of B_2O_3 by Na_2O or K_2O has a gradually changing influence upon the network. At lower alkali-oxide content groups with BO_4 units are again probably formed, to be gradually replaced by other groups requiring more space on increase of the alkali-oxide content.

REFERENCES

9–1) M. Coenen, Glastechn. Ber. **35**, 14, 1962.
9–2) F. C. Eversteijn, J. M. Stevels and H. I. Waterman, Phys. Chem. Glasses **1**, 123, 1960.
9–3) H. Scholze, Glas, Friedr. Vieweg, Braunschweig, Germany, 1965.
9–4) K. Fajans and N. J. Kreidl, J. Am. ceram. Soc. **31**, 105, 1948.

10. THE STRUCTURE OF BOROSILICATE GLASSES

It is generally known that the structure of glasses has to be studied by several experimental methods if a reliable picture of the structure is to be obtained. Therefore a number of different methods have been applied to study the structure of the borosilicate glasses. The results of all these measurements, the discussion of and the conclusions from these are given in chapters 3 to 9. The purpose of the present chapter is to compare the different measurements with each other and with those of the literature and to come to final conclusions on the structure of borosilicate glasses.

From the measurements of the Raman and infrared spectra, the viscosity, the thermal expansion and the internal friction as a function of the composition of the glasses it becomes clear that the structural characteristics of the binary borate glasses are to a large extent retained in the borosilicate glasses. The alkali ions are all, or nearly all, bonded by the boron ions to form certain borate groups when the alkali-to-boron ratio is about 0·5 or less. Above this ratio detectable amounts of alkali ions are bonded to silicate groups, amounts that increase on increase of the alkali-oxide content. This is most clearly indicated by the Raman and infrared spectra and confirmed by the viscosity, thermal-expansion and internal-friction measurements.

The Raman and infrared spectra further suggest that phase separation on a very fine scale takes place over the whole glass-forming area of the borosilicate systems. This is confirmed by electron microscopy of these systems by many authors, for example by Ohlberg et al. [10-1]) and Konijnendijk et al. [10-2]). This is further confirmed by leaching experiments such as, for instance those done by Hair and Chapman [10-3]). It may be recalled that wet-chemical preparation methods generally lead to more-homogeneous borosilicate glasses but that with these methods a fine microphase separation remains present in the borosilicate glasses even outside the generally accepted regions of subliquidus metastable phase separation (Konijnendijk et al. [10-2])). The structural units that are present in the borosilicate glasses resemble strongly those of the binary borate and silicate glasses, which in their turn resemble strongly those of binary crystalline borates and silicates.

This is most clearly indicated by the Raman spectra but also to some extent by the infrared spectra.

Binary borate glasses

The conclusion is that in alkali-borate glasses in the composition range 0 to 20 mol % alkali oxide the boroxol groups are to a major extent gradually replaced by six-membered borate rings with one BO_4 tetrahedron. The six-membered borate rings are to a large extent ordered to form tetraborate groups in the sodium- and potassium-borate glasses. In the composition region 20 to 35 mol %

alkali oxide the six-membered borate rings with one BO_4 tetrahedron are gradually replaced by those with two BO_4 tetrahedra. In these borate glasses the rings with two BO_4 units seem to a large extent to be connected to form diborate groups.

The conclusion of the presence of six-membered borate rings in the binary alkali borates is based on X-ray, n.m.r. and Raman data. As pointed out in chapter 1 the X-ray-diffraction patterns of some borate glasses suggest that the alkali and alkaline-earth ions are not uniformly distributed over the borate network but that there is a tendency to a characteristic distance of first-neighbour alkali and alkaline-earth ions and that this distance is nearly the same as in comparable crystalline compounds. This suggests that in small areas the structure of borate glasses resembles the structure of crystalline compounds.

From nuclear-magnetic-resonance measurements, done by Rhee [10–4]), on sodium-borate glasses it also becomes clear that probably the same types of borate groups are present in the glasses as in the crystalline sodium-borate compounds. His results clearly indicate that up to about 20 mol % Na_2O, BO_4 tetrahedra are present in the borate glasses which are not connected to each other. Above 20 mol % Na_2O, BO_4 tetrahedra are in gradually increasing amounts connected to each other. These unconnected and connected BO_4 tetrahedra are also observed in many crystalline borates. Above 30 mol % alkali oxide, reasonable amounts of non-bridging oxygen ions are formed in the alkali-borate glasses which, to a large extent, are grouped together in orthoborate, pyroborate and ring-type metaborate groups. This result is obtained from the Raman spectra. The formation of increasing and gradually detectable amounts of non-bridging oxygen ions in borate glasses further correlates with viscosity, thermal-expansion and internal-friction data.

In the mixed alkali-borate glasses in the composition range 40 to 50 mol % alkali oxide the formation of non-bridging oxygen ions connected to orthoborate, pyroborate and ring-type metaborate groups is evidenced. This conclusion is based on the Raman spectra of these glasses.

Borosilicate glasses

In the borosilicate glasses with 15 mol % SiO_2 the same types of borate groups are formed primarily as in the binary borate glasses. The SiO_2 seems mainly to be present in a vitreous silica-like structure and agglomerated into small areas. Above the alkali-to-boron ratio of 0·5, increasing but small amounts of non-bridging oxygen ions are formed connected to silicon ions in a disilicate-like structure. This is most strongly indicated by the Raman spectra. The viscosity, thermal-expansion and internal-friction data also indicate the increased formation of non-bridging oxygen ions compared to the binary borates at equal mol percentage of alkali oxide above the alkali-to-boron ratio of 0·5. This suggests that the formation of two paired BO_4 tetrahedra is preferably circumvented and

that the added alkali oxide leads to the formation of non-bridging oxygen ions connected to silicon as well as boron ions.

The formation of ring-type metaborate groups can be observed in these borosilicate glasses at a lower mol percentage of alkali oxide than in the binary borate glasses. This is primarily based on the Raman spectra but is confirmed by the infrared spectra, the viscosity, the thermal-expansion and the internal-friction measurements.

The ^{11}B n.m.r. data on borosilicate glasses obtained by Scheerer et al. [10–5]) and Milberg et al. [10–6]) confirm the conclusions above.

In the alkali-borosilicate glasses with 35 mol% SiO_2 the tendency to the formation of non-bridging oxygen ions is again stronger than in the glasses with 15 mol% SiO_2. Again the formation of ring-type metaborate groups and SiO_4 tetrahedra with one non-bridging oxygen ion is observed at a lower Na_2O or K_2O mol percentage than is the case for the glasses with 15 mol% SiO_2. In these glasses the six-membered borate rings with a BO_4 tetrahedron are also formed, and the gradual decrease of the amount of boroxol groups observed.

In the borosilicate glasses with 65 mol% SiO_2 the formation of non-bridging oxygen ions takes place in already detectable amounts at about 10 mol % alkali oxide. This is based on the Raman and infrared spectra and the viscosity, thermal-expansion and internal-friction measurements. The Raman spectra again indicate the resistance to the formation of paired BO_4 tetrahedra in the alkali-borosilicate glasses. The non-bridging oxygen ions are primarily present in the ring-type metaborate groups as evidenced mainly by the Raman spectra and to some extent by the infrared spectra. BO_4 tetrahedra are not incorporated in the silicate network like AlO_4 tetrahedra. Borosilicate-compound formation in this concentration area is not indicated. Most probably SiO_2 is present in a nearly vitreous silica-like structure with only a limited number of non-bridging oxygen ions when enough boron ions are available for the formation of ring-type metaborate groups, which latter seem to be grouped together in small areas.

Lithium-borosilicate glasses show in general the same characteristic structural units as the sodium- and potassium-borosilicate glasses. It may, however, be observed that replacement of an Na or K ion by Li decreases the amount of ring-type metaborate groups when these last are present in the original sodium- and potassium-borosilicate glasses. This is evidenced by Raman spectroscopy of these glasses.

The introduction of alkaline-earth oxides in borosilicate glasses leads in general to the same type of units as for the alkali-borosilicate glasses, as is evidenced mainly by the Raman and infrared spectra. However, the relative number of the various groups is influenced. For instance, CaO in borosilicate glasses counteracts the formation of ring-type metaborate groups. This may be understood if one keeps in mind that the compound $CaO \cdot B_2O_3$ is not built

up of ring-type metaborate groups but of chain-type groups. These chain-type groups could not be detected in the borosilicate glasses.

Introduction of Al_2O_3 at low alkali-oxide concentration leads to the disappearance of BO_4 tetrahedra and formation of boroxol groups. At higher alkali-oxide and SiO_2 concentrations, that is, when enough non-bridging oxygen ions are present, the latter are removed first to form AlO_4 tetrahedra. In these cases it is not clear in what form boron ions are present in the network structure at higher Al_2O_3 content. From the thermal-expansion measurements it is suggested that in the high-silica range the introduction of Al_2O_3 leads primarily to the disappearance of the ring-type metaborate groups before the non-bridging oxygen ions of SiO_4 tetrahedra are replaced.

As well as in the borate glasses as in the borosilicate glasses, part of the boron ions is not present in typical large borate groups but forms a random network of BO_3 triangles and BO_4 tetrahedra.

REFERENCES

10–1) S. M. Ohlberg, H. R. Golub, J. J. Hammel and R. R. Lewchuck, J. Am. ceram. Soc. **48**, 178, 331, 1965.
10–2) W. L. Konijnendijk, M. van Duuren and H. Groenendijk, Verres Réfract. **27**, 11, 1973.
10–3) M. L. Hair and D. Chapman, J. Am. ceram. Soc. **49**, 651, 1966.
10–4) C. Rhee, J. Korean phys. Soc. **4**, 51, 1971.
10–5) J. Scheerer, W. Müller-Warmuth and H. Dutz, Glastechn. Ber. **46**, 109, 1973.
10–6) M. E. Milberg, J. G. O'Keefe, R. A. Verhelst and H. O. Hooper, Phys. Chem. Glasses **13**, 79, 1972.

APPENDIX

This appendix contains some tables of viscosity, thermal-expansion, electrical-conduction, density and refractive-index results. Tables A-I to A-VII consist of viscosity measurements. Tables A-VIII to A-XIV consist of thermal-expansion measurements. Tables A-XV to A-XXI consist of electrical-conduction measurements. Tables A-XXII and A-XXIII consist of density and refractive-index measurements.

In the tables of viscosity measurements E_η stands for the activation energy of viscous flow and A for the logarithm of the pre-exponential factor. Thus A is calculated from the experimental measurements using the experimentally observed relation

$$\log_{10} \eta = A + \frac{E_\eta}{4{\cdot}57\,T}.$$

By this equation E_η is given in kcal/mole.

In the tables of the electrical-conduction measurements E_ϱ stands for the activation energy of ionic conduction. A stands again for the logarithm of the pre-exponential factor, calculated from the experimentally observed relation

$$\log_{10} \varrho = A + \frac{B}{T}.$$

From the B in this relation E_ϱ is calculated in eV.

TABLE A-I

Viscosity measurements. System Li_2O–B_2O_3–SiO_2; x = mol % Li_2O, y = mol % B_2O_3, z = mol % SiO_2

x	y	z	E_η (kcal/mol)	$T(\log\eta = 12)$ (°C)	$T(\log\eta = 7{\cdot}6)$ (°C)	A
0	85	15	75	315	425	—15·87
5	80	15	83	367	484	—16·38
7	78	15	89	384	499	—17·59
10	75	15	118	418	510	—25·46
20	65	15	183	503	575	—39·55
30	55	15	225	515	574	—50·89
40	45	15	250	485	534	—60·10
30	35	35	178	502	576	—38·14

TABLE A-II

Viscosity measurements. System Na_2O–B_2O_3–SiO_2; x = mol % Na_2O, y = mol % B_2O_3, z = mol % SiO_2

x	y	z	E_η (kcal/mol)	$T(\log\eta = 12)$ (°C)	$T(\log\eta = 7{\cdot}6)$ (°C)	A
0	100	0	78·3	289	383	—18·54
5	95	0	87·8	338	438	—19·39
10	90	0	109·5	384	474	—24·55
20	80	0	217	476	532	—51·26
30	70	0	216	482	540	—50·63
10	85	5	116	386	472	—26·35
20	75	5	162	478	555	—35·21
30	65	5	199	495	561	—44·78
0	85	15	75	315	425	—15·87
3	82	15	95·5	348	442	—21·72
5	80	15	97·1	366	464	—21·66
7	78	15	106	382	475	—23·56
10	75	15	118	415	507	—25·47
20	65	15	146	494	584	—29·76
30	55	15	223	517	579	—49·37
5	70	25	88·2	382	498	—17·46
30	46·5	23·5	221	515	575	—49·25
10	60	30	110	409	506	—23·19
0	65	35	57·5	344	514	— 8·37
1	64	35	63·7	355	510	—10·21
3	62	35	64·7	375	540	— 9·82
5	60	35	60·5	401	596	— 7·63
10	55	35	89·0	445	584	—15·15
20	45	35	163	527	615	—32·62
30	35	35	198	522	593	—42·52
40	25	35	165	457	528	—37·36
0	55	45	62·4	377	549	— 9·01
30	23·5	46·5	170	527	610	—34·44
20	30	50	191	579	662	—37·16
0	45	55	62·2	420	619	— 7·69
10	30	60	82·5	545	722	—12·79
20	20	60	162	586	689	—29·26
30	11·5	58·5	145	522	621	—27·91
0	35	65	65·4	475	699	— 7·12
1	34	65	67·5	490	714	— 7·40

TABLE A-II (continued)

x	y	z	E_η (kcal/mol)	$T(\log\eta = 12)$ (°C)	$T(\log\eta = 7{\cdot}6)$ (°C)	A
5	30	65	90·0	543	725	—12·13
10	25	65	126	562	689	—21·18
20	15	65	159	580	683	—28·85
30	5	65	125	501	612	—23·28
10	14·5	75·5	145	622	747	—23·52

TABLE A-III

Viscosity measurements. System K_2O–B_2O_3–SiO_2; x = mol % K_2O, y = mol % B_2O_3, z = mol % SiO_2

x	y	z	E_η (kcal/mol)	$T(\log\eta = 12)$ (°C)	$T(\log\eta = 7{\cdot}6)$ (°C)	A
0	100	0	78·3	289	383	—18·54
5	95	0	99·5	325	407	—24·37
10	90	0	116	371	452	—27·34
20	80	0	154	437	509	—35·49
30	70	0	159	450	522	—36·26
10	85	5	113	382	469	—25·86
30	65	5	154	453	529	—34·62
0	85	15	75	315	425	—15·87
3	82	15	91·4	339	435	—20·63
10	75	15	109	393	486	—23·96
14·5	70·5	15	129	423	509	—28·54
20	65	15	151	461	547	—32·78
30	55	15	176	478	548	—39·43
10	60	30	119	420	512	—25·73
0	65	35	57·5	344	514	— 8·37
5	60	35	63·8	371	536	— 9·69
10	55	35	111	431	533	—22·66
14	51	35	116	470	579	—22·34
20	45	35	147	515	611	—28·84
10	30	60	137	560	674	—24·21
30	11·5	58·5	132	526	639	—24·16
0	35	65	65·4	475	699	— 7·12
1	34	65	84·8	494	665	—12·20
10	25	65	121	569	706	—19·50
20	15	65	175	629	732	—30·45
30	5	65	127	537	655	—22·38
10	14·5	75·5	141	670	816	—20·66

TABLE A-IV

Viscosity measurements. System $NaKO–B_2O_3–SiO_2$; x = mol % NaKO, y = mol % B_2O_3, z = mol % SiO_2

x	y	z	E_η (kcal/mol)	$T(\log\eta = 12)$ (°C)	$T(\log\eta = 7{\cdot}6)$ (°C)	A
0	85	15	75	315	425	—15·87
3	82	15	78	333	446	—16·20
10	75	15	106	388	483	—23·07
14·5	70·5	15	135	433	516	—29·97
20	65	15	142	459	544	—30·38
30	55	15	159	456	531	—35·59
0	35	65	65·4	475	699	— 7·12
1	34	65	71	487	697	— 8·44
5	30	65	—	512	712	—
10	25	65	100	535	692	—15·14
20	15	65	154	563	665	—28·26
30	5	65	116	469	577	—22·40

TABLE A-V

Viscosity measurements. System $Na_2O–B_2O_3–SiO_2$ + 5 mol % Al_2O_3; x = mol % Na_2O, y = mol % B_2O_3, z = mol % SiO_2

x	y	z	E_η	$T(\log\eta = 12)$ (°C)	$T(\log\eta = 7{\cdot}6)$ (°C)	A
0	85	15	no glass			
3	82	15	116	382	464	—27·00
5	80	15	104	389	487	—22·28
10	75	15	113	406	499	—24·38
12	73	15	110	417	517	—22·81
14·5	70·5	15	115	433	532	—23·69
20	65	15	148	472	561	—31·39
30	55	15	142	490	562	—39·34
0	35	65	no glass			
5	30	65	68·5	495	718	— 7·53
10	25	65	104	538	688	—16·15
20	15	65	127	591	727	—20·25
30	5	65	126	517	632	—22·79

TABLE A-VI

Viscosity measurements. System K_2O–B_2O_3–SiO_2 + 5 mol % Al_2O_3; x = mol % K_2O, y = mol % B_2O_3, z = mol % SiO_2

x	y	z	E_η (kcal/mol)	$T(\log\eta = 12)$ (°C)	$T(\log\eta = 7{\cdot}6)$ (°C)	A
0	85	15	no glass			
3	82	15	81·5	375	499	—15·57
10	75	15	111	397	489	—24·31
14·5	70·5	15	129	427	513	—28·39
20	65	15	130	457	549	—27·06
30	55	15	200	470	531	—46·88
0	35	65	no glass			
1	34	65	70	550	805	— 6·63
5	30	65	63·7	495	739	— 6·15
10	25	65	92·5	541	712	—12·99
20	15	65	135	647	792	—20·13
30	5	65	109	572	728	—16·10

TABLE A-VII

Viscosity measurements. System NaKO–B_2O_3–SiO_2 + 5 mol % Al_2O_3; x = mol % NaKO, y = mol % B_2O_3, z = mol % SiO_2

x	y	z	E_η (kcal/mol)	$T(\log\eta = 12)$ (°C)	$T(\log\eta = 7{\cdot}6)$ (°C)	A
0	85	15	no glass			
3	82	15	85·2	367	482	—17·08
10	75	15	87·1	378	493	—17·25
14·5	70·5	15	120	418	509	—25·83
20	65	15	134	454	541	—28·42
30	55	15	164	461	533	—36·90
0	35	65	no glass			
5	30	65	67·2	487	710	— 7·36
10	25	65	97·8	521	677	—14·97
20	15	65	134	562	683	—23·04
30	5	65	114	492	612	—20·53

TABLE A-VIII

Linear-thermal-expansion measurements. System Li_2O–B_2O_3–SiO_2; x = mol % Li_2O, y = mol % B_2O_3, z = mol % SiO_2

x	y	z	$\alpha_{200\,°C}$		$\alpha_{250\,°C}$		$\alpha_{300\,°C}$	
			heating	cooling	heating	cooling	heating	cooling
3	82	15	87·9	105	89·6	106	88·7	116
			88·2	104	89·4	105	88·5	113
5	80	15	85·9	95·4	85·6	95·1	80·6	102
			83·0	91·8	82·6	92·7	77·9	99·0
7	78	15	71·6	84·9	72·5	85·4	69·8	89·1
			67·6	85·8	68·6	85·8	65·9	90·1
10	75	15	73·7	75·7	74·1	76·6	74·1	79·0
			73·8	78·0	74·5	78·4	74·7	79·9
20	65	15	70·7	73·3	72·1	74·5	72·4	76·3
			74·2	74·4	75·0	75·2	76·8	76·6
30	55	15	85·3	88·8	86·5	89·8	89·0	91·4
			90·0	86·0	91·2	86·9	92·6	88·5
40	45	15	108	109	109	110	111	111
			105	109	105	109	105	111
30	35	35	92·0	92·5	92·9	93·4	94·6	95·0
			89·9	92·2	91·3	93·3	93·3	94·8
40	25	35	112	115	114	115	116	117
			110	113	112	112	114	113

TABLE A-IX

Linear-thermal-expansion measurements. System Na_2O–B_2O_3–SiO_2; x = mol % Na_2O, y = mol % B_2O_3, z = mol % SiO_2

x	y	z	$\alpha_{200\,°C}$		$\alpha_{250\,°C}$		$\alpha_{300\,°C}$	
			heating	cooling	heating	cooling	heating	cooling
0	100	0	154	162	150	180		
			156	165	153	178		
5	95	0	120	132	119	132	117	136
			104	114	104	113	102	121
10	90	0	99·0	105	99·0	105	99·3	106
20	80	0	95·3	97·7	95·3	97·8	96·9	102
			96·3	96·8	96·7	97·7	97·4	99·6

TABLE A-IX (continued)

x	y	z	$\alpha_{200°C}$		$\alpha_{250°C}$		$\alpha_{300°C}$	
			heating	cooling	heating	cooling	heating	cooling
30	70	0	108	110	109	112	111	115
			106	112	108	114	111	116
10	85	5	91·4	99·6	92·3	98·4	92·9	99·2
			90·8	98·1	92·1	97·9	92·3	99·5
20	75	5	91·0	96·7	91·3	96·4	89·9	97·3
			96·2	101	95·7	99·9	93·7	101
30	65	5	114	119	115	118	116	119
			115	118	114	117	115	117
30	58·5	11·5	121	117	120	118	120	119
			123	120	120	123	119	126
0	85	15	114	125				
			115	127				
3	82	15	95·6	104	95·4	104	92·2	109
			104	106	102	106	98·7	111
5	80	15	97·5	99·1	97·0	101	96·8	106
			95·2	97·0	94·2	96·7	92·9	99·5
7	78	15	86·8	93·8	87·3	93·4	87·8	94·9
			86·1	93·0	86·6	92·9	86·8	94·9
10	75	15	88·4	96·4	89·5	94·9	89·3	94·8
			86·6	91·8	86·6	89·9	86·9	90·3
14·5	70·5	15	90·1	91·9	90·2	91·7	90·4	92·4
			91·7	94·1	91·5	94·3	91·9	94·9
17	68	15	91·6	93·6	91·1	93·1	91·8	93·5
			89·6	91·5	90·0	91·6	90·9	92·7
20	65	15	93·2	95·4	93·3	95·2	94·2	95·6
			92·8	95·6	93·3	95·2	94·3	95·9
30	55	15	117	119	117	118	117	118
			115	116	115	116	116	116
30	46·5	23·5	113	117	113	116	114	116
			119	122	119	122	119	122
5	70	25	75·8	84·0	76·6	84·2	74·9	79·2
			84·0	85·2	82·3	84·7	78·9	86·5
10	60	30	85·0	88·3	85·6	88·2	86·8	88·9
			91·6	93·7	91·5	92·9	92·1	93·7
0	65	35	81·9	85·3	80·3	85·1	77·2	89·0
			76·2	86·8	76·6	86·1	74·9	89·4

TABLE A-IX (continued)

x	y	z	$\alpha_{200°C}$		$\alpha_{250°C}$		$\alpha_{300°C}$	
			heating	cooling	heating	cooling	heating	cooling
1	64	35	77·6	80·9	75·8	80·5	70·6	83·4
			76·7	81·7	74·0	81·3	67·3	85·3
3	62	35	62·1	77·9	64·2	77·5	65·1	86·1
			70·5	77·0	69·8	76·5	68·3	78·5
5	60	35	63·6	75·7	65·2	74·4	67·0	74·2
			64·0	73·5	66·1	73·5	67·6	74·9
7·5	57·5	35	73·7	75·3	72·6	74·5	72·3	74·9
			75·7	76·7	75·7	76·2	75·2	76·5
10	55	35	72·8	73·6	73·5	74·4	74·1	75·0
			72·9	77·6	73·3	77·2	73·6	77·3
11·5	53·5	35	76·1	77·6	75·4	76·9	76·0	77·1
			75·5	78·7	77·3	78·8	77·9	79·1
14	51	35	80·1	83·3	80·6	83·6	81·4	84·2
			77·3	79·5	77·6	79·2	78·6	79·6
			76·9	78·8	77·1	81·6	76·9	82·0
20	45	35	99·4	98·6	98·7	98·4	99·1	98·5
			98·4	99·3	97·5	101	98·7	102
30	35	35	117	119	116	118	117	118
			123	127	121	124	121	123
40	25	35	153	156	152	154	151	151
			154	153	151	152	151	152
10	45	45	61·4	67·9	62·4	68·6	64·0	68·7
			66·9	65·7	67·8	66·6	68·9	67·3
			67·7	70·1	68·1	70·2	69·2	71·0
			70·0	69·5	69·7	69·0	70·1	69·5
30	23·5	46·5	122	120	120	119	120	119
			117	118	116	118	117	118
20	30	50	91·7	92·4	91·8	92·4	92·7	93·3
			93·5	94·4	93·7	94·9	95·0	95·6
30	11·5	58·5	130	126	127	129	127	132
			124	125	123	124	124	124
20	20	60	94·4	94·6	94·0	94·0	94·3	94·1
			91·3	95·1	92·2	95·2	93·5	95·9
0	35	65	45·6	47·5	45·3	47·4	45·5	47·8
			41·4	49·5	42·6	48·9	43·5	49·1
2	33	65	45·6	46·6	45·4	46·4	46·2	46·9
			47·2	48·7	46·8	48·1	47·4	48·1

TABLE A-IX (continued)

x	y	z	$\alpha_{200\,°C}$		$\alpha_{250\,°C}$		$\alpha_{300\,°C}$	
5	30	65	52·3	50·3	51·2	50·7	50·9	51·4
			48·7	49·9	49·9	51·0	51·1	52·2
10	25	65	62·9	64·1	63·7	64·0	65·5	64·8
			64·8	66·1	65·9	66·9	67·8	68·4
20	15	65	92·8	94·4	93·6	94·8	95·0	95·9
			94·8	96·7	94·6	95·4	95·8	95·9
30	5	65	132	134	131	133	131	133
			128	134	126	131	125	130
10	14·5	75·5	65·6	63·4	65·7	63·7	67·5	65·2
			57·1	60·9	59·3	61·6	61·1	62·8
			60·2	59·7	61·5	60·8	63·3	62·0
			61·1	62·0	62·5	62·5	64·2	63·0

TABLE A-X

Linear-thermal-expansion measurements. System K_2O–B_2O_3–SiO_2; x = mol % K_2O, y = mol % B_2O_3, z = mol % SiO_2

x	y	z	$\alpha_{200\,°C}$		$\alpha_{250\,°C}$		$\alpha_{300\,°C}$	
			heating	cooling	heating	cooling	heating	cooling
5	95	0	79·1	114	85·9	118		
			81·2	116	87·7	120		
10	90	0	102	109	105	112	106	118
			107	112	110	114	111	121
20	80	0	111	118	114	121	115	123
			106	114	108	116	110	120
30	70	0	113	117	116	118	110	122
			110	121	113	117	116	126
30	65	5	132	135	131	134	131	134
			130	135	129	133	129	132
30	58·5	11·5	119		118		117	
			124	127	123	126	122	126

TABLE A-X (continued)

x	y	z	$\alpha_{200°C}$		$\alpha_{250°C}$		$\alpha_{300°C}$	
			heating	cooling	heating	cooling	heating	cooling
3	82	15		106		109		121
				105		111		128
10	75	15	102	103	101	103	101	104
			101	105	101	105	102	106
20	65	15	113	117	113	116	113	116
			115	117	114	116	115	116
30	55	15	131	132	130	131	130	130
			130	133	129	132	129	131
10	60	30	90·2	89·9	89·9	89·6	90·3	90·3
			86·7	89·9	87·6	89·9	88·6	90·9
5	60	35	80·2	84·8	79·5	84·3	77·9	86·9
			83·4	87·4	81·9	86·4	79·5	88·2
10	55	35	86·1	87·9	85·7	87·6	85·7	88·7
			89·1	88·7	87·8	87·8	87·3	88·4
14	51	35	96·2	101	97·0	100	97·0	99·8
			100	99·4	99·0	98·4	98·9	98·8
20	45	35	105	111	104	108	104	108
			102	107	102	106	103	106
10	45	45	79·0	80·9	79·4	80·4	80·7	81·0
			81·4	80·7	80·9	80·0	81·6	80·3
30	11·5	58·5	137	149	139	146	139	145
			140	150	137	147	136	146
10	30	60	76·0	76·0	75·7	75·8	76·3	76·1
			75·0	76·1	74·9	75·7	75·3	76·2
1	34	65	37·7	43·6	39·5	44·4	38·8	43·7
				43·2		44·4		43·6
			43·9	45·1	43·7	45·1	42·2	44·4
			43·6	44·9	43·3	45·2	41·8	44·1
5	30	65	53·7	51·4	52·9	51·6	51·9	50·9
			45·4	48·2	46·4	49·3	46·3	49·8
10	25	65	63·9	67·6	65·6	67·8	66·4	67·6
			68·2	68·4	69·1	68·8	68·9	70·8
20	15	65	97·0	98·0	97·4	98·4	97·5	98·1
			98·7	100	99·1	101	99·3	101
30	5	65	140	147	140	147	142	150
			146	147	146	147	147	150
10	14·5	75·5	70·7	70·0	69·7	69·9	70·6	70·3
			69·4	71·6	70·1	71·3	71·9	72·2

TABLE A-XI

Linear-thermal-expansion measurements. System $NaKO–B_2O_3–SiO_2$; x = mol % NaKO, y = mol % B_2O_3, z = mol % SiO_2

x	y	z	$\alpha_{200°C}$		$\alpha_{250°C}$		$\alpha_{300°C}$	
			heating	cooling	heating	cooling	heating	cooling
3	82	15		103		104		112
				103		105		115
10	75	15	88·0	94·0	89·7	95·6	91·6	99·1
			85·4	93·6	87·2	93·9	89·5	94·1
14·5	70·5	15	86·5	95·2	89·5	97·0	91·2	99·4
			91·5	95·0	94·1	96·8	96·3	100
20	65	15	106	106	108	109	110	112
			97·5	101	101	103	104	106
30	55	15	116	118	118	120	121	122
			120	121	122	122	125	126
1	34	65	45·0	47·3	45·6	47·1	46·7	47·9
			45·7	47·1	45·9	47·0	46·8	47·8
5	30	65	55·0	52·2	53·8	52·6	53·2	53·5
			50·0	51·2	50·8	51·7	52·1	52·6
10	25	65	65·1	69·4	66·6	69·7	68·5	70·9
			66·2	68·3	67·0	68·8	68·7	70·1
20	15	65	103	104	103	104	103	104
			103	105	104	105	104	106
30	5	65	158	157	156	156	155	155
			156	156	155	156	155	156

TABLE A-XII

Linear-thermal-expansion measurements. System Na_2O–B_2O_3–SiO_2 + 5 mol % Al_2O_3; x = mol % Na_2O, y = mol % B_2O_3, z = mol % SiO_2

x	y	z	$\alpha_{200\,°C}$		$\alpha_{250\,°C}$		$\alpha_{300\,°C}$	
			heating	cooling	heating	cooling	heating	cooling
3	82	15	78·0	73·6	77·4	78·2		
			73·6	84·9	73·0	87·4		
5	80	15	114	98·9	113	102	112	108
			87·3	95·8	87·8	94·8	88·0	99·2
10	75	15	89·6	91·6	89·6	91·1	90·3	92·0
			89·8	92·5	89·2	91·6	89·6	92·9
12	73	15	109	113	107	111	107	110
			92·4	90·3	91·5	91·7	92·2	94·7
14·5	70·5	15	92·0	91·0	91·7	91·2	92·5	92·3
			87·1	91·4	87·7	91·2	88·2	93·0
20	65	15	98·3	98·1	97·7	97·2	97·8	98·2
			94·2	96·7	93·9	96·8	95·3	96·8
30	55	15	110	111	111	113	114	115
			111	113	112	113	114	115
5	30	65	52·0	52·2	52·4	52·4	49·3	49·3
			50·0	51·2	51·0	51·8	48·1	48·6
10	25	65	60·6	60·8	61·4	62·5	61·0	62·1
			59·8	59·2	60·5	60·2	60·6	60·7
20	15	65	85·7	85·2	88·6	87·4	90·0	88·9
			81·6	82·9	84·4	85·5	85·8	86·1
30	5	65	115	117	117	118	119	120
			114	115	116	119	115	122

TABLE A-XIII

Linear-thermal-expansion measurements. System K_2O–B_2O_3–SiO_2 + 5 mol % Al_2O_3; x = mol % K_2O, y = mol % B_2O_3, z = mol % SiO_2

x	y	z	$\alpha_{200°C}$		$\alpha_{250°C}$		$\alpha_{300°C}$	
			heating	cooling	heating	cooling	heating	cooling
10	75·5	14·5	103	104	103	105	103	107
			101	105	102	108	102	111
3	82	15	86·4	94·4	85·3	95·2	78·1	104
			77·3	96·1	77·5	97·3	69·6	107
14·5	70·5	15	104	107	106	108	106	109
			100	106	102	108	102	108
20	65	15	111	113	111	113	113	115
			113	114	113	114	114	115
30	55	15	116	117	119	121	119	121
			120	121	122	120	124	123
1	34	65	39·5	40·3	40·5	41·1	40·6	41·4
			39·5	40·2	40·6	41·1	40·8	41·2
			37·4	38·9	37·8	39·2	36·8	38·0
			38·1	37·6	38·2	38·3	37·2	37·9
			38·0	39·1	38·6	39·6	37·3	38·4
			36·3	37·3	36·0	37·4	35·4	36·9
5	30	65	56·7	58·9	56·7	58·9	56·0	58·0
			57·9	61·7	58·0	59·2	57·1	58·8
			57·9	59·4	57·7	58·9	57·0	58·1
			59·3	59·0	58·9	59·2	57·5	58·2
			57·1	59·2	57·8	59·7	58·1	59·6
			55·5	55·5	56·4	56·6	56·0	56·8
10	25	65	69·7	69·2	70·0	69·7	69·8	69·9
			68·8	68·7	69·0	68·6	68·2	67·8
20	15	65	87·3	89·0	87·4	88·9	87·8	88·3
			84·4	87·0	85·7	87·8	86·1	87·9
			84·9	86·1	86·7	85·9	87·6	87·0
			85·0	87·1	86·2	88·4	87·4	89·3
30	5	65	134	134	134	134	134	137
			127	134	128	134	129	135

TABLE A-XIV

Linear-thermal-expansion measurements. System $NaKO–B_2O_3–SiO_2$ + 5 mol % Al_2O_3; x = mol % NaKO, y = mol % B_2O_3, z = mol % SiO_2

x	y	z	$\alpha_{200°C}$		$\alpha_{250°C}$		$\alpha_{300°C}$	
			heating	cooling	heating	cooling	heating	cooling
10	75	15	92·7	94·4	94·6	96·0	94·8	98·5
			94·4	95·3	96·9	96·6	98·6	99·7
3	82	15	88·3	91·3	87·7	94·2	81·7	102
			73·8	93·1	75·0	91·9	69·3	92·3
			81·2	91·7	79·9	93·9	69·5	105
			86·0	93·7	83·0	96·0	71·8	109
14·5	70·5	15	94·8	96·0	97·1	98·7	99·1	102
			96·4	96·2	98·8	98·9	100	101
20	65	15	104	105	107	108	109	110
			108	106	110	108	112	112
30	55	15	114	115	117	117	119	120
			114	116	117	119	120	122
5	30	65	54·6	56·4	55·0	56·8	54·1	56·3
			56·0	54·2	56·3	55·0	55·6	54·6
10	25	65	69·0		69·5		70·5	
			69·5	71·8	70·0	72·8	70·5	72·7
20	15	65	93·4	111	98·9	112	101	113
			95·0	96·7	96·8	97·7	97·9	98·4
30	5	65	132	134	132	135	134	137
			134		135		137	
			134	130	131	131	133	133
			133	134	134	136	134	138
			127	127	129	129	132	131
			130	130	132	132	134	135

TABLE A-XV

Electrical-conduction measurements. System Li_2O–B_2O_3–SiO_2; x = mol % Li_2O, y = mol % B_2O_3, z = mol % SiO_2

x	y	z	E_ϱ (eV)	$T(\log \varrho = 7)$ (°C)	A	remarks *)
3	82	15	2·90	456	—13·10	$T > T_g$
5	80	15	2·66	437	—11·97	$T > T_g$ **)
7	78	15	1·58 (402–429 °C)		— 4·20	
			2·41 (429–496 °C)	433	—10·25	$T > T_g$ **)
10	75	15	1·32 (361–413 °C)	408	— 2·77	
			1·82 (413–456 °C)		— 6·45	$T > T_g$ **)
20	65	15	0·91	243	— 1·85	
30	55	15	0·64	119	— 1·28	
40	45	15	0·55	58	— 1·46	
30	35	35	0·68	109	— 1·97	
40	25	35	0·58	55	— 1·98	

*) No remarks means that $T < T_g$.
**) Visible phase separation developed during measurement.

TABLE A-XVI

Electrical-conduction measurements. System Na_2O–B_2O_3–SiO_2; x = mol % Na_2O, y = mol % B_2O_3, z = mol % SiO_2

x	y	z	E_ϱ (eV)	$T(\log \varrho = 7)$ (°C)	A	remarks *)
5	95	0	2·88	425	—14·01	$T > T_g$
10	90	0	3·39	427	—17·51	$T > T_g$
20	80	0	0·91	271	— 1·39	
30	70	0	0·72	174	— 1·07	
10	85	5	2·74	423	—12·89	$T > T_g$
20	75	5	0·91	264	— 1·51	
30	65	5	0·68	156	— 0·96	
30	58·5	11·5	0·72	158	— 1·39	
3	82	15	3·17	460	—14·46	$T > T_g$
5	80	15	2·67	450	—11·67	$T > T_g$
7	78	15	2·90	436	—13·63	$T > T_g$
10	75	15	2·59	421	—11·87	$T > T_g$
17	68	15	0·96	307	— 1·34	
20	65	15	0·88	249	— 1·55	

TABLE A-XVI (continued)

x	y	z	E_ϱ (eV)	$T(\log \varrho = 7)$ (°C)	A	remarks *)
30	55	15	0·66	143	— 0·97	
5	70	25	2·68	443	—11·89	$T > T_g$
30	46·5	23·5	0·72	142	— 1·73	
10	60	30	2·64	420	—12·24	$T > T_g$
0	65	35	1·66	572	— 2·94	$T > T_g$
1	64	35	2·84	500	—11·58	$T > T_g$
3	62	35	2·58	463	—10·73	$T > T_g$
5	60	35	2·58	448	—11·10	$T > T_g$
7·5	57·5	35	2·40 (419–468 °C)	424	—10·51	$T > T_g$
			1·17 (374–419 °C)		— 1·50	
10	55	35	1·12	383	— 1·65	
11·5	53·5	35	1·00	349	— 1·09	
14	51	35	0·96	298	— 1·46	
20	45	35	0·82	229	— 1·23	
30	35	35	0·60	125	— 1·10	
40	25	35	0·52	51	— 1·02	
10	45	45	0·93	329	— 0·84	
30	23·5	46·5	0·60	103	— 1·08	
20	30	50	0·75	194	— 1·05	
10	30	60	0·90	294	— 0·99	
20	20	60	0·71	138	— 1·12	
30	11·5	58·5	0·59	84	— 1·39	
0	35	65	1·40	569	— 1·43	$T > T_g$
1	34	65	1·59	537	— 2·94	$T > T_g$
5	30	65	1·02	379	— 0·92	
10	25	65	0·87	275	— 1·00	
20	15	65	0·69	155	— 1·09	
30	5	65	0·59	75	— 1·59	
10	14·5	75·5	0·81	243	— 0·87	

*) No remarks means measurements in temperature range $T < T_g$.

TABLE A-XVII

Electrical-conduction measurements. System K_2O–B_2O_3–SiO_2; x = mol % K_2O, y = mol % B_2O_3, z = mol % SiO_2

x	y	z	E_ϱ (eV)	$T(\log \varrho = 7)$ (°C)	A	remarks *)
5	95	0	3·35 (425–463 °C)	439	—16·78	$T > T_g$
			2·36 (463–501 °C)		— 9·97	$T > T_g$
10	90	0	3·88 (421–467 °C)	442	—20·42	$T > T_g$
			2·70 (467–515 °C)		—12·41	$T > T_g$
20	80	0	1·36	340	— 4·17	
30	70	0	0·85	254	— 1·15	
30	65	5	0·81	215	— 1·35	
30	58·5	11·5	0·78	229	— 0·88	
3	82	15	2·70	467/453	—11·35/	
					—11·85	$T > T_g$
10	75	15	3·24	455	—15·52	$T > T_g$
14·5	70·5	15	1·20 (388–425 °C)		— 1·50	
			2·97 (425–482 °C)	432	—14·30	$T > T_g$
20	65	15	0·95	301	— 1·33	
30	55	15	0·77	207	— 1·12	
10	60	30	2·90	448	—13·32	$T > T_g$
0	65	35	1·66	572	— 2·94	$T > T_g$
5	60	35	3·06	472	—13·80	$T > T_g$
10	55	35	2·93	457	—13·27	$T > T_g$
14	51	35	1·04	382	— 0·99	
10	45	45	1·28 (407–452 °C)		— 1·80	
			2·70 (452–501 °C)	456	—11·69	$T > T_g$
0	35	65	1·40	569	— 1·43	$T > T_g$
1	34	65	1·50	559	— 2·08	$T > T_g$
5	30	65	2·34	497	— 8·36	$T > T_g$
10	25	65	1·08	433	— 0·72	
20	15	65	0·75	212	— 0·80	
30	5	65	0·59	96	— 1·10	
10	14·5	75·5	1·09	423	— 0·93	

*) No remarks means $T < T_g$.

TABLE A-XVIII

Electrical-conduction measurements. System $NaKO–B_2O_3–SiO_2$; x = mol % NaKO, y = mol % B_2O_3, z = mol % SiO_2

x	y	z	E_ϱ (eV)	$T(\log \varrho = 7)$ (°C)	A	remarks *)
3	82	15	2·73	454	—11·97	$T > T_g$
10	75	15	3·31	451	—16·10	$T > T_g$
14·5	70·5	15	1·38 (381–419 °C)		— 2·82	
			2·68 (419–484 °C)	428	—12·27	$T > T_g$
20	65	15	1·23	375	— 2·58	
30	55	15	1·04	306	— 2·09	
1	34	65	1·59	556	— 2·70	$T > T_g$
5	30	65	1·59 (421–483 °C)	467	— 3·84	
			2·30 (483–515 °C)		— 8·61	$T > T_g$
10	25	65	1·24	397	— 2·35	
20	15	65	1·05	306	— 2·15	
30	5	65	1·03	224	— 3·42	

*) No remarks means $T < T_g$.

TABLE A-XIX

Electrical-conduction measurements. System $Na_2O–B_2O_3–SiO_2$ + 5 mol % Al_2O_3; x = mol % Na_2O, y = mol % B_2O_3, z = mol % SiO_2

x	y	z	E_ϱ (eV)	$T(\log \varrho = 7)$ (°C)	A	remarks *)
3	82	15	2·31 (430–475 °C)	467	— 8·76	$T > T_g$; $T < T(\log\eta = 7{\cdot}1)$
			3·42 (475–530 °C)		—16·33	$T > T_g$; $T > T(\log\eta = 7{\cdot}1)$
5	80	15	3·03	439	—14·51	$T > T_g$
10	75	15	1·71 (376–406 °C)		— 5·55	
			2·53 (406–470 °C)	412	—11·65	$T > T_g$
12	73	15	1·04 (342–384 °C)		— 0·71	
			1·56 (384–437 °C)	398	— 4·71	$T > T_g$
14·5	70·5	15	1·11	368	— 1·76	
20	65	15	0·93	270	— 1·64	
30	55	15	0·75	166	— 1·64	
5	30	65	0·96	323	— 1·09	
10	25	65	0·89	255	— 1·50	
20	15	65	0·80	169	— 2·12	
30	5	65	0·66	80	— 2·30	

TABLE A-XX

Electrical-conduction measurements. System K_2O–B_2O_3–SiO_2 + 5 mol % Al_2O_3; x = mol % K_2O, y = mol % B_2O_3, z = mol % SiO_2

x	y	z	E_ϱ (eV)	$T(\log \varrho = 7)$ (°C)	A	remarks *)
3	82	15	1·78	473	—11·85	$T > T_g$
10	75	15	3·66	448	—18·62	$T > T_g$
14·5	70·5	15	1·15 (368–412 °C)		— 1·34	
			2·68 (412–463 °C)	417	—12·59	$T > T_g$
20	65	15	0·88	312	— 0·61	
30	55	15	0·83	224	— 1·48	
1	34	65	1·32	517	— 1·47	
5	30	65	1·27	460	— 1·74	
10	25	65	1·29	403	— 2·61	
20	15	65	0·79	245	— 0·69	
30	5	65	0·59	98	— 1·10	

*) No remarks means temperature range $T < T_g$.

TABLE A-XXI

Electrical-conduction measurements. System NaKO–B_2O_3–SiO_2 + 5 mol % Al_2O_3; x = mol % NaKO, y = mol % B_2O_3, z = mol % SiO_2

x	y	z	E_ϱ (eV)	$T(\log \varrho = 7)$ (°C)	A	remarks *)
3	82	15	2·60	474	—10·61	$T > T_g$
10	75	15	3·16	439	—15·41	$T > T_g$
14·5	70·5	15	1·40 (385–424 °C)		— 3·00	
			2·66 (424–480 °C)	431	—12·07	$T > T_g$
20	65	15	1·09	363	— 2·45	
30	55	15	0·97	311	— 1·44	
5	30	65	1·26	390	— 2·63	
10	25	65	1·00	341	— 1·26	
20	15	65	1·04	312	— 2·00	
30	5	65	1·02	228	— 3·23	

*) No remarks means temperature range $T < T_g$.

TABLE A-XXII

Density and refractive index of sodium-borosilicate glasses

composition (mol %)				density	refractive index n_D
Na_2O	B_2O_3	SiO_2	Al_2O_3	$(g/cm)^3$, 24 °C	24 °C
0	85	15	—	1·779	
3	82	15	—	1·834	1·468
5	80	15	—	1·883	1·4741
7	78	15	—	1·942	1·4800
10	75	15	—	2·002	1·4850
14·5	70·5	15	—	2·085	1·4943
17	68	15	—	2·148	1·4992
20	65	15	—	2·244	1·5042
30	55	15	—	2·441	1·5205
3	82	15	+5	1·950	1·4668
5	80	15	+5	1·965	1·4740
10	75	15	+5	2·040	1·4818
12	73	15	+5	2·063	
14·5	70·5	15	+5	2·101	
20	65	15	+5	2·215	1·4989
30	55	15	+5	2·429	1·5152
1	34	65	—	2·035	1·4580
5	30	65	—	2·105	1·4720
15	20	65	—	2·345	1·5075
20	15	65	—	2·462	1·5176
25	10	65	—	2·507	1·5153
30	5	65	—	2·537	1·5094
5	30	65	+5	2·117	1·4720
10	25	65	+5	2·193	1·4848
20	15	65	+5	2·422	1·5134
30	5	65	+5	2·458	1·5101

TABLE A-XXIII

Density and refractive index of potassium-borosilicate glasses

composition (mol %)				density	refractive index n_D
K_2O	B_2O_3	SiO_2	Al_2O_3	(g/cm³), 24 °C	24 °C
3	82	15	—	1·842	1·4647
10	75	15	—	2·014	1·4829
14·5	70·5	15	—	2·083	1·4860
20	65	15	—	2·223	1·4931
30	55	15	—	2·448	1·5050
3	82	15	+5	1·938	1·4659
10	75	15	+5	2·044	1·4760
14·5	70·5	15	+5	2·130	
20	65	15	+5	2·208	1·4875
30	55	15	+5	2·444	1·4974
1	34	65	—	2·038	1·4580
5	30	65	—	2·130	1·4729
20	15	65	—	2·468	1·5099
1	34	65	+5	2·107	1·467
5	30	65	+5	2·164	1·468
10	25	65	+5	2·267	1·4824
20	15	65	+5	2·425	1·5046
30	5	65	+5	2·461	1·5049

Summary

In this thesis an attempt has been made to determine the types of structural units in borosilicate glasses. Therefore a number of investigations have been carried out on the relation between the composition of the glasses and the properties. In a preliminary study the importance of wet-chemical preparation techniques was revealed. Together with the application of wet-chemical techniques, vacuum melting of the borosilicate glasses was also necessary to obtain reliable and useful results.

The Raman and infrared spectra of many borosilicate glasses were recorded, and the viscosity, the electrical conduction, the thermal expansion and the internal friction as a function of temperature was measured. Finally the density and refractive index of a limited number of compositions were measured. Of all these measurements the Raman spectra were especially useful in the determination of the different types of structural groups in the borosilicate glasses. The viscosity, thermal-expansion and internal-friction measurements also added much to reveal the structure of these glasses.

This study is primarily confined to sodium- and potassium-borosilicate glasses. For a limited number of compositions the influence of lithium, calcium and barium has been studied. The influence of Al_2O_3 on the structure has been studied more extensively.

For the binary alkali-borate glasses it has been found that in the concentration range 0 to about 25 mol % alkali oxide the boroxol groups, originally present in vitreous B_2O_3, are replaced by six-membered borate rings with one BO_4 tetrahedron which to a certain extent are ordered to tetraborate groups. In the range 20 to 35 mol % alkali oxide, gradually six-membered borate rings with two paired BO_4 tetrahedra are formed which to a certain extent are condensed to diborate groups. Unmixed sodium- and potassium-borate glasses cannot be made in the range above about 40 mol % alkali oxide. In mixed alkali-borate glasses with 40 to 50 mol % alkali oxide the presence of orthoborate, pyroborate and ring-type metaborate groups is indicated, together with diborate groups.

In the sodium- and potassium-borosilicate glasses the alkali ions are primarily bonded to borate groups of the same type as in the binary sodium- and potassium-borate glasses. On increasing the mole fraction of SiO_2 and at a constant alkali-to-boron ratio relatively increasing amounts of non-bridging oxygen ions are formed. These non-bridging oxygen ions are primarily grouped together in the ring-type metaborate groups. BO_4 tetrahedra are not incorporated in the silicate network like AlO_4 tetrahedra.

Lithium-, calcium- and barium-containing borosilicate glasses generally contain the same type of structural units as the corresponding sodium- and potassium-borosilicate glasses. The tendency to the formation of ring-type metaborate groups is not observed in these glasses.

The introduction of Al_2O_3 leads to the disappearance of BO_4 tetrahedra when not enough non-bridging oxygen ions are present to allow the conversion of all aluminum ions into AlO_4 tetrahedra. When enough non-bridging oxygen ions are present in the borosilicate glasses, then those connected to ring-type metaborate groups disappear first as compared to those present in SiO_4 tetrahedra with one non-bridging oxygen ion. At relatively low alkali-oxide concentration the introduction of Al_2O_3 results in the reoccurrence of boroxol groups.

Part of the boron ions is not present in typical large borate groups but forms a random network of BO_3 triangles and BO_4 tetrahedra.

It is indicated that microphase separation extends to the whole area of glass formation and is not confined to the well-known area in the ternary borosilicate system.

Samenvatting

Deze dissertatie beschrijft een onderzoek naar de struktuur van borosilikaatglazen. Hiertoe zijn metingen verricht naar de relatie tussen de eigenschappen van het glas en de samenstelling. In een voorgaand onderzoek werd het belang van nat-chemische bereidingsmethoden al aangetoond. Naast toepassing van deze methoden bleek het eveneens noodzakelijk alle borosilikaatglazen in vakuum te smelten opdat betrouwbare en reproduceerbare gegevens verkregen werden.

De Raman en infrarood spektra van vele borosilikaatglazen werden opgenomen en daarnaast de viskositeit, het elektrisch geleidingsvermogen, de thermische uitzetting en de inwendige wrijving als funktie van de temperatuur bepaald. Tenslotte werd voor een beperkt aantal samenstellingen de dichtheid en de brekingsindex gemeten. Van al deze metingen zijn vooral de Raman spectra erg nuttig geweest voor het ophelderen van de diverse struktuurelementen. De metingen van de viskositeit, thermische uitzetting en inwendige wrijving hebben eveneens bijgedragen tot het ophelderen van de struktuur.

Dit onderzoek heeft voornamelijk betrekking op natrium- en kalium-borosilikaatglazen. Voor een beperkt aantal samenstellingen is de invloed van lithium, calcium en barium op de struktuur bestudeerd. De invloed op de struktuur van het toevoegen van Al_2O_3 aan het glas is uitvoeriger onderzocht.

Voor de binaire alkali-boraatglazen is gevonden dat in het koncentratiegebied 0 tot ongeveer 25 mol % alkali oxide, de oorspronkelijk in B_2O_3-glas aanwezige boroxolgroepen vervangen worden door boraat-zesringen met één BO_4 tetraeder. Deze zesringen zijn tot op zekere hoogte geordend tot tetraboraatgroepen. In het gebied 20 tot 35 mol % alkali oxide worden langzamerhand boraat-zesringen gevormd met twee verbonden BO_4 tetraeders. Deze zesringen zijn tot op zekere hoogte met elkaar verbonden tot diboraatgroepen. Natrium- en kalium-boraatglazen met meer dan 40 mol % alkali oxide zijn niet bekend. Echter, in gemengde alkali-boraatglazen met 40 tot 50 mol % alkali oxide is de aanwezigheid van orthoboraat, pyroboraat en ring-type metaboraatgroepen aangetoond, alsmede diboraatgroepen.

In de natrium- en kalium-borosilikaatglazen zijn de alkali ionen voornamelijk aan boraatgroepen gebonden welke van hetzelfde type zijn als in de binaire boraatglazen. Bij toename van het SiO_2 gehalte en bij gelijke alkali/borium verhouding neemt het aantal zwevende zuurstofionen toe. Deze zijn voornamelijk gebonden aan ring-type metaboraatgroepen. BO_4 tetraeders worden, in tegenstelling tot AlO_4 tetraeders, nauwelijks in het silikaatnetwerk opgenomen.

Lithium-, calcium- en bariumhoudende borosilikaatglazen bevatten in het algemeen dezelfde struktuureenheden als korresponderende natrium- en kalium-borosilikaatglazen. Echter, de neiging tot het vormen van ring-type metaboraatgroepen is niet waargenomen.

Toevoeging van Al_2O_3 leidt tot het verdwijnen van BO_4 tetraeders als er niet

voldoende zwevende zuurstofionen aanwezig zijn, onder gelijktijdige vorming van AlO_4 tetraeders. Als er voldoende zwevende zuurstofionen aanwezig zijn dan verdwijnen in de eerste plaats die welke tot ring-type metaboraatgroepen behoren vergeleken met die welke tot SiO_4 tetraeders behoren. Bij relatief lage koncentraties van alkali oxide leidt het toevoegen van Al_2O_3 tot het heroptreden van boroxolgroepen.

Een gedeelte van de borium-ionen is niet aanwezig in typische grote boraatgroepen maar vormen een ongeordend netwerk van BO_3 driehoeken en BO_4 tetraeders.

Fasenscheiding treedt in het gehele borosilikaatglasvormingsgebied op en beperkt zich niet tot de reeds bekende gebieden.

Levensbericht

Willem Leendert Konijnendijk werd op 4 april 1945 te Oss geboren. Kort daarop, na het definitieve einde van de oorlog, konden zijn ouders naar Eindhoven terugkeren.

De middelbare schoolopleiding, die hij aan het Gemeentelijk Lyceum te Eindhoven ontving, sloot hij met het behalen van het einddiploma h.b.s.-b in 1962 af. In datzelfde jaar liet hij zich inschrijven als student aan de Technische Hogeschool Eindhoven in de Afdeling der Scheikundige Technologie. Op 10 januari 1968 legde hij met gunstig gevolg het ingenieursexamen af. Zijn afstudeeronderzoek voerde hij uit onder leiding van Prof. Dr. G. C. A. Schuit in de groep Anorganische Chemie.

Na het behalen van het ingenieursdiploma trad hij op 15 januari 1968 als wetenschappelijk medewerker in dienst van het Natuurkundig Laboratorium van de N.V. Philips' Gloeilampenfabrieken. Hij was werkzaam in de groep Glas, welke tot 30 april 1973 onder leiding stond van Prof. Dr. J. M. Stevels.

Het experimentele werk dat in deze dissertatie beschreven wordt, is uitgevoerd in de periode eind 1971 tot midden 1974.

Op 12 oktober 1973 trad hij in het huwelijk met Paloma Vivancos, arts.

STELLINGEN

bij het proefschrift van

W. L. Konijnendijk

11 april 1975

I

Drie waarden voor het relatieve aantal borium atomen in tetraeder omringing (N_4) in natrium borosilikaatglazen, welke met behulp van n.m.r. door Scheerer, Müller-Warmuth en Dutz werden gemeten en gepubliceerd, zijn hoger dan de theoretisch meest waarschijnlijke maximale waarden.

J. Scheerer, W. Müller-Warmuth en H. Dutz, Glastechn. Ber. **46**, 109, 1973.

II

Het is onwaarschijnlijk dat in gesmolten alkali boraten en borosilikaten de fraktie borium atomen in tetraeder omringing sterk afwijkt van de fraktie in het glas van overeenkomstige samenstelling bij kamertemperatuur.

P. Beekenkamp, Proefschrift 1965, T.H. Eindhoven.
Th. J. M. Visser, Proefschrift 1971, T. H. Eindhoven.
E. F. Riebling, J. Am. ceram. Soc. **50**, 46, 1967.
Dit proefschrift.

III

De verklaring dat spinodale fasenscheiding in multikomponent oxyde glazen zou kunnen optreden is aan bedenkingen onderhevig.

J. W. Cahn, J. chem. Phys. **42**, 93, 1964.
G. F. Neilson, Phys. Chem. Glasses, **10**, 54, 1969.
W. Haller en P. B. Macedo, Phys. Chem. Glasses **9**, 153, 1968.

IV

Grenzen van gebieden met metastabiele fasenscheiding in glas dienen opgegeven te worden tezamen met de gevolgde meetmethode.

V

Arseen, dat in de vorm van As_2O_3 dikwijls aan silikaatglas als loutermiddel wordt toegevoegd, wordt onder andere als geïsoleerde AsO_4^{3-} groepen in het glas opgenomen.

W. L. Konijnendijk en J. H. J. M. Buster, J. non-cryst. Solids, in druk.

VI

Het op ruime schaal beschikbaar komen van rasterelektronenmikroskopen kan een nieuwe impuls geven aan het onderzoek van koncentratiefluktuaties op submikronschaal in vaste stoffen met behulp van autoradiografie.

VII

Het relatief sterker optrekken van de kollektieve voorzieningen in Nederland vergeleken met andere Westeuropese landen heeft een remmende invloed op de toevloed van gastarbeiders naar ons land.

VIII

Voor een gezonde industriële ontwikkeling in de Nederlandse samenleving, is deze meer gediend met het toetsen van investeringsbeslissingen van partikuliere ondernemingen aan een door het parlement vooraf aanvaard industrialisatiebeleid, dan met het invoeren van wettelijke maatregelen achteraf waardoor de rentabiliteit van ondernemingen veelal nodeloos wordt gedrukt.

IX

Voor de demonisering van de faktor "kapitaal" door vele linkse politici bestaat weinig grond.

X

Een goede remedie tegen maagzweren bij Spaanse gastarbeiders is de overkomst van hun echtgenotes naar Nederland.

Huisartspraktijk van P. Konijnendijk-Vivancos.

Eindhoven, 11 april 1975 W. L. Konijnendijk